Gravity of Light, Light in Gravitational Fields, and Metrological Implications

Dissertation

der Mathematisch-Naturwissenschaftlichen Fakultät
der Eberhard Karls Universität Tübingen
zur Erlangung des Grades eines
Doktors der Naturwissenschaften
(Dr. rer. nat.)

vorgelegt von
Fabienne Schneiter
aus Bern, Schweiz

Tübingen
2018

Gedruckt mit Genehmigung der Mathematisch-Naturwissenschaftlichen Fakultät
der Eberhard Karls Universität Tübingen.

Tag der mündlichen Qualifikation: 30. Januar 2019
Dekan: Prof. Dr. Wolfgang Rosenstiel
1. Berichterstatter: Prof. Dr. Daniel Braun
2. Berichterstatter: Prof. Dr. Martin Wilkens

Abstract

This thesis deals with the interplay of gravitation and light. It is split into four parts, each of them giving an overview of one of our projects: In the first and second part, we study the gravitational properties of laser light and use other light rays to illustrate these properties. In the third part, light rays are used as a tool to determine the frequency spectrum of an optical resonator in a background gravitational field. Finally, in the fourth part, light plays both the role of the source of the gravitational field and the means to perform a measurement. As the gravitational field of light is weak, its effects are too small to be experimentally measured. However, with the progress of technology, they might be detected in the future. They are of conceptual interest, revealing fundamental properties of the nature of light.

In the first part, we determine the gravitational field of a laser beam: The laser beam is described as a solution of Maxwell's equations and has a finite wavelength and circular polarization. This description is beyond the short-wavelength approximation, and allows to find novel gravitational properties of light. Among these are frame-dragging due to the laser beam's spin angular momentum and the deflection of parallel co-propagating test light-rays that overlap with the source laser-beam.

Further, the polarization of a test light-ray in the gravitational field of the laser beam is rotated. This is analyzed in the second part. The rotation consists of a reciprocal contribution associated to the gravitational analogue of optical activity, and a non-reciprocal part identified as the gravitational analogue of the electromagnetic Faraday effect. Therefore, letting light propagate back and forth between two mirrors, the gravitational Faraday effect accumulates, while the effect due to the gravitational optical activity cancels. Interestingly, using only classical general relativity, our analysis shows gravitational spin-spin coupling, which is a known effect in perturbative quantum gravity.

In the third part, we study the effect of a gravitational field and proper acceleration on the frequency spectrum of an optical resonator. The resonator is modelled in two different ways: As a rod of matter with two attached mirrors at its ends, and as a dielectric rod whose ends function as mirrors. The resonator can be deformed in the gravitational field depending on the material properties of the rod. The frequency spectrum turns out to depend on the radar length, which is the length an observer measures by sending a light signals back and forth between the mirrors and measuring the time difference. The results for the frequency spectrum may be used for measuring gravitational fields or acceleration based on frequency shifts of the light.

Also in the fourth part we look at an optical resonator, this time a cubic cavity. While in the third part we considered a background gravitational field, now the light inside the cubic cavity is the source of the gravitational field. With this setup, we consider an observer making a specific measurement of the speed of light and analyze the precision of the measurement. Using quantum parameter estimation theory and analyzing the effect of the gravitational field, we determine the number of photons inside the cavity which leads to the best precision of the measurement.

Zusammenfassung

Das Thema dieser Dissertation ist das Zusammenspiel von Gravitation und Licht. Die Arbeit ist in vier Teile unterteilt, die jeweils einen Überblick über eines unserer vier Projekte geben. Im ersten und zweiten Teil beschäftigen wir uns mit dem Gravitationsfeld eines Laserstrahls und verwenden weitere Lichtstrahlen um dessen Eigenschaften zu illustrieren. Im dritten Teil benutzen wir Lichtstrahlen um das Frequenzspektrum eines optischen Resonators in einem Gravitationsfeld zu berechnen. Letztendlich, im vierten Teil, ist das Licht sowohl die Quelle des Gravitationsfelds wie auch das Mittel um eine Messung durchzuführen. Das Gravitationsfeld von Licht is schwach, deshalb sind seine Effekte momentan zu klein um in einem Experiment gemessen zu werden. Mit dem Fortschritt der Technologie könnte dies jedoch in Zukunft möglich sein. Jedenfalls sind die Effekte von konzeptionellem Interesse, da sie fundamentale Eigenschaft von Licht enthüllen.

Im ersten Teil bestimmen wir das Gravitationsfeld von einem Laserstrahl. Dieser gehorcht den Maxwell Gleichungen und hat eine endliche Wellenlänge und zirkulare Polarisation. Unsere Beschreibung des Laserstrahls unterliegt nicht der paraxialen Näherung und ermöglicht deshalb, neue gravitative Eigenschaften von Laserlicht zu sehen: frame-dragging aufgrund des Spin-Drehimpulses und die Ablenkung von parallel co-propagierenden Lichtstrahlen, die mit dem Laserstrahl überlappen.

Weiter wird die Polarisation eines Lichtstrahls gedreht, wenn dieser im Gravitationsfeld des Laserstrahls propagiert. Dies ist das Thema des zweiten Teils. Die Rotation besteht aus einem reziproken und einem nicht-reziproken Anteil, die respektive dem gravitativen Analogon zur optischen Aktivität und dem gravitativen Analogon zum elektromagnetischen Faraday Effekt zugeordnet werden können. Lässt man Licht zwischen zwei Spiegeln hin und her propagieren, wird der gravitative Faraday Effekt verstärkt, während sich der Effekt aufgrund der gravitativen optischen Aktivität aufhebt. Interessanterweise illustrieren unsere Überlegungen im Rahmen der klassischen Relativitätstheorie eine gravitative Spin-Spin Wechselwirkung, die man in der perturbativen Quantengravitation findet.

Im dritten Teil betrachten wir den Effekt eines Gravitationsfelds und einer Beschleunigung auf das Frequenzspektrum eines optischen Resonators. Der Resonator ist entweder als Materiestab modelliert, an dessen Enden zwei Spiegel angebracht sind, oder als Stab, der aus einem dielektrischen Medium besteht, an dessen Enden das Licht reflektiert wird. Je nach den materiellen Eigenschaften des Stabs, kann der Resonator im Gravitationsfeld verformt werden. Das Frequenzspektrum hängt von der Radarlänge ab. Dies ist die Länge, die ein Beobachter bestimmt, indem er ein Lichtsignal zwischen den Spiegeln hin und her sendet und die Zeitdifferenz misst. Mit dem Ergebnis lässt sich möglicherweise die Stärke eines Gravitationsfelds oder einer Beschleunigung bestimmen, indem man die Frequenz des Lichts im Resonator misst.

Auch im vierten Teil betrachten wir einen optischen Resonator, dieses Mal einen kubischen. Während im dritten Teil ein beliebiges Gravitationsfeld angenommen wurde, wird letzteres nun vom Laserstrahl verursacht. Wir betrachten eine Messung der Lichtgeschwindigkeit, die ein Beobachter durchführt, und analysieren die Präzision mittels Quanten-Parameterschätzung. Unter Berücksichtigung des Effekts des Gravitationsfelds bestimmen wir die Anzahl Photonen im Resonator, welche die präziseste Messung erlaubt.

Acknowledgements

During my PhD, I was supported, motivated and inspired by various people. I would like to mention some of them.

First, I thank Daniel Braun for the supervision of the thesis, especially for always finding time to look at my work and to discuss problems in detail. I appreciated his broad and deep knowledge in physics and his open-mindedness when it came to the choice of the projects. He gave me the chance to work in collaborations, do research stays and attend conferences and therefore get to know the latest progresses in my field, which I was very grateful for.

Most of the work was done together with Dennis Rätzel. I thank Dennis for guiding the projects into interesting directions, for pointing out relevant literature, for his advice and critical reviews. Further, I was grateful for the discussions concerning life in science, for giving me the chance to meet people and present our work. Working with him has been a pleasure, and his passion and understanding of physics have always been very motivating for me.

I thank Julien Fraïsse for the many discussions about physics, quantum metrology and my projects. Most importantly, I thank him for making life in Tübingen beautiful from the first day on.

I thank József Fortágh for introducing me in Tübingen, which gave me the possibility to obtain my current position. I am very grateful for his support and helpful advice during the thesis.

I appreciated the further collaborations: I thank Uwe Fischer for interesting discussions, during the ongoing project and during his visits in Tübingen. Further, I thank David Bruschi and Sofia Qvarfort for the collaboration. Working and spending time with them during my stay in Vienna has been a pleasure.

Further, I thank our group and our floor for the convenient atmosphere, and Annette Lorösch for doing the administration and helping me with paperwork. Especially, I thank Cornelia Hille for discussions concerning the thesis and all the nice time we spent together in the evenings and on weekends.

Last but not least, I thank my family for the nice days I regularly spent with them.

I thank Daniel Braun, Dennis Rätzel and Julien Fraïsse for proofreading the manuscript.

Fabienne Schneiter

Contents

Introduction

The twentieth century has seen the emergence of two theories lying at the core of modern physics: general relativity and quantum mechanics. In both of these theories, light plays an important role. Indeed, light is both a quantum and a relativistic object: It has been experimentally confirmed that light behaves according to the predictions of quantum mechanics. On the other hand, light enters the postulates of general relativity and is by construction of the theory a relativistic object. By knowing precisely the gravitational properties of light, it might be possible to gain insight into the role of gravity in quantum mechanics, or the other way around, to learn about the role of quantum mechanics in general relativity.

In our work, we studied on one side how light beams gravitate, and on the other side how the behavior of light rays in a gravitational field influences specific measurements. The latter includes the deflection of light rays, the rotation of their polarization and the frequency shift they obtain in a gravitational field. We analyzed theoretical and specific setups that could be used in a laboratory. The difficulty in experiments is the distinction and detection of the gravitational effects, as they are very small even when using the most powerful lasers of nowadays.

We worked on four different but related projects, and accordingly the thesis is split into four main chapters, each of them giving an overview of one of our four projects. The first chapter deals with the gravitational field of a laser beam as one creates in a laboratory, its gravitational characteristics and its influence on small particles or light rays [C]. The second chapter focusses on one of these effects, namely the rotation of the polarization of another light ray propagating in the gravitational field of the laser beam [D]. In the third chapter, we consider a given gravitational field and study its influence on light rays in order to give an expression for the frequency spectrum of an optical resonator in a gravitational field [B]. Importantly, in this chapter the gravitational field could be, but is not necessarily, generated by the light itself. In the fourth chapter, we consider a different optical resonator, this time affected by the gravitational field of light itself [A]. In this setup, we study the gravitational influence when making a specific measurement.

Two technical points concerning general relativity deserve to be explained before starting with the main projects. One of them is the coordinate-invariance of general relativity and the related difficulty to distinguish between actual physical effects and coordinate-artefacts. We were careful to either work with coordinate-invariant quantities, or to work with covariant quantities and to explain to which observer they correspond. In some cases, it turned out to be useful to do the calculations in the proper detector frame, which is a locally inertial frame for an observer and reduces to the Fermi normal coordinates if the observer is freely falling. In other cases, it was possible to find expressions for the effects containing the Riemann curvature tensor, which is invariant under coordinate transformations in the linearized approximation to general relativity, which can be applied

if the gravitational field is weak. Summarized, one needs to verify that the effect is actually physical, and to make sure that it is analyzed in the frame of the observer measuring it.
Another important point, especially in the third chapter for the description of the optical resonator, is the concept of length and extended objects: General relativity is a local theory, which makes it hard to describe extended objects, implying that it is not possible to associate a physical concept of length to them. For example, a one-dimensional extended object has to be described by a sequence of segments, and a possibility to define its length is in an operational way using light signals, therefore making it clearly observer-dependent.
The projects are not ordered in a chronological way: Our first article [A] left some points that were interesting to study in more detail, such as the resonance frequency in a curved spacetime, the gravitational field of laser light, and how they can be linked to measurements. The gravitational field of laser light is studied in article [C], and the resonance frequency in article [B]. Article [C] then provided the tools to look at the rotation of polarization discussed in article [D]. The following four chapters aim to give an overview of our work and to explain the ideas intuitively.
We use the following conventions and notations: The metric is assumed to have the signature $(-1, 1, 1, 1)$. Greek indices like α denote to spacetime indices, latin indices like a denote to spatial indices, curly capital latin indices like $\mathcal{A}$ denote to spacetime indices in the Minkowski frame, and ordinary capital latin indices like A denote to spatial indices in the Minkowski frame. Further, c stands for the speed of light, $\hbar$ for the Planck constant, G for Newton's constant, and ϵ_0 for the electric permittivity.

Chapter 1

Gravitational Field of a Laser Beam beyond the Short-Wavelength Approximation

The gravitational field of light was already studied in the year 1931 by Tolman, Ehrenfest and Podolski [1]. They considered the most simple model for light: an infinitely thin pencil of constant energy density which is moving at the speed of light. Later on this description was generalized in various ways. Among these models are cylindrical beams, infinitely extended plane waves, or single photons (compare Appendix A). All of them have one important feature in common: They describe light in the short-wavelength approximation, or equivalently, the paraxial approximation, meaning that they describe light in the framework of geometric ray optics. In this approximation, there is no divergence, no spreading, of the beam. This means that the wave-like nature of light is not taken into account, and the Maxwell equations are not satisfied.[1]

In our project [C], we give a realistic description of a laser beam including the wave-like nature of light and fulfilling the Maxwell equations. This description reveals features of the gravitational field of a laser beam that are not visible in the short-wavelength approximation: First, due to the helicity of the laser beam, frame-dragging appears. This means that a particle moving initially radially outwards from the beamline of the laser beam moves on a bent line. Second, a parallel co-propagating light ray, this means a light ray propagating parallel to the beamline of the laser beam and in the same direction as the laser beam, is deflected by the gravitational field of the laser beam. This is in contrast to the statements obtained with the previous models. Third, the polarization vector of a light ray propagating in the gravitational field of the laser beam is rotated. This is the gravitational analogue of the Faraday effect appearing in electromagnetism, and the subject of the next chapter. None of these features is visible in the short-wavelength approximation, which indicates that they can be attributed to the wave-like nature of light.

The gravitational effects are too small to be experimentally detected with current technology, but with the fast improvement of the sensitivity of measurements, it might be possible in the future. The effects are of conceptual interest, revealing fundamental properties of light.

[1] For the plane wave metrics the Maxwell equations are fulfilled. However, they do not describe realistic situations as the energy density of the beam does not decrease with the distance in any direction.

In this chapter we introduce the description of the laser beam beyond the short-wavelength approximation, outline the calculation of the gravitational field, and present some of its characteristics. Various models for light beams in the short-wavelength approximation are presented in Appendix B. Our calculations are done in the linearized approximation to general relativity, which is introduced in Appendix A.

1.1 Description of the Laser Beam

We describe the laser beam as electromagnetic radiation satisfying the Maxwell equations. This ensures that it has wave-like characteristics. In previous models for light beams, this was not the case: They used the short-wavelength approximation, which means that the momentum of the light beam diverges, while its wavelength vanishes - implying that there is no wave-like behavior of the light beam. In these models, the light is moving along null geodesics. The metric describing the gravitational fields of these beams has always the same structure (Appendix B), which is typical for any energy densities moving at the speed of light. In this case, it turns out that a test light-ray co-propagating parallel to the source light-ray is not deflected. For our description of the laser beam beyond the short-wavelength approximation, this is not the case, as we will explain.

More specifically, our laser beam is described as a perturbative solution to the Maxwell equations, an expansion in the beam-divergence angle θ, which is the opening angle of the beam and assumed to be small. Making the ansatz of an electromagnetic almost plane wave, this solution turns out to be a Gaussian beam, which has the property that its intensity distribution decreases with a Gaussian factor with the distance to the beamline of the laser beam.

The solution is obtained as follows. First, in order to keep track of the orders of magnitude more easily, we introduce the dimensionless coordinates $\tau = ct/w_0$, $\xi = x/w_0$, $\chi = y/w_0$, $\zeta = z/w_0$, where w_0 is the beam waist, a measure of the radius of the beam at its focal point. The vector potential describing the laser beam is given by a plane wave multiplied by an amplitude which is slowly varying in the direction of propagation, as the beam divergence is small. Further, the laser beam is considered to be propagating in positive ζ-direction, such that its beamline lies on the ζ-axis. Corresponding to these features, one makes the ansatz for the four-vector potential

$$A_\alpha(\tau, \xi, \chi, \zeta) = \mathcal{A} v_\alpha(\xi, \chi, \theta\zeta) e^{i\frac{2}{\theta}(\zeta - \tau)} \,, \tag{1.1}$$

where $\mathcal{A}$ is the amplitude and v_α the envelope function. The exponential factor describes a plane wave propagating in ζ-direction with angular wave number $k = \frac{2}{\theta w_0}$. A schematic illustration of the laser beam is shown in Figure 1.1

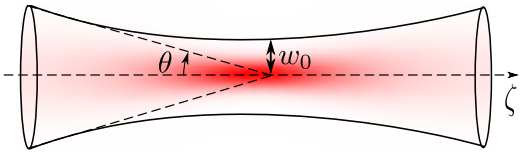

Figure 1.1: Schematic illustration of the laser beam: The opening angle is described by the beam-divergence angle θ, and is assumed to be small. The beam waist w_0 is a measure for the radius of the laser beam at its focal point, more precisely the radius at which the intensity of the beam falls to $1/e^2$ of its value on the beamline. The typical property of the laser beam is that its intensity distribution decreases with a Gaussian factor with the distance from the beamline.

We then impose the Maxwell equations for the vector potential, which in the Lorentz gauge $\eta^{\alpha\beta}\partial_\alpha A_\beta = 0$ reduce to wave equations,

$$\left(-\partial_\tau^2 + \partial_\xi^2 + \partial_\chi^2 + \partial_\zeta^2\right) A_\mu(\tau, \xi, \chi, \zeta) = 0 \,. \tag{1.2}$$

The envelope function is assumed to vary slowly in the direction of propagation, which implies that the Maxwell equations for the four-vector potential take the form of a Helmholtz equation for the envelope function,

$$\left(\partial_\xi^2 + \partial_\chi^2 + \theta^2\partial_{\theta\zeta}^2 + 4iw_0\partial_{\theta\zeta}\right) v_\alpha(\xi, \chi, \theta\zeta) = 0 \,. \tag{1.3}$$

This equation is solved by writing the envelope function as a power series in the beam-divergence angle θ,

$$v_\alpha(\xi, \chi, \theta\zeta) = \sum_{n=0}^{\infty} \theta^n v_\alpha^{(n)}(\xi, \chi, \theta\zeta) \,. \tag{1.4}$$

This leads to a differential equation for each order, where in even/odd orders the solution of a lower even/odd order appears as a source term. The two lowest order equations have a similar structure to a Schrödinger equation, and therefore their solutions are similar to Gaussian wave packets.
We consider the laser beam to be rotationally symmetric about the beamline and to have circular polarization, as in this case strongly oscillating terms in the energy-momentum tensor cancel, making it possible to calculate the gravitational field.[2]
In the following we consider two different scenarios. In the first scenario, both the distance of the emission and the absorption to the focal point of the laser beam are assumed to be large. This has the advantage that there is no abrupt change in the energy distribution at the location of the emission or absorption, as due to the spreading of the laser beam, the energy density decreases with the distance to the focal point of the beam, such that far away it is close to zero. In this case, as the envelope function has the argument $\theta\zeta$ rather than ζ, this is also the case for the energy-momentum tensor, and one finds $T_{\alpha\beta} = c^2\epsilon_0 \,\mathrm{Re}\left(F_\alpha{}^\sigma F^*_{\beta\sigma} - \frac{1}{4}\eta_{\alpha\beta}F^{\delta\rho}F^*_{\delta\rho}\right)/2$.

[2]The polarization of light is defined with the duality transformation of the electromagnetic field, $D_\varphi = e^{i\varphi\Lambda} : \; F_{\mu\nu} \mapsto F_{\mu\nu}\cos(\varphi) + \star F_{\mu\nu}\sin(\varphi)$, where the Hodge dual of the field strength is given by $\star F_{\mu\nu} = \frac{1}{2}\omega_{\mu\nu\rho\sigma}F^{\rho\sigma}$ and $\omega_{\mu\nu\rho\sigma}$ is the completely anti-symmetric tensor. The generator Λ of the duality transformation is found to be the operator $\Lambda : \; F_{\mu\nu} \mapsto -i \star F_{\mu\nu}$. The laser beam has right or left handed circular polarization, if its field strength $F_{\mu\nu} = \partial_\mu A_\nu - \partial_\nu A_\mu$ is an eigenvector of Λ with eigenvalue ± 1, such that $\Lambda F_{\mu\nu} = \pm F_{\mu\nu}$.

Different approach: optical vortices

Before starting the discussion of the gravitational field of the laser beam, we mention the to our knowledge only other two results about the gravitational field of laser beams beyond the short-wavelength approximation. They both deal with optical vortices. Optical vortices are laser beams that carry orbital angular momentum; one can think of them as winding around the optical axis like a corkscrew. A certain class of them are the Laguerre-Gaussian beams, which are constructed with the generalized Laguerre polynomials. In [2], the laser beam is described perturbatively. They consider the two leading orders, which they call the paraxial approximation, equivalent to the short-wavelength approximation. In comparison, in [C] we study the five leading orders and associate only the leading order to the short-wavelength approximation. In [2], frame-dragging arises due to orbital angular momentum, while in [C], it is due to spin angular momentum. In a subsequent article [3] which appeared after [C], the gravitational field is again calculated for the optical vortex. The energy-momentum tensor has the same structure as in our case up to the first order,[3] and frame-dragging due to spin and orbital angular momentum is discussed and illustrated by looking at massive test particles. They do not find a deflection of the parallel co-propagating light ray, as this only appears in higher orders, as we will explain.

1.2 Characteristics of the Gravitational Field

The metric describing the gravitational field is determined using the linearized approximation of general relativity, introduced in Appendix A. This is possible since the gravitational field is expected to be weak. Then, the metric $g_{\alpha\beta}$ consists of the Minkowski metric $\eta_{\mu\nu}$ plus a small perturbation $h_{\mu\nu}$.
In the first scenario, where the laser beam is considered to be long, the metric perturbation is written in a power series of the beam divergence,

$$h_{\alpha\beta}(\xi,\chi,\theta\zeta) = \sum_{n=0}^{\infty} \theta^n h^{(n)}_{\alpha\beta}(\xi,\chi,\theta\zeta) \ , \tag{1.5}$$

and the Einstein equations are solved order by order. In this case they simplify to a two-dimensional Poisson equation for the metric perturbation, with the energy momentum tensor plus lower order solutions of the metric perturbation as source terms. They are solved with the Green's function for the Poisson equation.
In the second scenario, we consider the laser beam to be short; it is assumed to be emitted at $\zeta = \alpha$ and absorbed at $\zeta = \beta$, chosen such that $\theta\zeta \ll 1$ holds. In this case, the metric perturbation can be calculated with the retarded solution of the wave equation and is given by

$$h_{\alpha\beta}(\tau,\xi,\chi,\theta) = \frac{4Gw_0^2}{c^4} \int_{-\infty}^{\infty} d\xi' d\chi' d\zeta' \frac{T_{\alpha\beta}\left(\tau - \sqrt{(\xi-\xi')^2+(\chi-\chi')^2+(\zeta-\zeta')^2}, \xi', \chi', \theta\zeta'\right)}{\sqrt{(\xi-\xi')^2+(\chi-\chi')^2+(\zeta-\zeta')^2}} \ . \tag{1.6}$$

Acceleration of massive test particles

The leading order of our perturbation corresponds to a laser beam with vanishing opening angle, and thus to the laser beam described in the paraxial approximation. The metric

[3] Compare Eq. (4.1-4.3) in [3] and Eq. (40,52) in [C].

has the characteristic structure for light beams in the short-wavelength approximation

$$h^{(0)}_{\tau\tau} = h^{(0)}_{\zeta\zeta} = -h^{(0)}_{\tau\zeta} = I^{(0)} \,, \tag{1.7}$$

where $I^{(0)}$ is obtained solving the Poisson equation in the case of the long beam or using the retarded solution in the case of the short beam.[4] For the case of the long laser beam, the solution looks the same as the exact solution found by Bonnor [4] (Model 4 in Appendix B2) for a light-like medium without divergence. For the case of a short laser beam, letting the beam waist go to zero, one reproduces the solution for the thin beam found by Tolman, Ehrenfest and Podolski [1] (Model 1 in Appendix B2).
The acceleration of massive test particles at rest due to the gravitational field of the laser beam is given by the geodesic equation $\ddot{\gamma}^\mu = -\Gamma^\mu_{\nu\rho}\dot{\gamma}^\nu\dot{\gamma}^\rho$, where γ^μ describes the trajectory of the particle and the dot refers to the derivative with respect to proper time. The acceleration transverse to the beamline of the laser beam $\ddot{\gamma}^\rho$ is proportional to $\partial_\rho I^{(0)}$, and the acceleration along the beamline $\ddot{\gamma}^\zeta$ is proportional to $\partial_\zeta I^{(0)}$. These quantities are illustrated in Figure 1.2.

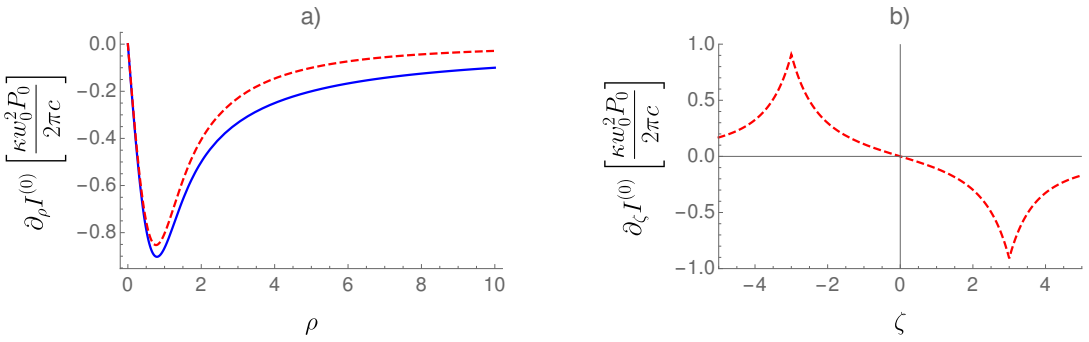

Figure 1.2: Behaviour of the acceleration of massive test particles initially at rest: The plain blue line corresponds to the long laser beam, and the dashed red line to the short laser beam. The plot a) shows the behaviour of the acceleration towards the beamline, as a function of the distance to the beamline. The plot b) illustrates the behaviour of the longitudinal acceleration in the direction of propagation as a function of the longitudinal distance from the beam waist. The two derivatives of $I^{(0)}$ are plotted in units of $\kappa w_0^2 P_0/(2\pi c)$, where $\kappa = 16\pi G/c^4$ and P_0 is the power of the source laser-beam. For the short source laser-beam, emission and absorption take place at $\zeta = -3$ and $\zeta = 3$, respectively. In the plot a), we set $\zeta = 1$, and in the plot b) we set $\rho = 1/2$.

The plot shows that the particle is accelerated towards the beamline of the laser beam. The acceleration is zero on the beamline, reaches a maximum at a certain distance from the beamline and then decreases with increasing distance to the beamline. The existence of a maximal acceleration can be explained with Green's theorem: As only the energy enclosed in a cylinder whose radius is the distance of the particle to the beamline contributes to the acceleration, the increase in the strength of the acceleration due to the increasing volume of

[4] For the long beam, it is given by $I^{(0)} = 8GPw_0^2/c^5\left(\mathrm{Ei}(-2|\mu|^2\rho^2) - 2\log(\rho)\right)$, where $|\mu|^2 = 1/\left(1+(\theta\zeta)^2\right)$, P_0 is the power of the laser beam and Ei is the exponential integral function. For the short beam, it is given by $I^{(0)} = 8Gw_0^2P_0/c^5 e^{-2\rho^2}\int_0^\infty d\rho'\ \rho'\log\left(\frac{\beta-\zeta+\sqrt{(\beta-\zeta)^2+\rho'^2}}{\alpha-\zeta+\sqrt{(\alpha-\zeta)^2+\rho'^2}}\right) J_0(i4\rho\rho')e^{-2\rho'^2}$, where J_0 is the Bessel function of the first kind.

the cylinder competes with the decrease of the acceleration due to the increasing distance from the beamline. Generally, the long laser beam induces a stronger acceleration than the short laser beam, since the absolute amount of energy is larger. Parallel to the beamline, there is no acceleration for the long laser beam, as in the zeroth order the beam is perfectly cylindrical and its shape does not change in this direction. The energy-distribution of the short laser beam however has a discontinuity at the points of emission and absorption. In this case, the acceleration is maximal at these two points and vanishes in the middle between the point of emission and the point of absorption.

With a numerical example, one sees that the acceleration is weak: For a long laser beam with a power $P_0 \sim 10^{15}\,\mathrm{W}$, a beam waist $w_0 \sim 10^{-3}\,\mathrm{m}$, a particle at rest at the location $z = 0$ and $r = \sqrt{x^2 + y^2} = w_0$ feels the radial acceleration of $\ddot{\gamma}^r \sim -10^{-18}\,\mathrm{ms}^{-2}$, where γ is the worldline of the particle parametrized by its proper time. The same order of magnitude is found in [5] (Model 1 and Model 2 in Appendix B2).

Frame-dragging

In the first order, the following components contribute to the metric perturbation:

$$h^{\lambda}_{\tau\xi}{}^{(1)} = -\, h^{\lambda}_{\xi\zeta}{}^{(1)} = I^{\lambda(1)}_{\xi}\,, \tag{1.8}$$

$$h^{\lambda}_{\tau\chi}{}^{(1)} = -\, h^{\lambda}_{\chi\zeta}{}^{(1)} = I^{\lambda(1)}_{\chi}\,, \tag{1.9}$$

where $I^{\lambda(1)}_{\xi}$ and $I^{\lambda(1)}_{\chi}$ are determined by $I^{(0)}$.[5] With the index λ we make explicit that the solution depends on whether the laser beam has left-handed circular polarization ($\lambda = \pm 1$). The result coincides with the exact solution for a rotating null fluid presented in [6] for a certain set of parameters.[6]

In the first order, frame-dragging appears. Frame-dragging is the effect that a rotating energy distribution draggs along the spacetime with it - other than in Newtonian gravity, where a body generates the same gravitational field when it is rotating as when it is not rotating. Frame-dragging can be illustrated by looking at the motion of a test particle: Letting a massive test particle move radially outward from the beamline, the frame-dragging causes it to move on a bent trajectory, i.e. letting the particle initially move in the ξ-direction, one finds that the acceleration in the χ-direction is different from zero, therefore forcing the particle to move on a bent line. This is schematically illustrated in Figure 1.3. In particular, we find that the sign of the acceleration depends on whether the laser beam is left- or right-handed circularly polarized, and that it falls off with the distance to the beamline of the laser beam in the same way as the energy-density of the laser beam. In our case, the effect is due to the spin angular momentum. Frame-dragging effects for optical vortices were shown in [2], where they stem from orbital angular momentum.

[5] They are given by $I^{\lambda(1)}_{\xi} = \frac{1}{4}\left(\theta\zeta\partial_{\xi} + \lambda\partial_{\chi}\right) I^{(0)}$ and $I^{\lambda(1)}_{\chi} = -\frac{1}{4}\left(\lambda\partial_{\xi} - \theta\zeta\partial_{\chi}\right) I^{(0)}$.

[6] The parameters in [6] need to be chosen as $\alpha = \theta I^{\lambda(1)}_{\chi}/\sqrt{2}$, $\beta = \theta I^{\lambda(1)}_{\xi}/\sqrt{2}$ and $A = I^{(0)}$.

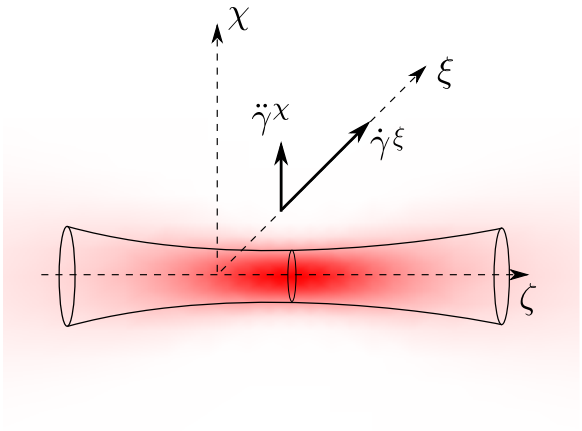

Figure 1.3: Schematic illustration of the frame-dragging effect: A massive particle moving radially outwards from the beamline, here in ξ-direction with the velocity $\dot{\gamma}^{\xi}$, is accelerated in the transverse direction, here in χ-direction with the acceleration $\ddot{\gamma}^{\chi}$. The worldline of the particle is described by the curve γ and parametrized with proper time.

As an example, for a particle moving radially outwards in ξ-direction with a velocity $v \sim 10\,\mathrm{m/s}$ from the location $x = w_0$, $y = 0$ and $z = 0$ and for a power of the laser beam $P_0 \sim 10^{15}\,\mathrm{W}$, a beam-divergence angle $\theta \sim 10^{-3}$, a beam waist $w_0 \sim 10^{-3}\,\mathrm{m}$, the acceleration is given by $d^2\gamma^y/dt^2 \sim \pm 10^{-29}\,\mathrm{m/s^2}$, where γ is the worldline of the particle.

Deflection of parallel co-propagating light rays

Interestingly, for any light beam described in the short-wavelength approximation, a test light-ray propagating parallel to the source light-beam and in the same direction is not deflected, while any other test light-ray is deflected (Appendix B3). This is not true for the laser beam when it is described beyond the short-wavelength approximation - intuitively, it is clear that the parallel co-propagating test light-ray should be deflected: As the laser beam has an opening angle, one can think of it as a bundle of not exactly parallel light rays. Then, the parallel co-propagating test light-ray is not parallel to the rays in this bundle and gets deflected. Another argument is based on the observation that the parallel co-propagating test light-ray is only not deflected from the source light-beam described in the short-wavelength approximation when the latter propagates at the speed of light (Model 7 in Appendix B2). It is clear intuitively, as locally the energy flow in the laser beam is not parallel to the beamline, and was shown both theoretically [7] and experimentally [8] that the laser beam moves slower than the speed of light. This means that the parallel co-propagating test light-ray should be deflected.
Indeed, we find a deflection of the parallel co-propagating light ray in the fourth order of our expansion in the beam-divergence angle θ: From the geodesic deviation equation, we find that the relative acceleration between two nearby geodesics is given by

$$a^{\xi} = -\frac{GP_0\theta^4}{16\pi w_0^2 c^3} e^{-2\rho^2} \left(\rho^2(4\xi^2+3) - 6\xi^2\right) \ , \tag{1.10}$$

where for simplicity we gave the expression for the region where $\theta\zeta \ll 1$. The deflection is schematically illustrated in Figure 1.4.

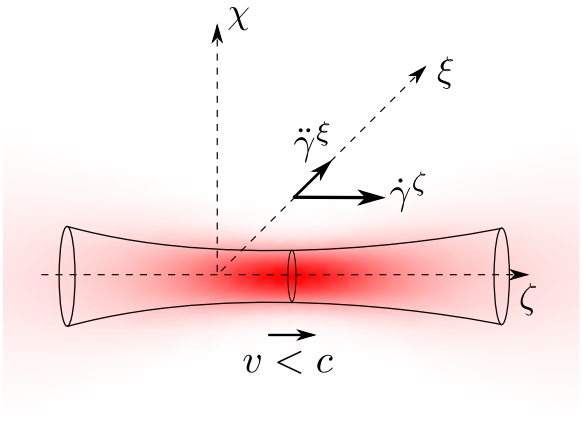

Figure 1.4: Schematic illustration of the deflection of a parallel co-propagating light ray. The parallel co-propagating light ray, described by the tangent $\dot{\gamma}^{\zeta}$, is radially deflected; it has the acceleration $\ddot{\gamma}^{\xi}$ (at $\chi = 0$).

As a numerical example, for a power of the source laser-beam $P_0 \sim 10^{15}\,\mathrm{W}$, a beam-divergence angle $\theta \sim 10^{-3}$, a beam waist $w_0 \sim 10^{-3}\,\mathrm{m}$ and at the location $x = w_0$ and $y = 0$, the acceleration towards the beamline between two nearby geodesics is given by $a^x \sim -10^{-31}\,\mathrm{m/s^2}$.
The deflection decays in the same way as the energy-distribution of the laser beam, as a Gaussion with the distance to the beamline of the laser beam. This means that the parallel co-propagating test light-ray is only deflected when it propagates within the energy-distribution of the laser beam. In our article we show that this is in contrast to the deflection of a test light-ray in the gravitational field of a massive cylindrical rod which moves at the propagation speed of the laser beam, as in this case the parallel co-propagating test light-ray is deflected when propagating in the exterior of the massive rod. This shows that focussed light and massive matter moving at the same speed do not have the same gravitational properties.
Our result reveals that contrarily to the statements made in the short wave-length approximation, the parallel co-propagating light ray is deflected when using an accurate description of the source laser-beam which takes into consideration the wave-like nature of light and respects Maxwell's equations.

Chapter 2

Rotation of Polarization - Faraday Effect and Optical Activity

The electromagnetic Faraday effect describes the rotation which the polarization of light obtains when propagating in an electromagnetic field. The Faraday effect is non-reciprocal; the effect does not cancel when the light propagates back and forth along the same path. Additionally, there is a reciprocal rotation of the polarization of light due to the optical activity. The analogy between the Maxwell equations in an electromagnetic field and in a curved spacetime suggests that there is a gravitational analogue for the electromagnetic Faraday effect and the rotation due to the optical activity. Indeed, it was shown that the gravitational rotation of polarization of light occurs in spacetimes that are stationary and non-static [9]. These are spacetimes for which there exists a coordinate-system such that all components of the metric tensor are time-independent, but there exists no such coordinate system such that the metric components that mix time and space vanish. The gravitational field of the laser beam satisfies these conditions (Section 1.1). The gravitational rotation of the polarization of light was first studied by Skrotsky [10] and by Balazs [11], and later a coordinate-invariant description for the change of the polarization for a light ray coming from flat spacetime, passing through a weak gravitational field, and going to flat spacetime again was found by Plebanski [12]. The gravitational rotation of polarization of light was studied for several systems: for moving gravitational lenses [13, 14, 15], in astrophysics [16, 17], in the context of gravitational waves [18], for a rotating ring [19] and for a ring laser [20]. It was also treated more formally in [21, 22, 23].

In this chapter we describe the rotation of polarization of a light ray propagating in the gravitational field of a long laser beam [D]. We identify the non-reciprocal contribution to the rotation as the gravitational Faraday effect and the reciprocal contribution as the gravitational analogue of the optical activity. Notice that a strict analogy is only present when the contribution of the outward propagation of the light ray is the same as the contribution of the backward propagation. In the first section we explain the result [12] which we use to calculate the rotation angle. Its application to test light-rays propagating in the gravitational field of the laser beam is explained in the second section. As the gravitational Faraday effect is non-reciprocal, it adds up when a test light-ray propagates back and forth a cavity consisting of two mirrors. On the other hand, as the gravitational analogue of optical activity is reciprocal, a ring cavity can be used to obtain the gravitational optical activity as the leading order contribution. This is discussed in the third section, where we also give a bound on the possible measurement precision.

For the plots and numerical examples we choose the power $P_0 = 10^{15}\,\mathrm{W}$, the beam waist $w_0 = 10^{-6}\,\mathrm{m}$, the beam divergence $\theta = 0.3$ (this implies that the wavelength is given by $\theta\pi w_0 \simeq 10^{-6}\,\mathrm{m}$) and the polarization $\lambda = 1$ and consider the parallel light rays to be at $\chi = 0$ and the orthogonal light ray to propagate in ξ-direction and to be at $\chi = 0.1$.

2.1 Rotation of polarization

Both the Faraday effect and the optical activity rotate the polarization vector within the plane of polarization, which is always perpendicular to the tangent to the path of the light ray. When the light ray is deflected, the plane of polarization is tilted such that it is again orthogonal to the tangent to the path of the light ray. This results in an additional change $\delta\vec{\omega}$ of the polarization vector $\vec{\omega}$. The change $\delta\vec{\omega}$ depends on the initial polarization $\vec{\omega}$ of the light ray,[1] is not within the plane of polarization and does not contribute to the gravitational Faraday effect nor to the gravitational optical activity. The rotation angle for these two effects for the rotation within the plane of polarization is derived using the formal analogy of Maxwell's equations in a dielectric medium and in a gravitational field, and using geometric ray optics [12]. For a light ray starting and ending in flat spacetime, it is given by [12]

$$\Delta = \frac{1}{2w_0^2}\int_{-\infty}^{\infty} d\tau\, \dot{\gamma}^a \epsilon_{abc}\partial_b h_{\alpha c}\dot{\gamma}^\alpha\,, \tag{2.1}$$

where $\dot{\gamma}^\alpha$ is the tangent to the path of the light ray parametrized by proper time τ and ϵ_{abc} is the Levi-Civita tensor with $\epsilon_{abc} = 1$. The positive sign refers to right-handedness. The rotation of polarization Δ and the change of polarization $\delta\vec{\omega}$ are illustrated in Figure 2.1.

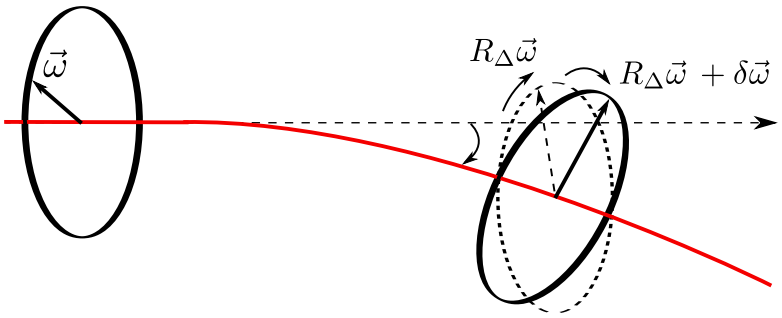

Figure 2.1: Change of the initial polarization vector $\vec{\omega}$ of a light ray γ: The initial polarization vector $\vec{\omega}$ in the plane orthogonal to the tangent of the light ray is rotated within this plane by the angle Δ into $R_\Delta\vec{\omega}$ (dashed arrow on the right) due to the gravitational field, where R_Δ is the corresponding rotation matrix. In addition, this plane is tilted due to the deflection of the laser beam (solid circle on the right), such that it is orthogonal to the tangent of the light ray. This leads to an additional change $\delta\vec{\omega}$ of the polarization vector. The rotation about the angle Δ is due to the gravitational Faraday effect and the gravitational optical activity.

The above result can be applied when the metric perturbation and its first derivatives vanish as $(\sqrt{\xi^2+\chi^2+\zeta^2})^{-1}$ for $\sqrt{\xi^2+\chi^2+\zeta^2} \to \infty$. It is invariant under coordinate transformations that approach the identity at spatial infinity.

[1] The explicit expression is given in Sec. 6 in [12].

The interpretation of the rotation is the following: The polarization vector $\vec{\epsilon}_\xi = (1,0,0)$ describing linear polarization in ξ-direction is rotated into $R_\Delta \vec{\epsilon}_\xi = \big(\cos(\Delta), \sin(\Delta), 0\big)$, where R_Δ is the matrix rotating by the angle Δ. The polarization vector $\vec{\epsilon}_{\lambda_{\text{test}}} = \frac{1}{\sqrt{2}}(1, -\lambda_{\text{test}} i, 0)$ for a test light-ray with circular polarization with helicity $\lambda_{\text{test}} = \pm 1$ becomes $R_\Delta \vec{\epsilon}_{\lambda_{\text{test}}} = e^{i\lambda_{\text{test}}\Delta}\vec{\epsilon}_{\lambda_{\text{test}}}$; the circularly polarized test light-ray obtains the phase $\lambda_{\text{test}}\Delta$.

2.2 Test light-rays

In this section, we look at infinitely long test light-rays and a finitely long source laser-beam. A test light-ray propagating parallel to the source laser-beam is described by the tangent vector $\dot{\gamma}^\alpha_\pm = \frac{c}{w_0}\big(1,0,0,\pm 1\big)$, where the "+" corresponds to the parallel co-propagating and the "−" to the parallel counter-propagating test light-ray.[2] The corresponding rotation angle for the parallel propagating light rays is given by

$$\Delta_\pm = -\frac{1}{2w_0^2}\int_{-\infty}^{\infty} d\zeta \Big(\partial_\chi \left(h_{\xi\zeta} \pm h_{\tau\xi}\right) - \partial_\xi \left(h_{\chi\zeta} \pm h_{\tau\chi}\right)\Big)\,, \tag{2.2}$$

where $h_{\alpha\beta}$ is the metric perturbation (1.5) introduced in Chapter 1. The rotation of polarization for the parallel co-propagating test light-ray is illustrated schematically in Figure 2.2 and the value of the rotation angle is plotted in Figure 2.3 for the parallel test rays.

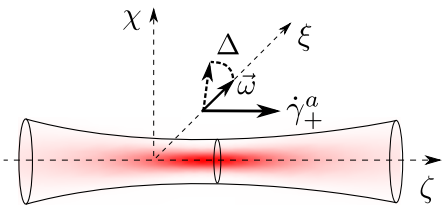

Figure 2.2: Schematic illustration of the rotation of the polarization vector $\vec{\omega}$ (here it originally has only a component in the ξ-direction) of a parallel co-propagating test light-ray with tangent $\dot{\gamma}^\alpha_+$ in the gravitational field of the laser beam.

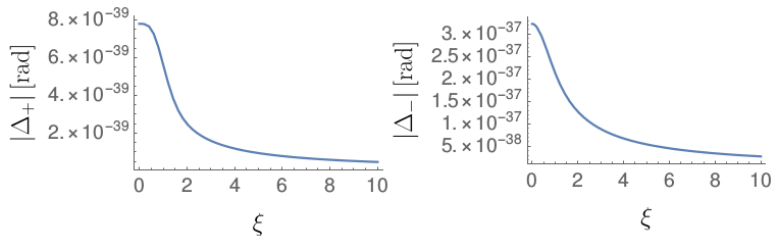

Figure 2.3: The absolute value of the rotation angle for the parallel co-propagating and the parallel counter-propagating test light-rays, Δ_+ and Δ_-, as a function of the orthogonal distance ξ from the beamline and for the parameter values specified in the introduction.

[2] To ensure the null condition, and taking into account the deflection of the parallel counter-propagating test light-ray, the tangents to the parallel and the anti-parallel test light-rays read $\dot{\gamma}^\alpha_\pm = \frac{c}{w_0}\big(1, \epsilon^\pm_\xi, \epsilon^\pm_\chi, \pm(1 - f^\pm)\big)$, where $\epsilon^\pm_\xi$, $\epsilon^\pm_\chi$ and $f^\pm$ are of the same order as the metric perturbation and turn out to be negligible in the calculation.

We also consider an orthogonal test light-ray which propagates in ξ-direction. Its tangent reads[3] $\dot{\gamma}_{\pm} = \frac{c}{w_0}\big(1, \pm 1, 0, 0\big)$. The rotation angle for the transversally propagating light ray is given by

$$\Delta_{t^{\pm}} = \pm \frac{1}{2w_0^2} \int_{-\infty}^{\infty} d\xi \, \partial_\chi h^{(0)}_{\tau\zeta} - \frac{\theta}{2w_0^2} \int_{-\infty}^{\infty} d\xi \, \partial_\chi h^{(1)}_{\tau\xi} \, , \tag{2.3}$$

where we gave the result up to the first order in the metric perturbation.
The rotation angle Δ turns out to depend on the helicity λ of the source laser-beam. As the rotation angle is equivalent to the phase $\lambda_{\text{test}}\Delta$ for the circularly polarized light ray, it contains terms proportional to $\lambda\lambda_{\text{test}}$. This product is positive if the source beam and the test light-ray have the same helicity, and negative if they have opposite helicity. This means that the phase depends on the relative helicity of the two beams, which is gravitational spin-spin coupling. With our analysis and using only classical general relativity, we thus find a phenomenon which appears in perturbative quantum gravity.
Equations (2.2) and (2.3) give the rotation angle due to the gravitational Faraday effect and the gravitational optical activity. The contribution from the gravitational Faraday effect, which is the non-reciprocal part, is (in leading order) given by[4]

$$\Delta^F_{+-} = \Delta_+ - \Delta_- = -\frac{\theta}{w_0^2} \int_{-\infty}^{\infty} d\zeta \Big(\partial_\chi h^{(1)}_{\tau\xi} - \partial_\xi h^{(1)}_{\tau\chi} \Big) \, , \tag{2.4}$$

for one forth- and back-propagation of a light ray propagating parallel to the source laser-beam, and by

$$\Delta^F_{t^+t^-} = \Delta_{t^+} - \Delta_{t^-} = \frac{1}{w_0^2} \int_{-\infty}^{\infty} d\xi \, \partial_\chi h^{(0)}_{\tau\zeta} \, , \tag{2.5}$$

for one forth- and back-propagation for a light ray propagating transversally to the source laser-beam. The reciprocal contribution to the rotation angle is the gravitational analogue of optical activity. It is (in leading order and for the propagation in one direction) given by

$$\Delta^{OA}_{+-} = \frac{\Delta_+ + \Delta_-}{2} = -\frac{\theta}{2w_0^2} \int_{-\infty}^{\infty} d\zeta \Big(\partial_\chi h^{(1)}_{\xi\zeta} - \partial_\xi h^{(1)}_{\chi\zeta} \Big) \, , \tag{2.6}$$

for the parallel light rays, and by

$$\Delta^{OA}_{t^+t^-} = \frac{\Delta_{t^+} + \Delta_{t^-}}{2} = \frac{\theta}{2w_0^2} \int_{-\infty}^{\infty} d\xi \, \partial_\chi h^{(1)}_{\xi\zeta} \, , \tag{2.7}$$

for the transversal light rays.
For light beeing emitted from or passing through a rotating spherical body [10, 11] or a rotating shell [16], it has been shown that the rotation angle for the polarization decreases with the inverse of the square of the distance to the rotating object. If however the light is only passing by these objects or any other stationary object, the polarization of the light is not rotated [9, 24]. The statement is not true if the objects are in motion; then the rotation of polarization is non-zero (see [15] for a moving point mass, [14, 9] for moving gravitational lenses, [13] for a moving Schwarzschild object and [12] for moving stars).

[3] Again in order to satisfy the null-condition and taking into account the deflection of the light ray, the tangent reads $\dot{\gamma}_{\pm} = \frac{c}{w_0}\big(1, \pm(1 - f^{\pm}), \epsilon^{\pm}_\chi, \epsilon^{\pm}_\zeta\big)$, where $\epsilon^{\pm}_\chi$, $\epsilon^{\pm}_\zeta$ and $f^{\pm}$ are of the order of magnitude of the metric perturbation and turn out to be negligible in the calculation.

[4] As the rotation angle is defined with respect to the propagation direction, the absolute rotation accumulated on the way back and forth is given by the difference between the rotation angle acquired during the propagation in the two directions.

Even though the laser beam's spacetime metric is stationary, it consists of an energy-distribution in motion. Therefore, our results agree with the literature in the sense that the rotation of polarization should be non-zero.
For parallel test rays, we find that the effect decreases with the inverse of the distance to the beamline of the source beam if there is an overlap between the test ray and the source beam's region of largest intensity,[5] and falls off with a Gaussian factor with the distance to the beamline if there is no overlap between the test ray and the source beam's region of largest intensity. Instead, for transversal test rays, the effect always decays with the inverse of the distance to the beamline. Even though formula (2.1) is not strictly applicable, the test ray and the source beam can under some conditions both be considered as finitely or infinitely extended. Then, the results are slightly different.

2.3 Cavities

Letting light propagate back and forth between two mirrors, the Faraday effect adds up, since it is non-reciprocal. On the other hand, the reciprocal effect associated to the gravitational optical activity cancels. The latter can be obtained as the leading order accumulating effect when using a certain ring cavity.
In order to magnify the Faraday effect, we consider a cavity consisting of two mirrors at locations $\zeta = \mathcal{A}$ and $\zeta = \mathcal{B}$, between which the light propagates, as illustrated in Figure 2.4. Orienting the cavity such that its axis is parallel to the beamline of the source laser-beam, the light travels undeflected up to the third order in θ from $\mathcal{A}$ to $\mathcal{B}$ and obtains a deflection of zeroth order when propagating back, which vanishes when the light ray propagates at the center of the source laser-beam. When placing the cavity at a slightly larger distance from the beamline of the source laser-beam, the Faraday effect becomes smaller. When the light propagates during the time $\tau = LF/(\pi c)$, where F is the finesse of the cavity, the total angle of rotation is given by $\Delta_p^F = F\Delta_{+-}^F/(2\pi)$. For a finesse $F = 10^6$ [25], and the parameters given in the introduction, the rotation angle is of the order of magnitude $\Delta_p^F \sim 10^{-32}$ rad. Rotating the cavity by ninety degrees (Figure 2.4), the accumulating angle is given by $\Delta_t^F = F\Delta_{t+t-}^F/(2\pi)$. For the same finesse and the same measuring time, it is also of the order of magnitude $\Delta_t^F \sim 10^{-32}$ rad.

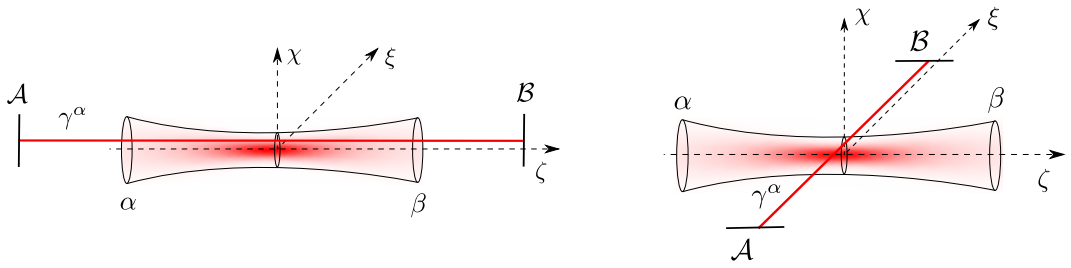

Figure 2.4: Schematic illustration of the parallel (left) and the orthogonal (right) cavity in the gravitational field of the laser beam: The laser beam starts at α and ends at β. The test light-ray propagates on the worldline γ^α between the mirrors of the cavity, $\mathcal{A}$ and $\mathcal{B}$. The Faraday rotation adds up after each roundtrip, while the rotation associated to the gravitational optical activity vanishes.

[5] The region of the source beam's largest intensity can be defined by a drop of the intensity by a factor e^{-2}. Then, this region has a radius $w(\zeta) = \sqrt{1 + (\theta\zeta)^2}$.

Using a ring cavity, it is possible to have the rotation due to the optical activity as the leading order effect which accumulates. Considering the ring cavity as in Figure 2.5, where again the mirrors are far enough away from the beamline or the beam waist, the polarization vector is rotated when the light propagates from $\mathcal{A}$ to $\mathcal{B}$, but not when it propagates from $\mathcal{B}$ to $\mathcal{C}$ to $\mathcal{D}$ to $\mathcal{A}$. If we choose the light ray between $\mathcal{A}$ and $\mathcal{B}$ to be propagating at $\chi = 0$, it turns out that the gravitational Faraday effect vanishes and the gravitational rotation of polarization is purely due to the gravitational analogue of optical activity. The accumulated rotation angle is of the order of magnitude $\Delta_t^{OA} \sim 10^{-33}\,\mathrm{rad}$.

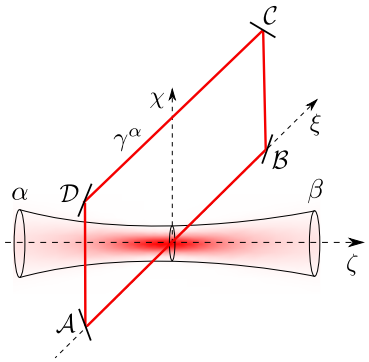

Figure 2.5: Schematic illustration of the ring cavity: The test light-ray propagates along the path γ^α and is reflected at the mirrors $\mathcal{A}$, $\mathcal{B}$, $\mathcal{C}$ and $\mathcal{D}$. The laser beam is emitted at $\zeta = \alpha$ and absorbed at $\zeta = \beta$.

Since for the circularly polarized light rays the rotation angle is equivalent to a phase, the precision of the measurement of the rotation angle is restricted by the shot noise. Using classical light, the minimal uncertainty of the estimation of the phase $\phi = \lambda_{\mathrm{test}}\Delta$ is of the order of magnitude of $\delta\phi \sim 1/\sqrt{nM}$, where n is the number of photons in the cavity and M the number of measurements [26]. If the cavity has the finese F and length L and is driven by a laser with frequency $\omega/(2\pi)$ and power P_{dr}, the number of photons inside the cavity is given by $n = P_{\mathrm{dr}}FL/(\pi\hbar\omega c)$, and the average time a photon is inside the cavity is found to be $T_{\mathrm{av}} = LF/(2\pi c)$. In the time T, $M = T/T_{\mathrm{av}}$ measurements can be made. Therefore, it follows that $\delta\phi \sim \sqrt{\hbar\omega/(2P_{\mathrm{dr}}T)}$. Using a cw-laser with the power $P_{\mathrm{dr}} = 100\,\mathrm{kW}$ [27] with a wavelength of 500 nm and measuring during $T = 10^6\,\mathrm{s}$ (approximately two weeks), the minimal standard deviation scales as $\delta\phi \sim 10^{-15}\,\mathrm{rad}$. The same order of magnitude is obtained when using a squeezed state and using quantum metrology (Appendix C) for the analysis.

Chapter 3

Resonance Frequency of an Optical Resonator in a Curved Spacetime

In this chapter we explain our work on the influence of a gravitational field on the frequency spectrum of an optical resonator [B]. While in the previous chapter light was the source of the gravitational field, in this chapter it will only be the tool to probe the effects of a given gravitational field, serving as test rays. The resonator is modelled as a rod with two mirrors attached at its ends, between which the light is propagating back and forth. In flat spacetime, it is clear how to describe the resonance frequency of the resonator: It is defined as one of the harmonics, which are determined by the length of the resonator. When the resonator is in a gravitational field, this concept needs to be changed, as in general relativity, being a local theory, the meaning of length of an extended object is not a priori clear. It turns out that the radar length has to be used in order to describe the resonance frequency, which is defined in an operational way by an observer: The observer sends out a light signal, measures the duration it takes to come back and infers the distance from it. This makes it evident that the resonance frequency is observer-dependent. Compared to a resonator in flat spacetime, there is another difficulty with the resonator in a gravitational field: While in flat spacetime it is possible to describe the resonator by a rigid rod, this is more complicated in curved spacetime. Strictly speaking, perfectly rigid objects do not exist. We use the concept of "Born rigidity", where the proper length between two segments of the rod is kept constant, as a first model of the resonator. In a second model, the resonator is deformable: It consists of thin segments which are accelerated in the gravitational field but stick together due to the material forces. The resonance frequency in curved spacetime thus deviates from its definition in flat spacetime for two reasons: First, for the concept of length the observer-dependent radar length is used, and second, the resonator deforms in the gravitational field.

Through the dependence of the frequency spectrum on the gravitational field, it is possible to determine the curvature of spacetime by performing a frequency measurement. This is important for example for the measurement of gravitational waves with electromagnetic resonators [28, 29, 30], tests of general relativity, or the measurement of the expansion of the universe. Also, the influence of the gravitational field on the frequency spectrum can be seen as a limitation of the precision of frequency measurements in the presence of a gravitational field, which has to be taken into account.

In the first section of this chapter, we explain how to describe a resonator in a gravitational field. Its frequency spectrum is determined in the second section. The result is applied to three examples in the third section.

3.1 Resonator in a Gravitational Field

The resonator consists of single segments. To these segments belongs a worldline, which allows to construct spatial geodesics representing the rod. We will explain this in the first subsection, while in the second subsection, we introduce the proper detector frame, a locally inertial frame for an observer. This will simplify the calculations for the subsequent discussions.

Describing the Resonator

We start by describing the resonator in a gravitational field or under acceleration. The resonator consists of a rod with two attached mirrors (Figure 3.2). The rod is constructed using worldlines and spatial geodesics: Each segment of the resonator is characterized by a worldline $\gamma_\varsigma(\varrho)$ with $\varsigma \in [a, b]$, where $\gamma_a(\varrho)$ and $\gamma_b(\varrho)$ are the worldlines of the mirrors A and B located at $\varsigma = a$ and $\varsigma = b$ respectively. The parameter ϱ is chosen such that the curves $s_\varrho(\varsigma) = \gamma_\varsigma(\varrho)$ are space-like geodesics.[1] To each worldline of the segments, which is a time-like curve, we associate a spatial slice defined by the vectors that are orthogonal to the worldline. In this spatial slice lie the tangents to the space-like curve $s_\varrho(\varsigma)$. This construction is illustrated in Figure 3.1.

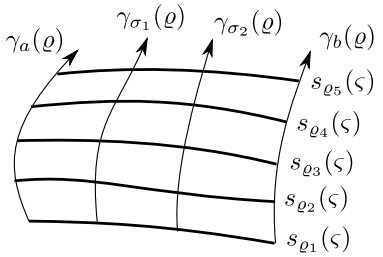

Figure 3.1: Representation of the rod by space-like and time-like curves: The space-like curves $s_\varrho(\varsigma)$ represent the rod. They are orthogonal to the time-like curves $\gamma_\varsigma(\varrho)$ that represent the worldline of the segments of the rod.

The rod is additionally accelerated, in the sense that the rod has a support on which the non-gravitational acceleration (the spatial part of the proper acceleration with respect to a local freely falling frame at the location of the observer) $\vec{a}$ is exerted.[2] In terms of the proper length L_p of the rod, the support is at a distance $\beta L_p/2$ from the center of the rod, where $\beta \in [-1/2, 1/2]$. Later, when we consider an observer performing a measurement, the observer will do so at a distance $\sigma L_p/2$ from the center, where $\sigma \in [-1/2, 1/2]$. The resonator is illustrated in Figure 3.2.

[1] With this choice, the world lines $\gamma_\varsigma(\varrho)$ do not need to be geodesics; the parameter ϱ is not assumed to be the proper time of the segments.

[2] We do not consider rotation of the resonator, as this effect leads to higher order terms in the eikonal expansion for the light field inside the cavity, which we neglect in our description.

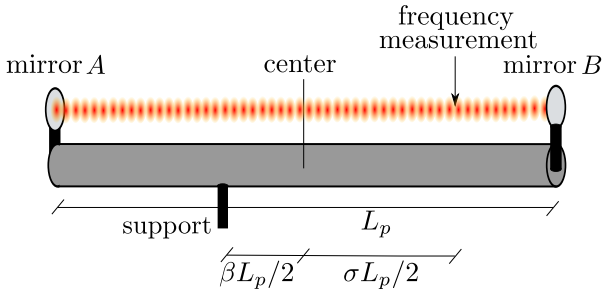

Figure 3.2: Illustration of the resonator: The mirrors A and B are attached to the beginning and the end of the rod. The rod is supported at a distance $\beta L_p/2$ from the center of the rod, and an observer performs a measurements at a distance $\sigma L_P/2$ from the center of the rod.

Proper Detector Frame

The proper detector frame is the natural frame for an observer: It is a locally inertial frame in the neighbourhood of an observer in a gravitational field under acceleration. This means that close to the worldline of an observer, the time coordinate is the proper time of the observer and the coordinate distance is the proper distance. The proper detector frame is thus a generalization of the Fermi normal coordinates, which are locally inertial coordinates in the neighbourhood of a geodesic.

The proper detector frame is obtained by constructing a tetrad consisting of a time-like and three space-like vectors, where the time-like vector corresponds to the tangent vector to the worldline of the observer. The metric in the proper detector frame [31, 32] for vanishing rotation, small acceleration $\vec{a}$ and small curvature (in the proper detector frame) reads

$$g^P_{00}(\mathbf{x}) = -\left(1 + \frac{2}{c^2} a_J(\tau) x^J + R_{0I0J}\left(\gamma(\tau)\right) x^I x^J\right) , \tag{3.1}$$

$$g^P_{0J}(\mathbf{x}) = -\frac{2}{3} R_{0KJL}\left(\gamma(\tau)\right) x^K x^L , \tag{3.2}$$

$$g^P_{IJ}(\mathbf{x}) = \delta_{IJ} - \frac{1}{3} R_{IKJL}\left(\gamma(\tau)\right) x^K x^L , \tag{3.3}$$

where R_{IJKL} is the Riemann curvature tensor, $\gamma(\tau)$ the worldline and τ the proper time of the observer. The construction of the proper detector frame is illustrated in Figure 3.3. For the validity of the proper detector frame, the gravitational field can vary only slowly. We make the assumption that it varies slowly enough such that during the time the light needs to make one round trip inside the cavity, the curvature can be considered as constant in time. The linearization of the metric in the proper detector frame is possible when the gravitational field varies only slowly; the gravitational field does not need to be weak.

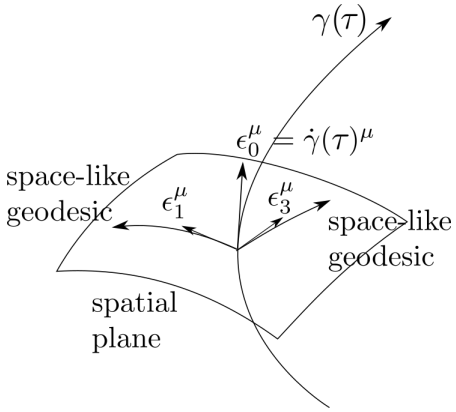

Figure 3.3: Construction of the proper detector frame: For a worldline of an observer $\gamma(\tau)$, one defines a tetrad by ϵ_0^μ, which is the tangent to the worldline, and three spatial vectors ϵ_J^μ, with $J = 1, 2, 3$. This tetrad gives rise to a coordinate system in which the coordinate time along the worldline corresponds to the proper time of the observer, and in a neighbourhood of the worldline, the coordinate distance corresponds to the proper distance.

3.2 Frequency Spectrum in a Gravitational Field

One can expect the definition for the resonance frequency in flat spacetime, $\omega_n = cn\pi/L$, to have a similar form in curved spacetime, with the length L replaced by some well-defined quantity in general relativity. In this section, we show that this is the case, and explain the concept of length which gives an appropriate replacement for L.
The resonance frequency of the cavity ω_n corresponding to the n^{th} mode of the light is determined by $\psi_n = \omega_n T$, where ψ_n is the phase with which the n^{th} mode evolves and T is a time difference measured by an observer. Therefore, the time difference is observer-dependent, while the phase is not, making it already clear that the resonance frequency will depend on the observer who measures it. In order to determine the resonance frequency, one thus needs to know the evolution of the phase. This could be done by solving the Maxwell equations in the curved background. Instead of doing so, we choose to describe the light inside the cavity in the short-wavelength approximation, which allows us to find the phase difference of the left- and the right-moving part of a standing light wave inside the resonator. Using the short-wavelength approximation restricts the validity of our results to the high frequency modes; for the lower modes, the short-wavelength approximation breaks down.
Doing so, one finds that a meaningful notion of distance in the formula $\omega_n = cn\pi/L$ is the radar length $\mathcal{R}_{\gamma_\sigma}$, which is the distance determined by an observer by sending back and forth a light signal and measuring the time duration T_{γ_σ} the light takes to travel. The radar distance is given by $\mathcal{R}_{\gamma_\sigma} = \frac{c}{2} T_{\gamma_\sigma}$. Thus, the frequency spectrum reads

$$\omega_{\sigma,n} = \frac{cn\pi}{\mathcal{R}_{\gamma_\sigma}} \,. \tag{3.4}$$

To ensure that we only consider wavelengths much shorter than the resonator and that the short-wavelength approximation is justified, we need the restriction $n \gg 1$. In the following sections, we will calculate the resonance frequency explicitly for both a rigid and a deformable cavity.

Born Rigid Resonator

We start by describing the resonance frequency for a rigid resonator, i.e. a resonator as in Figure 3.2 with a rigid rod to which the mirrors are attached. Strictly speaking, rigid objects do not exist in general relativity. What we call rigid in the following is thus rigidity as defined by Born [4]: The proper length between any two segments of the rod is kept constant when measured along a spatial geodesic defined by either of the two worldlines of the segments.[3]

As the resonance frequency depends on the radar length, we need to determine the latter: To do so, we consider that the observer sends out a light signal, which satisfies the null condition $g^P_{\mu\nu}\big(\xi(\iota)\big)\dot{\xi}^\mu(\iota)\dot{\xi}^\nu(\iota) = 0$ and the geodesic equation $\ddot{\xi}^\mu(\iota) = -\Gamma^{P\mu}_{\nu\delta}\big(\xi(\iota)\big)\dot{\xi}^\mu(\iota)\dot{\xi}^\nu(\iota)$, from which one obtains an expression for the tangent vectors to the path of the light ray. Integrating over them, one finds the difference in proper time of the observer which the light ray needs for one roundtrip, and from it the radar distance. One obtains for the resonance frequency

$$\omega_{\sigma,n} = \frac{cn\pi}{L_p}\left(1 - \frac{a^z(\tau)}{2c^2}\sigma L_p - \frac{R_{\tau z\tau z}\big(\gamma(\tau)\big)}{24}\left(3\sigma^2 + 6\sigma\beta - 1\right)L_p^2\right) . \tag{3.5}$$

The first term in the bracket is the resonance frequency one obtains in flat spacetime. The second term is a redshift due to the acceleration of the support of the cavity. Due to symmetry reasons, it vanishes if the observer makes the measurement in the center of the cavity. The third term is a gravitational redshift. In curved spacetime, it is always there; only parts of it vanish if the measurement is done at the center of the rod or if the rod is supported at its center. Summarized, the resonance frequency of the Born rigid resonator consists of the resonance frequency one obtains in flat spacetime (first term) plus corrections depending on the acceleration, the curvature, the location of the measurement and the location of the support of the resonator.

Deformable Resonator

In this section we describe the frequency spectrum of an optical resonator which is deformed due to a gravitational field. The rod of the resonator is modeled as sequence of segments that would follow geodesics due to the gravitational field, but are hold back by material forces between the segments.

The segments are assumed to have density ρ and crosssection A. The acceleration of a segment at rest in the gravitational field is given by the geodesic equation $\ddot{\gamma}^\mu_{\text{rest}} = -\Gamma^{P\mu}_{\sigma\rho}\dot{\gamma}^\sigma_{\text{rest}}\dot{\gamma}^\rho_{\text{rest}}$, and in our case the acceleration is approximately equal to the the proper acceleration a^μ_P. The acceleration leads to a force $F^z = ma^z_P$ acting on the segments.[4] The force induces a stress in the material, $\sigma_{zz} = F^z/A = \rho L_p a^z_P$, which is linked to strain ϵ_{zz} via the Young's modulus Y by $\epsilon_{zz} = \sigma_{zz}/Y$. The change of proper length of the rod due to these deformations is given by integrating over the strain at every location of the resonator. Incorporating the change of proper length in the expression for the resonance frequency of the rigid resonator (3.5), one obtains

$$\omega_{\sigma,n} = \frac{cn\pi}{L_p}\left(1 + \frac{a^z(\tau)}{2c^2}\left(\frac{c^2}{c_s^2}\beta - \sigma\right)L_p + \frac{R_{\tau z\tau z}\big(\gamma(\tau)\big)}{24}\left(2\frac{c^2}{c_s^2}\left(3\beta^2+1\right) - 3\sigma^2 - 6\sigma\beta + 1\right)L_p^2\right) , \tag{3.6}$$

[3] As any other definition of rigidity, the definition by Born has an issue: The motion of a Born rigid object is completely defined by one of its points, which means that the body cannot be accelerated or put into rotation without violating causality [33, 34].

[4] The forces transversal to the rod turn out to be negligible.

where we replaced the Young's modulus with the speed of sound in the material c_s according to $c_s = \sqrt{Y/\rho}$.

This description of a deformable rod is consistent with the result for the deformable resonator: Letting the speed of sound approach infinity, the change in proper length vanishes and one recovers the frequency spectrum of the rigid resonator given in equation (3.5). Letting the speed of sound approach the speed of light, the resonance frequency agrees with the result one obtains with the definition of rigidity given in [35].

As an example we look at carbyne, which is a stiff material and has a very high Young's modulus. In this case, the speed of sound is $c_s^2 = Y/\rho \sim 10^9\,\mathrm{m}^2/\mathrm{s}^2$. Therefore, the ratio $c^2/c_s^2 \sim 10^8$ is large, which means that the effect due to the change of the proper length is dominating the effect due to the curvature of the spacetime and the acceleration of the cavity. As the speed of sound in the stiffest materials is much smaller than the speed of light, this observation remains valid for all materials. The effects due to the curvature and the acceleration become relevant once the deformation effects are taken into account and the frequency spectrum needs to be determined to a precision of the order of magnitude of the redshift effects due to curvature and acceleration.

Dielectric Rod as Resonator

The resonator can also be modeled as a cylinder of a dielectric media in which light is propagating and reflected at the rod's ends, as illustrated in Figure 3.4.

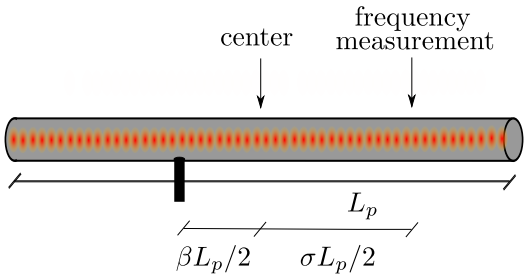

Figure 3.4: Illustration of the resonator consisting of a cylinder of a dielectric medium: The light propagates inside the medium and is reflected at the ends of the resonator. Again, the resonator has the proper length L_p, the support lies at a distance $\beta L_p/2$ from the center of the resonator, and the observer performs the measurement at the distance $\sigma L_p/2$ from the center of the resonator.

The metric tensor for the proper detector frame inside the dielectric medium is given by [36, 37]

$$g^{P,\mathrm{diel}}_{\mathcal{MN}} = g^{P}_{\mathcal{MN}} - \left(\frac{c^2_{\mathrm{diel}}}{c^2} - 1\right) u_{\mathcal{M}} u_{\mathcal{N}}\,, \tag{3.7}$$

where c_{diel} is the speed of light inside the medium and $u^{\mathcal{M}}$ the tangent vector to the worldline of a segment of the rod. For the metric in the proper detector frame one obtains

$$g_{00}^{P,\text{diel}}(\mathbf{x}) = -\frac{c_{\text{diel}}^2}{c^2}\left(1 + \frac{2}{c^2}a_J(\tau)x^J + R_{0I0J}(\tau)x^I x^J\right) , \tag{3.8}$$

$$g_{0J}^{P,\text{diel}}(\mathbf{x}) = -\frac{2}{3}\frac{c_{\text{diel}}^2}{c^2}\, R_{0KJL}(\tau)x^K x^L , \tag{3.9}$$

$$g_{IJ}^{P,\text{diel}}(\mathbf{x}) = \delta_{IJ} - \frac{1}{3}R_{IKJL}(\tau)x^K x^L . \tag{3.10}$$

The calculations for the resonance frequency can be done analogously, and one finds that it differs by a factor c_{diel}/c from the results for the resonator consisting of a rod with attached mirrors, where the light is propagating in free space,

$$\omega_{\sigma,n}^{\text{diel}} = \frac{c_{\text{diel}}}{c}\omega_{\sigma,n} . \tag{3.11}$$

3.3 Applications

The result for the resonance frequency is valid in any gravitational field which is varying slowly enough such that the proper detector frame can be used, and for high enough frequencies of the light inside the resonator such that the short-wavelength approximation can be used. In this section we apply the results to a uniformly accelerated resonator, to a resonator which is falling into a black hole, and to a resonator in front of an oscillating massive sphere. With these examples we illustrate that by measuring the resonance frequency, the resonator could be used to indirectly measure other parameters, in our examples the acceleration, the Schwarzschild radius or the mass of the sphere. For the numerical examples, we consider the relative frequency shift, defined by $\delta_{\sigma,n} = (\omega_{\sigma,n} - \bar{\omega}_n)/\bar{\omega}_n$, where $\bar{\omega}_n$ denotes to the resonance frequency of a resonator at rest in flat spacetime.

Uniform Acceleration

For an observer which is uniformly accelerated in flat spacetime, the relative frequency shift is given by

$$\delta_{\omega,\sigma} = \left(\frac{\beta}{c_s^2} - \frac{\sigma}{c^2}\right)\frac{a^x}{2}L_p . \tag{3.12}$$

As a numerical example, we consider a rod made of aluminium. Aluminium has the speed of sound $c_s \sim 10^3\,\text{ms}^{-1}$. We consider the resonator to have the length $L_p = 2\,\text{cm}$ and to be supported at one of the mirrors, therefore setting $\beta = \pm 1$, and to be accelerated with $10\,\text{ms}^{-2}$. The relative frequency shift turns out to be of the order of magnitude $\delta_{\omega,\sigma} \sim 10^{-7}$. In this case, the first term in equation (3.12) dominates, which stems from the deformation of the resonator. In order to look at the effect coming purely from the acceleration, which means the effect for a rigid cavity, we let the speed of sound go to infinity and are left with the second term. Then, the relative frequency shift measured at one of the mirrors is of the order of magnitude of $\delta_{\omega,\pm 1} \sim \pm 10^{-18}$. This is in principle measurable with the most precise clocks [38, 39].

Falling into a Black Hole

To illustrate that the result for the frequency spectrum is also true in strong gravitational fields, we look at a resonator which is falling into a Schwarzschild black hole, as illustrated

in Figure 3.5. If the resonator is oriented such that its rod points vertically towards the black hole, the observer makes the measurement at the center of the resonator and the speed of sound is taken equal to the speed of light, the relative frequency shift is found to be

$$\delta_{\omega,0}(\tau) = -\frac{r_S L_p^2}{8r^3} \,, \tag{3.13}$$

where r_S is the Schwarzschild radius and r the radial distance from the center of the black hole. There is nothing special happening at the event horizon of the black hole.

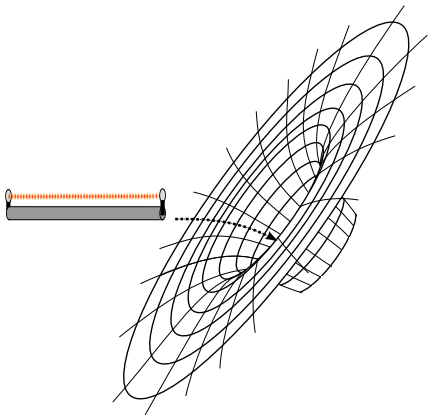

Figure 3.5: Artistic illustration of the resonator falling into a tilted Schwarzschild black hole.

Oscillating Mass

As the last example, we consider the resonator in front of an oscillating massive sphere, as illustrated in Figure 3.6. Our description of the frequency spectrum remains valid as long as the variation of the gravitational field of the oscillating sphere is slow enough such that the proper detector frame can be used.

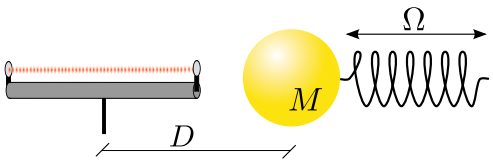

Figure 3.6: Illustration of the resonator in the gravitational field of an oscillating mass: The sphere of mass M is attached to a spring and oscillates with frequency Ω, and the support of the resonator is at a distance $R(\tau)$ from the center of the massive sphere when it is in the spring's equilibrium position.

The sphere is attached to a spring and oscillating at the frequency Ω, such that the distance between the center of the sphere and the center of the resonator is given by $R(\tau) = R_0 + \delta R_0 \sin(\Omega\tau)$. Describing the sphere's gravitational field with the Schwarzschild metric, one obtains

$$\delta_{\omega,\sigma} = -\frac{r_S L_p}{4R_0^2}\left(\left(\frac{c^2}{c_S^2}\beta - \sigma\right) + \left(2\frac{c^2}{c_S^2}(3\beta^2+1) - 3\sigma^2 - 6\beta\sigma + 1\right)\frac{L_p}{6R_0}\right) . \tag{3.14}$$

For the numerical example, we consider a gold sphere of mass $m = 100\,\mathrm{g}$, which oscillates with an amplitude $\delta R_0 \sim 1\,\mathrm{mm}$. The resonator is assumed to have length $L_p \sim 1\,\mathrm{cm}$ and be at a distance $R_0 \sim 1\,\mathrm{cm}$ from the sphere, and to consist of a material with speed of sound $c_s \sim 10^3\,\mathrm{ms}^{-1}$. If the rod is supported at one of the mirrors, the relative frequency shift is of the order of magnitude $\delta_{\omega,\pm 1} \sim 10^{-18}$ and purely due to the deformation of the rod.

Chapter 4

A Measurement of the Speed of Light in a Cavity

In project [A], we look at an observer performing a measurement of the speed of light in vacuum: In a cubic cavity containing light, the observer determines the speed of light according to $c = \omega\lambda/(2\pi)$, where ω is the frequency and λ the wavelength of the light. The measurement is both analyzed in the framework of quantum parameter estimation and in the framework of general relativity. In the former we derive a lower bound on the quantum mechanical uncertainty in the measurement, which decreases with increasing energy. However, when increasing the energy, the measurement does not take place in empty free space any more due to the self-gravitation of light. This means that the observer makes a systematic error when measuring the speed of light in vacuum. This error has two different origins, the systematic error in the frequency measurement is due to the gravitational redshift, and the systematic error in the calculation of the wavelength is due to the deformation of the cavity. These two effects are discussed in detail in Chapter 3. Another way to set up the experiment would be to measure the time period a light signal needs to make one round trip in the cavity and to infer the speed of light from it. Both the quantum mechanical uncertainty and the systematic error remain the same; the systematic error arising because the observer does not take into account that coordinate time and length have to be replaced by proper time and proper length.
In the current definition of the SI units the speed of light is defined the constant $c = 299\,792\,458\,\mathrm{ms}^{-1}$, the second is defined by transition properties of the caesium atom, and the meter is defined by the distance a light signal travels in a certain amount of time, when propagating at the speed c. The experiment could be reformulated in SI units: with the speed of light and measuring a time span, a length is inferred. The two approaches are equivalent, one leading to a minimal uncertainty in the measurement of the speed of light and the other giving a minimal uncertainty in the measurement of distance.
The chapter is organized as follows: In the first section we describe the cavity and the light and determine its gravitational field. The quantum mechanical uncertainty and the systematic error are analyzed in the second section.

4.1 The Gravitational Field of Light inside a Cubic Cavity

In the first subsection we explain how one obtains the vector potential and the energy-momentum tensor corresponding to the light inside the cavity, and in the second subsection we calculate the corresponding gravitational field. The calculations are performed in the

linearized approximation to general relativity (Appendix A) and using the semiclassical approximation. In the latter, the light field is treated quantum mechanically and the gravitational field classically, meaning that in the Einstein equations, the expectation value with respect to a certain quantum state is taken of the energy-momentum tensor.

Describing the Light

The light is contained in a cubic cavity of side length L with one corner in the origin of the coordinate system. It is assumed to have perfectly reflecting walls, to whom the electric field of the light is perpendicular and the magnetic field parallel. The electromagnetic vector potential $\vec{A}$ satisfies the Maxwell equations

$$\Box\vec{A}(x,y,z) = 0 \,, \tag{4.1}$$

where the Lorenz gauge condition $\vec{\nabla}\vec{A} = 0$ is imposed (we set the electric scalar potential to zero) and where $\Box = -\frac{1}{c^2}\partial_t^2 + \vec{\nabla}^2$ and $\vec{\nabla} = (\partial_x, \partial_y, \partial_z)$. A solution is given by

$$\vec{A}(x,y,z) = \frac{1}{\sqrt{\varepsilon_0}} q(t) \left(\frac{2}{L}\right)^{\frac{3}{2}} \begin{pmatrix} 1 \\ 0 \\ 0 \end{pmatrix} \cos(k_x x)\sin(k_y y)\sin(k_z z) \,, \tag{4.2}$$

where $q(t)$ is the time-dependent amplitude, ϵ_0 is the electric permittivity and $\vec{k} = (k_x, k_y, k_z)$ is the wave vector. We assume that the mode in x-direction vanishes, the mode in y-direction is in the first harmonic and the mode in z-direction is in the m^{th} harmonic. Then the vector potential reads

$$\vec{A}(x,y,z) = \frac{1}{\sqrt{\varepsilon_0}} q(t) \left(\frac{2}{L}\right)^{\frac{3}{2}} \begin{pmatrix} 1 \\ 0 \\ 0 \end{pmatrix} \sin\left(\frac{\pi}{L}y\right) \sin\left(\frac{m\pi}{L}z\right) , \tag{4.3}$$

where we used that the wavelength corresponding to the m^{th} harmonic is given by $\lambda_m = 2L/m$ and the wave number by $k_m = 2\pi/\lambda_m$. The corresponding electric field is given by $\vec{E} = -\dot{\vec{A}}$ and the magnetic field by $\vec{B} = \vec{\nabla}\times\vec{A}$. Quantizing them, q and its time-derivative $\dot{q}$ turn into the quadrature operators $\hat{q}$ and $\hat{p}$ respectively,[1]

$$q \;\rightarrow\; \hat{q} = \sqrt{\frac{\hbar}{2\omega c}}\left(\hat{a}_\omega + \hat{a}_\omega^\dagger\right) , \tag{4.4}$$

$$\dot{q} \;\rightarrow\; \hat{p} = -i\sqrt{\frac{\hbar\omega c}{2}}\left(\hat{a}_\omega - \hat{a}_\omega^\dagger\right) , \tag{4.5}$$

with the frequency $\omega = \sqrt{k_x^2 + k_y^2} = \frac{\pi}{L}\sqrt{1+m^2}$. From the electromagnetic field, the energy-momentum tensor is calculated according to $\hat{T}_{00} = \frac{\epsilon_0}{2}\left(\hat{\vec{E}}^2 + c^2\hat{\vec{B}}^2\right)$, $\hat{T}_{0a} = -\frac{1}{c}\left[\hat{\vec{E}}\times\hat{\vec{B}}\right]_a$ and $\hat{T}_{ab} = -\epsilon_0\left(\hat{E}_a\hat{E}_b + c^2\hat{B}_a\hat{B}_b\right) + \hat{T}_{00}\delta_{ab}$. The light field is chosen to be in the quantum state which is optimal for a frequency measurement [40],

$$|\psi_{\text{optimal}}\rangle = \frac{|0\rangle_\omega + |n_{\text{tot}}\rangle_\omega}{\sqrt{2}} \,, \tag{4.6}$$

[1] We label operators by hats.

where n_{tot} is the total number of available photons. In the following, we consider both the total number of photons n_{tot} and the mode number in z-direction m to be much larger than one. Further, we assume symmetric operator ordering, which means that products of annihilation and creation operators $\hat{a}\hat{a}^\dagger$ and $\hat{a}^\dagger\hat{a}$ are replaced by $(\hat{a}\hat{a}^\dagger + \hat{a}^\dagger\hat{a})/2$. Calculating the expectation values of the energy-momentum tensor with respect to the quantum state above, it turns out that only the components $\langle T_{00}\rangle$, $\langle T_{11}\rangle$, $\langle T_{22}\rangle$, $\langle T_{33}\rangle$ and $\langle T_{23}\rangle$ are different from zero.

Gravitational Field

In our description of the light field, we consider the light to be quantized, and determine its gravitational field. We make the semi-classical approximation of general relativity: We treat the fields quantum mechanically and the metric classically. In order to have well-defined Einstein equations, we need to take the expectation value of the energy-momentum tensor,

$$R_{\alpha\beta} - \frac{1}{2} g_{\alpha\beta} = 8\pi G \left\langle \hat{T}_{\alpha\beta} \right\rangle \ , \tag{4.7}$$

where $R_{\alpha\beta}$ is the Ricci tensor. The semiclassical approximation [41, 42] can be used if the quantum fluctuations of the energy-momentum tensor are small, i.e. $\text{Var}(\hat{T}_{\alpha\beta}) = \langle \hat{T}^2_{\alpha\beta}\rangle - \langle \hat{T}_{\alpha\beta}\rangle^2 \ll \langle \hat{T}_{\alpha\beta}\rangle^2$. In the linearized approximation of general relativity (Appendix A), the energy is assumed to be weak and terms quadratic in the energy-momentum tensor are neglected. In this case, the above condition for the variance is satisfied and the semi-classical approximation can be applied. The metric perturbation is thus given by

$$h_{\mu\nu}(\vec{x}) = \frac{4G}{c^4} \int_0^L d^3x' \, \frac{\left\langle \hat{T}_{\mu\nu}(\vec{x}') \right\rangle}{|\vec{x} - \vec{x}'|} \ . \tag{4.8}$$

Since the mode number m is assumed to be large, terms containing a sine or cosine function with m appearing as an argument are strongly oscillating, and thus vanish to a sufficient approximation when integrating over them. In our case, this means that only two components of the metric perturbation are different from zero, namely h_{tt} and h_{zz}.

4.2 Measurement Precision

The precision of the measurement is limited due to the quantum mechanical nature of the light; there is always a fundamental quantum mechanical uncertainty. As speed is not a quantum mechanical observable, the uncertainty in its measurement is not given by the Heisenberg uncertainty relation. Instead the observer performs measurements[2] on quantum mechanical observables, and infers the speed o flight from them. The uncertainty in this procedure is described in the framework of quantum parameter estimation theory, which offers an expression for the best achievable precision for the estimation of the parameter c, idealized over every possible measurement (Appendix C). The uncertainty δc turns out to be lower bounded by

$$\delta c \geq \frac{1}{\sqrt{M F_Q(c)}} \ , \tag{4.9}$$

[2]In general, quantum measurements are not constrained to observables, but belong to the larger class of POVM (positive-operator valued measure) measurements.

where M is the number of measurements the observer performs and F_Q the quantum Fisher information, defined in Appendix C. The observer, when performing the frequency measurement, will be limited in the precision by this bound. In our case, the relative minimal uncertainty δc_{CRLB} is given by

$$\frac{\delta c_{\mathrm{CRLB}}}{c} \sim \frac{1}{t n_{\mathrm{tot}} \omega \sqrt{M}} \sim \frac{1}{t c \sqrt{M} \frac{n_{\mathrm{tot}}}{\lambda}} , \tag{4.10}$$

where t is the measuring time, ω the frequency and $\lambda = c/\omega$ the wavelength of the light. From this equation it becomes clear that one way for the observer to lower the uncertainty in his measurement is to increase the number of photons in the cavity, and thus the energy. However, when increasing the energy, a systematic error in the setup of the measurement becomes more and more relevant: The observer does not take into consideration the gravitational field of the light. This leads to problems when the observer determines the speed of light in vacuum in the described way, as the observer thinks to be doing the measurement in flat spacetime, while he is not. When the observer determines the speed of light by doing a frequency measurement, he will make an error because he does not take into account the gravitational redshift.[3] The corresponding relative error in our case scales as

$$\frac{\delta c_{\mathrm{err}}}{c} \sim \left(\frac{l_{\mathrm{Pl}}}{L_p}\right)^2 n_{\mathrm{tot}}\, m \sim \frac{\hbar G}{c^3 L} \frac{n_{\mathrm{tot}}}{\lambda}. \tag{4.11}$$

The systematic error and the quantum mechanical uncertainty are different in nature. By increasing the number of measurements, the measuring time or the ratio n_{tot}/λ, the quantum mechanical uncertainty can become arbitrarily small, without affecting the systematic error. This corresponds to a sharp estimation of the wrong parameter. On the other hand, increasing the size of the cavity or decreasing the ratio n_{tot}/λ, the systematic error can become arbitrarily small. This corresponds to an imprecise (high variance) estimation of the actual parameter. Saying the measurement to be the most accurate when the systematic error and the quantum mechanical uncertainty are of the same order of magnitude, we adjust the ratio n_{tot}/λ and obtain the scaling for the relative minimal uncertainty

$$\frac{\delta c_{\mathrm{min}}}{c} \sim \frac{1}{c^2} \sqrt{\frac{\hbar G}{L t \sqrt{M}}} , \tag{4.12}$$

as illustrated in Figure 4.1. Again, it can be lowered by increasing the size of the cavity, the measuring time or the number of measurements. For the measurement time $t = LF/(\pi c)$ (the time in which the intensity of the light in the cavity decreases by a factor $1/e$), with the length $L = 1\,\mathrm{m}$, the finesse $F = 10^4$ and $M = 10^6$ repetitions of the measurement, the best possible precision scales as $\delta c_{\mathrm{min}}/c \sim 10^{-38}$.

[3] When performing the analysis in more detail, one would need to take into account the gravitational effects discussed in Chapter 3.

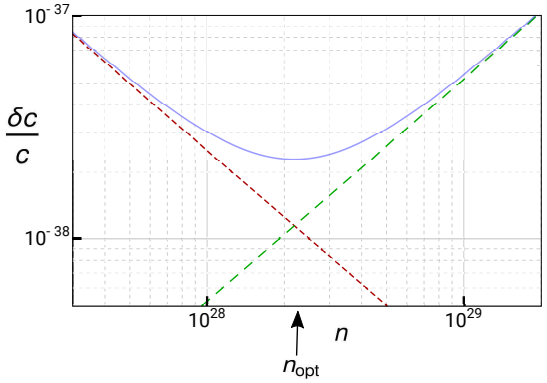

Figure 4.1: The quantum mechanical uncertainty $\delta c_{\mathrm{QCRB}}/c$ (short-dashed, red) and the systematic error $\delta c_{\mathrm{err}}/c$ (long-dashed, green) and the sum of both of them $\delta c/c$ (plain, blue) as a function of the number of photons n. The minimal uncertainty $\delta c_{\mathrm{min}}/c$ corresponds to the minimum of $\delta c/c$. For the plot we chose the wavelength $\lambda = 5 \cdot 10^{-7}\,\mathrm{m}$, the measuring time $t = L/c$, the length of the cavity $L = 1\,\mathrm{m}$ and the number of measurements $M = 10^6$. The arrow indicates the optimal number of photons n_{opt}, which minimizes the uncertainty.

In an experiment, a coherent state is more easily obtained than the optimal state (4.6). The coherent state is defined by $|\psi_{\mathrm{coh}}\rangle_\omega = \exp\left(\alpha \hat{a}_\omega^\dagger - \alpha^* \hat{a}_\omega\right)|0\rangle_\omega$ and has the average excitation number $n^{\mathrm{av}} = |\alpha|^2$. The minimal relative error in this case scales as

$$\frac{\delta c_{\mathrm{min}}}{c} \sim \left(\frac{\hbar G \lambda}{L c^5 t^2 M}\right)^{\frac{1}{3}}, \tag{4.13}$$

and for the same parameters as in the previous numerical example and $\lambda = 10^{-6}\,\mathrm{m}$, one obtains $\delta c_{\mathrm{min}}/c \sim 10^{-30}$.

Conclusion and Outlook

Summarized, in projects [C] and [D], we studied the gravitational properties of laser beams, finding novel features due to an accurate description of the laser beam. We studied some of them in detail, with the hope that they might be experimentally detected in the future, when technology becomes more advanced to measure small effects. More specifically, the novel results are the following: A light ray which co-propagates parallel to the beamline of the source laser-beam is gravitationally deflected by the latter. This statement is in contradiction to previous results, which were obtained in the short-wavelength approximation. In the short-wavelength approximation, the wave-like nature of light is not taken into account. We conclude from our analysis that the wave-like nature of light is essential when looking at the gravitational properties of light. Further, there is a gravitational spin-spin coupling: due to the effect of the spin angular momentum of the source laser-beam on its gravitational field, the polarization of test light-rays is rotated.

Three next steps for further investigations could be the following: First, in order to improve the measurability of the effects in an experiment, it would be better to use a laser pulse rather than a steady laser beam. To do so, our analysis needs to be generalized to laser pulses. Second, the laser beam we described carries spin angular momentum. We want to extend our description to laser beams carrying additionally orbital angular momentum. Third, it would be interesting to study the gravitational interaction of two laser beams characterized according to our description.

In project [B] we analyzed the frequency spectrum of an optical resonator in a gravitational field. The effect of the gravitational field on the frequency spectrum consists of a direct influence of the curvature of spacetime and an indirect influence through the deformation of the rod, depending on its material properties. As we show in examples, the order of magnitude of the gravitational effect is big enough such that the effect could possibly be measured in experiments. Also this article provides results that are useful for further investigations. In subsequent articles, we provide tools in order to apply quantum metrology for the analysis of the measurement precision which we want to apply to the resonator after describing it quantum mechanically, therefore extending the analysis in [B]. In this way, the statements on the measurability of the gravitational effects should become more precise, and a link to quantum mechanics would be built. It would also be interesting to take rotation of the resonator in to account. This requires a description including higher orders of the eikonal expansion of the light field inside the resonator.

In project [A] we consider relativistic effects in a specific measurement of the speed of light and analyze the measurement precision using quantum metrology. Understanding the procedure in a slightly different way, it is equivalent to the question of the minimal length which is in principle measurable with this setup. While projects [B], [C] and [D] were done using classical general relativity only, in project [A] we combine arguments from quantum mechanics with general relativity. This is done in the realm of the semi-classical

theory of general relativity, where the light field is treated quantum mechanically and the gravitational field classically. The next step could be to describe the gravitational effects on the frequency spectrum of the cavity as in project [B], expanding the results of [B] to three-dimensional deformable cavities. This would improve the precision of the analysis performed in project [A].
Summarized, this thesis deals with gravitation and light. Since light is both a relativistic and a quantum object, knowing its characteristics in detail might lead to some hint concerning the matching of gravity and quantum mechanics. Looking for gravitational effects in quantum mechanics or quantum mechanical effects in general relativity is a possible approach to tackle the problem, although not necessarily the right one. With our work we do not address this question, but provide tools and ideas upon which further investigations could build.

Appendix A: Linearized Theory of General Relativity

Assuming that the energy of the Gaussian beam is sufficiently small, we use the linearized theory of general relativity [43] to describe its gravitational field. Then the metric $g_{\alpha\beta}$ consists of the metric for flat spacetime $\eta_{\alpha\beta}$ plus a small perturbation $h_{\alpha\beta}$ with $|h_{\alpha\beta}| \ll 1$,

$$g_{\alpha\beta} = \eta_{\alpha\beta} + h_{\alpha\beta} \ . \tag{A1}$$

Therefore one neglects terms quadratic in the metric perturbation. In this case, one sees that the inverse of the metric reads $g^{\alpha\beta} = \eta^{\alpha\beta} - h^{\alpha\beta}$. In this appriximation, the Einstein equations[4] $R_{\alpha\beta} - \frac{1}{2}g_{\alpha\beta}R = 8\pi G T_{\alpha\beta}$ can be simplified to a set of equations linear in the metric perturbation.
We assume the metric perturbation to obey the Lorenz gauge condition, $\partial^\alpha h_{\alpha\beta} = 0$, which is equivalent to implying the harmonic gauge condition for the metric perturbation, $\partial^\alpha h_{\alpha\beta} = \partial_\beta h^\alpha_{\ \alpha}/2$. The conservation of the energy-momentum tensor, $\eta^{\alpha\beta}\partial_\alpha T_{\beta\gamma} = 0$ implies that the continuity equation is satisfied [31, 5]. Taking into account that the energy-momentum tensor is traceless for the electromagnetic field, the linearized Einstein equations are found to be [43]

$$\Box h_{\alpha\beta} = -\kappa T_{\alpha\beta} \ , \tag{A2}$$

where we define $\kappa = 16\pi G/c^4$ and $\Box = -c^{-2}\partial_t^2 + \partial_x^2 + \partial_y^2 + \partial_z^2$ is the d'Alembertian. This is a wave equation, which has the retarded solution

$$h_{\alpha\beta}(t, \vec{x}) = \frac{4G}{c^4}\int_{-\infty}^{\infty} d^3x' \frac{T_{\alpha\beta}\left(t - |\vec{x} - \vec{x}'|, \vec{x}'\right)}{|\vec{x} - \vec{x}'|} \ , \tag{A3}$$

where $\vec{x} = (x, y, z)$. As the full theory has an invariance under coordinate transformation, its linearized approximation is invariant under linear coordinate transformations $x^\alpha \to \tilde{x}^\alpha = x^\alpha + \xi^\alpha$, where the metric transforms as $h_{\alpha\beta} \to \tilde{h}_{\alpha\beta} = h_{\alpha\beta} - \partial_\alpha\xi_\beta - \partial_\beta\xi_\alpha$ (it is assumed that $|\partial_\alpha\xi_\beta|$ is of the same order of magnitude as $h_{\alpha\beta}$). In order to not violate the gauge condition, ξ_α has to satisfy $\Box\xi_\alpha = 0$. Since curvature is described by the second derivatives of the metric, quantities depending on the curvature are invariant under linear coordinate transformations. The Riemann curvature tensor in the linear approximation is given by

$$R^\alpha_{\beta\gamma\delta} = \frac{1}{2}\eta^{\alpha\rho}\left(\partial_\beta\partial_\gamma h_{\delta\rho} - \partial_\beta\partial_\delta h_{\gamma\rho} - \partial_\gamma\partial_\rho h_{\beta\delta} + \partial_\delta\partial_\rho h_{\beta\gamma}\right) \ . \tag{A4}$$

[4] $R_{\alpha\beta}$ is the Ricci tensor and R the Ricci scalar, which are contractions of the Riemann curvature tensor describing the curvature of spacetime. $T_{\alpha\beta}$ is the energy-momentum tensor, describing the energy distribution. The Einstein equations thus relate the curvature of spacetime to the energy distribution.

In Appendix B2, we present models for light rays in the short-wavelength approximation. In this case, the only non-zero components of the energy-momentum tensor are T_{tt}, T_{tz} and T_{zz}. If the radiation is moving at the speed of light, we have $T_{tt} = -T_{tz} = T_{zz}$. The metric is given by $ds^2 = -(1-h)dt^2 + (1+h)dz^2 - 2hdtdz + dx^2 + dy^2$, with $h = h_{tt} = -h_{tz} = h_{zz}$. In this case, the metric has similarities with the pp-wave metric, which is introduced in Appendix B1.

Appendix B: Models of Light Beams in the Short-Wavelength Approximation

Appendix B1: Plane Wave Metrics - pp-waves

For the different descriptions of light beams, either the linearized theory of general relativity or the pp-wave solutions to the Einstein equations are used: The linear approximation of general relativity is applied if one deals with finitely extended energy distributions, as then the metric perturbation remains small and the linear approximation remains valid. On the other hand, for infinitely extended sources, the pp-wave solutions are useful, as they are exact results not restricted to any domain of validity.
Heuristically, pp-wave metrics are obtained from the line element $ds^2 = (\eta_{\mu\nu} + h_{\mu\nu})dx^\mu dx^\nu$ for electromagnetic radiation in the linearized theory by dropping the assumption that the energy and thus the metric perturbation is small - therefore promoting the solution to an exact solution to the Einstein equations [44].
More rigorously, they are obtained as follows [44]: They are defined to describe spacetimes where there exists a covariantly conserved null vector field, i.e. a vector field Z^α whose norm and whose covariant derivative vanish, i.e. $Z_\alpha Z^\alpha = 0$ and $\nabla_\alpha Z^\beta = 0$. Changing from the coordinates $\{x^\mu\} = (t, x, y, z)$ to the coordinates $\{y^\alpha\} = (u, x, y, v)$ with $u = z - t$ and $v = z + t$, one finds the line element

$$g_{\alpha\beta}dy^\alpha dy^\beta = 2dudv + K(u, y^\alpha)du^2 + 2B_a(u, y^c)dudy^a + g_{ab}(u, y^c)dy^a dy^b \ , \tag{B1}$$

where $y^a, y^b, y^c \in \{x, y\}$. This metric is called a plane wave metric if $g_{ab} = \delta_{ab}$, $B_a = 0$ and $K(u, y^a) = A_{ab}y^a y^b$, where $A_{ab} = A_{ab}(u)$, and thus

$$g_{\alpha\beta}dy^\alpha dy^\beta = 2dudv + A_{ab}(u)y^a y^b du^2 + \delta_{ab}dy^a dy^b \ . \tag{B2}$$

Then, the Ricci tensor has the only non-zero component $R_{uu} = -\delta^{ab}A_{ab}$. Accordingly, the only non-vanishing component of the Einstein equations is

$$R_{uu} = 8\pi G T_{uu} \ , \tag{B3}$$

and therefore one finds the relation $\delta^{ab}A_{ab} = -8\pi G T_{uu}$. Changing back from the coordinates $\{y^\alpha\}$ to coordinates $\{x^\mu\}$ and defining $A = A_{ab}y^a y^b$, we obtain

$$g_{\mu\nu}dx^\mu dx^\nu = -(1 + A)dt^2 + (1 + A)dz^2 - 2Adtdz + \delta_{ab}dx^a dx^b \ . \tag{B4}$$

To show the mentionned similarity to the linearized theory of relativity, we define the tensor $h_{\mu\nu}$ with the only non-vanishing components $h_{00} = h_{33} = -h_{03} = -A$, which

allows us to write the metric as $g_{\mu\nu} = \eta_{\mu\nu} + h_{\mu\nu}$. Here however, the expression is exact. That the exact metric can be written in the same structure as the linearized version is not surprising, as neither the Ricci tensor nor the Ricci scalar contain any non-linear terms in the energy-momentum tensor. Therefore the Einstein equations are already linear, and one expects an analogy to the linearized theory.
For an electromagnetic plane wave, which is given by the vector potential $A_\mu = \mathcal{A}\epsilon_\mu e^{-iku}$, the only non-vanishing component of the energy-momentum tensor[5] is $T_{uu} = \delta^{ab}\partial_u A_a \partial_u A_b$. Therefore, from $\delta^{ab}A_{ab} = -8\pi G T_{uu}$, it follows that the plane wave metric (B2) reads

$$g_{\alpha\beta}dy^\alpha dy^\beta = 2dudv + Adu^2 + \delta_{ab}dy^a dy^b, \quad A = -8\pi G\partial_u A_a \partial_u A_b y^a y^b \ . \tag{B5}$$

Appendix B2: Models of Light Beams in the Short-Wavenength Approximation

For most descriptions of the gravitational fields of light beams, the short-wavelength approximation is used. This means that the beams have a diverging momentum and a vanishing wavelength. As the beam divergence angle is proportional to the inverse of the wave number and thus proportional to the wavelength (Section 1.1), also the beam divergence angle vanishes, such that these beams have a cylindrical symmetry. As intuitively clear by letting the wavelength go to zero, in this approximation the wave-like nature of the light is not visible. This is confirmed by noticing that the Maxwell equations, whom electromagnetic waves underlie, are not fulfilled.
We review the most important models of laser beams in the short-wavelength approximation. Starting by the simplest ones, a single light ray and an infinitely extended plane wave, we continue with beams whose energy density depends on the distance from the beamline or falls off abruptly at a finite distance from the beamline, describing a cylinder of light. In addition to static spacetimes, we also discuss a thin light pulse both in free space and in a wave guide, and a single photon.

Model 1: infinitely thin, finitely long beam

The gravitational field of light was first studied in 1931 by Tolman, Ehrenfest and Podolsky [1]. They considered the most simple description of a light beam: a single light ray, this means an infinitely thin beam, which is emitted at $z = a$ and absorbed at $z = b$, and which is assumed to have constant energy per length. The metric is calculated using the linearized theory of general relativity. Instead of assuming constant energy per length, the same beam was also described as consisting of electromagnetic plane waves [5]. We discuss the description of the light beam consisting of plane waves, keeping in mind that for circular polarization, the energy per length is constant and the result concides with the one found by Tolman, Ehrenfest and Podolski [1].
The vector potential of a transversally polarized plane electromagnetic wave travelling in z-direction is given by

$$A_\mu(t-z) = \mathcal{A}\epsilon_\mu e^{-i\omega(t-z)} \ , \tag{B6}$$

where $\mathcal{A}$ is the amplitude and the polarization vector is given by $\epsilon_\mu = (0, \epsilon_1, \epsilon_2, 0)$. The field strength tensor $F_{\mu\nu} = \mathrm{Re}\left(\partial_\mu A_\nu - \partial_\nu A_\mu\right)$ has the only non-zero independent components

[5]The energy-momentum tensor is given by $T_{\mu\nu} = F_{\mu\sigma}F^\sigma_{\ \nu} - \frac{1}{4}F_{\sigma\delta}F^{\sigma\delta}$, with the field strength tensor $F_{\mu\nu} = \partial_\mu \mathrm{Re}(A_\nu) - \partial_\nu(\mathrm{Im}A_\mu)$.

$F_{01} = F_{13} = -i\omega\mathcal{A}\epsilon_1 e^{-i\omega(t-z)}$ and $F_{02} = F_{23} = -i\omega\mathcal{A}\epsilon_2 e^{-i\omega(t-z)}$. The energy-momentum tensor $T_{\mu\nu} = \mathrm{Re}(F_{\mu\sigma})\mathrm{Re}(F_\nu{}^\sigma) - \frac{1}{4}\mathrm{Re}(F_{\mu\nu})\mathrm{Re}(F^{\mu\nu})$ is then found to be

$$T_{\mu\nu} = u(t-z)M_0 \ , \quad M_0 = \begin{pmatrix} 1 & 0 & 0 & -1 \\ 0 & 0 & 0 & 0 \\ 0 & 0 & 0 & 0 \\ -1 & 0 & 0 & 1 \end{pmatrix} \ , \tag{B7}$$

where u is the energy density, the energy per length (sometimes in the literature the energy per volume is used, and multiplied by a small cross-section). This structure of the energy-momentum tensor is characteristic for an energy density moving at the speed of light, when it does not change its shape and is not rotating. Therefore, the matrix M_0 appears in any model of light beams using the short-wavelength approximation. The energy density for circular polarization $\epsilon_\mu^{\mathrm{circ}} = \frac{1}{\sqrt{2}}(0,1,i,0)$ and for linear polarization $\epsilon_\mu^{\mathrm{lin}} = \frac{1}{\sqrt{2}}(0,1,0,0)$ is given by $u^{\mathrm{circ}} = \mathcal{A}^2\omega^2/2$ and $u^{\mathrm{lin}}(t-z) = \mathcal{A}^2\omega^2/2\,\sin^2(\omega(t-z))$. As mentionned before, for circular polarization the energy density for the circular polarization is constant and the description coincides with the model by Tolman, Ehrenfest and Podolski [1]. The metric perturbation (A3) in the linearized theory of relativity is found to be

$$h_{\mu\nu}(t,x,y,z) = 4G\int_a^b dz' \, \frac{u\big(t-z'-\sqrt{x^2+y^2+(z-z')^2}\big)}{\sqrt{x^2+y^2+(z-z')^2}} M_0 \ . \tag{B8}$$

The integral may be solved conveniently by introducing the coordinate $\xi = z - z' + \sqrt{x^2+y^2+(z-z')^2}$. Together with $d\xi = \frac{\xi}{\sqrt{x^2+y^2+(z-z')^2}}dz'$, one finds for the metric perturbation [5]

$$h_{\mu\nu}(t,x,y,z) = 4G\int_{\xi(a)}^{\xi(b)} d\xi \, \frac{u(t-z-\xi)}{\xi} \ . \tag{B9}$$

Inserting the energy density for the circular and the linear polarization leads to

$$h_{\mu\nu}^{\mathrm{circ}}(t,x,y,z) = -2\Sigma^2 k^2 G \log\left(\frac{z-b+\sqrt{r^2+(z-b)^2}}{z-a+\sqrt{r^2+(z-a)^2}}\right) M_0 \ , \tag{B10}$$

for the circular polarization, and a somewhat longer expression for the linear polarization.[6]

Model 2: infinitely long beam of an infinite radius and an energy density which does not depend on the transverse distance to the beamline

A formally simple, but not very realistic model of a light beam is an infinitely extended plane wave, describing an infinitely long and infinitely wide light beam. For this beam, there exists an exact solution to the Maxwell equations, the pp-wave metric (Appendix B1). In [45], the solution is explicitly given for circular and linear polarization of the light. It is obtained from the plane wave metric for electromagnetic fields (B5) by writing the Einstein equations in the form $\delta^{ab}A_{ab} = -8\pi G T_{uu}$ as $\frac{1}{2}\left(\partial_1^2+\partial_2^2\right)A = 8\pi G T_{uu}$.[7] For the vector potential for electromagnetic waves $A_\mu(t-z) = \mathcal{A}\epsilon_\mu e^{-ik(t-z)}$, where $\mathcal{A}$ is the amplitude

[6] See Appendix A in [5].
[7] Compare Eq. (15) in [45].

and ϵ_μ the polarization vector and integrating over the transverse directions, one obtains for circular and linear polarization

$$A^{\text{circ}} = 4\pi G\mathcal{A}^2\omega^2\left(x^2+y^2\right) \ , \tag{B11}$$

$$A^{\text{lin}} = 4\pi G\mathcal{A}^2\omega^2\sin^2\left(\omega(t-z)\right)\left(x^2+y^2\right) \ . \tag{B12}$$

where A^{circ} and A^{lin} stand for the function A in the metric (B5) for circular and linear polarization.

Model 3: infinitely long beam with an infinite radius and an energy density depending on the transverse distance to the beamline

Making a step towards a more realistic description of the light beam, in [46] the same beam as in Model 2 is considered, but with an energy density that depends on the radial distance to the beamline. While in the previous models, the spacetime metric was determined based on a known energy distribution, here one proceeds in the opposite direction for this model; for a certain structure of the metric, the energy distribution is analyzed. The metric given in [46][8] is obtained from the plane wave metric (B4) as follows: Changing to cylindrical coordinates according to $x = r\cos(\vartheta)$ and $y = r\sin(\vartheta)$, one obtains

$$g_{\mu\nu}dx^\mu dx^\nu = -(1+A)dt^2 - 2dtdz + (1-A)dz^2 + dr^2 + r^2 d\vartheta^2 \ . \tag{B13}$$

Setting $A = 1$ and rescaling the t- and z-coordinates by $t \to t/\sqrt{2}$ and $z \to \sqrt{2}z$, leads to

$$g_{\mu\nu}dx^\mu dx^\nu = -dt^2 - 2dtdz + dr^2 + r^2 d\vartheta^2 \ . \tag{B14}$$

The only non-zero components of the Ricci tensor turn out to be

$$R_{00} = -R_{03} = R_{33} = -\,\sigma \ . \tag{B15}$$

With the Einstein equations $R_{tt} = 8\pi G T_{tt}$, $R_{tz} = 8\pi G T_{tz}$ and $R_{zz} = 8\pi G T_{zz}$, one identifies σ as the energy density. In [46] it is shown that it may be written as $\sigma = Dr^C$, with constants C and D, thus showing that the energy density depends on the transverse distance to the axis of the beam. However, this scaling with r of the energy density is not the scaling one has in a typical laser beam, where it decreases by a Gaussian factor with the distance to the beamline (Section 1.1).

Model 4: infinitely long beam with a finite radius and an energy density not depending on the transverse distance to the beamline

In 1969, Bonnor described a cylindrical light beam. This beam has constant energy density within a cylinder around the beamline, whereas outside of the cylinder the energy density is zero. Again, the Einstein equations for this beam are solved by a plane wave metric. However, since in this model the light beam is a described as a continuous fluid and not as an electromagnetic wave, one does not start with the form for electromagnetic plane waves of Eq. (B5), but with the more general form given in Eq. (B1), where one sets $B_a = 0$ and $J_{ab} = \delta_{ab}$. The line element then reads

$$g_{\alpha\beta}dy^\alpha dy^\beta = 2dudv + K(u,y^a)du^2 + \delta_{ab}dy^a dy^b \ . \tag{B16}$$

[8] Compare Eq. (4) in [46].

The cylinder is assumed to have radius a. Choosing both a solution to the Einstein equations for the interior region of the beam where $\sqrt{y_1^2+y_2^2} \leq a$ and the exterior region where $\sqrt{y_1^2+y_2^2} \geq a$ and demanding continuity at $r=a$, the following solution is obtained in [4],

$$K_{\text{ext}}(u,y^1,y^2) = -8Gm\phi(u)\left(\log\left(\frac{\sqrt{y_1^2+y_2^2}}{a}\right)+\frac{1}{2}\right) , \quad \sqrt{y_1^2+y_2^2} \geq a , \tag{B17}$$

$$K_{\text{int}}(u,y^1,y^2) = -4Gm\phi(u)\frac{y_1^2+y_2^2}{a^2}, \quad \sqrt{y_1^2+y_2^2} \leq a , \tag{B18}$$

where m is a parameter and ϕ a function of the coordinate u. Finally, it remains to identify the energy density of the beam. To do so, one calculates the Ricci tensor, $R_{uu} = -\delta^{ab}\partial_a\partial_b K(u,y^a)$, and obtains with the Einstein equations the energy-momentum tensor, $T_{uu} = \delta^{ab}\partial_a\partial_b K(u,y^a)/(8\pi G)$. For the interior and the exterior region of the cylinder, one finds

$$T_{uu}^{\text{ext}} = 0 , \tag{B19}$$

$$T_{uu}^{\text{int}} = \frac{m\phi(u)}{a^2\pi} . \tag{B20}$$

Altogether, this is a cylindrically symmetric solution, whose energy-momentum tensor is non-zero within the radius a and vanishes outside of it. Therefore, this solution is interpreted as a cylindrical beam of light with energy per unit length $m\phi(u)/(a^2\pi)$. As a consistency check, by taking the radius of the cylinder to be infinite, one recovers the plane wave metric (B5).

Model 5: single photon

So far we discussed steady laser beams, which is the main interest in [C]. For completeness, in this and the following two paragraphs, we discuss two other descriptions of light: single photons and a thin laser pulse.

The gravitational field of a massless point particle,[9] a single photon, was described both in the linearized approximation of general relativity [49][10] and as a plane wave solution [50]. In [49] they also find an exact result by boosting the Schwarzschild metric. Their result coincides with the exterior solution found in [50], where they proceed as follows: Setting $\phi(u) = \delta(u)$ in equation (B17) for the solution of the beam of circular cross-section and locating the entire energy at $u=0$ or $t=z$, one obtains

$$K_{\text{ext}}(u,y^1,y^2) = -4\pi Gm\delta(u)\left(\log\left(\frac{y_1^2+y_2^2}{a}\right)+\frac{1}{2}\right) , \tag{B21}$$

$$K_{\text{int}}(u,y^1,y^2) = -2\pi Gm\delta(u)\frac{y_1^2+y_2^2}{a^2} . \tag{B22}$$

This describes an infinitely thin slice of radius a moving at the speed of light. Considering only the exterior solution and assuming the radius a to be small, it may be interpreted as

[9] This particle is moving in flat spacetime. The analogous situation of a single photon in a Schwarzschild background is analyzed in [47, 48].

[10] As they explain, the calculation does not work by simply multiplying the energy-momentum tensor of the one-dimensional beam with a Dirac-Delta function - there is a problem since the source is moving at the speed of light.

the description of a photon. If this photon is travelling on the path given by $x_0 = t_0$, it is causally connected to the points (t, x, y, z) that satisfy $x^2 + y^2 + (z - z_0)^2 = (t_0 - t)^2$. This means that its gravitational field reaches a point (t_1, x_1, y_1, z_1) if $t_0 = (t_1^2 - x_1^2 - y_1^2 - z_1^2)/\big(2(t_1 - z_1)\big)$. Since one deals with a retarded potential, one has $t_1 \geq t_0$. The case $t_1 > t_0$ is equivalent to $t_1 > z_1$. In this region, spacetime turns out to be flat. For $t_1 = z_1$, one finds $x_1 = y_1 = 0$, which means that the point of evaluation of the metric, the observer, lies on the path of the photon, as well as $t_0 = -\infty$, which means that the source of the gravitational field lies infinitely back in the past. By looking at the Riemann curvature tensor, it was found that the gravitational field depends only on the energy of the photon for small distances from the beamline; further away, it is independent of the energy of the photon. These two observations suggest that the gravitational field arises from the emission process only, and that there is no gravitational effect due to the propagating photon.

Model 6: infinitley thin pulse

That propagating light does not have any gravitational influence is supported by studying a thin laser pulse. From the solution for the infinitely thin beam, one can derive the gravitational field of an infinitely thin light pulse. Here we review the calculation performed in [5][11]. The pulse is assumed to be emitted at $z = z_a$, propagate along the z-axis and be absorbed at $z = z_b$. The front of the pulse leaves the emitter at time $t = 0$ and the end of the pulse at $t = L$; the pulse has thus the length L. The pulse is described by taking the energy-momentum tensor for the infinitely thin beam and boxing its support, i.e. by cutting out a piece of length L of the beam and letting it propagate from z_a to z_b.
The metric perturbation then reads

$$h_{\mu\nu} = 4G \int_{z_a}^{z_b} dz' \frac{u\left(t - \sqrt{x^2 + y^2 + (z - z')^2} - z'\right)}{\sqrt{x^2 + y^2 + (z - z')^2}} M_0 \,, \tag{B23}$$

where u stands for the energy density corresponding to linear or circular polarization and the integration boundaries z_a and z_b will be determined in the following: The boundary of integration is the intersection of the past light cone of the observer with the world sheet of the pulse - in order to ensure that the observer is causally connected with the pulse. The front and the end of the pulse at $z = \tilde{z}_b$ and $z = \tilde{z}_a$ intersect the past light cone of the observer at the point (t, x, y, z) if

$$\bar{z}_b = z + \frac{(t - z)^2 - x^2 - y^2}{2(t - z)} \,, \tag{B24}$$

$$\bar{z}_a = z + \frac{(t - L - z)^2 - x^2 - y^2}{2(t - L - z)} \,. \tag{B25}$$

Respecting the location of emission and absorption, the region of integration is given by

$$[z_a, z_b] = \begin{cases} \emptyset \,, \quad \mathrm{I}_-, \mathrm{I}_+ \,, \\ [a, \bar{z}_b] \,, \quad \mathrm{II} \,, \\ [\bar{z}_a, \bar{z}_b] \,, \quad \mathrm{III} \,, \\ [\bar{z}_a, b] \,, \quad \mathrm{IV} \,, \\ [a, b] \,, \quad \mathrm{V} \,. \end{cases} \tag{B26}$$

[11] Compare also [51].

The regions I through V are defined by (compare Figure 4.2)

- Region I: There is no causal connection between the observer and the pulse.
- Region II: The observer is causally connected with the emission process.
- Region III: The observer is causally connected with the propagating pulse, but not with the emission nor the absorption process.
- Region IV: The observer is causally connected to the absorption process.
- Region V: The observer is causally connected with the emission process, the propagation of the pulse, as well as the absorption process.

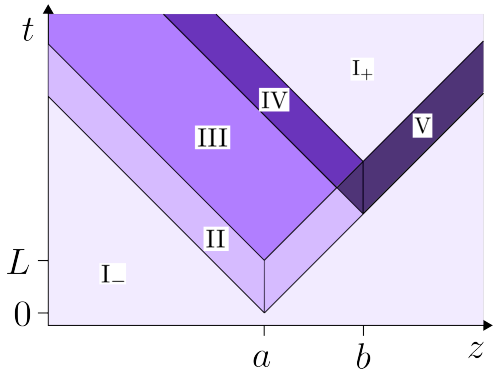

Figure 4.2: Spacetime diagram showing the different regions of causal connection.

With a substitution, the metric perturbation (A3) can be written in a simple way: Introducing $\xi = z - z' + \sqrt{x^2 + y^2 + (z - z')^2}$, one obtains

$$h_{\mu\nu} = 4G \int_{\xi(z_a)}^{\xi(z_b)} d\xi \frac{u\,(t - \xi - x_1)}{\xi} M_0 \; . \tag{B27}$$

In region III, one has $\xi(z_b) = t - z$ and $\xi(z_a) = t - z - L$. Therefore, the metric perturbation is a function of $t - z$. In this case, the only non-zero component of the Riemann curvature tensor is $R_{tztz} = -\frac{1}{2}\left(\partial_0 + \partial_3\right)^2 u(t - z)$. However, also this component vanishes as $(\partial_0 + \partial_1)h(t - x) = \frac{\partial h}{\partial(t-x)}\frac{\partial t}{\partial t} + \frac{\partial h}{\partial(t-x)}\frac{\partial(-x)}{\partial x} = 0$. Therefore, the curvature is zero in region III, where neither the emission nor the absorption process have any influence. One may thus conclude that the propagation of the pulse does not produce a gravitational field. This is in agreement with the result found in [50] that the propagation of a single photon does not have any gravitational effect, and has been derived in the way we described in [52].

Model 7: infinitely thin pulse in a wave guide

In the previous sections, the light was propagating in free space and therefore at the speed of light. In [53] an infinitely thin pulse in a wave guide is studied. The light in the wave guide travels at the speed $v < c$, slower than the speed of light. In this case, the metric takes a form which is different to the cases where the light is propagating at the speed of light.

In [53] the electric field is assumed to have transverse polarization and is of the form,

$$E_2 = \mathcal{A}^2 \sin\big(\omega(vt-z)\big)\,, \tag{B28}$$

$$B_1 = \mathcal{A}^2 v \sin\big(\omega(vt-z)\big)\,, \tag{B29}$$

$$B_3 = \mathcal{A}^2 \sqrt{1-v^2} \cos\big(\omega(vt-z)\big)\,, \tag{B30}$$

where $\mathcal{A}$ is the amplitude. The pulse is constructed as in the previous section. In the spacetime region which is causally connected to the propagation of the pulse, but not the emission nor the absorption process (region III as defined in the previous paragraph), this leads to the metric perturbation $h_{\mu\nu} = hM_{\mu\nu}$, where the function h is given by

$$h = -2G\mathcal{A}^2 \log\left(\frac{vt-z+\sqrt{(vt-z)^2+(1-v^2)(x^2+y^2)}}{vt-z-L+\sqrt{(vt-z-L)^2+(1-v^2)(x^2+y^2)}}\right)\,, \tag{B31}$$

and the matrix $M_{\mu\nu}$ is defined by

$$M_{\mu\nu} = \begin{pmatrix} 1 & 0 & 0 & -v \\ 0 & 1-v^2 & 0 & 0 \\ 0 & 0 & 0 & 0 \\ -v & 0 & 0 & v^2 \end{pmatrix}\,. \tag{B32}$$

The metric perturbation has thus a different structure for light propagating at the speed of light and light propagating slower than the speed of light.

Other models

There exist further models which we will not present in detail. We will just mention some of them. In [54], a plane wave solution carrying angular momentum is presented. An exact solution for a planar shell of null matter of constant and arbitrary energy density is found in [55] and [56]. There exist further exact solutions to the Einstein equations for an infinitely extended circular or elliptical beam whose energy density depends on the radial distance to the beamline [57], and for the same beam but whose radius varies in time [58][12]. In [59], a solution in the linearized approximation for a beam of a rectangular cross-section is given.

Appendix B3: The parallel co-propagating test light ray

As already noticed by Tolman, Ehrenfest and Podolski [1], there is an interesting effect regarding the gravitational interaction of light when the light is described in the short-wavelength approximation: A light ray propagating parallel to another light ray is not deflected in the gravitational field of the latter. It is neither deflected if the beam is described by the plane wave metric. This holds as long as the source beam is propagating with the speed of light; when it is slower than the speed of light, the parallel propagating light ray will be deflected [53].
More specifically, the parallel co-propagating test light-ray is defined by the tangent to its geodesic γ (parametrized by ϱ), $\dot\gamma^\mu(\varrho) = \frac{c}{w_0}(1,0,0,1-f)$, where f is determined by the null condition $g_{\mu\nu}\dot\gamma^\mu(\varrho)\dot\gamma^\nu(\varrho) = 0$. It follows that f is of the same order of magnitude

[12] These solutions have been criticized as they do not satisfy the Maxwell equations

as the metric perturbation and may be neglected in the following. The originally parallel test light-ray remains parallel, i.e. is not deflected, if the radial acceleration vanishes. The acceleration is calculated with the geodesic equation $\ddot{\gamma}^\mu(\varrho) = -\Gamma^\mu_{\nu\lambda}\dot{\gamma}^\nu(\varrho)\dot{\gamma}^\lambda(\varrho)$.
For a laser beam in the short-wavelength approximation (such as in the models 1-4), for which the metric perturbation is proportional to the matrix M_0, we obtain, using that the metric is independent of time, that the acceleration in the direction transverse to the beamline (here in x-direction, for the y-direction the expression is analogous) vanishes,

$$\ddot{\gamma}^x = \frac{1}{2}\partial_x \left(h_{tt} + h_{zz} + 2h_{tz}\right) = 0 \; . \tag{B33}$$

For the single photon (Model 5) and the infinitely thin light pulse (Model 6), the acceleration vanishes in the region which is not causally connected to the emission or absorption, as there the curvature and thus the gravitational field vanishes. For the infinitely thin pulse moving at velocity v in a wave guide (Model 7), one obtains the following [53]: A parallel propagating light pulse at velocity v' has the transverse acceleration

$$\ddot{\gamma}^x = -\frac{1}{2}\partial_x^2 h(1 - vv')^2 \; . \tag{B34}$$

The light pulse travelling parallel to the source pulse is thus deflected unless both pulses propagate at the speed of light.
Since coordinate acceleration does not have a proper meaning in general relativity, we also look at the geodesic deviation equation,[13] $a^\mu = \frac{Ds^\mu(\varrho)}{d\varrho} = R^\mu_{\nu\rho\sigma}\big(\gamma(\varrho)\big)\dot{\gamma}^\nu(\varrho)\dot{\gamma}^\rho(\varrho)s^\sigma(\varrho)$, which describes the difference $s^\mu(\varrho)$ between two nearby geodesics $\gamma(\varrho)$ and $\gamma'(\varrho)$, and where $\frac{D^2 s^\mu}{d\varrho^2} = \dot{\gamma}^\mu(\varrho)\nabla_\mu$ is the covariant derivative along the curve $\gamma(\varrho)$, compare Figure 4.3.

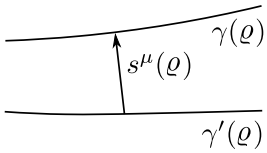

Figure 4.3: Illustration of the geodesic deviation equation: Two nearby geodesics $\gamma(\varrho)$ and $\gamma'(\varrho)$ are separated by the vector $s^\mu(\varrho)$.

Considering two geodesics which are separated by $s^\mu = (0, 1, 0, 0)$, we obtain for the Models 1-4,

$$a^x = R_{xttx} + R_{xzzx} + 2R_{xtzx} = \frac{1}{2}\partial_x^2 \left(h_{tt} + h_{zz} + 2h_{tz}\right) = 0 \; , \tag{B35}$$

meaning that the distance in the transverse direction between two nearby geodesics is constant. We conclude that a test light ray co-propagating parallel to the beamline is not deflected by the gravitational field of the light beam described by one of the models 1-4.
For the pulse in a wave guide (Model 7), we obtain for the acceleration in x-direction

$$a^x = R_{xttx} + R_{xzzx} + 2R_{xtzx} = \frac{1}{2}\partial_x^2 \left(h_{tt} + h_{zz} + 2h_{tz}\right) = \frac{1}{2}\partial_z^2 \left(h_{tt} + h_{zz} + 2h_{tz}\right) + \frac{1}{2}\partial_z^2 h_{xx} \; . \tag{B36}$$

[13] The equation $\ddot{\gamma}^\alpha = 0$ is not tensorial. Therefore, if $\ddot{\gamma}^\alpha = 0$ holds in one coordinate system, it does not necessarily hold in every coordinate system. The second covariant derivative a of the separation vector in the geodesic deviation equation is a tensor. Therefore, when it vanishes in one coordinate system, it vanishes in every coordinate system. The geodesic deviation equation can thus be used to decide whether the parallel light ray is deflected or not.

Using that the first term vanishes and $h_{xx} \sim (1 - v^2)$ leads to

$$a^x \sim (1 - v^2) \,, \tag{B37}$$

showing that the acceleration transverse to the beamline is non-vanishing if and only if the pulse inducing the gravitational field moves slower than the speed of light.[14,15]
As we explain in Section 1.2, the parallel co-propagating test light-ray is deflected in the gravitational field of the laser beam. The deflection appears if one describes the laser beam beyond the short-wavelength approximation.

[14]The same statement can be shown for light beams propagating slower than the speed of light.

[15]That a parallel propagating light ray is not deflected is confirmed by the result that a superposition of two plane wave metrics is again a solution to the Einstein equations [4]. There exist solutions for two counter-propagating beams, which are not superpositions of two solutions for the two individual beams [60, 61].

Appendix C: Quantum Metrology

For a quantum mechanical observable, the quantum mechanical uncertainty is given by the Heisenberg relation. However, often we are interested to infer the value of a parameter which does not correspond to an observable. In this case, quantum parameter estimation can be used to determine the fundamental quantum mechanical uncertainty that will remain when performing an optimal estimation procedure. More precisely, consider a system that depends on the parameter θ. The state of the system is described by the density matrix $\hat{\rho}(\theta)$. The value of the parameter θ is estimated by performing M measurements on the system to collect the data $\{x_1, x_2, ..., x_M\}$, which can be used to make the estimate $\theta_{\text{est}}(x_1, x_2, ..., x_M)$. The precision of the measurement procedure is determined by how close the estimated value θ_{est} is to the actual value θ. Assuming that there is no systematic error and therefore the expectation value of the estimator θ_{est} is equal to the actual value θ, the precision of the measurement corresponds to the variance of the estimator θ_{est}. A lower bound therefore is given by the Cramér-Rao Lower Bound,

$$\text{Var}(\theta_{\text{est}}) \geq \frac{1}{MF_Q(\theta)} \,, \tag{C1}$$

which states that the lower bound is inversely proportional to the number of measurements M and the quantum Fisher information F_Q. This bound can be saturated in the limit of a large number of repetitions of the measurement. The quantum Fisher information is a measure for the sensitivity of the quantum state on the parameter: Given a change of the parameter, if the quantum state changes a lot the quantum Fisher is large, and if it changes only a little bit the quantum Fisher information is small. In Chapter 4 we use the quantum Fisher information for pure states $|\psi_\theta\rangle$ depending on the parameter θ, which is given by

$$F_Q(\theta) = 4\big(\langle \partial_\theta \psi_\theta | \partial_\theta \psi_\theta \rangle - | \langle \psi_\theta | \partial_\theta \psi_\theta \rangle |^2 \big) \,. \tag{C2}$$

Bibliography

[1] Richard C. Tolman, Paul Ehrenfest, and Boris Podolsky. On the gravitational field produced by light. *Physical Review*, 37:602–615, Mar 1931.

[2] James Strohaber. Frame dragging with optical vortices. *General Relativity and Gravitation*, 45(12):2457–2465, 2013.

[3] James Strohaber. General relativistic manifestations of orbital angular and intrinsic hyperbolic momentum in electromagnetic radiation. *arXiv: 1807.00933*, 2018.

[4] W. B. Bonnor. The gravitational field of light. *Communications in Mathematical Physics*, 13(3):163–174, 1969.

[5] Dennis Rätzel, Martin Wilkens, and Ralf Menzel. Gravitational properties of lightthe gravitational field of a laser pulse. *New Journal of Physics*, 18(2):023009, 2016.

[6] W. B. Bonnor. Spinning null fluid in general relativity. *International Journal of Theoretical Physics*, 3(4):257–266, 1970.

[7] M. V. Federov and S. V. Vintskevich. Diverging light pulses in vacuum: Lorentz-invariant mass and mean propagation speed. *Laser Physics 27, 036202*, 2017.

[8] Daniel Giovannini, Jacquiline Romero, Václav Potocek, Gergely Ferenczi, Fiona Speirits, Stephen M. Barnett, Daniele Faccio, and Miles J. Padgett. Spatially structured photons that travel in free space slower than the speed of light. *Science*, 347, 2015.

[9] I. Yu. Kobzarev and K. G. Selivanov. Rotation of the polarization vector in a non-stationary gravitational field. *Zh. Eksp. Teor. Fiz.*, 94(1-4), 1988.

[10] G. V. Skrotskii. The influence of gravity on the propagation of light. *Doklady Akademii Nauk SSSR*, 114(1):73–76, 1957.

[11] N. L. Balazs. Effect of a gravitational field, due to a rotating body, on the plane of polarization of an electromagnetic wave. *Physical Review*, 110(1), 1958.

[12] Jerzy Plebanski. Electromagnetic waves in gravitational fields. *Physical Review*, 118:1396–1408, 1960.

[13] Maxim Lyutikov. Rotation of polarization by a moving gravitational lens. *Physical Review D*, 95:124003, 2017.

[14] Sergei Kopeikin and Bahram Mashoon. Gravitomagnetic effects in the propagation of electromeagnetic waves in variable gravitational fields of arbitrary-moving and spinning bodies. *Physical Review D*, 65:064025, 2002.

[15] Ue-Li Pen, Xin Wang, and I-Sheng Yang. Gravitational rotation of polarization: Clarifying the gauge dependence and prediction for a double pulsar. *Physical Review D*, 95:044034, 2017.

[16] Mauro Sereno. Gravitational Faraday rotation in a weak gravitational field. *Physical Review D*, 69:087501, 2004.

[17] Bin Chen. Probing the gravitational Faraday rotation using quasar X-ray microlensing. *Scientific Reports*, 5(16860), 2015.

[18] Tsvi Piran and Pedro N. Safier. A gravitational analogue of Faraday rotation. *Nature*, 318(21), 1985.

[19] H. Dehnen. Gravitational Faraday-effect. *International Journal of Theoretical Physics*, 7(6):467–474, 1973.

[20] David Eric Cox, James G. O'Brien, Ronald L. Mallett, and Chandra Roychoudhuri. Gravitational Faraday effect produced by a ring laser. *Foundation of Physics*, 2006.

[21] N. Yu. Gnedin and I. G. Dymnikova. Rotation of the plane of polarization of a photon in a Petrov type $\mathcal{D}$ space-time. *Zh. Eksp. Teor. Fiz.*, 94:26–31, 1988.

[22] Aharon Brodutch, Tommaso F. Demarie, and Daniel R. Terno. Photon polarization and geometric phase in general relativity. *Physical Review D*, 84:104043, 2011.

[23] Aharon Brodutch and Daniel R. Terno. Polarization rotation, reference frames, and Mach's principle. *Physical Review D*, 84:121501(R), 2011.

[24] V. Faraoni. On the rotation of polarization by a gravitational lens. *Journal of Astrophysics and Astronomy*, 272:385–388, 1993.

[25] F. Della Valle, E. Milotti, A. Ejlli, U. Gastaldi, G. Messineo, L. Piemontese, G. Zavattini, R. Pengo, and G. Ruoso. Extremely long decay time optical cavity. *Optics Express*, 22(9):11570, 2014.

[26] W. Schottky. Über spontane Stromschwankungen in verschiedenen Elektrizitätsleitern. *Annalen der Physik*, 57:541567, 1918.

[27] E. A. Shcherbakov, V. V. Fomin, A. A. Abramov, A. A. Ferin, D. V. Mochalov, and V. P. Gaspontsev. Industrial grade 100 kw power cw fiber laser. In *Advanced Solid-State Lasers Congress*, page ATh4A.2. Optical Society of America, 2013.

[28] S. P. Tarabrin. Interaction of plane gravitational waves with a Fabry-Perot cavity in the local Lorentz frame. *Physical Review D*, 75(102002), 2007.

[29] F. Pegoraro, E. Picasso, and L. A. Radicati. On the operation of a tunable electromagnetic detector for gravitational waves. *Journal of Physics A*, 11:1949, 1978.

[30] F. Pegoraro, L. A. Radicati, and E. Picasso. Electromagnetic detector for graivtational waves. *Physical Letters A*, 68:156–8, 1978.

[31] Michele Maggiore. *Gravitational Waves: Theory and Experiments*. Oxford University Press, New York, 2008.

[32] Wei-Tou Ni and Mark Zimmermann. Inertial and gravitational effects in the proper reference frame of an accelerated, rotating observer. *Physical Review D*, 17(6), 1978.

[33] F. Noether. Zur Kinematik des starren Körpers in der Relativtheorie. *Annalen der Physik*, 336(919):44, 1910.

[34] G. Herglotz. Über den Standpunkt des Relativitätsprinzips aus als starr zu bezeichnenden Körper. *Annalen der Physik*, 336(993):415, 1910.

[35] José Natarió. Relativistic elasticity of rigid rods and strings. *General Relativity and Gravity*, 46:1816, 2014.

[36] Walter Gordon. Zur Lichtfortpflanzung nach der Relativitätstheorie. *Annalen der Physik*, 377:421–356, 1923.

[37] Volker Perlick. *Ray optics, Fermat's principle, and applications to general relativity.* Lecture notes in physics. Monographs m61. Springer, 1 edition, 2000.

[38] N. Hinkley, J. A. Sherman, N. B. Phillips, M. Schioppo, N. D. Lemke, K. Beloy, M. Pizzocaro, C. W. Oates, and A. D. Ludlow. An atomic clock with 10^{-18} instability. *Science*, 341(1215):8, 2013.

[39] I. Ushijima, M. Takamoto, M. Das, T. Ohkubo, and H. Katori. Cryogenic optical lattice clocks. *Nature Photonics*, 9(185):9, 2015.

[40] D. Braun. Ultimate quantum bounds on mass measurements with a nano-mechanical resonator. *EPL*, 94:68007, 2011.

[41] L. H. Ford. Gravitational radiation by quantum systems. *Annals of Physics*, 144:238–248, 1982.

[42] Chung-I Kuo and L. H. Ford. Semiclassical gravity theory and quantum fluctuations. *Physical Review D*, 47(10), 1993.

[43] Charles W. Misner, Kip S. Thorne, and John Archibald Wheeler. *Gravitation.* W. H. Freeman and Company, San Francisco, 1973.

[44] Matthias Blau. Plane waves and Penrose limits, 2011. *http://www.blau.itp.unibe.ch/Lecturenotes.html (2018).*

[45] J. W. van Holten. The gravitational field of a light wave. *Fortschritte der Physik*, 59:284–295, 2011.

[46] A. Banerjee. Cylindrically symmetric stationary beam of electromagnetic radiation. *Journal of Mathematical Physics*, 16:1188, 1975.

[47] Tevian Dray and Gerard't Hooft. The gravitational shock wave of a massless particle. *Nuclear Physics B253*, pages 173–188, 1985.

[48] Tevian Dray and Gerard't Hooft. The effect of spherical shells of matter on the schwarzschild black hole. *Communications in Mathematical Physics*, 99:613–625, 1985.

[49] P. C. Aichelburg and R. U. Sexl. On the gravitational field of a massless particle. *General Relativity and Gravitation*, 2(4):303–312, 1971.

[50] W. B. Bonnor. The gravitational field of photons. *General Relativity and Gravitation*, 41:77–85, 2009.

[51] N. A. Voronov and I. Yu. Kobzarev. On the gravitational field of a massless particle. *Sov. Phys. JETP*, 39(4), 1974.

[52] J. C. Hegarty. Gravitational effect of electromagnetic radiation. *Il nuovo cimento*, LXIB(1), 1968.

[53] Marlan O. Scully. General-relativistic treatment of the gravitational coupling between laser beams. *Physical Review D*, 19(12):3582–3591, 1979.

[54] Valeri P. Frolov and Dimiti V. Fursaev. Gravitational field of a spinning radiation beam pulse in higher dimensions. *Physical Review D*, 71:104034, 2005.

[55] Tevian Dray and Gerard't Hooft. The gravitation effect of colliding planar shells of matter. *Classical and Quantum Gravity*, 3:825, 1986.

[56] V. Ferrari, P. Pendenza, and G. Veneziano. Beam-like gravitational waves and their geodesics. *General Relativity and Gravitation*, 20(11), 1988.

[57] Raymond W. Nackoney. The gravitational influence of a beam of light. *Journal of Mathematical Physics*, 14(9), 1973.

[58] Raymond W. Nackoney. The gravitational influence of a beam of light of variable flux. *Journal of Mathematical Physics*, 18(11), 1977.

[59] Raymond W. Nackoney. Gravitational solutions, including radiation, for a perturbed light beam. *Journal of Mathematical Physics*, 27(9), 1986.

[60] B. V. Ivanov. Colliding beams of light. *Classical and Quantum Gravity*, 20:397–405, 2003.

[61] D. Kramer. The gravitational field of two counter-propagating beams of light. *Classical and Quantum Gravity*, 15:L73–L76, 1998.

Publications

[A] Daniel Braun, Fabienne Schneiter, Uwe R. Fischer. Intrinsic measurement errors for the sped of light in vacuum. Classical and Quantum Gravity, 34(17), 2017.

[B] Dennis Rätzel, Fabienne Schneiter, Daniel Braun, Tupac Bravo, Richard Howl, Maximilian P. E. Lock, Ivette Fuentes. Frequency spectrum of an optical resonator in a gravitational field. New Journal of Physics, 20(5), 2018.

[C] Fabienne Schneiter, Dennis Rätzel, Daniel Braun. The gravitational field of a laser beam beyond the short wavelength approximation. Classical and Quantum Gravity, 35(19), 2018.

[D] Fabienne Schneiter, Dennis Rätzel, Daniel Braun. Rotation of polarization in the gravitational field of a focused laser beam - Faraday effect and optical activity. arXiv: 1812.04505.

[A] Intrinsic measurement errors for the speed of light in vacuum

Daniel Braun, Fabienne Schneiter, Uwe R. Fischer
Classical and Quantum Gravity, 34(17), 2017
DOI: 10.1088/1361-6382/aa8058
URL: http://stacks.iop.org/0264-9381/34/i=17/a=175009

IOP Publishing Classical and Quantum Gravity
Class. Quantum Grav. **34** (2017) 175009 (21pp) https://doi.org/10.1088/1361-6382/aa8058

Intrinsic measurement errors for the speed of light in vacuum

Daniel Braun[1], **Fabienne Schneiter**[1] **and Uwe R Fischer**[2]

[1] Institut für Theoretische Physik, Eberhard-Karls-Universität Tübingen, 72076 Tübingen, Germany
[2] Department of Physics and Astronomy, Center for Theoretical Physics, Seoul National University, 08826 Seoul, Republic of Korea

E-mail: uwe@phya.snu.ac.kr

Received 20 February 2017, revised 22 June 2017
Accepted for publication 18 July 2017
Published 3 August 2017

Abstract

The speed of light in vacuum, one of the most important and precisely measured natural constants, is fixed by convention to $c = 299\,792\,458$ m s^{-1}. Advanced theories predict possible deviations from this universal value, or even quantum fluctuations of c. Combining arguments from quantum parameter estimation theory and classical general relativity, we here establish rigorously the existence of lower bounds on the uncertainty to which the speed of light in vacuum can be determined in a given region of space-time, subject to several reasonable restrictions. They provide a novel perspective on the experimental falsifiability of predictions for the quantum fluctuations of space-time.

Keywords: speed of light, quantum metrology, general relativity

(Some figures may appear in colour only in the online journal)

1. Introduction

It is generally accepted that the speed of light in vacuum c is a universal natural constant, isotropic, independent of frequency, and independent of the motion of the inertial frame with respect to which it is measured. These properties have been experimentally demonstrated with very high precision, e.g. isotropy up to a relative uncertainty of the order of $\sim 10^{-9}$ [1], and lie at the basis of special relativity. By 1972, measurements of the speed of light became more precise than the definition of the meter [2], leading in 1983 to the definition of the speed of light in vacuum $c = 299\,792\,458$ m s^{-1}. But attempts to quantize gravity have led to the concept of space-time as a fuzzy 'quantum foam' on the Planck length $l_{\rm Pl} = \sqrt{\hbar G/c^3} \simeq 1.62 \times 10^{-35}$ m

[3–5] that implies an uncertainty or dispersion of c [6–9]. Experimental data based on gamma-ray bursts, pulsars, and TeV-flares from active galaxies imply upper bounds on deviations of c over cosmic distances [10–16]. Quantum fluctuations of c were also proposed due to virtual fermion-anti-fermion pairs, leading to a scaling of the jitter of the arrival time of light pulses with propagation distance [17, 18]. Satellite experiments are being planned to verify fundamental space-time properties with unprecedented precision, such as the isotropy of c and its independence from the laboratory frame velocity [1].

Here we establish how precisely c in a given region of space–time may be determined *in principle*, i.e. independent of any technical challenges. Our approach is based on the firmly established quantum parameter estimation theory (q-pet) [19–26] and general relativity (GR) in semiclassical approximation [27]. Q-pet allows one to obtain a lower bound on the uncertainty with which a parameter θ may be estimated that parametrizes a quantum state specified by a density matrix $\rho(\theta)$. The power of q-pet is due to the facts that (i.) the bound is reachable in the limit of a large number of measurements, and (ii.) it is optimized over all possible quantum mechanical measurements (positive operator valued measures, POVM [28]) and all data-analysis schemes (unbiased estimator functions). This so-called quantum Cramér–Rao bound (QCRB) [19–22] becomes relevant once all technical noise problems have been solved, and only the fundamental quantum uncertainties remain. It is the ultimate achievable lower bound on the uncertainty with which any parameter can be measured. Recently, the q-pet formalism was applied to the measurement of parameters in relativistic quantum field theory such as proper times and accelerations, the Unruh effect, gravitation, or the estimation of the mass of a black hole [29–32]. In the present work we go a step further by examining the back-action of the quantum probe on the metric of space-time. Taking back-action into account was proposed before [33–37] but to the best of our knowledge we combine for the first time modern q-pet with a precise calculation of the back-action of the probe on the space-time metric. We show that there is an optimal photon number at which the perturbation of the space-time metric due to the probe equals the quantum uncertainty of the measurement itself, establishing thus an ultimate lower bound on the uncertainty with which c can be determined.

2. Quantum parameter estimation

Any *direct* measurement of the speed of light has to use a light signal. Indirect measurements, e.g. through measuring the fine-structure constant, the electron charge and Planck's constant, may need no light but do not reflect the definition of c as a speed and need an elaborate theoretical framework for their interpretation. We consider definitions of c through $c = \Delta x/\Delta t$ (i.e. runtime measurements of a light pulse) as well as through $c = \omega/k$ (where ω is (2π times) the frequency and k the wavevector of a monochromatic e.m. wave) as direct measurements, as these (i.) use a light signal; (ii.) correspond to how c has actually been determined experimentally (in particular the most precise determinations of c to date use $c = \omega/k$ [2]), and (iii.) are based on simple three-letter formulas that need no elaborate theoretical framework for extracting c. These two definitions give c the meaning of a propagation speed or phase speed, respectively. Note that we only need $c = \omega/k$ at the frequency considered, not over all frequencies. For wave-lengths comparable to quantum-gravity length scales (assumed to be of order Planck-length), modifications of this linear dispersion relation have been proposed (see the discussion on rainbow gravity in section 5.2), but we restrict ourselves to frequencies where the linear dispersion is well verified experimentally. We emphasize that these definitions of speed are only needed to determine a systematic experimental error due to GR effects. The quantum-mechanical uncertainty of c obtained from q-pet on the other hand is optimized

over all possible (POVM) measurements of the light signal and analysis schemees of the data, including those that measure the propagation distance Δx of a light pulse over a time-interval Δt. We therefore do not have to worry about additional uncertainties of measurements of positions or times.

Any light signal can be decomposed in modes of the electromagnetic (e.m.) field which are the fundamental dynamical objects in quantum optics. Q-pet shows that with m modes the sensitivity can be improved at most by a factor $1/m$ [25]. Below we find that with at most n photons in a single mode the best sensitivity scales as $\propto 1/n$; one can thus achieve for given maximum photon number nm the same sensitivity scaling as $\propto 1/(nm)$ as with m modes (for a strict proof see appendix A). In [38] the problems of positioning and clock synchronization were analyzed. They were reduced to measuring a travel time of a light pulse with constant c, which is closely related to measuring c for a known propagation distance. Also there it was shown that the best uncertainty in the arrival time of the pulse for a squeezed m-mode state scales as $1/(nm)$. Furthermore, using the Margolus–Levitin quantum speed limit theorem, it was argued in [38] that this is the optimal scaling possible for any state. The scaling $\propto 1/\bar{n}$ for large average photon number $\bar{n}$ was also obtained for phase estimation with two-mode squeezed light in [39]. As for relativistic effects, if we are interested in knowing c in a given space-time region, they cannot be diluted by using several modes in parallel in different space-regions or sequentially. We can thus restrict ourselves to studying a single mode. For concreteness, we consider a cubic cavity with edges of length L, and perfectly reflecting walls or symmetric boundary conditions.

Maxwell's equations in vacuum with appropriate boundary conditions impose quantized modes with wave vectors $\boldsymbol{k}$ that are independent of c, whereas the frequency $\omega = c|\boldsymbol{k}|$. Obtaining the best possible precision of c is thus equivalent to the optimal frequency measurement of a harmonic oscillator, for which the quantum Cramér–Rao bound was calculated in [40]. The smallest $\delta\omega/\omega$, and hence smallest $\delta c/c$ for fixed maximum excitation $2n$ and for $\tau = \omega t \gg 1$, is achieved with the optimal state $|\psi_{\rm opt}\rangle = (|0\rangle + |2n\rangle)/\sqrt{2}$. In a single measurement, it leads to a minimal c-uncertainty

$$\frac{\delta c}{c} \simeq \frac{1}{2\tau n}. \tag{1}$$

For existing measurements with large n, coherent states are more relevant than the optimal state. A coherent state with amplitude α at time $t = 0$, $|\psi_{\rm coh}\rangle = |\alpha\rangle$, evolves according to $\alpha(t) = \alpha e^{-i\omega t}$ [41] and leads to

$$\frac{\delta c}{c} = \frac{1}{2}\frac{1}{|(\frac{1}{2}+n)\sin^2\tau + n\tau(\tau+\sin(2\tau))|^{1/2}} \simeq \frac{1}{2\tau\sqrt{n}}, \tag{2}$$

where the last equality is for large $\tau = \omega t$ and large average photon number $n = \alpha^2$ ($\tau^2\alpha \gg 1$) [40].

From these results one is tempted to conclude that $\delta c/c$ can be made arbitrarily small by increasing n. However, the energy-momentum tensor increases $\propto n$ for $n \gg 1$, and will at some point perturb itself the metric of space-time. We argue that the ultimate sensitivity is reached when the general relativistic modification of space-time becomes comparable to the minimal quantum uncertainty of the measurement. This leads to a finite optimal number of photons, and a finite optimal sensitivity. Increasing the photon number even more will modify space-time to a point where one cannot speak of light propagation in vacuum anymore. In principle one may re-calculate from the measured value using GR what the speed of light in vacuum *would* be, but this is a counterfactual reasoning and not a direct measurement of c. On the other hand,

reducing the photon number would increase the quantum noise. The situation is very similar to the optimization of the photon number in LIGO-type gravitational wave interferometers, where one balances photon-shot noise against radiation pressure noise [42–44]. However, whereas radiation pressure noise is specific to the measurement instrument, in our case the properties of space-time itself and thus the very meaning of light propagation in vacuum are affected when increasing the photon number further, and this effect is unavoidable.

The gravitational effects sought here are well in the regime where Einstein's field equations are valid: Firstly, we consider light at wavelengths λ and structures of the energy-momentum tensor on scales much larger than the Planck-length (e.g. $\lambda = 500$ nm and a standard (possibly lossy) cavity of size $L = 1$ km). Secondly, we consider light fields of very large intensity and effects linear in the perturbation of the metric, for which the energy-momentum tensor should be well approximated by its quantum mechanical expectation value [45]. It is the effect of this average energy-momentum tensor on space-time that we calculate and compare to the minimal uncertainty of c obtained from q-pet, not the fluctuations of space-time themselves. The former is established on the solid ground of general relativity, whereas the latter would require a quantum gravity theory to make reliable predictions. The quantum fluctuations that we *are* interested in here are those of light probing the space-time, which are reliably described by quantum optics. Our results therefore rely only on well-tested theories, in distinction to predictions of the fluctuations of space-time obtained by various theories of quantum gravity.

3. Perturbation of metric due to light intensity

The modification of the metric of space-time is found from the weak field limit of the Einstein field equations, where the metric tensor is given by $g_{\mu\nu} = \eta_{\mu\nu} + h_{\mu\nu}$, i.e. the flat Minkowski metric $\eta_{\mu\nu} = \mathrm{diag}(-1,1,1,1)$ (in terms of ct, x, y, z) plus a small perturbation, $|h_{\mu\nu}| \ll 1$. Einstein's equations yield a wave equation for the trace inverse, $\bar{h}^{\mu\nu} = h^{\mu\nu} - \frac{1}{2}\eta^{\mu\nu}\eta^{\alpha\beta}h_{\beta\alpha}$,

$$\Box\bar{h}^{\mu\nu} = -16\pi\frac{G}{c^4}T^{\mu\nu}, \tag{3}$$

where the (flat space-time) Lorenz gauge (FLG) condition $\bar{h}^{\mu\nu}{}_{,\nu} = 0$ is used; see equation (18.8b) in [46]. The energy-momentum tensor $T^{\mu\nu}$ of the e.m. field reads [46]

$$\begin{aligned} T^{00} &= \frac{1}{2}(\epsilon_0\boldsymbol{E}^2 + \mu_0\boldsymbol{H}^2), \quad T^{0i} = T^{i0} = \frac{1}{c}(\boldsymbol{E}\times\boldsymbol{H})_i, \\ T^{ij} &= -(\epsilon_0 E_i E_j + \mu_0 H_i H_j) + T^{00}\delta_{ij}, \end{aligned} \tag{4}$$

where $i,j \in \{1,2,3\} = \{x,y,z\}$. We use the q.m. expectation value of $T^{\mu\nu}$ as source term in (3) for the (0 1 1) and the (01M) modes ($k_i = l_i\pi/L$, $l_x = 0, l_y = 1$, and $l_z = 1$ or $l_z = M$, respectively; $\Omega_l = c|\boldsymbol{k}|$, and $V = L^3$). This 'semiclassical approximation' is justified if one is interested only in effects to first order in $h_{\mu\nu}$ [45]. Using the (0 1 1) mode is motivated by the fact that it has lowest frequency and hence expected lowest GR impact. This will be verified by comparing to the (01M) mode with large M. For $|\psi_{\mathrm{opt}}\rangle$ with $n \gg 1$, the solution of (3) for the (0 1 1) mode reads ($\boldsymbol{\xi} = \pi\boldsymbol{x}/L$)

$$\begin{aligned} \bar{h}^{\mu\nu}(\boldsymbol{\xi}) &= \mathcal{P}\int_0^\pi\int_0^\pi \mathrm{d}\eta'\mathrm{d}\zeta' I(\xi, \eta-\eta', \zeta-\zeta')t^{\mu\nu}(\eta',\zeta'), \\ \mathcal{P} &= \frac{4\sqrt{2}n}{\pi}\kappa, \qquad \kappa = \left(\frac{l_{\mathrm{Pl}}}{L}\right)^2, \end{aligned} \tag{5}$$

$$I(\xi,\eta,\zeta)=\ln\left(\frac{\xi+\sqrt{\xi^2+\eta^2+\zeta^2}}{\xi-\pi+\sqrt{(\xi-\pi)^2+\eta^2+\zeta^2}}\right), \tag{6}$$

with dimensionless trigonometric functions $t^{\mu\nu}:=T^{\mu\nu}/(n\hbar\Omega_l/V)$ of order one inside the cavity, and zero outside (see appendix B). $T^{\mu}_{\mu}=0$ for the e.m. field [47], hence $h^{\mu}_{\mu}=0$ and $h^{\mu\nu}=\bar{h}^{\mu\nu}$.

The deviations of $\bar{h}^{\mu\nu}$ in (5) from FLG are of second order in h and can be neglected [48]. For $|\psi_{\rm coh}\rangle$, $\bar{h}^{\mu\nu}$ is the same as for $|\psi_{\rm opt}\rangle$ plus retarded oscillation on top of it, with an amplitude of the same order. We therefore restrict the analysis to the time-independent part. For the $(01M)$ mode, and $n,M\gg 1$, only h^{00} and h^{33} are non-negligible,

$$h^{00}=h^{33}\simeq 4\mathcal{P}M\int_0^{\pi}\int_0^{\pi}\mathrm{d}\eta'\mathrm{d}\zeta' I(\xi,\eta-\eta',\zeta-\zeta')\sin^2\eta'.$$

From the geodesic condition $\mathrm{d}s^2=g_{\mu\nu}\mathrm{d}x^{\mu}\mathrm{d}x^{\nu}=0$, the local modification of the coordinate speed of light

$$\delta c(x)/c=-\frac{1}{2}(h_{00}+h_{11}) \tag{7}$$

is obtained for the $(0\,1\,1)$ mode, with similar expressions for $\delta c(y)$ and $\delta c(z)$ (see also figure B1 in appendix B). For the $(01M)$ mode with $n,M\gg 1$, $\delta c(x)/c=\delta c(y)/c=-\frac{1}{2}h_{00}$, $\delta c(z)/c=2\delta c(x)/c$. One may object that according to the equivalence principle one could always find a coordinate system (CS) in which $c(x)=c(y)=c(z)=c$, and that by the definition of c one *should* go to the free falling CS for measuring c, where c is always the same. However, one has to distinguish between the universal constant c entering Lorentz-transformations, and the experimental value $c_{\rm exp}$ of the propagation speed of light obtained in measurements. The experimental definition of c, $c_{\rm exp}=\Delta x/\Delta t$, where Δx is the distance that a light signal travels in time Δt implies that for any finite Δx the measurement is non-local, which precludes transforming the discussed GR effect away by a local transformation. It is to be expected that this non-local effect can be made arbitrarily small by moving the two points arbitrarily close to each other. More importantly, however, the measurement apparatus cannot be free falling in the gravitational field of the light it contains, as it carries that light with it. A time delay can be measured with a single clock by passing a short light pulse through a beam splitter (BS), reflecting it on a mirror and sending it back to the BS. The two passes through the BS trigger start/stop of the clock by light scattered into detectors adjacent to the BS. The clock measures its proper time, $\mathrm{d}\tau=\sqrt{-g_{00}}\mathrm{d}t$. Δx has to be measured independently, i.e. with standard measurement rods. Hence, Δx corresponds to the 'proper length' of the apparatus (distance between BS and mirror for a runtime experiment or length of the cavity when using $\omega=ck$). 'Proper length' (not to be confused with 'proper distance') is defined as the length measured with standard measurement rods in the frame where the object is at rest [49]. We may assume the measurement rods as well as the measurement apparatus as sufficiently 'rigid' (gravitational forces and modification of the e.m. forces that determine the shapes of these objects much smaller than the e.m. forces that determine their shape and arrangement [50, 51]), which means that Δx remains unchanged when the light intensity is increased. In the limit $R\gg L$ ($R=$ typical radius of curvature of space time), the experimentally found value $c_{\rm exp}(x)=\Delta x/\Delta\tau\simeq \mathrm{d}x/\mathrm{d}\tau=c(x)/\sqrt{-g_{00}}$ is then directly related to the coordinate speed $c(x)$ determined above. This gives $\delta c_{\rm exp}/c=-h_{11}/2$ for the $(0\,1\,1)$ mode, where $\delta c_{\rm exp}(x):=c_{\rm exp}(x)-c$ can be considered a systematic error in the determination of c.

Since q-pet was based on the uncertainties $\delta\omega$, we also compare q-pet and GR based on the GR shift of the cavity resonance frequencies by solving the e.m. wave equation in the entire cavity with mirrors at $0, x_L$ and symmetric boundary conditions (SBC), $A^\mu(0,y,z) = A^\mu(x_L,y,z)$ (and correspondingly for the other directions). The unperturbed single modes are plane waves $A^3(t,x,y,z) = (\hbar/(2\omega\epsilon_0 V))^{1/2}(\mathrm{e}^{\mathrm{i}k(x-ct)}a + \mathrm{h.c.})$, $A^\mu = 0$ for $\mu \in \{0,1,2\}$, and $k := k_0 = k_1 > 0$. This leads to $T^{\mu\nu} = -\hbar\omega/(2\epsilon_0 V)\langle(a\,\mathrm{e}^{\mathrm{i}k(x-ct)} + \mathrm{h.c.})^2\rangle$ for $(\mu,\nu) \in \{00,01,10,11\}$ inside the cavity, and $T^{\mu\nu} = 0$ else or outside. For $|\psi_{\mathrm{opt}}\rangle$, $T^{\mu\nu}$ is time-independent, and for $|\psi_{\mathrm{coh}}\rangle$ we once more consider only the time-independent part. Then, $h^{\mu\nu}(\boldsymbol{\xi}) = \epsilon(\boldsymbol{\xi})$ for $(\mu,\nu) \in \{00,01,10,11\}$ and $h^{\mu\nu} = 0$ else, where

$$\epsilon(\boldsymbol{\xi}) := \sqrt{2}\mathcal{P}M \int_0^\pi \int_0^\pi \mathrm{d}\eta'\mathrm{d}\zeta' I(\xi, \eta-\eta', \zeta-\zeta'). \tag{8}$$

The wave equation describing the propagation of light in curved space-time reads $\nabla_\beta F^{\alpha\beta} = 0$ (see (22.17a) in [46]), with $F^{\alpha\beta} = g^{\alpha\mu}g^{\beta\nu}(A_{\nu,\mu} - A_{\mu,\nu})$. Using FLG for A and h, and $h^\nu_\nu = 0$, we obtain to first order in ϵ

$$0 = -A^{\alpha,\nu}{}_{,\nu} + (h^\alpha_{\mu,\nu} - h^\alpha_{\nu,\mu})A^{\mu,\nu}, \tag{9}$$

where indices are pulled up or down by the full metric $g^{\mu\nu}$. Equation (9) is solved exactly by the original plane wave despite the changed metric, as the ϵ-correction in A^3 is $\propto (\partial_x + \partial_{ct})^2$. This reflects the well-known result that two parallely propagating beams of light do not affect each other gravitationally [52, 53]. The existence of a mode with unchanged dispersion relation suggests that judging whether the vacuum may still be considered as such based on the change of a single mode frequency can be insufficient. In such a case, the change of the metric can normally still be probed using other modes. In the example above the frequencies of modes propagating in different directions, e.g. $A^3 \propto \exp(\mathrm{i}k(x+ct))$, are modified locally by a relative amount of order $\epsilon(\boldsymbol{x})$, as can be shown by solving (9) in eikonal approximation.

To summarize, up to numerical prefactors of order 1, both systematic errors δc_{exp} obtained by measuring length over time or a shift of a cavity resonance, possibly in another mode, scale as

$$\frac{\delta c_{\mathrm{exp}}}{c} \sim -\kappa\, n\, M \tag{10}$$

for $n, M \gg 1$. With this, we can now obtain the smallest possible uncertainty with which c can be determined in a given region of space-time.

4. Minimal uncertainty of speed-of-light measurements

For $|\psi_{\mathrm{opt}}\rangle$, equating (1) and the absolute value of (10) leads with $M \sim L/\lambda$ to an optimal photon number $n_{\mathrm{opt}} \sim (\lambda/l_{\mathrm{Pl}})\sqrt{L/(cT)}$, and a minimal

$$\frac{\delta c}{c} \sim \frac{l_{\mathrm{Pl}}}{(c\,T\,L)^{1/2}}, \tag{11}$$

independent of frequency: the gain in quantum mechanical sensitivity due to longer dimensionless evolution time for more energetic photons is exactly cancelled by the increased perturbation of the metric.

In an experiment, the measurement time is bounded from above by the finite photon-storage time of the photons in the cavity. While obtaining optimal bounds including photon loss requires mixed state q-pet [54, 55], the sensitivity cannot be better than that obtained from the

pure states from which the state is mixed [56]. For known dissipation and decoherence mechanisms one can try to find an adapted optimal state. However, the sensitivity cannot be better than if one had access to the full system and its environment. For photon loss the environment can be modelled by additional modes coupled to the central mode by beam-splitter couplings, and including such ancilla modes cannot improve the estimation of a parameter of the original system when optimized over all initial states [57, 58], if the ancillas are independent of the c we are interested in (which is the case for the modes outside the cavity and hence outside the space-time region considered). Our q-pet bound calculated for the ideal situation without photon loss therefore remains valid, but can in general in the presence of dissipation or decoherence not be reached anymore. For a cavity of length L and finesse F, the measurement time is bounded by $T = LF/(\pi c)$. This leads to an optimal number of photons *independent of the length of the cavity*, $n \sim \lambda/(l_{\rm Pl}F^{1/2})$. For numerical estimates we use in the following a standard situation: visible light with $\lambda = 500$ nm, a finesse $F = 10\,000$, and $L = 1000$ m. The optimal n for the optimal state is then $n \sim 10^{26}$, and the minimal uncertainty $\delta c/c \sim l_{\rm Pl}/(LF^{1/2}) \sim 10^{-40}$.

For $|\psi_{\rm coh}\rangle$, equating (2) and (10) leads to $n_{\rm opt} \sim (L\lambda^2/(l_{\rm Pl}^2 cT))^{2/3}$, and a minimal uncertainty

$$\frac{\delta c}{c} \sim \left(\frac{l_{\rm Pl}^2\lambda}{L(cT)^2}\right)^{1/3}. \tag{12}$$

For a cavity with finesse F, the length of the cavity is again irrelevant for the optimal photon number, $n_{\rm opt} \sim (\lambda/l_{\rm Pl})^{4/3}/F^{2/3}$, and $\delta c/c \sim l_{\rm Pl}^{2/3}\lambda^{1/3}/(LF^{2/3})$. Contrary to $|\psi_{\rm opt}\rangle$, the minimal uncertainty depends here on the wavelength. In principle, $\delta c/c$ could therefore be smaller for $|\psi_{\rm coh}\rangle$ than for $|\psi_{\rm opt}\rangle$, but only for wavelengths $\lambda < l_{\rm Pl}\sqrt{cT/L}$ in lossless cavities, and for $\lambda < l_{\rm Pl}\sqrt{F}$ in cavities with finesse F, which are outside the validity of the theory. For the lossy cavity considered, the optimal coherent state photon number is $n \sim 10^{35}$ and $\delta c/c \gtrsim 10^{-31}$, demonstrating the superiority of $|\psi_{\rm opt}\rangle$. We display the various n-scaling regimes and the optimal photon numbers located at the minima of the overall dependence of $\delta c/c$ on n in figure 1.

5. Comparison with similar bounds

The minimal uncertainties of c and hence the metric of flat space-time that we have derived are reminiscent of ideas about the fuzziness of space-time on the Planck scale, their different physical meaning not withstanding. The minimal uncertainty of δc that we have derived here translates, in experiments where a length L is measured through $L = cT$, to fluctuations δL of L. There has been a vast amount of work aiming at demonstrating a minimal length scale in physics and working out its consequences, see [59] for an excellent review. The majority of these works has tried to establish smallest uncertainties of positions or length measurements, but there have also been attempts to find minimal uncertainties of volumes, areas, gravitational fields, event horizons, and others. Here we focus on previous predictions of minimal uncertainties of lengths or positions. For simplicity we set $\hbar = c = 1$ in the rest of this section and neglect factors of order 1, unless otherwise noted.

5.1. Previous thought experiments

Closest to our analysis are previous thought experiments that one way or another use classical gravity effects to bound quantum uncertainties from below. An illustrative example is the Heisenberg microscope with gravity [60]. In addition to the familiar Heisenberg microscope,

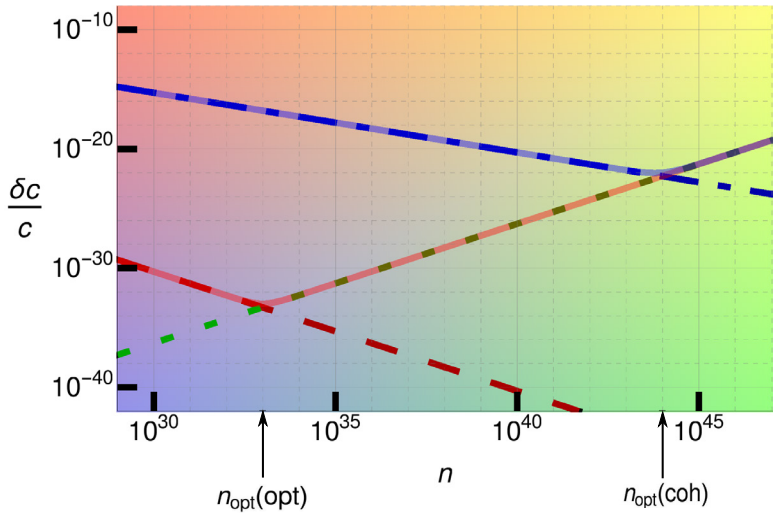

Figure 1. Minimal uncertainty $\delta c/c$ as a function of the number of photons n: The dashed red/blue line shows the minimal uncertainty obtained from the quantum Cramér–Rao bound for the optimal and coherent states given in equations (1) and (2), respectively. The dashed green line corresponds to the unavoidable systematic error in the measurement of c due to the light's own gravitational effect. The sum of the minimal uncertainty given by the quantum Cramér–Rao bound and the systematic error for the optimal/coherent state is shown by the solid orange/light blue lines. The optimal number of photons minimizing $\delta c/c$ for either optimal or coherent states lies at the minima of the solid orange/light blue lines. Parameters are $\lambda = 500$ nm, $\tau = 1$, $L = 1$ km und $M = L/\lambda$.

where attempts to resolve the position of a particle by scattering light from it result in an unknown momentum kick of order ω onto the particle, while limiting the spatial resolution to roughly the wavelength of the light $\delta x_{QM} \sim 1/\omega$, one also considers the gravitational interaction of the photon with the particle. This leads to an acceleration of the particle of at least $G\omega/R^2$ if the photon is detected at distance R, and a corresponding displacement between the photon-particle interaction and the photon detection of order $\delta x_{GR} \sim G\omega$. Taking the geometric mean of the two uncertainties gives immediately $\delta x \sim \sqrt{G} = l_{\mathrm{Pl}}$. Alternatively, we can take the sum of the two uncertainties and minimize it over ω. This gives $\omega \sim 1/\sqrt{G} = m_{\mathrm{Pl}}$, the Planck mass, and, up to a factor 2, again $\delta x \sim l_{\mathrm{Pl}}$.

Another popular argument goes back at least to Bronstein in 1936 [61], who, in the context of investigating how precisely a gravitational field might possibly be measured, came up with the request that the test particle should not collapse to a black hole. Later, Wigner and Salecker introduced a similar limitation to length measurements with light pulses [33, 34], where the clock should not become a black hole. The idea was refined for the measurement of lengths based on 'material reference systems' (MRS) [36], consisting of reference points of size s and mass M that contain a clock, light-gun and detector, arranged in space. The request that no event-horizon should form around the reference points beyond s implies $M < s/l_{\mathrm{Pl}}^2$.

We can apply the black-hole argument to the Heisenberg-microscope, requesting that the photon's event horizon should be at least smaller than the distance R, i.e. $\omega < R/l_{\mathrm{Pl}}^2$. Then $\delta x_{\mathrm{QM}} \gtrsim l_{\mathrm{Pl}}^2/R$, a bound obviously much weaker than the previous one for $R \gg l_{\mathrm{Pl}}$. On the other hand, for the MRS the black-hole criterion leads again to $\delta L \gtrsim l_{\mathrm{Pl}}$ if we assume $s \sim L$ and argue that the quantum mechanical uncertainty for a material particle scales as $\delta L \gtrsim \sqrt{L/M}$.

This latter scaling is based on a semi-classical picture [36] with an initial width of a wave-package leading to a minimal width in momentum space, that is interpreted as particles spreading out with a corresponding momentum distribution, giving a correspondingly larger uncertainty for the position measurement at a later time T. The argument can be made more rigorous by minimizing the quantum-mechanically calculated expectation value $\langle \delta x(0)\delta x(t)\rangle$ of a particle by minimizing over its mass [62]. One also recognizes in $\delta L \gtrsim \sqrt{L/M}$ the standard quantum limit (SQL), and in particular for $M = N\omega$ for a device dominated by the mass of N photons a scaling with $1/\sqrt{N}$.

5.2. Quantum gravity theories and phenomenological models

For most microscopic theories of quantum gravity it is difficult to extract bounds on minimal uncertainties of lengths. In [59], a generalized uncertainty principle (GUP) of the form $\delta x^\nu \delta p^\nu \gtrsim 1 + l_s E$ is given as a prediction of string theory, as well as a space-time uncertainty $\delta x \delta T \gtrsim l_s^2$, where l_s is a (yet unknown) string scale that might be of the order of $l_{\rm Pl}$, and E the energy with which the string is tested. In [15] it was stated that Lie-algebra non-commutative space-times with non-commuting position coordinates, $[x_\alpha, x_\beta] = \mathrm{i}R^\gamma_{\alpha\beta}x_\gamma/m_{\rm Pl}$, lead to a δT of the form $\delta T \sim L^n E^m/m_{\rm pl}^{1+m-n}$ where m, n are some model-dependent powers with $1 + m - n > 0$. The lowest-order non-trivial case $n = m = 1$ that gives an energy dependence, corresponds to $\delta T \sim LE/m_{\rm Pl}$. Considering T as the travel time of a particle from source to detector, δT implies an uncertainty of the radar length. Combining this δT with the standard contribution from the Heisenberg uncertainty principle and minimizing over the energy gives a minimal length uncertainty that can be written in the form

$$\delta L \gtrsim l_{\rm Pl}^\alpha L^{1-\alpha} \tag{13}$$

with some real value $\alpha \in [0, 1]$ [15].

Given the mentioned difficulty to extract predictions of fluctuations of positions or lengths from microscopic quantum gravity theories, mostly phenomenological GUPs have been used to generalize lower bounds based on the standard uncertainty principle. It is clear from dimensional grounds that (13) is the generic form of a power law scaling with $l_{\rm Pl}$ if only $l_{\rm Pl}$ and L exist as length scales. Such a form is therefore also obtained in many other phenomenological theories, notably models that assume fluctuations on the scale of the Planck length and then ask how these accumulate during the propagation of a light signal. The simplest case are random walk models, which lead to $\alpha = 1/2$ [63, 64]; $\alpha = 2/3$ is known as the holographic model. If one assumes a fluctuation $\delta\lambda$ of the wavelength λ of the light used to measure distances with $\alpha = 1/2$, $\delta\lambda \gtrsim l_{\rm Pl}(\lambda/l_{\rm Pl})^{1/2}$, the fluctuations of the total length are given in the random walk model by $\delta L \gtrsim \delta\lambda(L/\lambda)^{1/2} = l_{\rm Pl}^{1/2}L^{1/2}$, i.e. the new length-scale λ drops out. However, if the fluctuations $\delta\lambda$ are added up coherently, i.e. all with the same sign, a much larger value results,

$$\delta L \gtrsim (l_{\rm Pl}L)^{1/2}(L/\lambda)^{1/2}. \tag{14}$$

The choice of model has therefore important implications for the falsifiability of the predicted minimal fluctuations. E.g. in [65] the coherence of Hubble-space telescope images of distant galaxies was used to bound possible quantum fluctuations of space-time from below. No fluctuations were found, but the coherent addition of the fluctuations was subsequently questioned [66].

Modified commutation relations lead in general to a generalized uncertainty principle. In as much as this implies a fluctuating speed of light, Lorentz invariance can be violated, but need not (see e.g. the model of discrete space-time with modified commutation relations without violation of Lorentz invariance due to Snyder in 1947 [3]). In the same way, the (deterministic) dispersion relation of e.m. waves can be modified; such theories have become known as 'rainbow gravity'. This class of theories contains doubly (or deformed) special relativity (DSR), with a kappa-deformed Poincaré group [67–72]. DSR is based on the idea that not only the speed of light is independent of the reference-frame, but also the small length-scale $l_{\rm QG}$ on which quantum-gravity effects become important, identified typically with the Planck-length. DSR has recently been elaborated further into 'relative locality' [73], a theory that emphasizes the importance of phase-space and suggests that momentum-space might be curved, which would imply non-linear conservation laws of energy and momentum, and a relativity of 'locality'. Another formulation of DSR considered an energy-dependence of space-time [74, 67]. Earlier theories also proposed a time-dependent speed of light as solution to cosmological problems [75, 76].

In [77, 78] it was proposed that a non-linear dispersion relation might arise from averaging a quantum-fluctuating metric over a relevant length scale of a test particle. Considering a 'measurement process' in relativistic rather than quantum terms, it was suggested that the metric relevant for a measurement process of the momentum p_α of a particle with energy E is the 'classical' metric of GR plus an averaged perturbation of quantum-gravitational origin, assumed non-vanishing when averaging over the de Broglie wavelength $\lambda = 1/E$ of a deeply relativistic particle, thus introducing an extra energy-dependence into the (inverse) dispersion relation $p_\alpha(E)$.

In [79] a modified dispersion relation was found in the context of a non-critical-string approach to quantum gravity. It leads to a minimal total uncertainty of a length measurement based on the propagation of massless particles

$$\delta L \gtrsim \sqrt{\eta L l_{\rm Pl}} + l_{\rm Pl}, \tag{15}$$

where η is a dimensionless parameter of order one, and clearly the first term dominates for $L \ll l_{\rm Pl}$, giving (13) with $\alpha = 1/2$, but $\alpha = 1$ for $L \simeq l_{\rm Pl}$. Underlying (15) is an assumption about the form of a decoherence-term in the modified quantum Liouville equation that arises from coupling matter to the degrees of freedom of space-time fluctuations that scales as $E^2/m_{\rm Pl}$ with Planck-mass $m_{\rm Pl}$ and energy E of a particle. When generalizing this to a scaling $E^n/m_{\rm Pl}^{n-1}$, a dependence

$$\delta L \gtrsim L^{1/n} l_{\rm Pl}^{1-1/n} \tag{16}$$

was predicted, which is again of the form (13).

In [80], it was argued that a finite minimal uncertainty of time measurements is linked to the perturbative approach to quantization, whereas in a non-perturbative approach in principle infinite resolution could be achieved, as long as particle energies are not bound from above (as might happen with a modified dispersion relation). On the other hand, the authors find a finite minimum resolution both in perturbative and non-perturbative approaches, with a minimum length uncertainty

$$\delta L \gtrsim l_{\rm Pl}, \tag{17}$$

whereas for large background times $\bar{T}$

$$\delta L \gtrsim \sqrt{l_{\rm Pl} c \bar{T}}, \tag{18}$$

as in the Wigner–Salecker case [33, 34]. In [64], other estimates of length fluctuations were discussed, one of them scaling as $\delta L \gtrsim (l_{\rm QG}\, c\, T)^{1/2}$, where $l_{\rm QG}$ is expected to be $l_{\rm QG} \gtrsim l_{\rm Pl}$, which for $L = cT$ is again in line with (13) with $\alpha = 1/2$.

5.3. Comparison with our bounds

When trying to compare these previously found bounds with ours, the first thing to keep in mind, is that our bounds are fundamentally for $\delta c/c$, not $\delta L/L$. This is important as there is no quantum mechanical operator for the speed of light, hence one cannot apply directly the standard Heisenberg uncertainty principle. Rather, we resorted to q-pet, which gives generalized uncertainty relations [22]. Secondly, our bounds are based directly on the light field itself, not the quantum mechanical uncertainty in the position of a clock, an MRS point, or a test-particle. We have furthermore the choice of the state of the probe, notably it can be a multi-photon state, whereas previous derivations typically considered single-particle uncertainty relations, with a state that saturates Heisenberg's uncertainty relation. Moreover, since the QCRB is optimized over all possible measurements of the light field and has a clear interpretation in terms of the minimal uncertainty of an estimator of c, there are no conceptual issues with the meaning of the measurement on very small length scales. Questions on how fluctuations at smaller length-scale add up do not arise. In random-walk models one might wonder why one should add up fluctuations of the wavelength, as no measurements are made at that length scale. In the q-pet approach, measurements on the length-scale of the wavelength are included just as any other measurement of the light field, and the uncertainty is the one of the best possible estimator of c, rather than fluctuations of a measured observable (whose existence at a very small length scale might be questionable; this issue was indeed recognized as one of the most important ones in the field, see section 4.2.5 in [59]).

By using a light signal, another length-scale comes into play, namely the wavelength λ of the light, as well as the propagation time, which in a cavity can be much larger than the length of the cavity. Depending on the quantum state used, λ is still present in the final result for the lower bound.

If we do translate our bounds for $\delta c/c$ into a bound for fluctuations of length estimations δL by assuming $\delta L = T\delta c$ with fixed T, we see from (11) that for the optimal state we get back $\delta L \gtrsim l_{\rm Pl}$ for $L = c\,T$, i.e. this corresponds to $\alpha = 1$ in (13). However, for $T \gg L/c$, one can get uncertainties much smaller than the Planck length, a fact that was not reflected by previous bounds. This insight results naturally from the use of q-pet, where time appears as a resource for more precise measurements, in sync with experimentalists' habit to provide uncertainties per square root of Hz for fair comparison.

For a coherent state in a lossless cavity, the lower bound of δL implied by (12) reads $\delta L \gtrsim l_{\rm Pl}^{2/3}\lambda^{1/3}(L^2/(c\,T)^2)^{1/3}$. If $L = c\,T$, this is as (13) for $\alpha = 2/3$, but with L replaced by λ. One might wonder if there is a deeper reason behind the fact that a classical light signal reproduces the holographic model concerning the scaling of the smallest δL with $l_{\rm Pl}$. Compared to the coherently added up fluctuations equation (14), this is, in the optical domain, still a much smaller value for any L larger than about 10^{-12} m.

Given their fundamental measurement-based nature, our bounds can serve for judging the falsifiability of quantum gravity theories and phenomenological models: predictions of fluctuations in a given space-time region that are smaller than those given by our bounds can never be falsified through direct measurement *as a matter of principle* (subject to the made assumptions). While the prefactors depending on L, λ, T for the coherent state matter, as a rule of thumb, predictions of fluctuations with $\alpha > 2/3$ could not be measured with light in a

coherent state, as the measurements own smallest possible uncertainty $\propto l_{\rm Pl}^{2/3}$ is larger. Length uncertainties $\propto \sqrt{l_{\rm Pl}L}$ of Wigner–Salecka-type theories as well as the bound in (15) are at least in principle falsifiable with light in a coherent state. The fluctuations (16) cannot be measured with light in a coherent state as soon as $n > 3$, but they would be accessible at least in principle to 'quantum enhanced measurements' using the optimal quantum state of light. However, it is unlikely that an optimal state of light with a sufficiently large photon number can ever be built, given the experimental difficulties of producing superpositions of Fock states with even a few photons. The fluctuations predicted in [17] are well above our bounds for any cavity of realistic size.

Several works discussed the possibility to measure fluctuations of space-time created on the Planck-scale with gravitational wave interferometers such as LIGO [37, 64, 81]. Bounds on $l_{\rm QG}$ were obtained from experimental data from Caltech's 40 m interferometer [82]. In [81] it was argued that the stated displacement noise level of that interferometer of order $3 \cdot 10^{-19}$ m $\sqrt{\rm Hz}^{-1}$ in the neighborhood of 450 Hz already rules out length fluctuations of the interferometer arms of order $l_{\rm Pl}$ per Planck-time interval for the random-walk accumulation of individual Planck-cell fluctuations to a total uncertainty. References [10–16] attempted to bound the supposed quantum fluctuations of space-time using the broadening of light pulses from far-away astronomical sources, but so far the uncertainty in the emission time of the light pulses as well as other sources of spreading the pulse are too large to say much about quantum fluctuations of the metric [13].

6. Concluding discussion

Our results imply that *one should not think of quantum fluctuations of space-time as existing independently of the measurement devices that probe them*, but rather as something that can only be defined in conjunction with them. This is in line with the modern theory of quantum measurement, where the possible measurement results do not only depend on the quantum system, but also on the quantum probe and its initial quantum state.

Accordingly, we find different lower bounds for $\delta c/c$ for the optimal state and a coherent state. The former reproduces $\delta L \gtrsim l_{\rm Pl}$ when translated to the uncertainty of a length and assuming a measurement time $T \simeq L/c$, whereas the latter is substantially enhanced and still depends on the wavelength, scaling only as $l_{\rm Pl}^{2/3}$. Their derivation from standard quantum optics and GR is similar in nature to those of previous bounds based on Gedanken-experiments (see section 5.1) within QM and GR, but provides a conceptual advance by the use of q-pet, which includes the optimization over all possible measurements, and precise calculations rather than orders of magnitude arguments. Simple scaling arguments can be insufficient, as the discussions in the literature about how fluctuations on small scales add up on long distances have shown. Another example: in the Heisenberg microscope including gravity, one might arrange the particle half way between light source and detector. In that case the acceleration due to the gravitational pull will average to zero and it is not clear why the quantum uncertainty should be bounded from below by a gravitational effect—not to talk about questions of how the photon is supposed to be localized in space-time, when only its wavelength is specified. Such questions on how exactly the measurement is done, and whether a different setup might not avoid the limitations, do not arise in our q-pet approach.

Nevertheless, our bounds are of course subject to several (reasonable) restrictions as well: We consider direct measurements of the propagation speed or phase speed of an e.m. wave. Note, however, that the QCRB bounds the uncertainty for any measurement and estimation scheme,

as long as c is imprinted on the quantum state through the standard time evolution in quantum optics with (A.1) as hamiltonian. Ambiguities arising from a proper definition of arrival time of the pulse pertain to the level of different data analysis schemes and are fully covered by the QCRB.

We want to know the value of c in a given region of space-time, and we assume a sufficiently rigid measurement apparatus whose length remains unchanged when the photon number is increased. Apparatuses with finite rigidity could deform under the influence of the gravity of the light signal and the modification of Coulomb's law. For any realistic material that deformation should be negligible, however, compared to the one due to the light pressure; this will be examined in more detail in another publication [83]. The gravitative effect of the elastic energy was already shown in [50] to be smaller than the one of the e.m. field by a factor c_s/c, where c_s is the speed of sound in the cavity walls. We rely on the validity of quantum mechanics (more precisely quantum optics and q-pet) and GR in semiclassical approximation (i.e. $T^{\mu\nu}$ calculated as q.m. expectation value), and the validity of the linear dispersion relation $\omega = ck$ for wave-lengths well above the quantum-gravity/Planck length. For finding the optimal state, we assume a maximum possible photon number in the state. We neglect uncertainties in c due to the expansion of the Universe [51], non–inertial observers, local gravitation potentials e.g. from Earth or a (stochastic) gravitational-wave (GW) background [84], and quantum fluctuations of the mirror positions. In the quantum foam picture, also the latter should depend on the way they are measured, but in any case can only lead to reduced precision. The GW background at optical frequencies is expected to be extremely small, but might dominate at frequencies around 100–1000 Hz, where a large number of gravitational sources is expected to exist, see [85]. However, to cavities much shorter than the GW wavelength (300–3000 km for the above frequencies), the modified metric due to the GW appears as uniform, and the GW effect can hence in principle be eliminated by a cavity in free fall, in contrast to the GR effect of the light inside the cavity. More generally, any additional source of modification of the speed of light may lead to tighter lower bounds on the uncertainty of $\delta c/c$ than ours, but will not invalidate them.

Acknowledgments

We thank Kostas Kokkotas, Nils Schopohl, Claus Zimmermann, Julien Fraïsse, Dennis Rätzel and Friedrich Wilhelm Hehl for discussions and a critical reading of the manuscript. The research of URF was supported by the NRF of Korea, grant Nos. 2014R1A2A2A01006535 and 2017R1A2A2A05001422.

Appendix A. Single mode reduction of q-pet

We here prove that very generally for a given maximum amount of energy the optimal quantum measurement of c can be reduced to measuring a single mode of fixed frequency put into the optimal state $|\psi_{\text{opt}}\rangle = (|0\rangle + |2n\rangle)/\sqrt{2}$. Starting point is the Hamiltonian H for the e.m. field, decomposed into modes labelled by a mode-index k, consisting of wave-vector $\boldsymbol{k}$ and polarization ϵ. Then

$$H = \sum_k \hbar\omega_k n_k = \hbar c \sum_k k n_k, \tag{A.1}$$

with angular frequency $\omega_k = ck$ and $k = |\boldsymbol{k}|$. The Hamiltonian has the general form $H = cG$ with a Hermitian generator $G = \hbar \sum_k k n_k$. It leads in a given state $|\psi\rangle$ and propagation over total time T to QFI [22]

$$I_c = 4\Delta G^2 T^2 \equiv 4(\langle G^2\rangle - \langle G\rangle^2)T^2. \tag{A.2}$$

Let $G = \sum_i e_i|i\rangle\langle i|$ be the spectral decomposition of G, and $|\psi\rangle = \sum_{i=1}^N c_i|i\rangle$, where we assume that $|1\rangle$ ($|N\rangle$) are the states of lowest (largest) energy available. Then $\Delta G^2 = \sum_{i=1}^N p_i e_i^2 - (\sum_{i=1}^N p_i e_i)^2$ with $p_i = |c_i|^2$ and $\sum_{i=1}^N p_i = 1$. The Popoviciu inequality [86] states $\Delta G^2 \leqslant (e_N - e_1)^2/4$. It is saturated for $p_1 = p_N = 1/2$, $p_i = 0$ else. The state $|\psi\rangle = (|1> + \mathrm{e}^{\mathrm{i}\varphi}|N>)/\sqrt{2}$ with an arbitrary phase φ saturates the inequality and thus maximizes I_c. If e_N or e_1 is degenerate, only the total probability for the degenerate energy levels is fixed to 1/2, and arbitrary linear combinations in the degenerate subspace are allowed. But the value of ΔG^2 remains unchanged under such redistributions, and we may still choose just two non-vanishing probabilities $p_1 = p_N = 1/2$. The derivation did not make use of the multi-mode structure of the energy eigentstates. Hence, exactly the same minimal uncertainty of c can be obtained by superposing the ground state of a single mode with a Fock state of given maximum allowed energy as with an arbitrarily entangled multi-mode state containing components of up to the same maximum energy. Setting $N = 2n$ leads to the announced optimal single-mode state.

Appendix B. Calculation of the metric perturbation

The vector potential of the e.m. field in the cavity in Coulomb gauge $\boldsymbol{A}(\boldsymbol{r}, t) = \Upsilon q(t)\boldsymbol{v}(\boldsymbol{r})$, where Υ is a constant, $q(t)$ the time dependent amplitude, and $\boldsymbol{v}(\boldsymbol{r})$ the mode function, with components

$$\begin{aligned} v_x &= \mathcal{N} e_x \cos k_x x \sin k_y y \sin k_z z, \\ v_y &= \mathcal{N} e_y \sin k_x x \cos k_y y \sin k_z z, \\ v_z &= \mathcal{N} e_z \sin k_x x \sin k_y y \cos k_z z. \end{aligned} \tag{B.1}$$

The polarization vector $\boldsymbol{e} = (e_x, e_y, e_z)$ is normalized to length one, and is orthogonal to the $\boldsymbol{k}$-vector $\boldsymbol{k} = (k_x, k_y, k_z)$, where $k_i = l_i\pi/L$, and $l_i \in \mathbb{N}_0$, and at most one of three given l_i can be zero. Therefore, there are two polarization directions (transverse modes) for each $\boldsymbol{k}$ vector, with the exception of cases where one of the $l_i = 0$, where only one polarization is possible. The request that the modes be orthonormal,

$$\int \mathrm{d}^3 r \boldsymbol{v}_l(\boldsymbol{r}) \cdot \boldsymbol{v}_{l'}(\boldsymbol{r}) = \delta_{l,l'} \tag{B.2}$$

leads to $\mathcal{N} = \sqrt{8/V}$, and we can define the mode-volume $V_l = V/8$. Note that the index l stands here for both the discrete $\boldsymbol{k}$ vector and the polarization direction $(1, 2)$. Finally, we choose $\Upsilon = 1/\sqrt{\epsilon_0}$, such that

$$\begin{aligned} \boldsymbol{A}(\boldsymbol{r}, t) &= \sum_l \frac{1}{\sqrt{\epsilon_0}} q_l(t) v_l(\boldsymbol{r}), \\ \boldsymbol{E}(\boldsymbol{r}, t) &= -\sum_l \frac{1}{\sqrt{\epsilon_0}} \dot{q}_l(t) v_l(\boldsymbol{r}), \\ \boldsymbol{H}(\boldsymbol{r}, t) &= \sum_l \frac{1}{\mu_0\sqrt{\epsilon_0}} q_l(t) \nabla \times v_l(\boldsymbol{r}). \end{aligned} \tag{B.3}$$

After quantization, the amplitudes q_l become the quadrature operators of a harmonic oscillator, $\hat{q}_l = \sqrt{\frac{\hbar}{2\Omega_l}}(\hat{a}_l + \hat{a}_l^\dagger)$, $\hat{p}_l = \frac{1}{i}\sqrt{\frac{\hbar\Omega_l}{2}}(\hat{a}_l - \hat{a}_l^\dagger)$, where $\Omega_l = |\boldsymbol{k}_l|c$. In the semiclassical approach the energy-momentum tensor for a single mode with mode function $\boldsymbol{v}$ is given by the quantum mechanical expectation value [46, 87],

$$\begin{aligned} T^{00} &= \frac{\hbar\Omega}{4}\left(-\left\langle(\hat{a}-\hat{a}^\dagger)^2\right\rangle \boldsymbol{v}^2 + \left\langle(\hat{a}+\hat{a}^\dagger)^2\right\rangle (\nabla\times\boldsymbol{v})^2/k^2\right), \\ T^{0i} &= \frac{i\hbar\Omega}{2k}\left(\left\langle\hat{a}^2\right\rangle - \left\langle\hat{a}^{\dagger 2}\right\rangle\right)(\boldsymbol{v}\times(\nabla\times\boldsymbol{v}))_i, \\ T^{ij} &= \frac{\hbar\Omega}{2}\left(\left\langle\left(\hat{a}-\hat{a}^\dagger\right)^2\right\rangle v_i v_j,\right. \\ &\quad \left. -\left\langle\left(\hat{a}+\hat{a}^\dagger\right)^2\right\rangle (\nabla\times\boldsymbol{v})_i(\nabla\times\boldsymbol{v})_j/k^2\right) + T^{00}\delta_{ij}, \end{aligned} \tag{B.4}$$

where $k^2 = \boldsymbol{k}^2$, and we have used the symmetrized form $(\hat{q}\hat{p}+\hat{p}\hat{q})/2$ of the quantum mechanical operators for the T^{0i} components.

For a $(01M)$ mode, $l_x = 0, l_y = 1, l_z = M$ dictates $\boldsymbol{e} = (1,0,0)$ as unique possible polarization. For $M = 1$, the frequency $\Omega_l = \sqrt{2}\pi c/L$, and

$$\begin{aligned} \boldsymbol{v} &= \sqrt{\frac{8}{V}}\sin(\pi y/L)\sin(\pi z/L)\boldsymbol{e}_x, \\ \nabla\times\boldsymbol{v} &= \sqrt{\frac{8}{V}}\frac{\pi}{L}\sin(\pi y/L)\cos(\pi z/L)\boldsymbol{e}_y \\ &\quad -\sqrt{\frac{8}{V}}\frac{\pi}{L}\cos(\pi y/L)\sin(\pi z/L)\boldsymbol{e}_z. \end{aligned} \tag{B.5}$$

For $|\psi_{\rm opt}\rangle$ with $n \gg 1$, and neglecting terms of order $\mathcal{O}(n^0)$ (all other terms are of order n), we find that for the fundamental $(0\,1\,1)$ mode the only non-vanishing components of $T^{\mu\nu}$ can be expressed in terms of four functions,

$$T^{\mu\nu} = n\frac{\hbar\Omega_l}{V}t^{\mu\nu} \tag{B.6}$$

with the dimensionless tensor components $t^{00}(\eta,\zeta) = f_1(\eta,\zeta)$, $t^{11}(\eta,\zeta) = f_2(\eta,\zeta)$, $t^{22}(\eta,\zeta) = f_3(\eta,\zeta)$, $t^{33}(\eta,\zeta) = \tilde{f}_3(\eta,\zeta) = f_3(\zeta,\eta)$, $t^{23}(\eta,\zeta) = t^{32}(\eta,\zeta) = f_4(\eta,\zeta)$, and

$$\begin{aligned} f_1(\eta,\zeta) &= 2 - \cos(2\eta) - \cos(2\zeta) \\ f_2(\eta,\zeta) &= \cos(2\eta) + \cos(2\zeta) - 2\cos(2\eta)\cos(2\zeta) \\ f_3(\eta,\zeta) &= \frac{1}{2}(2 - 4\cos(2\zeta) + 2\cos(2\zeta)\cos(2\eta)) \\ f_4(\eta,\zeta) &= \sin(2\eta)\,\sin(2\zeta), \end{aligned} \tag{B.7}$$

where we write x, y, z in units of L/π, $\xi = x\pi/L$, $\eta = y\pi/L$, $\zeta = z\pi/L$, and thus $\xi, \eta, \zeta \in [0,\pi]$. Outside the cavity $T^{\mu\nu}$ vanishes. For this state the field equations are solved with a time-independent metric. The wave equation reduces to the Poisson equation,

$$\Delta\bar{h}^{\mu\nu} = -16\pi\frac{G}{c^4}T^{\mu\nu}. \tag{B.8}$$

The solution is obtained by integrating the inhomogeneity $T^{\mu\nu}$ over with the Green's function of the Poisson equation, i.e.

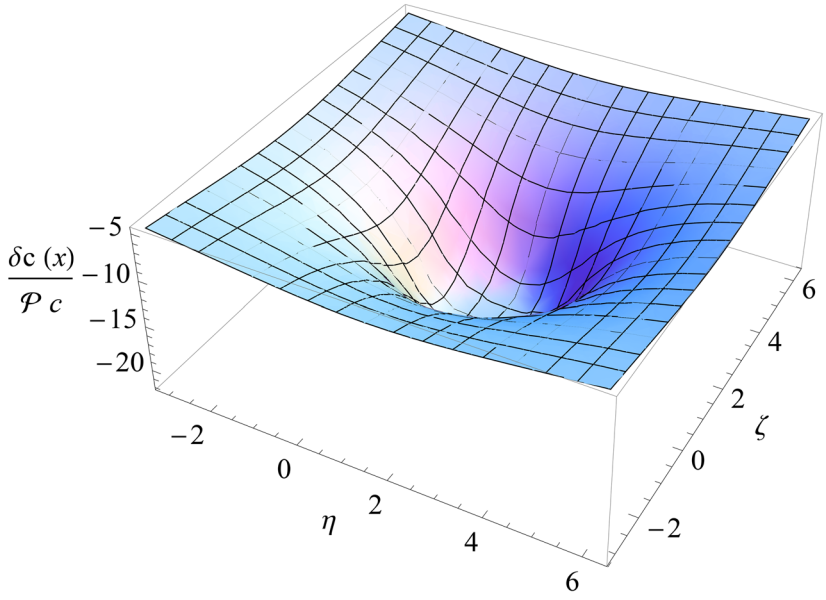

Figure B1. Relative change of the local coordinate speed of light in x-direction as function of dimensionless coordinates η, ζ at $\xi = 1.5$ in units of $\mathcal{P} = (4n/\pi)\kappa$ with $\kappa = (l_{\rm Pl}/L)^2$ (see equation (B.10)) for the (0 1 1) mode. The cavity extends from 0 to π in these units.

$$\begin{aligned}\bar{h}^{\mu\nu} &= \frac{4G}{c^4}\int \frac{T^{\mu\nu}(\boldsymbol{x}')}{|\boldsymbol{x}-\boldsymbol{x}'|}\mathrm{d}^3x' \\ &= \mathcal{P}\int_0^\pi\int_0^\pi \mathrm{d}\eta'\mathrm{d}\zeta' I(\xi,\eta-\eta',\zeta-\zeta')t^{\mu\nu}(\eta',\zeta'),\end{aligned} \tag{B.9}$$

where the parameter $\mathcal{P}$ is given by

$$\mathcal{P} = 4\sqrt{2}\frac{n\hbar G}{\pi c^3 L^2} = \frac{4\sqrt{2}n}{\pi}\kappa, \qquad \kappa = \left(\frac{l_{\rm Pl}}{L}\right)^2. \tag{B.10}$$

The integral kernel reads

$$I(\xi,\eta,\zeta) = \ln\left(\frac{\xi+\sqrt{\xi^2+\eta^2+\zeta^2}}{\xi-\pi+\sqrt{(\xi-\pi)^2+\eta^2+\zeta^2}}\right). \tag{B.11}$$

Numerical evaluation of the two remaining integrals in equation (B.9) shows that they are of order one inside the cavity, and decay rapidly outside, as is required by the boundary conditions of a flat metric far from the cavity.

For $|\psi_{\rm coh}\rangle$, we have to consider the full retarded solution of the wave equation according to

$$\bar{h}^{\mu\nu} = \frac{4G}{c^4}\int \frac{T^{\mu\nu}(t-|\boldsymbol{x}-\boldsymbol{x}'|/c,\boldsymbol{x}')}{|\boldsymbol{x}-\boldsymbol{x}'|}\mathrm{d}^3x'. \tag{B.12}$$

For example, the yz component reads $\bar{h}^{yz} = \bar{h}^{yz}_{\rm opt} + \frac{4n\hbar G\Omega}{c^4}\int \mathrm{d}\xi'\mathrm{d}\eta'\mathrm{d}\zeta' \frac{\sin[2\omega(t-|\boldsymbol{x}-\boldsymbol{x}'|/c)]\sin(2\eta')\sin(2\zeta')}{|\boldsymbol{x}-\boldsymbol{x}'|}$. This metric element is thus the solution of $|\psi_{\rm opt}\rangle$ (B.9) plus some retarded oscillation on top of it, which is of the same order. In the following we will therefore restrict our analysis to the time-independent part given by $|\psi_{\rm opt}\rangle$.

For the $(01M)$ mode, with $M > 1$, $l_x = 0, l_y = 1, l_z = M$, the general expressions for $T^{\mu\nu}$ are more complicated, but for $|\psi_{\rm opt}\rangle$ with $n \gg 2$, and in the limit of $M \gg 1$, we have $T^{00} = T^{33} = 4n(\hbar\Omega/V)\sin^2\eta$, $T^{11} = -T^{22} = 4n(\hbar\Omega/V)\sin^2\eta\cos(2M\zeta)$. Corrections are of order $1/M$. All other tensor elements of T vanish to order M^0. The rapidly oscillating term $\cos(2M\zeta)$ in T^{11}, T^{22} leads to a rapid decay of $\bar{h}^{11}$ and $\bar{h}^{22}$ as function of M. Numerics indicates that the decay is roughly as $1/M$ for fixed (ξ, η, ζ), including the factor M that is gained due to the prefactor $\Omega \propto M$ for large M. This means that for large n and M, only $T^{00} = T^{33}$ are non-negligible, with

$$\begin{aligned} \bar{h}^{00} &= \bar{h}^{33} \simeq \mathcal{P}M\tilde{h}(\xi,\eta,\zeta), \\ \tilde{h}(\xi,\eta,\zeta) &:= 4\int_0^\pi\int_0^\pi \mathrm{d}\eta'\mathrm{d}\zeta' I(\xi,\eta-\eta',\zeta-\zeta')\sin^2\eta', \end{aligned} \tag{B.13}$$

where the dimensionless function $\tilde{h}(\xi, \eta, \zeta)$ is once more of order 1 inside the cavity and falls off rapidly outside. So using a higher mode has the effect of reducing the perturbation of the metric essentially to two diagonal elements of the metric tensors, but increases the perturbation by a factor equal to the mode-index M.

In all cases, the amplitude of the space-time perturbation due to the e.m. field in the cavity scales as

$$\bar{h}^{\mu\nu} \sim \left(\frac{l_{\rm Pl}}{L}\right)^2 n\,M, \tag{B.14}$$

proportional to the number of photons n in the cavity, the mode index M, and the squared ratio $l_{\rm Pl}/L$ of Planck length $l_{\rm Pl} \simeq 1.62 \times 10^{-35}$ m and size L of the cavity. The expression remains valid for the fundamental mode with $M = 1$.

We note that throughout our analysis we tacitly assume that the photon densities in the cavity are small enough and the cavity sufficiently large, such that we stay well below the critical (electric) field strength $E_c = m_e^2c^3/(e\hbar) = 1.3 \times 10^{18}$ V m^{-1}, where m_e is the mass of the electron, beyond which nonlinear corrections to Maxwellian electrodynamics due to polarization of the quantum vacuum become important [88]. This condition may be translated into a minimal cavity size L using an energy density $\mathcal{O}(\hbar cnM/L^4)$ and a critical energy density $\mathcal{O}(\epsilon_0 E_c^2)$. We obtain that $L \gg (\hbar^{3/4}e^{1/2}\epsilon_0^{-1/4}m_e^{-1}c^{-5/4})(nM)^{1/4} = (2.1 \times 10^{-13}\ \mathrm{m})(nM)^{1/4}$ for linear electrodynamics in the cavity to hold. For the two types of cavities considered and all combinations of $n_{\rm opt}$ and M, the lower bound on L is satisfied by the cavity sizes considered.

From $h_{\mu\nu}$ we now calculate a local measure of the modification of the coordinate speed of light defined through the geodesics of the modified metric.

A finite $h_{\mu\nu}$ leads to a new line element

$$\mathrm{d}s^2 = -(1-h_{00})c^2\mathrm{d}t^2 + (1+h_{ii})(\mathrm{d}x^i)^2 + 2h_{23}dydz \tag{B.15}$$

where the metric elements are, for the (0 1 1) mode,

$$\begin{aligned} h_{00} &= \frac{1}{2}\mathcal{P}(g_1+g_2+g_3+\tilde{g}_3), \\ h_{11} &= \frac{1}{2}\mathcal{P}(g_1+g_2-g_3-\tilde{g}_3), \\ h_{22} &= \frac{1}{2}\mathcal{P}(g_1-g_2+g_3-\tilde{g}_3), \\ h_{33} &= \frac{1}{2}\mathcal{P}(g_1-g_2+\tilde{g}_3-g_3), \quad h_{23} = \mathcal{P}g_4, \end{aligned} \tag{B.16}$$

with the definitions, see (B.9),

$$g_i = \int_0^\pi \int_0^\pi \mathrm{d}\eta' \mathrm{d}\zeta' I(\xi, \eta - \eta', \zeta - \zeta') f_i(\eta', \zeta'),$$
$$\tilde{g}_i = \int_0^\pi \int_0^\pi \mathrm{d}\eta' \mathrm{d}\zeta' I(\xi, \eta - \eta', \zeta - \zeta') \tilde{f}_i(\eta', \zeta'). \tag{B.17}$$

For the $(01M)$ mode we have $h_{00} = h_{33}$ with h_{00} given by (B.16) whereas $h_{\mu\nu}$ vanishes for all other values of μ,ν. The light ray trajectories are determined through the geodesic condition $\mathrm{d}s^2 = 0$. The speed of light in x^1-direction (meaning all other $\mathrm{d}x^j = 0$, $j \neq 1$, i.e. locally straight paths along $x^1 = x$) is then $c(x) = c\sqrt{(1 - h_{00})/(1 + h_{11})}$, and correspondingly for the other directions. The relative change of the coordinate speed of light in x^i-direction then reads, for the (0 1 1) mode with $n \gg 1$,

$$\delta c(x)/c = -\frac{1}{2}(h_{00} + h_{11}) = -\frac{1}{2}\mathcal{P}(g_1 + g_2),$$
$$\delta c(y)/c = -\frac{1}{2}(h_{00} + h_{22}) = -\frac{1}{2}\mathcal{P}(g_1 + g_3),$$
$$\delta c(z)/c = -\frac{1}{2}(h_{00} + h_{33}) = -\frac{1}{2}\mathcal{P}(g_1 + \tilde{g}_3). \tag{B.18}$$

For the $(01M)$ mode with $n, M \gg 1$,

$$\delta c(x)/c = \delta c(y)/c = -\frac{1}{2}h_{00} = -\frac{\mathcal{P}M}{4}(g_1 + g_2 + g_3 + \tilde{g}_3),$$
$$\delta c(z)/c = 2\delta c(x)/c, \tag{B.19}$$

where the equalities in terms of the $g_i, \tilde{g}_i$ are for $|\psi_{\mathrm{opt}}\rangle$.

In figure B1, we plot the relative change of the coordinate speed of light in x—direction for the (0 1 1) mode. We see that up to position dependent functions of order 1 the relative change of speed of light is given by equation (5) in the main text. Very similar plots are obtained for other directions.

References

[1] Scheithauer S, Lämmerzahl C, Dittus H, Schiller S and Peters A 2005 The OPTIS satellite improved tests of special and general relativity *Aerosp. Sci. Technol.* **9** 357–65

[2] Evenson K M, Wells J S, Petersen F R, Danielson B L, Day G W, Barger R L and Hall J L 1972 Speed of light from direct frequency and wavelength measurements of the Methane–Stabilized laser *Phys. Rev. Lett.* **29** 1346–9

[3] Synder H S 1947 Quantized space-time *Phys. Rev.* **71** 38–41

[4] Doplicher S, Fredenhagen K and Roberts J E 1995 *The quantum structure of spacetime at the Planck scale and quantum fields Commun. Math. Phys.* **172** 187–220

[5] Ng Y J 2012 Quantum Foam *The 10th Marcel Grossmann Meeting* (Singapore: World Scientific) pp 2150–64

[6] Hawking S W, Page D N and Pope C N 1980 Quantum gravitational bubbles *Nucl. Phys.* B **170** 283–306

[7] Ashtekar A, Rovelli C and Smolin L 1992 Weaving a classical metric with quantum threads *Phys. Rev. Lett.* **69** 237–40

[8] Ford L H 1995 Gravitons and light cone fluctuations *Phys. Rev.* D **51** 1692–700

[9] Yu H and Ford L H 2000 Lightcone fluctuations in quantum gravity and extra dimensions *Phys. Lett.* B **496** 107–12

[10] Amelino-Camelia G, Ellis J, Mavromatos N E, Nanopoulos D V and Sarkar S 1998 Sensitivity of astrophysical observations to gravity-induced wave dispersion in vacuo (arXiv:astro-ph/9810483)

[11] Ellis J, Mavromatos N E and Nanopoulos D V 2000 Quantum-gravitational diffusion and stochastic fluctuations in the velocity of light *Gen. Relativ. Gravit.* **32** 127–44
[12] Biller S D *et al* 1999 Limits to quantum gravity effects on energy dependence of the speed of light from observations of TeV flares in active galaxies *Phys. Rev. Lett.* **83** 2108–11
[13] Kaaret P 1999 Pulsar radiation and quantum gravity *Astron. Astrophys.* **345** L32–L34
[14] Amelino-Camelia G 2014 Gravity in quantum mechanics *Nat. Phys.* **10** 254–5
[15] Vasileiou V, Granot J, Piran T and Amelino-Camelia G 2015 A Planck-scale limit on spacetime fuzziness and stochastic Lorentz invariance violation *Nat. Phys.* **11** 344–6
[16] Perlman E S, Rappaport S A, Christiansen W A, Ng Y J, DeVore J and Pooley D 2015 New constraints on quantum gravity from x-ray and gamma-ray observations *Astrophys. J.* **805** 10
[17] Urban M, Couchot F, Sarazin X and Djannati-Atai A 2013 The quantum vacuum as the origin of the speed of light *Eur. Phys. J.* D **67** 58
[18] Leuchs G and Sánchez-Soto L L 2013 A sum rule for charged elementary particles *Eur. Phys. J.* D **67** 57
[19] Helstrom C W 1967 Minimum mean-squared error of estimates in quantum statistics *Phys. Lett.* A **25** 101–2
[20] Helstrom C W 1969 Quantum detection and estimation theory *J. Stat. Phys.* **1** 231–52
[21] Braunstein S L and Caves C M 1994 Statistical distance and the geometry of quantum states *Phys. Rev. Lett.* **72** 3439–43
[22] Braunstein S L, Caves C M and Milburn G J 1996 Generalized uncertainty relations: theory, examples and Lorentz invariance *Ann. Phys.* **247** 135–73
[23] Wiseman H M and Milburn G J 2009 *Quantum Measurement and Control* 1st edn (Cambridge: Cambridge University Press)
[24] Giovannetti V, Loyd S and Maccone L 2004 Quantum-enhanced measurements: beating the standard quantum limit *Science* **306** 1330–6
[25] Giovannetti V, Lloyd S and Maccone L 2006 Quantum metrology *Phys. Rev. Lett.* **96** 010401
[26] Paris M G A 2009 Quantum estimation for quantum technology *Int. J. Quantum Inf.* **7** 125
[27] Davies P C W and Birrell N C 1982 *Quantum Fields in Curved Space* (Cambridge: Cambridge University Press)
[28] Peres A 1993 *Quantum Theory: Concepts and Methods* (Dordrecht: Kluwer)
[29] Ahmadi M, Bruschi D E, Sabín C, Adesso G and Fuentes I 2014 Relativistic quantum metrology: exploiting relativity to improve quantum measurement technologies *Sci. Rep.* **4** 4996
[30] Ahmadi M, Bruschi D E and Fuentes I 2014 Quantum metrology for relativistic quantum fields *Phys. Rev.* D **89** 065028
[31] Aspachs M, Adesso G and Fuentes I 2010 Optimal quantum estimation of the Unruh–Hawking effect *Phys. Rev. Lett.* **105** 151301
[32] Downes T G Milburn G J and Caves C M 2011 Optimal quantum estimation for gravitation (arXiv:1108.5220)
[33] Wigner E P 1957 Relativistic invariance and quantum phenomena *Rev. Mod. Phys.* **29** 255–68
[34] Salecker H and Wigner E P 1958 Quantum limitations of the measurement of space-time distances *Phys. Rev.* **109** 571–7
[35] Ahluwalia D V 1994 Quantum measurement, gravitation, and locality *Phys. Lett.* B **339** 301–3
[36] Amelino-Camelia G 1994 Limits on the measurability of space-time distances in the semiclassical approximation of quantum gravity *Mod. Phys. Lett.* A **09** 3415–22
[37] Ng Y J and van Dam H 2000 Measuring the foaminess of space-time with gravity-wave interferometers *Found. Phys.* **30** 795–805
[38] Giovannetti V, Lloyd S and Maccone L 2001 Quantum-enhanced positioning and clock synchronization *Nature* **412** 417–9
[39] Anisimov P M, Raterman G M, Chiruvelli A, Plick W N, Huver S D, Lee H and Dowling J P 2010 Quantum metrology with two-mode squeezed vacuum: parity detection beats the Heisenberg limit *Phys. Rev. Lett.* **104** 103602
[40] Braun D 2011 Ultimate quantum bounds on mass measurements with a nano-mechanical resonator *Europhys. Lett.* **94** 68007
Braun D 2012 Ultimate quantum bounds on mass measurements with a nano-mechanical resonator *Europhys. Lett.* **99** 49901 (erratum)
[41] Scully M O and Zubairy M S 1997 *Quantum Optics* (Cambridge: Cambridge University Press)
[42] Caves C M 1981 Quantum-mechanical noise in an interferometer *Phys. Rev.* D **23** 1693–708

[43] LIGO Collaboration 2011 A gravitational wave observatory operating beyond the quantum shot-noise limit *Nat. Phys.* **7** 962–5
[44] Demkowicz-Dobrzański R, Banaszek K and Schnabel R 2013 Fundamental quantum interferometry bound for the squeezed-light-enhanced gravitational wave detector GEO 600 *Phys. Rev.* A **88** 041802
[45] Ford L H 1982 Gravitational radiation by quantum systems *Ann. Phys.* **144** 238–48
[46] Misner C W, Thorne K S and Wheeler J A 1973 *Gravitation* (New York: Freeman)
[47] Landau L and Lifschitz E 1987 *Klassische Feldtheorie* (*Lehrbuch der Theoretischen Physik* vol II) German edn (Berlin: Akademie)
[48] Eddington A S 1920 *The Mathematical Theory of Relativity* (Cambridge: Cambridge University Press)
[49] Fayngold M 2009 *Special Relativity and How it Works* (New York: Wiley)
[50] Grishchuk L P and Sazhin M V 1974 Emission of gravitational waves by an electromagnetic cavity *JETP* **38** 215
[51] Kopeikin S M 2015 Optical cavity resonator in an expanding universe *Gen. Relativ. Gravit.* **47** 1–18
[52] Tolman R C, Ehrenfest P and Podolsky B 1931 On the gravitational field produced by light *Phys. Rev.* **37** 602–15
[53] Bonnor W B 1969 The gravitational field of light *Commun. Math. Phys.* **13** 163–74
[54] Escher B M, de Matos Filho R L and Davidovich L 2011 General framework for estimating the ultimate precision limit in noisy quantum-enhanced metrology *Nat. Phys.* **7** 406–11
[55] Kołodyński J and Demkowicz-Dobrzański R 2010 Phase estimation without *a priori* phase knowledge in the presence of loss *Phys. Rev.* A **82** 053804
[56] Braun D 2010 Parameter estimation with mixed quantum states *Eur. Phys. J.* D **59** 521–3
[57] Fraïsse J M E and Braun D 2016 Hamiltonian extensions in quantum metrology (arXiv:1610.05974)
[58] Boixo S, Flammia S T, Caves C M and Geremia J M 2007 Generalized limits for single-parameter quantum estimation *Phys. Rev. Lett.* **98** 090401
[59] Hossenfelder S 2013 Minimal length scale scenarios for quantum gravity *Living Rev. Relativ.* **16** 2
[60] Mead C A 1964 Possible connection between gravitation and fundamental length *Phys. Rev.* **135** B849–62
[61] Bronstein M 1936 Quantentheorie schwacher Gravitationsfelder *Phys. Z. Sowjetunion* **9** 140–57
[62] Calmet X, Graesser M and Hsu S D H 2004 Minimum length from quantum mechanics and classical general relativity *Phys. Rev. Lett.* **93** 211101
[63] Diósi L and Lukács B 1989 On the minimum uncertainty of space-time geodesics *Phys. Lett.* A **142** 331–4
[64] Amelino-Camelia G 1999 Gravity-wave interferometers as quantum-gravity detectors *Nature* **398** 216–8
[65] Lieu R and Hillman L W 2003 The phase coherence of light from extragalactic sources: direct evidence against first-order Planck-scale fluctuations in time and space *Astrophys. J. Lett.* **585** L77
[66] Ng Y J, Christiansen W A and van Dam H 2003 Probing Planck-scale physics with extragalactic sources? *Astrophys. J.* **591** L87
[67] Magueijo J and Smolin L 2003 Generalized Lorentz invariance with an invariant energy scale *Phys. Rev.* D **67** 044017
[68] Amelino-Camelia G 2002 Relativity in spacetimes with short-distance structure governed by an observer-independent (Planckian) length scale *Int. J. Mod. Phys.* D **11** 35–59
[69] Liberati S, Sonego S and Visser M 2005 Interpreting doubly special relativity as a modified theory of measurement *Phys. Rev.* D **71** 045001
[70] Sotiriou T P, Visser M and Weinfurtner S 2009 Quantum gravity without Lorentz invariance *J. High Energy Phys.* JHEP10(2009)033
[71] Visser M 2009 Lorentz symmetry breaking as a quantum field theory regulator *Phys. Rev.* D **80** 025011
[72] Weinfurtner S, Jain P, Visser M and Gardiner C W 2009 Cosmological particle production in emergent rainbow spacetimes *Class. Quantum Grav.* **26** 065012
[73] Amelino-Camelia G, Freidel L, Kowalski-Glikman J and Smolin L 2011 Principle of relative locality *Phys. Rev.* D **84** 084010
[74] Magueijo J and Smolin L 2002 Lorentz invariance with an invariant energy scale *Phys. Rev. Lett.* **88** 190403

[75] Moffat J W 1993 Superluminary universe: a possible solution to the initial value problem in cosmology *Int. J. Mod. Phys.* D **02** 351–65
[76] Albrecht A and Magueijo J 1999 Time varying speed of light as a solution to cosmological puzzles *Phys. Rev.* D **59** 043516
[77] Aloisio R, Galante A, Grillo A, Liberati S, Luzio E and Méndez F 2006 Deformed special relativity as an effective theory of measurements on quantum gravitational backgrounds *Phys. Rev.* D **73** 045020
[78] Aloisio R, Galante A, Grillo A F, Liberati S, Luzio E and Méndez F 2006 Modified special relativity on a fluctuating spacetime *Phys. Rev.* D **74** 085017
[79] Amelino-Camelia G, Ellis J, Mavromatos N E and Nanopoulos D V 1997 Distance measurement and wave dispersion in a Liouville–String approach to quantum gravity *Int. J. Mod. Phys.* A **12** 607–23
[80] Galán P and Marugán G A M 2005 Length uncertainty in a gravity's rainbow formalism *Phys. Rev.* D **72** 044019
[81] Amelino-Camelia G 2000 Gravity-wave interferometers as probes of a low-energy effective quantum gravity *Phys. Rev.* D **62** 024015
[82] Abramovici A *et al* 1996 Improved sensitivity in a gravitational wave interferometer and implications for LIGO *Phys. Lett.* A **218** 157–63
[83] Rätzel D *et al* 2017 Frequency spectrum of a Fabry–Pérot resonator in a weak gravitational field (to be published)
[84] LIGO Scientific Collaboration and Virgo Collaboration 2016 GW150914: implications for the stochastic gravitational-wave background from binary black holes *Phys. Rev. Lett.* **116** 131102
[85] Sorge F 2000 Do gravitational waves create particles? *Class. Quantum Grav.* **17** 4655
[86] Popoviciu T 1935 Sur les équations algébriques ayant toutes leurs racines réelles *Mathematica* **9** 129–45
[87] Deser S 1957 General relativity and the divergence problem in quantum field theory *Rev. Mod. Phys.* **29** 417–23
[88] Heisenberg W and Euler H 1936 Folgerungen aus der Diracschen Theorie des Positrons *Z. Phys.* **98** 714

[B] Frequency spectrum of an optical resonator in a curved spacetime

Dennis Rätzel, Fabienne Schneiter, Daniel Braun, Tupac Bravo, Richard Howl, Maximilian P. E. Lock, Ivette Fuentes
New Journal of Physics, 20(5), 2018
DOI: 10.1088/1367-2630/aac0ac
URL: http://stacks.iop.org/1367-2630/20/i=5/a=053046

New Journal of Physics
The open access journal at the forefront of physics

Deutsche Physikalische Gesellschaft DPG
IOP Institute of Physics

Published in partnership with: Deutsche Physikalische Gesellschaft and the Institute of Physics

OPEN ACCESS

RECEIVED
3 December 2017

REVISED
9 March 2018

ACCEPTED FOR PUBLICATION
27 April 2018

PUBLISHED
18 May 2018

PAPER

Frequency spectrum of an optical resonator in a curved spacetime

Dennis Rätzel[1], Fabienne Schneiter[2], Daniel Braun[2], Tupac Bravo[1], Richard Howl[1], Maximilian P E Lock[1,3] and Ivette Fuentes[1,4]

[1] Faculty of Physics, University of Vienna, Boltzmanngasse 5, A-1090 Vienna, Austria
[2] Institut für Theoretische Physik, Eberhard-Karls-Universität Tübingen, D-72076 Tübingen, Germany
[3] Imperial College, Department of Physics, SW7 2AZ London, United Kingdom
[4] School of Mathematical Sciences, University of Nottingham, University Park, Nottingham NG7 2RD, United Kingdom

E-mail: dennis.raetzel@univie.ac.at

Keywords: gravitational field, rigid rod, frequency spectrum, Fabry–Pérot, elastic body, optical cavity, geometrical optics

Abstract

The effect of gravity and proper acceleration on the frequency spectrum of an optical resonator—both rigid or deformable—is considered in the framework of general relativity. The optical resonator is modeled either as a rod of matter connecting two mirrors or as a dielectric rod whose ends function as mirrors. Explicit expressions for the frequency spectrum are derived for the case that it is only perturbed slightly and variations are slow enough to avoid any elastic resonances of the rod. For a deformable resonator, the perturbation of the frequency spectrum depends on the speed of sound in the rod supporting the mirrors. A connection is found to a relativistic concept of rigidity when the speed of sound approaches the speed of light. In contrast, the corresponding result for the assumption of Born rigidity is recovered when the speed of sound becomes infinite. The results presented in this article can be used as the basis for the description of optical and opto-mechanical systems in a curved spacetime. We apply our results to the examples of a uniformly accelerating resonator and an optical resonator in the gravitational field of a small moving sphere. To exemplify the applicability of our approach beyond the framework of linearized gravity, we consider the fictitious situation of an optical resonator falling into a black hole.

1. Introduction

In general relativity (GR), as coordinates have no physical meaning, there is no unique concept for the length of a matter system. Some notion of length can be covariantly defined using geometrical quantities or properties of matter. The ambiguity in the notion of length poses a problem for high accuracy metrological experiments, where gravitational fields or acceleration have a significant role to play. For example, the frequency spectrum of a resonator depends on its dimensions and hence knowledge of the precise values of these dimensions is of utmost importance. Cases in which the effects of gravitational fields and acceleration must be considered include those in which the gravitational field is to be measured, such as in proposals for the measurement of gravitational waves with electromagnetic cavity resonators [1–7] or other extended matter systems [8–14], tests of GR [15, 16] or the expansion of the universe [17, 18]. Other situations are those in which the metrological system is significantly accelerated [19–21]. A fundamental limit for the precision of a light cavity resonator as a metrological system can even be imposed by the gravitational field of the light inside the cavity [22].

The two most important concepts of length are the proper distance and the radar distance. The proper distance is a geometrical quantity usually associated with the length of a rod that is rigid in the sense of that given by Born [23]. The radar distance is the optical length that can be measured by sending light back and forth between two mirrors and taking the time between the two events as a measure of distance. It is this radar length that gives the resonance frequency spectrum of an optical resonator for large enough wave numbers. However, the resonators that are part of the metrological systems described in [1–22] are confined by solid matter systems, and therefore, the notion of proper length plays also a role.

In section 2, we start our considerations by modeling a one-dimensional resonator as a set of two end mirrors connected by a rod of matter. If this rod is assumed to be rigid, the resonator is called a rigid optical resonator. In section 3, we show that the resonance frequencies of an optical resonator are given by its radar length. The general results derived in sections 2 and 3 are applied in the following sections.

Since proper length and radar length are generally different, it turns out that the resonance frequencies of a Born rigid optical resonator change if the resonator is accelerated or is exposed to tidal forces. Furthermore, the frequency of a mode is dependent on the reference time, which, in turn, is dependent on the position of the resonator in spacetime. Taking all this into consideration leads to an expression for the resonance frequencies of a resonator that is dependent on acceleration and curvature. This is presented in section 4.

A realistic rod cannot truly be Born rigid; depending on its stiffness and mass density, it will be affected by the gravitational field and its internal interactions have to obey the laws of relativistic causality. In section 5, we derive expressions for the dependence of the resonance frequencies on the deformation of the rod and show that the change in resonance frequencies depends only on the speed of sound in the material of the rod. In this article, we restrict our considerations to cases where acceleration and tidal forces experienced by the optical resonator vary slowly. This way, we can neglect elastic resonances of rod. At the end of section 5, we compare the change of the resonance frequencies due to deformations of the rod to the change of the resonance frequencies due to the relativistic effects presented in section 4. Additionally, we discuss the notion of a causal rigid resonator which is based on the definition of a causal rigid rod as one composed of a material in which the speed of sound is equivalent to the speed of light.

The optical resonator can also be filled with a dielectric, or equivalently, the rod that sets the length of the resonator can be a dielectric material and the mirrors can be its ends. The case of homogeneous isotropic dielectric is discussed in section 6, and it is shown that the relative frequency shifts are independent of the refractive index of the dielectric material. In section 7, we consider the case of a uniformly accelerated resonator, in section 8 we consider the case of a resonator that falls into a black hole and in section 9, we consider the example of an optical resonator in the gravitational field of an oscillating massive sphere. In section 10 we give a summary and conclusions.

In this article, we assume that all effects on the optical resonator can be described as small perturbations. In section 5, we present a certain coordinate system $x^{\mathcal{M}}$ valid in a region around the world line of the resonator's center of mass in which the spacetime metric takes the form $g_{\mathcal{MN}} = \eta_{\mathcal{MN}} + h_{\mathcal{MN}}$, where $\eta_{\mathcal{MN}} = \mathrm{diag}(-1, 1, 1, 1)$ is the Minkowski metric and $h_{\mathcal{MN}}$ is a perturbation. $h_{\mathcal{MN}}$ is considered to be small in the sense that $|h_{\mathcal{MN}}| \ll 1$ for all $\mathcal{M}, \mathcal{N}$.

2. A rigid one-dimensional resonator in a curved spacetime

In GR, the gravitational field is represented by the spacetime metric $g_{\mu\nu}$ on a smooth four-dimensional manifold $\mathcal{M}$. We assume the metric to have signature $(-1, 1, 1, 1)$. Then, for every vector v^μ at a point p in $\mathcal{M}$, the metric delivers a number $g(v, v) = g_{\mu\nu} v^\mu v^\nu$, which is either positive, zero or negative. These cases are called, respectively, space-like, light like and time-like. For all space-like vectors v^μ, the square root of the positive number $g(v, v)$ is called the length of this vector. A curve $s(\varsigma)$ parameterized by $\varsigma \in [a, b]$ in the spacetime $\mathcal{M}$ that has tangents $s'(\varsigma) := \mathrm{d}s^\mu(\varsigma)/\mathrm{d}\varsigma$ that are always space-like is called a space-like curve. The geometrical distance along this curve is the quantity $L_p(s) = \int_a^b \mathrm{d}\varsigma \sqrt{g_{\mu\nu} s'^\mu s'^\nu}$, which is called the proper distance. To define a frequency we need to know how to measure time. A time measurement in GR is defined only with respect to an observer world line. An observer world line is a curve $\gamma(\varrho)$ whose tangents $\dot\gamma(\varrho) := \mathrm{d}\gamma(\varrho)/\mathrm{d}\varrho$ are always time-like. The time measured along the observer world line $\gamma(\varrho)$ between the parameter values ϱ_1 and ϱ_2 is $T_p(\varrho_1, \varrho_2) = \int_{\varrho_1}^{\varrho_2} \mathrm{d}\varrho \sqrt{-g_{\mu\nu} \dot\gamma^\mu \dot\gamma^\nu}$. This is the temporal counterpart to the proper distance, and it is called the proper time. Additionally, at every point of a world line $\gamma(\varrho)$, there is a corresponding set of spatial vectors v called the spatial slice in the tangent vector space at $\gamma(\varrho)$ with respect to $\dot\gamma(\varrho)$, which is defined by the condition $\dot\gamma^\mu(\varrho) v^\nu g_{\mu\nu}(\gamma(\varrho)) = 0$.

In GR, there exist different notions of rigidity as it turns out to be less than straightforward to formulate this basic concept of Newtonian mechanics in a relativistic way. Early attempts to understand rigidity in the framework of electrodynamics date back to before Einstein's formulation of the special theory of relativity [24–28]. These approaches turned out to be inconsistent with Lorentz symmetry, which then led to the formulation of a Lorentz invariant differential geometric definition of rigidity in [23] by Max Born after special relativity was established. Formulated in a modern way, it is the condition of constant distance between every two infinitesimally separated segments of a rigid body. Here, the measure of distance is the infinitesimal proper distance between the two world lines measured in the spatial slice defined by any of the two world lines. This concept of rigidity is denoted as Born rigidity in literature. A short time after the publication by Born in 1909, it

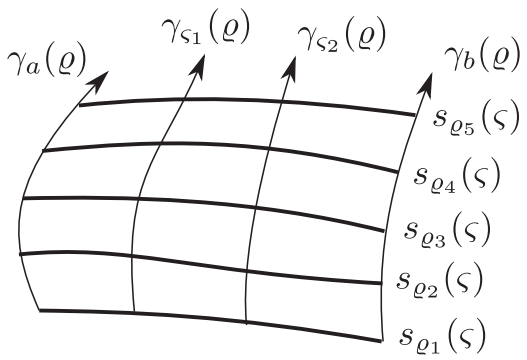

Figure 1. The world lines $\gamma_\varsigma(\varrho)$ of the segments of the rod are assumed to form a family of curves which give rise to the rod's world sheet. The curve parameter ϱ, which is not necessarily equivalent to their proper time, is the parameter for a family of space-like curves $s_\varrho(\varsigma)$ that represent the rod. We assume that the curves $s_\varrho(\varsigma)$ are space-like geodesics and cross the world lines of each segment orthogonally.

was found by Herglotz [29] and Nöther [30] that Born rigidity is too restrictive. In particular, they found that, with the exception of the singular case of uniform rotation, the motion of a Born rigid body is completely defined by the trajectory of one of its points. Subsequently, there were attempts to give a less restrictive definition of a rigid body which include the concept of quasi-rigidity in GR, a condition on the multipole-moments of a body [31, 32], and the model of a rigid body as a body in which the speed of sound is equal to the speed of light [33]. Here, we will use, as our starting point, a definition of a rigid rod that is Born rigid, and we will undertake a perturbative analysis for small length scales, small accelerations, small velocities and small gravitational fields. In this article, we will show that two types of effects are found; those due to spacetime properties alone and those due to small deformations of the rod which correspond to small deviations from Born rigidity. Since all effects can be considered to be small, we remain in the linear regime, where the different effects can be assumed to be independent.

Let us assume that we have a rod of very small diameter in comparison to its length, i.e., it is effectively one-dimensional. We assume that the world lines of the segments of the rod form a family of curves $\gamma_\varsigma(\varrho)$ parameterized by ς which we assume to be in the interval $\varsigma \in [a, b]$. The end points of the rod are $\gamma_a(\varrho)$ and $\gamma_b(\varrho)$. The spacetime surface $F(\varrho, \varsigma) = \gamma_\varsigma(\varrho)$ can be called the world sheet of the rod. See figure 1. for each curve, the curve parameter ϱ is chosen so that the curves $s_\varrho(\varsigma) \coloneqq F(\varrho, \varsigma)$ are space-like geodesics in the sense of the auto-parallel condition $\nabla_{s'_\varrho(\varsigma)} s'_\varrho(\varsigma) = 0$ with respect to the Levi-Cevita connection ∇ of the metric g given as $\nabla_\xi \zeta^\alpha = \xi^\beta \partial_\beta \zeta^\alpha + \Gamma^\alpha_{\beta\gamma} \xi^\beta \zeta^\gamma$ for any two vectors ξ and ζ, where

$$\Gamma^\alpha_{\beta\gamma} = \frac{1}{2} g^{\alpha\rho} (\partial_\beta g_{\gamma\rho} + \partial_\gamma g_{\beta\rho} - \partial_\rho g_{\beta\gamma}) \tag{1}$$

are the Christoffel symbols. Note that we do not assume that the world lines of the segments of the rod be geodesics. The segments move under the interior forces of the rod. We also do not assume that ϱ is the proper time of all the segments. Later we will assume that there is a single segment that has ϱ as its proper time.

For every point of the world sheet $F(\varrho, \varsigma)$ of the rod, we assume that the tangent $s'_\varrho(\varsigma)$ lies in the spatial slice defined by the tangent to the local segment's world line $\dot\gamma_\varsigma(\varrho)$, i.e. $g(\dot\gamma_\varsigma(\varrho), s'_\varrho(\varsigma)) = 0$. Later, we will find that, due to the condition that the curves $s_\varrho(\varsigma)$ be geodesics, the condition $g(\dot\gamma_\varsigma(\varrho), s'_\varrho(\varsigma)) = 0$ is fulfilled up to the second order in the proper length of the rod divided by a length scale l_{var}, which is associated with local curvature and acceleration. We say that the rod is rigid if the proper distance between every two points on the curve $s_\varrho(\varsigma)$ is independent of the parameter ϱ. To further elucidate the meaning of the concept of a rigid rod that we use here, we explain its relation to the concept of a rigid rod that may be familiar from special relativity in appendix A.

There are two possibilities to construct a rigid resonator from the rigid rod defined above. One option is that the rod itself is the resonator: for example, it could be a resonator for electromagnetic waves in different spectral ranges or a resonator for the many different quasiparticles inside and on the surface of a solid matter system such as phonons, plasmons and polaritons, to mention just a few, all of which may resonate between the ends of the rigid rod. The second option is to create a cavity resonator by attaching two mirrors at the end points of the rod such that the light is reflected between the mirrors. In practice, this would be achieved by maximizing the quality factor of the resonator. We denote such resonators as rigid resonators. The second option is the focus of this article, and it is illustrated in figure 2. The first option for a homogeneous isotropic dielectric is discussed in section 6.

A realistic matter system can only be rigid for negligible tidal forces and accelerations. We will discuss our model for a deformable resonator affected by tidal forces and acceleration in section 5. In section 3, we will

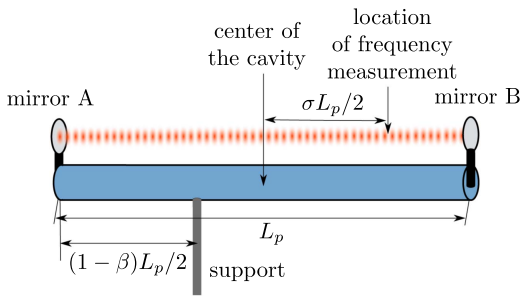

Figure 2. Illustration of our model of an optical resonator consisting of two mirrors that are attached to the ends of a rod. We assume that the resonator is moved along a trajectory $\gamma(\varrho)$ by a support which is attached at a distance $(1-\beta)L_p/2$ from mirror A. Since proper time depends on the position in the gravitational field so does the measured frequency of a resonator mode. We assume the frequency to be measured at a distance $\sigma L_p/2$ from the center of the resonator towards mirror B.

derive an expression for the resonance frequency spectrum of a resonator, rigid or deformable, under the condition that the timescale for light propagation between the mirrors is much smaller than the timescale on which the rigid resonator length is changing.

3. Resonance frequencies

In this section, we will derive an expression for the resonance frequencies of the resonator described above. As we are dealing with an extended object in GR, the obtained resonance frequencies are ambiguous as we will see in the following: first, every mode k existing in the resonator evolves with a certain phase ψ_k, this is a covariant quantity. In order to extract a frequency ω_k from the phase, we require a time T such that we can express the phase as $\psi_k = \omega_k T$. As stated in section 2, such a time measurement is defined only with respect to an observer and the time measured by the observer along the curve $\gamma(\varrho)$ is the proper time $T_p(\varrho_1, \varrho_2) = \int_{\varrho_1}^{\varrho_2} \mathrm{d}\varrho \sqrt{-g_{\mu\nu}\dot{\gamma}^\mu\dot{\gamma}^\nu}$. Through the family of curves associated with the rigid rod, we can define a family of observers along the curves $\gamma_\varsigma(\varrho) = s_\varrho(\varsigma)$. We see that every point in the resonator corresponds to a different observer and, therefore, we cannot give a proper time to the whole resonator, therefore the frequencies of the modes must depend on the point in the resonator where they are observed.

First, we will consider the case of an optical resonator, discussing other cases at the end of the section. The resonance frequencies can be obtained from the evolution of the phase ψ_k of a resonator mode. This can be found by explicitly solving Maxwell's equations in the curved spacetime under consideration. However, we can achieve the same result much faster by implementing the short wavelength expansion or geometric optical limit. The purpose of the following calculation is to prove the expression in equation (5), which gives the resonance frequencies in terms of the radar distance between the two ends of the resonator. Some readers may want to jump to equation (5) directly.

In the short wavelength expansion, the electromagnetic field strength tensor for a freely propagating, monochromatic light wave is given as [34]

$$F_{\mu\nu}(x) = \mathrm{Re}\left(\mathrm{e}^{\mathrm{i}\frac{\alpha}{\lambda}S(x)}\sum_{n=0}^{\infty}\phi_{n,\mu\nu}(x)\left(\frac{\lambda}{\alpha}\right)^n\right), \tag{2}$$

where the complex valued second rank tensors $\phi_{n,\,\mu\nu}(x)$ give the slowly varying amplitudes, λ is the wavelength, α is the length scale of the slow changes of the properties of the light field and the real function $S(x)$ is the eikonal function which describes the rapidly varying phase. In particular, α is the smallest of the length scales given by the waist of the resonator mode, the acceleration of the cavity and the spacetime curvature. This statement will get its full meaning in section 5, where the effects of the motion of the resonator and the spacetime curvature on the proper length of the resonator are considered explicitly by using a particular set of coordinates called the proper detector frame. We assume that $\lambda \ll \alpha$ and $\lambda < L_p$. We will only consider linear polarization in the following. We find that the results for the change of the frequency spectrum do not depend on the polarization. Therefore, the results also apply to circular and elliptic polarized fields as those can be obtained as superpositions of linearly polarized fields.

The raised gradient of the eikonal function $\hat{\xi}^\mu(x) := g^{\mu\nu}\partial_\nu S(x)$ is the normal vector field to the wave fronts defined by $S(x)$. Applying the Maxwell equations to the eikonal expansion in equation (2), we find in leading

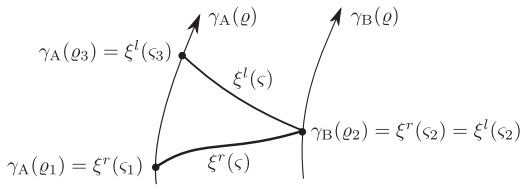

Figure 3. The resonance frequencies of a resonator can be derived in the geometric optical limit by considering light bouncing back and forth between the two mirrors of the optical resonator.

order that $\hat{\xi}^\mu(x)$ must be a light like vector field, i.e. $\hat{\xi}^\mu(x)\hat{\xi}^\nu(x)g_{\mu\nu}(x) = 0$ [35][5]. Additionally, the light like condition implies that the integral curves of the tangents $\hat{\xi}^\mu(x)$ are light like geodesics. In other words, there exist curves $\xi(\varsigma)$ that have the tangents $\hat{\xi}^\mu(\xi(\varsigma))$: the light rays of geometric optics. Furthermore, the light like property implies $\hat{\xi}^\mu(x)\partial_\mu S(x) = 0$, which means that the phase $\frac{\alpha}{\lambda}S(x)$ is constant along the light rays. We will use these properties of the eikonal function and its gradient to derive the frequency spectrum of the optical resonator in the following.

Inside a resonator, we create standing waves. Hence, we must assume that, for the resonator, there are stationary solutions of Maxwell's equations that fulfill the boundary conditions at the mirrors. This assumption is valid if we assume that coordinates exist in a small region containing the resonator such that the positions of the mirrors and the metric change only very slightly in the time span that light needs to propagate between the mirrors. Assuming that linearly polarized standing cavity mode solutions exist, we consider the superposition of two counter-propagating linearly polarized light waves $F^{\text{res}}_{\mu\nu}(x) = F^r_{\mu\nu}(x) + F^l_{\mu\nu}(x)$, where $F^r_{\mu\nu}(x)$ and $F^l_{\mu\nu}(x)$ are as in equation (2) with the eikonal functions $S^r(x)$ and $S^l(x)$, respectively. $F^l_{\mu\nu}(x)$ represents the wave propagating to the left (negative direction) and $F^r_{\mu\nu}(x)$ represents the wave propagating to the right (positive direction). We obtain

$$F^{\text{res}}_{\mu\nu}(x) = \text{Re}\left(e^{i\frac{\alpha}{\lambda}S^r(x)}\sum_{n=0}^{\infty}\phi^r_{n,\mu\nu}(x)\left(\frac{\lambda}{\alpha}\right)^n + e^{i\frac{\alpha}{\lambda}S^l(x)}\sum_{n=0}^{\infty}\phi^l_{n,\mu\nu}(x)\left(\frac{\lambda}{\alpha}\right)^n\right). \tag{3}$$

We defined a rigid cavity by assuming that there are two mirrors attached to the ends of a rigid rod. We consider the gravitational attraction of the two mirrors, all atoms in the rigid rod and the light itself to be negligible. We assume in the following that the mirrors are so close to the ends and so tightly attached that we can identify their world lines with those of the end points of the rod, i.e. $\gamma_A(\varrho) = \gamma_a(\varrho)$ and $\gamma_B(\varrho) = \gamma_b(\varrho)$. Starting at $\varrho = \varrho_1$ with the mirror at $\gamma_A(\varrho_1)$, we can define a curve $\xi^r(\varsigma)$ with $\varsigma \in [\varsigma_1, \varsigma_2]$ such that $\xi^r(\varsigma_1) = \gamma_A(\varrho_1)$ and $\xi^r(\varsigma_2) = \gamma_B(\varrho_2)$ for some ϱ_2 and $\mathrm{d}\xi^{r,\mu}(\varsigma)/\mathrm{d}\varsigma = \hat{\xi}^{r,\mu}(\xi(\varsigma)) = g^{\mu\nu}\partial_\nu S^r(\xi(\varsigma))$ (see figure 3 for an illustration). Since all tangents of $\xi^r(\varsigma)$ are light like, this is a light like curve and can be interpreted as the path of a massless point particle, a single photon, from mirror A to mirror B. At mirror B, the photon is reflected and the tangent of its path becomes $g^{\mu\nu}\partial_\nu S^l(\gamma_B(\varrho_2))$. We can define a curve $\xi^l(\varsigma)$ with$\varsigma \in [\varsigma_2, \varsigma_3]$ such that $\xi^l(\varsigma_2) = \gamma_B(\varrho_2)$ and $\xi^l(\varsigma_3) = \gamma_B(\varrho_3)$ for some ϱ_3 and $\mathrm{d}\xi^{l,\mu}(\varsigma)/\mathrm{d}\varsigma = \hat{\xi}^{l,\mu}(\xi(\varsigma)) = g^{\mu\nu}\partial_\nu S^l(\xi(\varsigma))$. This is the light like curve representing the path of the photon back to the mirror A. At mirror A, the photon is again reflected and the tangent becomes $g^{\mu\nu}\partial_\nu S^r(\gamma_A(\varrho_3))$.

Then, a condition can be formulated that is necessary to fulfill the boundary conditions at each of the mirrors: the phases of the left propagating and the right propagating parts of $F^{\text{res}}_{\mu\nu}(\gamma_A(\varrho))$ and $F^{\text{res}}_{\mu\nu}(\gamma_B(\varrho))$ have to match by a multiple of 2π. In appendix B, the derivation of this condition is given. Since the phase is constant along the geodesics ξ^r and ξ^l, we find that the change of the eikonal function at the position of the mirror must have been $\frac{\alpha}{\lambda}\delta S_A = \frac{\alpha}{\lambda}(S(\gamma_A(\varrho_3)) - S(\gamma_A(\varrho_1))) = 2\pi m$ where $m \in \mathbb{Z}$. An observer at mirror A can measure this phase and associate it with a frequency and a change in proper time as $\frac{\alpha}{\lambda}\delta S_A = \omega_A T_p(\varrho_1, \varrho_3)$. The proper time difference $T_p(\varrho_1, \varrho_3)$ is proportional to the radar length $R_A = cT_p(\varrho_1, \varrho_3)/2$ of the resonator measured at $\varrho_0 = (\varrho_3 + \varrho_1)/2$ by an observer traveling with mirror A. Therefore, we find that the frequencies of the modes of the resonator measured by an observer along the world line of mirror A are given as

$$\omega_{A,n} = \frac{cn\pi}{R_A}, \tag{4}$$

where we assume $n > 0$, i.e. we consider only positive frequencies. A similar analysis can be made for mirror B, which leads to $\omega_{B,n} = \frac{cn\pi}{R_B}$. Accordingly, for any other observer inside the cavity, we obtain

[5] For any matter field in the eikonal approximation, the gradient of the eikonal function has to fulfill the characteristic equations which derive from the highest derivative part of the matter field equations. In the case of Maxwells electrodynamics, the characteristic equations are simply given by the light cone condition. For more details about this analysis see [34, 36, 37].

$$\omega_{\gamma,n} = \frac{cn\pi}{R_\gamma}, \tag{5}$$

where R_γ is obtained by following a light like geodesic from the observer to one of the mirrors, after reflection, to the second mirror and, after the second reflection, back to the observer. It is clear that this is an approximate value; the notion of frequency means the rate of repetition of a signal. For this notion to make sense, it has to be constant at least for a few repetition cycles. Hence, the observer measuring the frequency has to move slowly in comparison to the time that a light pulse needs to propagate between the mirrors R_γ/c.

There is another way to understand equation (5): electrodynamics in a Lorentzian spacetime can be interpreted as electrodynamics in a non-dispersive, bi-anisotropic, impedance matched medium using the Plebanski constitutive equations [38]

$$D^i = \varepsilon_0 \varepsilon^{ij} E_j + \frac{1}{c}\epsilon^{ijk} w_j H_k, \tag{6}$$

$$B^i = \mu_0 \mu^{ij} H_j - \frac{1}{c}\epsilon^{ijk} w_j E_k, \tag{7}$$

where we define the spatial co-vector as $w_i := g_{i0}/g^{00}$ and the permittivity and permeability matrices $\varepsilon^{ij} = \mu^{ij} := -\sqrt{|\det g|}\, g^{ij}/g_{00}$. Maxwell's equations in the curved spacetime $g_{\mu\nu}$ take the form of Maxwell's equations in this effective dielectric medium in flat spacetime. Note that the spatial co-vector w_j, which mixes the electric and magnetic field components, is defined by the spacetime mixing components of the metric. If the metric is orthogonal in the chosen set of coordinates, w_j vanishes and we are left with a normal anisotropic medium.

Let us assume that the coordinate system was chosen such that the coordinate time t coincides with the proper time at mirror A and that z is the coordinate along the light ray. In this case, we find that the radar length of the resonator measured by an observer at mirror A can be written as

$$\begin{aligned} R_\mathrm{A} &= \frac{c}{2}(t_2 - t_1) = \frac{c}{2}\int_{t_1}^{t_2} \mathrm{d}t' = c\int_{z_a}^{z_b}\left(\frac{\mathrm{d}z}{\mathrm{d}t}\right)^{-1}\mathrm{d}z \\ &= \int_{z_a}^{z_b}\frac{c}{v_\mathrm{ph}}\mathrm{d}z = \int_{z_a}^{z_b} n_z\,\mathrm{d}z, \end{aligned} \tag{8}$$

where $v_\mathrm{ph} = \mathrm{d}z/\mathrm{d}t$ is the coordinate dependent phase velocity of the light and $n_z = c/v_\mathrm{ph}$ can be understood as an effective index of refraction. Equation (8) shows that the radar length can be understood as the optical path length measured by a ray sent from mirror A to mirror B. Hence, equation (5) is the condition that the frequencies measured at mirror A must be multiples of the speed of light divided by the optical path length.

At the end of this section, we would like to discuss the effect of higher order terms in the eikonal expansion. We derived the frequency spectrum (4) and (5) from a necessary condition for the existence of linearly polarized standing wave solutions of the electromagnetic field in the resonator. This is the condition at the leading order in the eikonal expansion. Terms in the eikonal expansion of higher order may be complex functions in general, this can lead to additional phase shifts at the boundaries which, in turn, can lead to frequency shifts. Such additional frequency shifts can be either considered as systematical errors that limit the predictive power of our approach or have to be evaluated independently to be subtracted from the result of the measurement. One particular source of additional frequency shifts is rotation of the resonator about an axis orthogonal to its optical axis. For earthbound experiments, such rotation will be induced by the rotation of the Earth, for example, which can be measured independently and taken into account explicitly. The effect of rotation may be calculated by taking higher orders of the eikonal expansion into account or using other methods of electrodynamics such as the paraxial wave equation. Here we assume that the optical resonator is non-rotating and we restrict our considerations to the expression for the frequency spectrum given in equation (5). In the next section, we will look at its application.

4. Born rigid optical resonators

In this section, we will derive the resonance frequencies of a Born rigid resonator in terms of its constant proper length. For this purpose, we choose to work in a particular coordinate system which we will introduce in the following.

Along the world line of an observer $\gamma(\tau)$, an orthonormal, co-rotating tetrad $\epsilon^\mu_\mathcal{M}(\tau)$ ($\mathcal{M} \in \{0, 1, 2, 3\}$, all calligraphic capital letters will run from 0 to 3 in the following) can be defined where $\epsilon^\mu_0 = \dot\gamma^\mu(\tau)$ is the tangent to the world line of the observer, $\epsilon^\mu_J(\tau)$ ($J \in \{1, 2, 3\}$, all capital non-calligraphic letters will run from 1 to 3 in the following) are space-like, $\epsilon^\mu_\mathcal{M}(\tau)\,\epsilon^\nu_\mathcal{N}(\tau) g_{\mu\nu}(\gamma(\tau)) = \eta_{\mathcal{M}\mathcal{N}}$ and $\eta_{\mathcal{M}\mathcal{N}} = \mathrm{diag}(-1, 1, 1, 1)$. There also exists a corresponding co-tetrad $\varepsilon^\mathcal{M}_\mu$ with $\varepsilon^\mathcal{M}_\mu \epsilon^\mu_\mathcal{N} = \delta^\mathcal{M}_\mathcal{N}$. The proper distance along the space-like geodesics

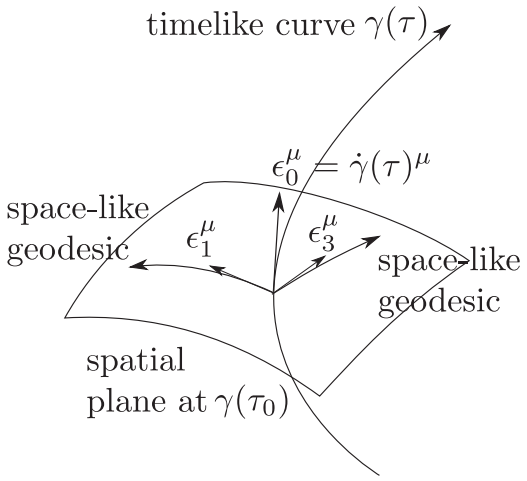

Figure 4. The proper detector frame can be defined along any time-like curve γ. The time coordinate is the proper time τ measured along the curve. The spatial coordinates at a proper time τ_0 are constructed from the proper distances along space-like geodesics that originate at $\gamma(\tau_0)$. The point with coordinates $(c\tau_0, x, y, z)$ is found by following the spatial geodesic with tangent $x^a \epsilon_a^\mu$ a proper distance $(x^2 + y^2 + z^2)^{1/2}$ from $\gamma(\tau_0)$.

extending from $\gamma(\tau)$ in the spatial directions generated from $\epsilon_J^\mu(\tau)$ and the proper time τ along the world line of the observer generate a coordinate system that is associated with the observer (see figure 4). This coordinate system only exists in the vicinity of the observer's world line, as it can only here be ensured that the spatial hyperplanes generated by $\epsilon_J^\mu(\tau)$ at different τ do not intersect. In these coordinates, the spacetime metric seen by a non-rotating observer can be given simply in terms of: the Riemann curvature tensor along $\gamma(\tau)$ given as $R_{\mathcal{MNKL}}(\tau) = \epsilon^\alpha_{\mathcal{M}}(\tau)\epsilon^\beta_{\mathcal{N}}(\tau)\epsilon^\gamma_{\mathcal{K}}(\tau)\epsilon^\delta_{\mathcal{L}}(\tau) g_{\alpha\sigma}(\gamma(\tau)) R^\sigma{}_{\beta\gamma\delta}(\gamma(\tau))$ where

$$R^\alpha{}_{\beta\gamma\delta} = \partial_\gamma \Gamma^\alpha_{\beta\delta} - \partial_\delta \Gamma^\alpha_{\beta\gamma} + \Gamma^\alpha_{\gamma\rho}\Gamma^\rho_{\beta\delta} - \Gamma^\alpha_{\delta\rho}\Gamma^\rho_{\beta\gamma}; \tag{9}$$

and the non-gravitational acceleration with respect to a local freely falling frame, represented by the spatial vector $\mathbf{a}^J := \varepsilon^J_\mu a^\mu$, where $a^\mu = (\nabla_{\dot{\gamma}}\dot{\gamma})^\mu$.

This coordinate system is called *Fermi normal coordinates* for a freely falling, non-rotational observer ($\mathbf{a} = 0$) [39] or *the proper detector frame* if proper acceleration occurs [9, 40]. The proper detector frame of a non-rotating observer is accurate for proper distances [40]

$$|\mathbf{x}| \ll l_{\text{var}} = \min\left\{\frac{c^2}{|\mathbf{a}^J|}, \frac{1}{|R^{\mathcal{M}}{}_{\mathcal{NPQ}}|^{1/2}}, \frac{|R^{\mathcal{M}}{}_{\mathcal{NPQ}}|}{|R^{\mathcal{M}}{}_{\mathcal{NPQ},\mathcal{R}}|}\right\}. \tag{10}$$

In the following, we will assume that the length of the resonator L_p is small in comparison to the scale l_{var}. We consider $\gamma(\tau)$ to be the world line of the point at which the rod that holds the resonator is supported. We assume that this point is somewhere inside the resonator. If it is not attached to any device, we assume that the center of acceleration is the rod's center of mass. We also assume that the resonator is not rotating in the frame of the observer. We orient the spatial geodesic representing the rigid rod along the z-direction at $\gamma(\tau)$, i.e. $s'_\tau(\varsigma) = (0, 0, 0, 1)$. By construction of the proper detector frame, the geodesics $s_\tau(\varsigma)$ run along the z-coordinate. Then, we consider two cases; for the first case we assume that

$$\frac{1}{|R^0{}_{z0z}|^{1/2}} \ll \min\left\{\frac{c^2}{|a^J|}\right\}, \tag{11}$$

and we take curvature into consideration. For the second case, we neglect curvature. In the following, we treat the first case directly and the second case can be obtained by setting the contributions of curvature to zero in the equations for the relative frequency shift. In particular, in both cases, we are allowed to consider only first order contributions of the proper acceleration. With this assumption, we can consider the metric in the proper detector frame as a linearly perturbed flat spacetime metric. We define the metric perturbation $h^P_{\mathcal{MN}} := g^P_{\mathcal{MN}} - \eta_{\mathcal{MN}}$. For example, in the gravitational field of the Earth, the inverse of the square root of the spatial curvature in the direction away from the center of the Earth is of the order of 10^{11} m, while the length scale given by c^2 over the gravitational acceleration is of the order of 10^{16} m. Therefore, the condition (11) is fulfilled by four orders of magnitude for the acceleration.

Neglecting quadratic terms in the acceleration, we obtain for the following components of the spacetime metric in the proper detector frame of a non-rotating observer [40] (as above, Latin indices are used for the spatial components with respect to the tetrads and spatial indices are raised and lowered with the spatial metric

$\delta_{IJ} = \mathrm{diag}(1, 1, 1)$)

$$g^P_{00}(c\tau, \mathbf{x}) \approx -\left(1 + \frac{2}{c^2}\mathbf{a}_J(\tau)\mathbf{x}^J + R_{0I0J}(\tau)\mathbf{x}^I\mathbf{x}^J\right)$$
$$g^P_{0J}(c\tau, \mathbf{x}) \approx -\frac{2}{3}R_{0KJL}(\tau)\mathbf{x}^K\mathbf{x}^L$$
$$g^P_{IJ}(c\tau, \mathbf{x}) \approx \delta_{IJ} - \frac{1}{3}R_{IKJL}(\tau)\mathbf{x}^K\mathbf{x}^L. \tag{12}$$

Since we assumed $s'_\tau(\varsigma) = (0, 0, 0, 1)$ and by construction of the proper detector frame, the proper length of the geodesics $s_\tau(\varsigma)$ is $L_p = b - a$, where the spatial positions of the mirrors are $(0, 0, b)$ and $(0, 0, a)$ with $b \geqslant 0$ and $a \leqslant 0$. Then, we find from equation (12) that $g^P_{0z}(c\tau, 0, 0, z) \approx 0$ for all τ and z along the resonator. Furthermore, by construction, all segments of the rod remain at fixed coordinate positions along the z-axis and we find that $\dot\gamma_\varsigma(\varrho)^{\mathcal{M}} = ((g^P_{00})^{-1/2}, 0, 0, 0)$. Since $s'_\tau(\varsigma) = (0, 0, 0, 1)$, we obtain $g^P_{\mathcal{MN}}\dot\gamma_\varsigma(\varrho)^{\mathcal{M}}s'^{\mathcal{N}}_\varrho(\varsigma) = (g^P_{00})^{-1/2}g^P_{0z}(c\tau(\varrho), 0, 0, z(\varsigma))$. From equation (12) and one of the symmetries of the Riemann tensor $R_{\mathcal{MNKL}} = -R_{\mathcal{MNLK}}$ follows that the condition $g^P_{\mathcal{MN}}\dot\gamma_\varsigma(\varrho)^{\mathcal{M}}s'^{\mathcal{N}}_\varrho(\varsigma) = 0$, which we assumed in our definition of a rigid resonator in section 2, is approximately fulfilled for a small proper length of the resonator[6].

To obtain the frequency of the rigid resonator measured by an observer at $\mathbf{x}$ using equation (5), we have to calculate the corresponding radar distance between the mirrors. The radar distance is obtained from the trajectories $\xi_\pm(\iota)$ of light like particles bouncing back and forth between the mirrors as described in section 3 and illustrated in figure 3. In section 3, we already assumed that acceleration and curvature only change very slowly with τ. Under this assumption, we can replace acceleration and curvature in equation (12) by their values at τ_0. The trajectories $\xi_\pm(\iota)$ have to fulfill the null condition $g^P_{\mathcal{M}\mathcal{N}}(\xi(\iota))\dot\xi^{\mathcal{M}}(\iota)\dot\xi^{\mathcal{N}}(\iota) = 0$ and the geodesic equation that governs the motion of test particles $\ddot\xi^{\mathcal{A}}(\iota) = -\Gamma^{\mathcal{A}}_{\mathcal{BC}}(\xi(\iota))\dot\xi^{\mathcal{B}}(\iota)\dot\xi^{\mathcal{C}}(\iota)$. In first order in $h^P_{\mathcal{MN}}$, one finds for the Christoffel symbols

$$\Gamma^{\mathcal{A}}_{\mathcal{BC}} = \frac{1}{2}\eta^{\mathcal{AR}}(\partial_{\mathcal{B}}h^P_{\mathcal{CR}} + \partial_{\mathcal{C}}h^P_{\mathcal{BR}} - \partial_{\mathcal{R}}h^P_{\mathcal{BC}}), \tag{13}$$

which shows that the Christoffel symbols are of the same order as $h^P_{\mathcal{M}}\mathcal{N}$. Then, to first order in $h^P_{\mathcal{M}}\mathcal{N}$, the trajectories are given by $\xi^{\mathcal{M}}_\pm(\iota) = c(\iota_{0,\pm} + \iota, 0, 0, \pm\iota) + \delta^{\mathcal{M}}_\pm(\iota)$, where $\iota_{0,\pm}$ are constants and the functions $\delta^{\mathcal{M}}_\pm(\iota)$ are of the same order as $h^P_{\mathcal{M}}\mathcal{N}$. With $R_{\mathcal{MNKL}} = -R_{\mathcal{MNLK}}$, we find that $g^P_{zz} \approx 1$ and $g^P_{0z} = g^P_{z0} \approx 0$ along $\xi_\pm(\iota)$, and we obtain that $\dot\delta^0_\pm(\iota) \approx ch^P_{00}(c\iota_{0,\pm}, 0, 0, \pm c\iota)$ and $\dot\delta^z_\pm(\iota) \approx \pm ch^P_{00}(c\iota_{0,\pm}, 0, 0, \pm c\iota)/2$ solve the light cone condition and the geodesic equation. The difference in coordinate time τ between sending and receiving the light pulse is given as

$$\delta\tau = \int_{\iota_{+,a}}^{\iota_{+,b}} \dot\xi^0_+(\iota)\mathrm{d}\iota + \int_{\iota_{-,b}}^{\iota_{-,a}} \dot\xi^0_-(\iota)\mathrm{d}\iota, \tag{14}$$

where $\iota_{\pm,a}$ and $\iota_{\pm,b}$ are the parameter values at which the ray intersects with the world lines of mirror A and mirror B, respectively. A transformation of the integration variable to $z_\pm = \xi^z_\pm(\iota)$ leads to

$$\delta\tau = \int_a^b \frac{\dot\xi^0_+(\iota(z_+))}{\dot\xi^z_+(\iota(z_+))}\mathrm{d}z_+ + \int_b^a \frac{\dot\xi^0_-(\iota(z_-))}{\dot\xi^z_-(\iota(z_-))}\mathrm{d}z_-, \tag{15}$$
$$\approx \int_a^b \frac{c + \dot\delta^0_+(z_+/c)}{c + \dot\delta^z_+(z_+/c)}\mathrm{d}z_+ + \int_b^a \frac{c + \dot\delta^0_-(-z_-/c)}{-c + \dot\delta^z_-(-z_-/c)}\mathrm{d}z_-, \tag{16}$$

which reduces to

$$\delta\tau \approx 2\int_a^b \mathrm{d}z_\pm\left(1 + \frac{h^P_{00}(c\tau_0, 0, 0, z_\pm)}{2}\right)$$
$$\approx 2\int_a^b \mathrm{d}z_\pm\left(1 - \frac{1}{2}\left(\frac{2}{c^2}\mathbf{a}^z(\tau_0)z_\pm + R_{0z0z}(\tau_0)z^2_\pm\right)\right)$$
$$\approx \frac{2}{c}L_p\left(1 - \frac{\mathbf{a}^z(\tau_0)}{2c^2}\beta L_p - \frac{R_{0z0z}(\tau_0)}{24}(3\beta^2 + 1)L^2_p\right), \tag{17}$$

where we defined $\beta \coloneqq 2b/L_p - 1$ and used $a = (\beta - 1)L_p/2$. Under the assumption of slowly changing acceleration and curvature, the coordinate time $\delta\tau$ needed for a round trip of a light pulse inside the resonator is independent of the point on the z-axis where it was sent from and received at, as long as it is sent and received at the same point. Therefore, we can calculate the radar length of the resonator measured at a given position

[6] Here small proper length means that the proper detector frame metric (12) is still a valid approximation to the actual spacetime metric.

$z_0 = (\sigma + \beta)L_p/2$ along the z-axis inside the resonator ($\sigma \in [-1, 1]$) as

$$R_\sigma \approx \sqrt{-g^P_{00}((\tau_0,\, 0,\, 0,\, z_0))}\,\frac{c}{2}\delta\tau = L_p\left[1 + \frac{\mathbf{a}^z(\tau_0)}{2c^2}\sigma L_p + \frac{R_{0z0z}(\tau_0)}{24}(3\sigma^2 + 6\sigma\beta - 1)L_p^2\right]. \tag{18}$$

Equation (18) was calculated for a given time τ_0 to make our assumption of slow changes of acceleration and curvature explicit. Of course, we are free to choose the value of τ_0. Therefore, we can replace τ_0 in equation (18) with τ. Then, the relative change of the resonance frequencies measured at $z_0 = (\sigma + \beta)L_p/2$ is given as

$$\delta_{\omega,\sigma} := \frac{\omega_n}{\bar{\omega}_n} - 1 \approx -\frac{\mathbf{a}^z(\tau)}{2c^2}\sigma L_p - \frac{R_{0z0z}(\tau)}{24}(3\sigma^2 + 6\sigma\beta - 1)L_p^2, \tag{19}$$

where $\bar{\omega}_n$ is the nth resonance frequency of the resonator for vanishing acceleration and curvature.

We find that the only linear contribution of the acceleration $\mathbf{a}^z$ to the resonance frequency spectrum in equation (19) is via a position-dependent red shift. It vanishes for $\sigma = 0$, which corresponds to a frequency measurement in the center of the resonator. The term $3\sigma^2$ corresponds to a pure red shift with respect to the center of the cavity. The term $6\beta\sigma$ is due to the displacement of the resonator's support from its center. In order to move the support along the trajectory $\gamma(\tau)$, while keeping the proper length of the resonator constant, the acceleration $\mathbf{a}^z_{\mathrm{cm}}(\tau) = \mathbf{a}^z(\tau) + c^2 R_{0z0z}(\tau)\beta L_p/2$ must be applied to the center of mass of the resonator[7]. Based on these considerations, we can rewrite equation (19) as

$$\delta_{\omega,\sigma} \approx -\frac{\mathbf{a}^z_{\mathrm{cm}}(\tau)}{2c^2}\sigma L_p - \frac{R_{0z0z}(\tau)}{24}(3\sigma^2 - 1)L_p^2. \tag{20}$$

However, a realistic rod can never be rigid. In the next section, we will consider the first order deviations from the rigid rod by taking the deformation of the rod due to small inertial and gravitational forces into account.

5. Deformable optical resonators

In the proper detector frame, every segment of the rod has a world line with constant spatial components. The acceleration of a segment of the rod at $\mathbf{x} = (c\tau, 0, 0, z)$, in comparison to a freely falling test particle initially at rest at the same position as that segment, can be derived from the geodesic equation

$$\ddot{\gamma}^{\mathcal{M}}_{\mathrm{rest},\mathbf{x}}(\tau_{\mathrm{rest}}) = -\Gamma^{\mathcal{M}}_{\mathcal{A}\mathcal{B}}(\gamma_{\mathrm{rest},\mathbf{x}})\dot{\gamma}^{\mathcal{A}}_{\mathrm{rest},\mathbf{x}}(\tau_{\mathrm{rest}})\dot{\gamma}^{\mathcal{B}}_{\mathrm{rest},\mathbf{x}}(\tau_{\mathrm{rest}}), \tag{21}$$

where, in first order in the metric perturbation, the tangent for a test particle at rest is $\dot{\gamma}_{\mathrm{rest},\mathbf{x}} = (c(-g^P_{00}(\mathbf{x}))^{-1/2},\, 0,\, 0,\, 0)$ with $(-g^P_{00}(\mathbf{x}))^{-1/2} \approx 1 + h^P_{00}(\tau,\, 0,\, 0,\, z)/2$. The dot means the derivative with respect to the curve parameter τ_{rest}. In first order in $h^P_{\mathcal{M}\mathcal{N}}$, the Christoffel symbols are given by equation (13) and are proportional to the metric perturbation. Therefore, expanding equation (21) in first order in the metric perturbation, we find $\ddot{\gamma}^{\mathcal{M}}_{\mathrm{rest},\mathbf{x}} \approx -c^2\Gamma^{\mathcal{M}}_{00}$. Since $c\mathrm{d}\tau/\mathrm{d}\tau_{\mathrm{rest}} = \dot{\gamma}^0_{\mathrm{rest},\mathbf{x}} \approx 1 + h^P_{00}(\tau,\, 0,\, 0,\, z)/2$, we obtain $\mathbf{a}^J_P \approx -c^2\Gamma^J_{00}$ for the proper and tidal accelerations.

We consider the effect of $\mathbf{a}_P$ on the resonator's end mirrors and the resulting deformation of the rod to be negligible in comparison to the direct effect of $\mathbf{a}_P$ on the rod. Then, we obtain the inertial and tidal forces on the rod by multiplication of $\mathbf{a}_P$ with the mass density ρ. These forces give rise to stresses within the rod, represented by the stress tensor σ_{KL}. For static forces and forces that change very slowly, the stresses are related to the strain via Hooke's law as

$$\varepsilon_{IJ} = (\mathcal{C}^{-1})_{IJKL}\sigma_{KL}, \tag{22}$$

where $\mathcal{C}^{-1}$ is the inverse of the stiffness tensor for the material the rod is composed of. From the strain, we can calculate the deformation of the rod by integration along the length of the rod from its center of mass. Since the change of diameter of the rod and its deformations in the x–y-plane are not of interest for us, we can restrict our considerations to ε_{zz}, ε_{xz} and ε_{yz}. We assume a constant cross section A of the rod, and we assume that the diameter of the rod is much smaller than its length. The contribution of ε_{xz} and ε_{yz} on the length of the rod are of second order in the metric perturbation and can be neglected (see appendix C) if

$$\mathbf{a}^z_{P,\mathrm{av}} \gg \max\left\{L_p^5\langle|\mathbf{a}^x_{P\,\max}|\rangle^2/c_s^2 w_x^4,\, L_p^5\langle|\mathbf{a}^y_{P\,\max}|\rangle^2/c_s^2 w_y^4\right\}. \tag{23}$$

where $\mathbf{a}^x_{P\,\max}$ and $\mathbf{a}^y_{P\,\max}$ are the maxima of proper acceleration in the x-direction and y-direction, respectively, w_x and w_y are the diameters of the rod in the x-direction and y-direction, respectively, and $\mathbf{a}^z_{P,\mathrm{av}}$ is the largest of

[7] This result can be directly obtained by considering the differential acceleration between the support and the center of the cavity by use of the geodesic deviation equation.

the values given by $\langle\beta|\mathbf{a}^z(\tau)|\rangle$ and $\langle(3\beta^2+1)L_pc^2|R_{0z0z}(\tau)|/6\rangle$, where $\langle\rangle$ denotes the averaging over the observation time (see appendix C for the derivation). With these considerations, the tidal accelerations in the proper detector frame in the transversal direction can be neglected if the following conditions hold

$$\mathbf{a}^z_{P,\mathrm{av}} \geqslant \max\{w_x c^2\langle|R_{0x0x}|\rangle,\ w_y c^2\langle|R_{0y0y}|\rangle\}, \tag{24}$$

Additionally, we assume that the various contributions to the transversal tidal acceleration do not oscillate on resonance with any elastic mode of the rod that is not already on resonance with the oscillations of the longitudinal acceleration and the longitudinal tidal acceleration. In most situations of interest, it should be easy to fulfill these conditions by choosing an appropriate orientation of the resonator and appropriate values for w_x and w_y. In particular, the conditions are fulfilled for the examples given in sections 7–9.

Under the above conditions, the only non-zero component of the stress tensor of interest for us is σ_{zz} and its relation to the strain is given as

$$\varepsilon_{zz} = \frac{1}{Y}\sigma_{zz}. \tag{25}$$

where Y is the Young's modulus of the rod material. If we assume a constant mass density, the force along the rod in the positive z-direction can be obtained as

$$F^z_+(\tau, z) = \int_z^b \mathrm{d}z'\rho A\ \mathbf{a}^z_P(z', \tau) \simeq -\rho A(b-z)\left(\mathbf{a}^z(\tau) + \frac{c^2}{2}(b+z)R_{0z0z}(\tau)\right). \tag{26}$$

where we made use of $\mathbf{a}^z_P(z,\tau) \simeq -c^2\Gamma^z_{00}(z,\tau) = -(\mathbf{a}^z(\tau) + c^2R_{0z0z}(\tau)z)$. For the force along the rod in the negative z-direction, we find

$$F^z_-(\tau, z) \simeq -\rho A(z-a)\left(\mathbf{a}^z(\tau) + \frac{c^2}{2}(z+a)R_{0z0z}(\tau)\right). \tag{27}$$

Since the support of the resonator is inside the resonator, we obtain the total deformation of the resonator by integrating the strains $\varepsilon^+_{zz} = F^z_+/A$ and $\varepsilon^-_{zz} = F^z_-/A$ on the two sides of the resonator from $z = 0$ to the ends, respectively. The effective change of the proper length is

$$\delta L_p \simeq \int_0^b \mathrm{d}z'\varepsilon^+_{zz}(z') + \int_a^0 \mathrm{d}z'\varepsilon^-_{zz}(z') = -\frac{c^2}{c_s^2}L_p\left(\frac{\mathbf{a}^z(\tau)}{2c^2}\beta L_p + \frac{R_{0z0z}(\tau)}{12}(3\beta^2+1)L_p^2\right). \tag{28}$$

where $c_s = \sqrt{Y/\rho}$ is the speed of sound in the rod material. The acceleration induces a contraction of one side of the resonator and an expansion of the other. Therefore, the acceleration amounts to a change of the proper length, proportional to the displacement $\beta L_p/2$ of the support with respect to the center of the resonator. The change of the proper length proportional to $R_{0z0z}(\tau)$ can be split into two terms. The term proportional to β^2 corresponds to the acceleration $\mathbf{a}^z_{\mathrm{cm}}(\tau_0) = \mathbf{a}^z(\tau_0) + c^2R_{0z0z}(\tau)\beta L_p/2$ of the center of mass of the resonator that we discussed at the end of section 4. For a freely falling resonator ($\beta = 0 = \mathbf{a}^z(\tau)$), only the second term in the brackets remains.

From equations (19) and (28), we find for the relative change of the resonance frequencies of the deformable resonator

$$\begin{aligned}\delta_{\omega,\sigma} &\approx -\frac{\delta L_p}{L_p} - \left(\frac{\mathbf{a}^z(\tau)}{2c^2}\sigma L_p + \frac{R_{0z0z}(\tau)}{24}(3\sigma^2+6\sigma\beta-1)L_p^2\right)\\ &\approx \frac{\mathbf{a}^z(\tau)}{2c^2}\left(\frac{c^2}{c_s^2}\beta-\sigma\right)L_p + \frac{R_{0z0z}(\tau)}{24}\left(2\frac{c^2}{c_s^2}(3\beta^2+1) - 3\sigma^2 - 6\sigma\beta + 1\right)L_p^2.\end{aligned} \tag{29}$$

Note that the deformation of the resonator changes the coordinate position of every point inside the resonator[8]. This leads to a change in the trajectory of a light pulse within the resonator, and the whole calculation we made in section 4 would be changed. However, this change would only amount to a change of the resonance frequencies in second order in the metric perturbation and we can neglect it.

Again, we can write the relative shift of the resonance frequencies in a neater way using the center of mass acceleration as

$$\delta_{\omega,\sigma} \approx \frac{\mathbf{a}^x(\tau)_{\mathrm{cm}}}{2c^2}\left(\frac{c^2}{c_s^2}\beta-\sigma\right)L_p + \frac{R_{0z0z}(\tau)}{24}\left(2\frac{c^2}{c_s^2}+1-3\sigma^2\right)L_p^2. \tag{30}$$

As expected, we would obtain the result in equation (20) for the Born rigid rod from equation (30) if the speed of sound in the material was infinite. This coincides with the observation that a Born rigid rod violates causality, as

[8] Any deformation of the rod also leads to a change of density and the speed of sound in the rod which, in turn, leads to a modulation of the deformation of the rod. We consider this effect to be negligible here. In particular, it corresponds to a nonlinear correction of Hook's law. Therefore, the result in equation (29) can be considered accurate as long as Hook's law can be applied. As the deformations considered are supposed to be small, Hook's law should hold with a very good accuracy.

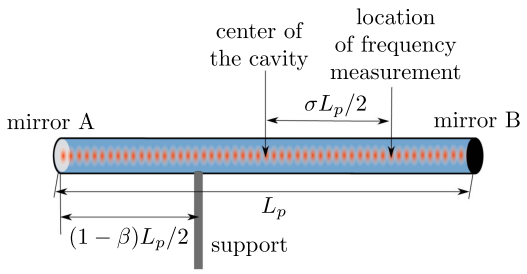

Figure 5. In the case of a dielectric optical resonator, we consider the rod itself to be the resonator.

its segments would need to interact with an infinite speed. A more realistic definition of a rigid rod was given in [33] as a rod in which the speed of sound is equivalent to the speed of light. In appendix D, we show that the approach of [33] leads to the same expression of the change of the length of the rigid rod as our equation (28). The relative shift of the resonance frequencies for such a causal rigid rod is found from equation (30) in the limit $c_s \to c$ as

$$\delta_{\omega,\sigma} \approx \frac{\mathbf{a}^z(\tau)_{\mathrm{cm}}}{2c^2}(\beta - \sigma)L_p + \frac{R_{0z0z}(\tau)}{8}(1 - \sigma^2)L_p^2. \tag{31}$$

In particular, we find that the contribution of curvature to the relative frequency shift vanishes if the frequency is measured at one of the mirrors corresponding to $\sigma = \pm 1$.

However, the speed of sound c_s in every realistic material is always much smaller than the speed of light: for example the speed of sound in aluminum is of the order $5 \times 10^3\ \mathrm{m\ s^{-1}}$. To date, the material with the highest ratio of Young's modulus and density $Y/\rho = c_s^2$ is carbyne, with a value of the order of $10^9\ \mathrm{m^2\ s^{-2}}$ [41], which would correspond to a speed of sound of the order of $3 \times 10^4\ \mathrm{m\ s^{-1}}$. Therefore, we find that the effect of the deformation of matter is by far the most dominant and the rod is far from rigid (may it be Born rigid or causal rigid) in all realistic situations. However, the relativistic effect of gravitational red shift gives a fundamental limit on the definition of the frequency spectrum of an optical resonator as a property of the resonator alone; when resonance frequencies of an optical resonator are to be specified with a precision of the order of this relativistic effect, the position of the frequency measurement has to specified.

Finally, we want to point out that the ratio of Young's modulus and density is called the specific modulus. In this sense, c^2 can be thought of as the specific modulus of spacetime. It is interesting to note that this value is off by a factor 4 from the value $4c^2$ given for the specific modulus of spacetime in [42].

6. Deformable dielectric optical resonators

Up to this point, we have only discussed the case of an empty cavity resonator. Now, let us assume that the rod itself is the optical resonator. In particular, we assume that it consists of an isotropic homogeneous dielectric medium (see figure 5). In [43], it was shown that light rays in an isotropic dielectric follow light like geodesics with respect to the dielectric metric tensor (see also [34, 44])

$$g^{P,\mathrm{diel}}_{\mathcal{MN}} = g^P_{\mathcal{MN}} - \left(\frac{c^2_{\mathrm{diel}}}{c^2} - 1\right)u_{\mathcal{M}}u_{\mathcal{N}}, \tag{32}$$

where $c^2_{\mathrm{diel}} = (\epsilon\mu)^{-1}$ is the speed of light inside the medium and $u^{\mathcal{M}} = g^{P\,\mathcal{MN}}u_{\mathcal{N}}$ is the normalized tangent vector to the world line associated with the local segments of the dielectric. In our case, these are the segments of the resonator, and therefore, $u^{\mathcal{M}}(z) = (1 + h^P_{00}/2,\ 0,\ 0,\ 0)$ and $u_{\mathcal{M}}(z) \approx (-1 + h^P_{00}/2,\ h^P_{01},\ h^P_{02},\ h^P_{03})$. From equation (32), we obtain the metric

$$\begin{aligned} g^{P,\mathrm{diel}}_{00}(c\tau,\ \mathbf{x}) &\approx -\frac{c^2_{\mathrm{diel}}}{c^2}\left(1 + \frac{2}{c^2}\mathbf{a}_J(\tau)\mathbf{x}^J + R_{0I0J}(\tau)\mathbf{x}^I\mathbf{x}^J\right) \\ g^{P,\mathrm{diel}}_{0J}(c\tau,\ \mathbf{x}) &\approx -\frac{2}{3}\frac{c^2_{\mathrm{diel}}}{c^2}R_{0KJL}(\tau)\mathbf{x}^K\mathbf{x}^L \\ g^{P,\mathrm{diel}}_{IJ}(c\tau,\ \mathbf{x}) &\approx \delta_{IJ} - \frac{1}{3}R_{IKJL}(\tau)\mathbf{x}^K\mathbf{x}^L. \end{aligned} \tag{33}$$

Now, all of the considerations made for the empty resonator above can also be made for a resonator composed of an isotropic, homogeneous dielectric by using the metric $g^{P,\mathrm{diel}}_{\mathcal{MN}}$ for the propagation of the phase fronts given by the eikonal function. Hence, we obtain the resonance frequencies in an isotropic homogeneous dielectric by

multiplying the result for the empty resonator with c_{diel}/c. This factor cancels in the relative frequency perturbation so that

$$\delta^{\text{diel}}_{\omega,\sigma} = \delta_{\omega,\sigma}. \tag{34}$$

A similar metric as in (32) has been shown to arise for particles or quasiparticles in other matter systems, e.g. for electrons in graphene [45]. Our analysis may also apply to these situations.

7. Example: uniform acceleration

To illustrate the applicability of our results, we will consider some examples in the following. A particularly straightforward example is the situation of a non-rotating resonator that is uniformly accelerated along the optical axis. From the equivalence principle follows that this situation is similar to the situation of an optical resonator kept vertically at a fixed position in the gravitational field of a massive object like the Earth. However, since we are considering an extended object, the curvature of the gravitational field would also enter the frequency spectrum of the resonator as in equation (30). Hence, the effect of uniform acceleration and a gravitational field do only coincide if the effect of curvature can be neglected. For uniform acceleration, we find

$$\delta_{\omega,\sigma} \approx \left(\frac{\beta}{c_s^2} - \frac{\sigma}{c^2}\right)\frac{\mathbf{a}^x L_p}{2}. \tag{35}$$

For $\beta = \pm 1$, a length of the resonator of $L_p \sim 2$ cm, an acceleration of the order of 10 ms^{-2}, which is similar to the gravitational acceleration of the Earth, and a speed of sound in the rod of the order of 10^3 ms^{-1} (similar to the speed of sound in aluminum), we obtain a relative frequency shift of the order of 10^{-7}. This frequency shift is given only by the first term in equation (35) as the second term is smaller by about 11 orders of magnitude. Since the first term is due to the deformation of the resonator it is a Newtonian effect.

For the case $\beta = 0$ the first term in (35) vanishes. What remains is a purely relativistic effect, the gravitational red shift, due to a difference in proper time between the center of the resonator and every other point along the optical axis. Setting the parameter σ to -1 and $+1$ means that the frequency is measured at the mirror A and mirror B, respectively. We find a relative frequency shift of the order of $\mp 10^{-18}$. The measurement of such a small frequency shift seems to be experimentally challenging but may be feasible with state of the art technology. For example, currently, optical clocks reach a relative precision of 10^{-18} over an integration time of 1 s [46, 47]. Of course, higher frequency shifts can be reached with longer cavities and larger accelerations. In particular, the effect of gravitational red shift was already measured on the length scale of about 33 cm [48]. As argued above, the effect of gravitational red shift gives a limit on the validity of the concept of the frequency spectrum as a property of the optical resonator itself. For the parameters of the example above, we find that a reference for the frequency measurement has to be given when the frequency spectrum is to be specified with a relative precision of 10^{-18}.

8. Example: plunge into a black hole

We consider the results derived in this article as a basis for optomechanics in relativity and gravity which implies their application to experiments in laboratories on the surface of the Earth or in space. However, our approach is not limited to spacetimes that only bear weak gravitational effects. It is the spacetime metric seen by the optical resonator in its proper detector frame that has to be a linearized metric. This is ensured by the condition $l_{\text{var}} \gg L_p$. To illustrate the applicability of our results to spacetimes with strong gravitational effects, we consider the situation of a non-rotating resonator that falls into a non-rotating black hole (see figure 6). To this end, we consider the Schwarzschild metric in spherical Schwarzschild coordinates (ct, r, ϑ, ϕ)

$$g = \text{diag}\left(-f(r), \frac{1}{f(r)}, r^2, r^2\sin^2(\vartheta)\right), \tag{36}$$

where $f(r) = 1 - r_S/r$ and r_S is the Schwarzschild radius. We assume that the support of the resonator falls radially from $r = R$ into the center of the black hole at $\phi = 0$ and $\vartheta = \pi/2$. The corresponding trajectory is given in [49] as

$$r(\varrho) = R\cos^2(\varrho/2), \tag{37}$$

$$c\tau(\varrho) = \frac{R}{2}\left(\frac{R}{r_S}\right)^{1/2}(\varrho + \sin\varrho), \tag{38}$$

parameterized by ϱ. We see that $r = 0$ for $\varrho = \pi$, which means that the singularity at the center of the black hole is reached in finite proper time $\tau = \pi R^{3/2}/2cr_S^{1/2}$. The tangent to the world line of the falling support of the

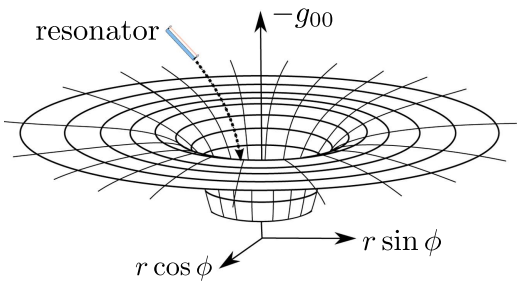

Figure 6. Artistic representation of the optical resonator plunging radially into a black hole.

resonator is

$$\dot{\gamma}^\mu = c\left(\frac{\sqrt{f(R)}}{f(r(\varrho))}, -\sqrt{\frac{r_S}{R}}\frac{\sin\varrho}{1+\cos\varrho}, 0, 0\right), \tag{39}$$

where $\varrho = \varrho(\tau)$ is implicitly given by equation (38), $\dot{\gamma}^1$ can be obtained directly from equations (37) and (38) and $\dot{\gamma}^0$ can be found from the normalization condition $\dot{\gamma}^\mu\dot{\gamma}^\nu g_{\mu\nu}(r(\varrho)) = -c^2$. Then, the time line can be found as $\gamma = (ct(\tau), r(\varrho(\tau)), \pi/2, 0)$, where $ct(\tau) = \int_0^\tau \mathrm{d}\tau'\ \dot{\gamma}^0(\varrho(\tau'))$. An orthonormal tetrad that is parallel transported along the time-like geodesic γ is given as

$$\begin{aligned}
\tilde{\epsilon}_0^\mu &= \dot{\gamma}^\mu/c,\\
\tilde{\epsilon}_1^\mu &= \left(-\sqrt{\frac{r_S}{R}}\frac{\tan(\varrho/2)}{f(r(\varrho))}, \sqrt{f(R)}, 0, 0\right),\\
\tilde{\epsilon}_2^\mu &= (0, 0, r(\varrho)^{-1}, 0) \quad \text{and}\\
\tilde{\epsilon}_3^\mu &= (0, 0, 0, r(\varrho)^{-1}).
\end{aligned} \tag{40}$$

All other orthonormal tetrads can be obtained by orthogonal transformations in three-dimensions on the spatial part of the tetrad (40). Due to the spherical symmetry of the spacetime and the radial trajectory of the resonator at $\vartheta = \pi/2$ and $\phi = 0$, we can restrict our considerations to rotations in the ϵ_1^μ–ϵ_3^μ-plane. Then, we define the rotated frame

$$\begin{aligned}
&\epsilon_0^\mu = \tilde{\epsilon}_0^\mu, \quad \epsilon_1^\mu = \cos\varphi\ \tilde{\epsilon}_1^\mu + \sin\varphi\ \tilde{\epsilon}_3^\mu,\\
&\tilde{\epsilon}_2^\mu = \tilde{\epsilon}_2^\mu \quad \text{and} \quad \epsilon_3^\mu = \cos\varphi\ \tilde{\epsilon}_3^\mu - \sin\varphi\ \tilde{\epsilon}_1^\mu,
\end{aligned} \tag{41}$$

where the angle $\varphi \in [0, \pi/2]$ gives the orientation of the resonator in the ϵ_1^μ–ϵ_3^μ-plane. From the tetrad (41), we obtain the proper detector frame. The z-direction is defined by ϵ_3^μ and we find from equation (29) that

$$\delta_{\omega,\sigma} \approx \frac{R_{0z0z}(\tau)}{24}\left(2\frac{c^2}{c_s^2}(3\beta^2+1) - 3\sigma^2 - 6\sigma\beta + 1\right)L_p^2,$$

where no proper acceleration appears since the resonator is assumed to be freely falling. The curvature tensor component $R_{0z0z}(\tau)$ is explicitly given as

$$\begin{aligned}
R_{0z0z}(\tau) &= \epsilon_0^\mu\epsilon_3^\nu\epsilon_0^\rho\epsilon_3^\sigma R_{\mu\nu\rho\sigma}(r(\varrho)))\\
&= \cos^2\varphi\left(\frac{f(R)}{f(r(\varrho))}\right)^2 R_{\bar{0}r\bar{0}r}(r(\varrho)),
\end{aligned} \tag{42}$$

$$+\frac{\sin^2\varphi}{R^2}\left(\frac{f(R)\sec^4(\varrho/2)}{f(r(\varrho))^2}R_{\bar{0}\phi\bar{0}\phi}(r(\varrho)) + \frac{r_S}{R}\frac{4\tan^2(\varrho/2)}{(1+\cos\varrho)^2}R_{r\phi r\phi}(r(\varrho))\right). \tag{43}$$

Here, we used that $R_{\bar{0}\phi r\phi} = 0$ for the Schwarzschild metric. The expressions for the other curvature tensor components appearing in equation (42) at $\vartheta = \pi/2$ are given as

$$\begin{aligned}
R_{\bar{0}r\bar{0}r}(r) = -\frac{r_S}{r^3}, \quad R_{\bar{0}\phi\bar{0}\phi}(r) = f(r)\frac{r_S}{2r}\\
\text{and} \quad R_{r\phi r\phi}(r) = -f(r)^{-1}\frac{r_S}{2r}.
\end{aligned} \tag{44}$$

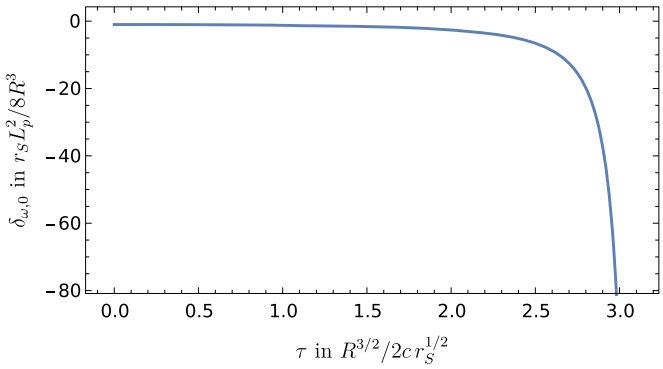

Figure 7. The frequency shift of a vertically oriented optical resonator falling into a black hole is plotted over the normalized proper time measured at the center of the resonator.

We obtain

$$R_{0z0z}(\tau) = -\frac{(1 + 3\cos(2\varphi))r_S}{4r(\varrho)^3}, \tag{45}$$

and we find that the specification of the angle of orientation of the rod φ gives rise to a numerical factor which vanishes only at $\varphi = \arccos(-1/3)/2$. Hence, for $\varphi \neq \arccos(-1/3)/2$, the frequency shift is proportional to the frequency shift at $\varphi = 0$, which corresponds to vertical orientation. For a vertically oriented causal rigid resonator supported at its center, we find the relative frequency shift at its center is given by

$$\delta_{\omega,0}(\tau) \approx -\frac{r_S L_p^2}{8r(\varrho)^3}. \tag{46}$$

The time evolution of this frequency shift is plotted in figure 7. We see that the frequency shift in equation (46) stays finite until $r = 0$ is reached at $\varrho(\tau) = \pi$. In particular, there is no effect due to the crossing of the event horizon at r_S. As stated at the beginning of this section, our approach is accurate only for $l_{\text{var}} \gg L_p$. From equation (45), we find that $l_{\text{var}} = \sqrt{r(\varrho)^3/r_S}$ for $\varphi = 0$. The stellar black hole has a Schwarzschild radius of the order of 10^3 m. For an optical resonator of a length of the order of 10^{-2} m, this implies that that our approach breaks down when a radius of the order of 1 m is reached which is far beyond the event horizon at $r = r_S$.

The effect of the event horizon can be seen by considering a situation in which the measured frequency is imprinted on a signal at the center of the resonator and sent out radially to an observer that stays at constant coordinate $r = R > r_S$. This observer receives a signal with frequency

$$\omega_{n,R}(t) \approx \sqrt{\frac{f(r(t))}{f(R)}}\left(\sqrt{f(R)} + \sqrt{\frac{r_S}{R}}\frac{\sin\varrho(\tau(t))}{1 + \cos\varrho(\tau(t))}\right)^{-1}\sqrt{f(r(t))}\,\frac{cn\pi}{L_p}(1 + \delta_{\omega,0}(\tau(t))), \tag{47}$$

where $r(t)$ and $\tau(t)$ are given implicitly by the time line $\gamma(\tau)$. The first factor on the right-hand side of equation (47) corresponds to the gravitational red shift and the second factor to the Doppler shift due to the relative velocity between the emitter and the receiver. The red shift factor $f(r(t))^{1/2}$ vanishes when the resonator passes the event horizon and becomes imaginary.

The above result can be applied as well to an optical resonator falling towards the Earth. For a distance from the center of the Earth of the same order as its radius, we find that the relative frequency shift in equation (46) is of the order of 10^{-27} for an optical resonator of 2 cm length. This relativistic effect is mostly gravitational red shift due to curvature. It is far from being observable with state of the art technology. However, it gives a fundamental limit of the validity of the concept of frequency spectrum as a property of the optical resonator without any reference as discussed above.

9. Example: an oscillating mass

As a third example, we consider the situation of a non-rotating resonator in the gravitational field of an oscillating solid sphere of massive matter. The result could be used to consider the possibility of detecting the gravitational field of a small sphere of dense material, like gold or tungsten (see figure 8). This situation is similar to the one considered in [50, 51], where the resonator is a second massive sphere on a support with restoring force. Here we will restrict ourselves to the derivation of the resonance frequency spectrum and an evaluation of its relative change for certain realistic experimental parameters. Also, we assume that the solid sphere is the only

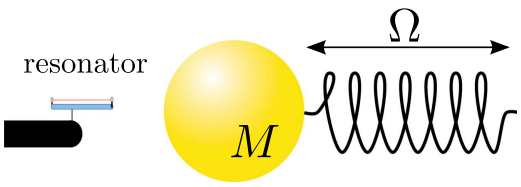

Figure 8. Illustration (not to scale) of the resonator placed in front of a gold sphere that oscillates by a lever with frequency $\Omega/2\pi$. The gravitational field of the sphere induces a change of the resonance frequencies of the resonator.

source of a gravitational field affecting the optical resonator. To model an earthbound experiment, the gravitational field of the Earth would have to be taken into account as well. To derive our model of the gravitational field of a massive sphere, we start from the Schwarzschild metric, which is given as

$$g^S_{\mu\nu} = \left(1 + \frac{r_S}{4R}\right)^4 \begin{pmatrix} -\frac{\left(1-\frac{r_S}{4R}\right)^2}{\left(1+\frac{r_S}{4R}\right)^6} & 0 & 0 & 0 \\ 0 & 1 & 0 & 0 \\ 0 & 0 & 1 & 0 \\ 0 & 0 & 0 & 1 \end{pmatrix}, \tag{48}$$

in isotropic Cartesian coordinates $(\tilde{x}^0 = c\tilde{t}, \tilde{x}, \tilde{y}, \tilde{z})$, where $r_S := 2GM/c^2$ is the Schwarzschild radius of the source mass and $R := (\tilde{x}^2 + \tilde{y}^2 + \tilde{z}^2)^{1/2}$. To first order in r_S/R, the difference of (48) from the Minkowski metric $\mathrm{diag}(-1, 1, 1, 1)$ has only four non-zero components, namely $h^S_{\tilde{0}\tilde{0}} = h^S_{\tilde{x}\tilde{x}} = h^S_{\tilde{y}\tilde{y}} = h^S_{\tilde{z}\tilde{z}} = \frac{r_S}{R}$. Let us assume that the sphere moves much more slowly than the speed of light and that we are close enough to the sphere so that all changes of the gravitational field can be considered to be instantaneous. With this, we can model the metric perturbation for the moving sphere by replacing R by $R(\tilde{t}) := ((\tilde{x} - \gamma^{\tilde{x}}_M(\tilde{t}))^2 + (\tilde{y} - \gamma^{\tilde{y}}_M(\tilde{t}))^2 + (\tilde{z} - \gamma^{\tilde{z}}_M(\tilde{t}))^2)^{1/2}$, where $\gamma^\mu_M(\tilde{t})$ is the trajectory of the source mass. The resulting metric perturbation becomes

$$h^M_{\tilde{0}\tilde{0}} = h^M_{\tilde{x}\tilde{x}} = h^M_{\tilde{y}\tilde{y}} = h^M_{\tilde{z}\tilde{z}} = \frac{r_S}{R(\tilde{t})} =: h^M, \tag{49}$$

$$h^M_{\mu\nu} = 0 \text{ for } \mu \neq \nu. \tag{50}$$

We assume that the support of the resonator is at rest in the isotropic coordinates on the $\tilde{z}$ axis in the negative $\tilde{z}$ direction. To be completely accurate, we would need to fix the proper distance between the support of the resonator and the average position of the sphere, as this corresponds to the assumption that the distance is fixed by another matter system. Furthermore, in every realistic situation, the proper distance would change as the matter system is affected by the gravitational field of the sphere and the gravitational force experienced by the resonator. However, any small error in the position of the resonator will be negligible, as it corresponds to a small change of the acceleration and curvature that we already assumed to be small. From equation (13), we find that an acceleration $a^{\tilde{z}}(\tau) = (\nabla_{\dot{\gamma}(\tau)}\dot{\gamma}(\tau))^z \approx c^2\Gamma^{\tilde{z}}_{\tilde{0}\tilde{0}} \approx -c^2 r_S/2R(\tau)^2$ along the $\tilde{z}$-axis is necessary to keep the resonator at a fixed position $\tilde{z}_0 < 0$ on the $\tilde{z}$-axis, i.e. $\gamma(\tau) = (\tau, 0, 0, \tilde{z}_0)$. For the linearly perturbed metric, the curvature tensor is given as

$$R^\alpha{}_{\beta\gamma\delta} \simeq \frac{1}{2}\eta^{\alpha\rho}(\partial_\beta\partial_\gamma h^M_{\delta\rho} - \partial_\beta\partial_\delta h^M_{\gamma\rho} - \partial_\gamma\partial_\rho h^M_{\beta\delta} + \partial_\delta\partial_\rho h^M_{\beta\gamma}). \tag{51}$$

We assume that the resonator is fixed along the $\tilde{z}$-axis. From the equation (51), we obtain the curvature component $R_{\tilde{0}\tilde{z}\tilde{0}\tilde{z}}(\tau) = -r_S/R(\tau)^3$.

To construct the proper detector frame, we need to fix the tetrad corresponding to the observer at the support of the cavity. Since we assume that the support stays at rest in the coordinates $(\tilde{x}^0, \tilde{x}, \tilde{y}, \tilde{z})$, we have $\epsilon^\mu_0 = ((g^S_{\tilde{0}\tilde{0}})^{-1/2}, 0, 0, 0)$. We define the three spatial vectors of the tetrad ϵ^μ_J with $J = 1, J = 2$ and $J = 3$ such that they point in the $\tilde{x}$-direction, $\tilde{y}$-direction and $\tilde{z}$-direction, respectively. Therefore, we find $\epsilon^\mu_1 = (0, (g^S_{\tilde{x}\tilde{x}})^{-1/2}, 0, 0)$, $\epsilon^\mu_2 = (0, 0, (g^S_{\tilde{y}\tilde{y}})^{-1/2}, 0)$ and $\epsilon^\mu_3 = (0, 0, 0, (g^S_{\tilde{z}\tilde{z}})^{-1/2})$. We conclude that the transformation to the proper detector frame is a linearized coordinate transformation. A linearized coordinate transformation leaves the curvature tensor invariant and we obtain $R_{0z0z}(\tau) = -r_S/R(\tau)^3$. Furthermore, $a^z(\tau) = \varepsilon^z_\mu a^\mu(\tau) \approx a^{\tilde{z}}(\tau)$ to first order in the metric perturbation.

Let us assume that the motion of the sphere can be described as $R(\tau) = R_0 + \delta R_0 \sin\Omega\tau$, where R_0 is the average distance between the sphere and the position of the support of the resonator, δR_0 is the amplitude of the sphere's oscillation and $2\pi\Omega$ its frequency. If we assume that δR_0 is much smaller than R_0, the proper acceleration and the curvature can be written as

$$a^z(\tau) \approx -\frac{c^2 r_S}{2R_0^2}\left(1 - \frac{2\delta R_0}{R_0}\sin(\Omega\tau + \varphi)\right), \tag{52}$$

$$R_{0z0z}(\tau) \approx -\frac{r_S}{R_0^3}\left(1 - \frac{3\delta R_0}{R_0}\sin(\Omega\tau + \varphi)\right). \tag{53}$$

The first terms in (52) and (53) are constant, and we can calculate their effect on the frequency spectrum using equation (29). The resulting time dependent resonance frequencies are given by equation (29) as

$$\delta_{\omega,\sigma} \approx -\frac{r_S L_p}{4R_0^2}\left(\left(\frac{c^2}{c_s^2}\beta - \sigma\right) + \left(2\frac{c^2}{c_s^2}(3\beta^2 + 1) - 3\sigma^2 - 6\beta\sigma + 1\right)\frac{L_p}{6R_0}\right). \tag{54}$$

Let us assume that the sphere is of gold or tungsten, that the mass of the sphere is 100 g (corresponding to a radius of the order of $r_{\mathrm{sph}} \sim 1$ cm), which corresponds to a Schwarzschild radius of the order of 10^{-27} m, the amplitude of the oscillations δR_0 is of the order 1 mm, while the length of the resonator and R_{min}, the minimal distance between the resonator and the sphere, are of the order of 1 cm. Then, we find that $R_0 = r_{\mathrm{sph}} + \delta R_0 + R_{\mathrm{min}} + L_p(1 + \beta)/2$ takes values between 2 and 3 cm. This results in values for acceleration and spacetime curvature of the order of 10^{-10} ms^{-2} and 10^{-25} m^{-2}, respectively. We mentioned above that the speed of sound in a rod of aluminum is about 5×10^3 m s^{-1}. Therefore, the relative change of the resonance frequencies of a resonator with its length fixed by an aluminum rod, in the gravitational field of the moving mass, yields $\delta_\omega \sim \mp 10^{-18}$ for $\beta = \pm 1$, where the acceleration is dominant, and $\delta_\omega \sim 10^{-19}$ for $\beta = 0$, where only the curvature contributes. The relativistic effects in equation (54) are ten orders of magnitude smaller. Hence, to detect them, the whole experimental setup would need to be under control with this precision.

For oscillation frequencies Ω far below any elastic resonances of the resonator rod, we can also derive the effect of the sinusoidally modulated terms in (52) and (53) with equation (29). We find

$$\delta^{\Omega}_{\omega,\sigma} \approx \frac{r_S L_p \delta R_0}{2R_0^3}\sin(\Omega\tau + \varphi)\left(\left(\frac{c^2}{c_s^2}\beta - \sigma\right) + \left(2\frac{c^2}{c_s^2}(3\beta^2 + 1) - 3\sigma^2 - 6\beta\sigma + 1\right)\frac{L_p}{4R_0}\right). \tag{55}$$

For the parameters used above, we find for $\beta = \pm 1$ an amplitude of the frequency oscillations of the order of 10^{-19}. The temporal modulation of the frequency shift may be an advantage in experimental situation as it may be used to increase sensitivity. As for the example of uniform acceleration, the values for the frequency shifts that we found for this setup seem to be challenging but not out of reach of state of the art experimental techniques. Oscillations of the source mass on resonance with the elastic modes of the resonator rod may be used to increase the effect on the frequency spectrum significantly. However, the consideration of this situation is beyond the framework developed in this article. It will be treated in a future article.

10. Conclusions and outlook

We derived an expression for the resonance frequencies of an optical resonator moving in a weak gravitational field in a relativistic setup. Firstly, we considered a Born rigid resonator, which we assumed to be constructed from a Born rigid rod. Secondly, we considered a deformable resonator, where we assumed the rod to consist of a realistic material with finite Young's modulus. In this context, we discussed the concept of a causal rigid rod. Besides gravitational effects, the expressions that we derived take proper acceleration of the resonator into account. As well as empty optical resonators, we considered optical resonators filled with a homogeneous dielectric material.

Our investigation revealed three fundamentally different effects. One is a simple gravitational red shift: the resonator is an extended object and time runs differently at different points inside the resonator. Therefore, the resonance frequencies of the resonator are not a global property of the resonator, but depend also on the position inside the resonator at which it is measured. The second effect is due to the difference between proper length and radar length, which leads to a shift of the resonance frequencies in the presence of non-zero curvature and acceleration even for a Born rigid resonator. The third effect is the deformation of the resonator due to curvature and acceleration, when the resonator is deformable. The deformation of the resonator is governed by only one parameter, the speed of sound c_s in the rod. It turns out that the effects of deformations are larger than the relativistic effects, red shift and difference between proper length and radar length, by a factor c^2/c_s^2. A causal rigid rod can be considered to be one with the speed of sound equivalent to the speed of light, overcoming the problems of Born rigidity [33]. We gave an expression for the resonance frequency spectrum of a causal rigid rod in equation (31). Since the largest speed of sound in any material is still many orders smaller than the speed of light, the deformations of realistic materials will dominate over the relativistic effects significantly. Therefore, a very high degree of control over the material parameters would be necessary to observe the relativistic effects. However, the relativistic effect of gravitational red shift can be seen as posing a fundamental limit on the validity

of the concept of the frequency spectrum as a property of the optical resonator alone; when resonance frequencies are to be specified with a precision of the order of the gravitational red shift, the position of frequency measurement has to be specified additionally.

The results derived in this article can be applied to general spacetime geometries if acceleration and tidal forces in the proper detector frame of the resonator are small enough. This includes freely falling resonators in strong gravitational fields like a black hole beyond the Schwarzschild radius or a uniformly accelerated cavity which we gave as examples in this article. As a third example calculation, we considered the gravitational effect of an oscillating tungsten or gold sphere on the resonance frequencies of an optical resonator in section 9. This situation is similar to the one considered in [50, 51], where the resonator is a second massive sphere on a support with a restoring force.

Note that our results can be applied to oscillating gravitational fields like that due to the oscillating source mass as long as the oscillation frequency is much smaller than the elastic resonances of the rod that constitutes the optical resonator. In the particular situation of an aluminum rod of a few centimeters and an oscillating source mass of a few gram, this is a very good approximation as the elastic modes of the rod have frequencies of the order of 100 kHz, which is hard to achieve with a source mass of this size. However, for longer resonators, smaller source masses or other oscillating gravitational fields like gravitational waves, elastic resonance may be achieved which can amplify the effect on the frequency spectrum significantly. A gravitational wave is a particular example of a situation in which the acceleration vanishes and only an oscillating curvature remains[9]. Since we already identified the deformation effects of a realistic rod as the dominant effect, the effect of oscillating curvature on the rod can be treated similar to the effect of a gravitational wave on the antenna of a resonant mass detector (see for example [9] and chapter 37 of [49] as a reference for the latter). A detailed description for a resonantly driven optical resonator as a follow up of this article will be given in a future publication.

The precision of metrological experiments with resonators depends strongly on the knowledge of the resonance frequencies of these resonators. On the one hand, the effects of acceleration and curvature on the resonance frequencies can be seen as an experimental systematic error which has to be taken into account. On the other hand, these effects can be used to measure a proper acceleration or spacetime curvature. In such experimental situations, the model we used will certainly not be fully valid and the effects have to be calculated for the precise apparatus that is used. However, the results of this article can serve as a basis for investigations of the accessibility of spacetime parameters and parameters of states of motion in the more advanced framework of quantum metrology [16].

In our analysis, the only non-Newtonian effects are the relativistic red shift and time dilation and the difference between radar length and proper length. However, the formalism employed here contains further relativistic effects (see table I of [40]) such as the Sagnac effect and magnetic type gravitational effects such as frame dragging, which induces the Lens–Thirring effect in gyroscopes. It would be interesting to include these effects in a more detailed analysis. One way could be an extension to three-dimensional optical resonator geometries and the inclusion of the polarization of the light field.

In the future, it would be desirable to have a description beyond the restrictions to small accelerations and curvatures. For that purpose, a fully relativistic description of elasticity has to be used such as those presented in [32, 33, 52]. For significant variations of the curvature on the length scale of the wavelength of the resonator modes, it would be necessary to abandon the eikonal approximation and to derive the resonance frequencies directly from solutions of the Maxwell equations in a curved spacetime. This is the case if the effect of the gravitational field of the light inside the resonator is to be considered in full generality [22]. Furthermore, the effect of rotation of the resonator has to be considered in the future. This can be done by considering higher orders of the eikonal expansion or using methods of electrodynamics like the paraxial approximation.

Acknowledgments

We thank Ralf Menzel, Jonas Schmöle, Tobias Westphal, Philipp Haslinger, José Natário, Luis Cortés Barbado, Jan Kohlrus, Ana Lucía Baez and Uwe R Fischer for interesting remarks and discussions and Kiri Mochrie for writing assistance. DR thanks the Humboldt Foundation for funding his research in Vienna with their Feodor-Lynen Felloship. RH and IF would like to acknowledge that this project was made possible through the support of the grant 'Leaps in cosmology: gravitational wave detection with quantum systems' (No. 58745) from the John Templeton Foundation. The opinions expressed in this publication are those of the authors and do not necessarily reflect the views of the John Templeton Foundation. IF would like to acknowledge that this project

[9] For example for a monochromatic gravitational wave of a particular linear polarization, we find the curvature component $R_{0z0z} = \omega^2 h/(2c^2)$, where h is the strain and ω is the frequency of the wave, when the z-axis is chosen in the polarization direction.

was made possible through the support of the grant 'Quantum Observers in a Relativistic World' from FQXi's Physics of the Observer program. The authors thank José Ignacio Latorre and the Centro de Ciencias de Benasque Pedro Pascual for hosting the workshop 'Gravity in the Lab' in 2016 where the collaboration started that led to this article. The publication of this article is funded by the Open Access Publishing Fund of the University of Vienna.

Appendix A. Relation to the concept of a rigid rod in special relativity

In special relativity, the proper length of a rod is given as the coordinate distance between its end points, calculated in the coordinate system defined by the rest frame of the rod. Here, we call $L_p(s_\varrho)$ the proper length of the rod and describe it in the following. By definition, for every ϱ_0 and every point $s_{\varrho_0}(\varsigma_0)$ of the space-like curve $s_{\varrho_0}(\varsigma)$ representing the rod, there is a space-like tangent $s'_{\varrho_0}(\varsigma_0) \coloneqq \mathrm{d}s_{\varrho_0}(\varsigma)\big/\mathrm{d}\varsigma|_{\varsigma_0}$. For every point of the curve $s_{\varrho_0}(\varsigma)$ representing the rod, there is an associated vector in the tangent space $T_{s_{\varrho_0}(\varsigma_0)}\mathcal{M}$ via the inverse of the exponential map, where the exponential map is given as $\exp_{s_{\varrho_0}(\varsigma_0)} : T_{s_{\varrho_0}(\varsigma_0)}\mathcal{M} \to \mathcal{M}$ and $\exp_{s_{\varrho_0}(\varsigma_0)}((\varsigma - \varsigma_0)s'_\varrho(\varsigma_0)) = s_{\varrho_0}(\varsigma)$. In particular, the two end points of the rod $s_{\varrho_0}(a)$ and $s_{\varrho_0}(b)$ are associated with the vectors $(\varsigma_0 - a)s'_{\varrho_0}(\varsigma_0)$ and $(b - \varsigma_0)s'_{\varrho_0}(\varsigma_0)$. Since $s_{\varrho_0}(\varsigma)$ is a space-like geodesic (in the sense of the auto-parallel property), the proper distance from $s_{\varrho_0}(\varsigma_0)$ to $s_{\varrho_0}(a)$ and $s_{\varrho_0}(b)$ is equivalent to the norm of $-(\varsigma_0 - a)s'_{\varrho_0}(\varsigma_0)$ and $(b - \varsigma_0)s'_{\varrho_0}(\varsigma_0)$, respectively, with respect to the metric $g_{\mu\nu}$ at $s_{\varrho_0}(\varsigma_0)$. Hence, for every point $s_{\varrho_0}(\varsigma_0)$ on the rod, there is a representation of the rod as a straight line $\varsigma s'_{\varrho_0}(\varsigma_0)$ in the tangent space to this point and the sum of the proper distances in both directions of the rod is equivalent to the length of the line given as $(b - a)g_{s_{\varrho_0}(\varsigma_0)}(s'_{\varrho_0}(\varsigma_0), s'_{\varrho_0}(\varsigma_0))$. We can find coordinates such that $(g_{s_{\varrho_0}(\varsigma_0)})_{\mu\nu} = \eta_{\mu\nu}$. This is called a local Lorentz frame at $s_{\varrho_0}(\varsigma_0)$. In the local Lorentz frame, the coordinate distance (in tangent space) between the end points of the line $\varsigma s'_{\varrho_0}(\varsigma_0)$ is equivalent to its length $(b - a)g_{s_{\varrho_0}(\varsigma_0)}(s'_{\varrho_0}(\varsigma_0), s'_{\varrho_0}(\varsigma_0))$. In special relativity, the spacetime and the tangent space to every point can be identified since spacetime is flat. Then, the length of the line representing the rod in tangent space is also the proper length of the rod. Therefore, we can identify $L_p(s_\varrho)$ as the generalization of the proper length of a rigid rod in GR.

Appendix B. Boundary conditions

In the following, we will will apply Maxwell's equations to the eikonal expansion in equation (2) along the same lines as in [35]. We will write $\nabla_\mu \zeta^\rho = \zeta^\rho{}_{;\mu}$ for the covariant derivative. In the following, we will apply the Lorenz gauge condition and Maxwell's equations to the eikonal expansion in equation (2). Maxwell's equations in vacuum imply that [35]

$$F_{\mu\nu;\lambda}{}^{;\lambda} + (R^\sigma{}_\mu F_{\nu\sigma} - R^\sigma{}_\nu F_{\mu\sigma}) + R_{\alpha\beta\mu\nu}F^{\alpha\beta} = 0, \tag{B1}$$

where $R_{\mu\nu}$ is the Ricci tensor. We have

$$F_{\mu\nu;\lambda} = \mathrm{Re}\left(\mathrm{e}^{\mathrm{i}\frac{\alpha}{\lambda}S(x)}\sum_{n=0}^{\infty}\left(\mathrm{i}\frac{\alpha}{\lambda}\phi_{n,\mu\nu}\hat{\xi}_\lambda + \phi_{n,\mu\nu;\lambda}\right)\left(\frac{\lambda}{\alpha}\right)^n\right) \quad \text{and} \tag{B2}$$

$$F_{\mu\nu;\lambda}{}^{;\lambda} = g^{\lambda\sigma}\,\mathrm{Re}\left(\mathrm{e}^{\mathrm{i}\frac{\alpha}{\lambda}S(x)}\sum_{n=0}^{\infty}\left(-\left(\frac{\alpha}{\lambda}\right)^2\phi_{n,\mu\nu}\hat{\xi}_\lambda\hat{\xi}_\sigma + \mathrm{i}\frac{\alpha}{\lambda}(\phi_{n,\mu\nu}\hat{\xi}_{\lambda;\sigma} + 2\phi_{n,\mu\nu;\lambda}\hat{\xi}_\sigma) + \phi_{n,\mu\nu;\lambda\sigma}\right)\left(\frac{\lambda}{\alpha}\right)^n\right). \tag{B3}$$

In leading order, we find the null condition $g^{\lambda\sigma}\hat{\xi}_\lambda\hat{\xi}_\sigma = 0$. By taking the covariant derivative of the null condition and taking into account that $\hat{\xi}_\mu = \partial_\mu S(x)$, we find

$$0 = (g^{\lambda\sigma}\hat{\xi}_\lambda\hat{\xi}_\sigma)_{;\mu} = 2\hat{\xi}^\sigma\hat{\xi}_{\sigma;\mu} = 2\hat{\xi}^\sigma S(x)_{;\sigma\mu} = 2\hat{\xi}^\sigma\hat{\xi}_{\mu;\sigma} \tag{B4}$$

which means that the integral curves of the vector field $\hat{\xi}^\sigma$ are light like geodesics. These are the light rays of geometrical optics. In the next to leading order, we find

$$0 = \phi_{0,\mu\nu}\hat{\xi}^{\ \lambda}_{;\lambda} + 2\phi_{0,\mu\nu;\lambda}\hat{\xi}^\lambda. \tag{B5}$$

We define the scalar

$$\phi_0 \coloneqq (g^{\alpha\gamma}g^{\beta\delta}\phi_{0,\alpha\beta}\phi^*_{0,\gamma\delta})^{1/2}, \tag{B6}$$

and the polarization tensor $f_{0,\mu\nu} = \phi_{0,\mu\nu}/\phi_0$. We find that

$$\hat{\xi}^\lambda f_{0,\mu\nu;\lambda} = \hat{\xi}^\lambda((\phi_0)^{-1}\phi_{0,\mu\nu;\lambda} - (\phi_0)^{-2}\phi_{0,\mu\nu}\phi_{0;\lambda}) \tag{B7}$$

$$=\hat{\xi}^{\lambda}\left((\phi_0)^{-1}\phi_{0,\mu\nu;\lambda}-\frac{1}{2}(\phi_0)^{-3}\phi_{0,\mu\nu}g^{\alpha\gamma}g^{\beta\delta}(\phi_{0,\alpha\beta;\lambda}\phi^{*}_{0,\gamma\delta}+\phi^{*}_{0,\alpha\beta;\lambda}\phi_{0,\gamma\delta})\right) \tag{B8}$$

$$=(\phi_0)^{-1}\phi_{0,\mu\nu;\lambda}\hat{\xi}^{\lambda}+\frac{1}{2}(\phi_0)^{-1}\phi_{0,\mu\nu}\hat{\xi}^{\ \lambda}_{;\lambda}=0. \tag{B9}$$

This means that the zeroth order polarization tensor is parallel transported along the light rays. Furthermore, for linear polarization, we can write $f_{0,\mu\nu}=\exp(\mathrm{i}\varphi_0)\bar{f}_{0,\mu\nu}$, where ϕ and $\bar{f}_{0,\mu\nu}$ are real. From $f_{\mu\nu;\lambda}\hat{\xi}^{\lambda}=0$, we find that $\varphi_{0,\lambda}\hat{\xi}^{\lambda}=0$. Therefore, the phase of the zeroth order amplitude function does not change along the light ray. In particular, we can assume that $\phi_{0,\mu\nu}$ is real everywhere as we can set the initial conditions accordingly.

With these considerations, we can investigate the boundary conditions at the mirrors. To express the boundary conditions in a covariant form, we define the frames of the mirrors in the following. The tangents $\dot{\gamma}_{\mathrm{A}}(\varrho)^{\mu}$ and $\dot{\gamma}_{\mathrm{B}}(\varrho)^{\mu}$ of the world lines of the mirrors define a spacetime split; the spatial slice at the mirror $(i)=\mathrm{A},\mathrm{B}$ is defined as the set of vectors $r^{(i)\mu}$ such that $g_{\mu\nu}r^{(i)\mu}\dot{\gamma}_{(i)}(\varrho)^{\nu}=0$ (no summation of i). Inside these spatial slices, we can define three orthonormal vectors $\epsilon^{(i)\mu}_{j}$ such that the vector $\epsilon^{(i)\mu}_{3}$ is orthogonal to the mirror and the normal vectors $\epsilon^{(i)\mu}_{1}$ and $\epsilon^{(i)\mu}_{2}$ are tangential to the mirror[10]. Furthermore, we choose $\epsilon^{(i)\mu}_{1}$ to be directed in the polarization direction of the right propagating light field at the mirror (i). Together with $\epsilon^{(i)\mu}_{0}=\dot{\gamma}_{(i)}(\varrho)^{\mu}\big/|\dot{\gamma}_{(i)}(\varrho)|$, the vectors $\epsilon^{(i)\mu}_{J}$ $(J\in\{1,2,3\})$ form an orthonormal tetrad. Using the tetrads, the components of the field strength tensor in the frame of the mirror are given as $F^{(i)}_{\mathcal{M}\mathcal{N}}(\varrho)=\epsilon^{(i)\mu}_{\mathcal{M}}\epsilon^{(i)\nu}_{\mathcal{N}}F_{\mu\nu}(\gamma_{(i)}(\varrho))$. Then, the boundary conditions at the mirrors are that the electric field is perpendicular and the magnetic field parallel to the mirrors, i.e. $F^{(i)}_{01}(\varrho)=0=F^{(i)}_{02}(\varrho)$ and $F^{(i)}_{12}(\varrho)=0$.

The tetrads were defined such that the polarization direction of the light field is in the direction of $\epsilon^{(i)\mu}_{1}$. We define $\phi^{(i)r/l}_{n,01}(\varrho):=\epsilon^{(i)\mu}_{0}\epsilon^{(i)\nu}_{1}\phi^{r/l}_{n,\mu\nu}(\gamma_{(i)}(\varrho))$ which are non-zero and we find the boundary conditions

$$0=F^{(i)\mathrm{res}}_{01}(\varrho)=\mathrm{Re}\left(\mathrm{e}^{\mathrm{i}\frac{\alpha}{\lambda}S^{r}(\gamma_{(i)}(\varrho))}\sum_{n=0}^{\infty}\phi^{(i)r}_{n,01}(\varrho)\left(\frac{\lambda}{\alpha}\right)^{n}+\mathrm{e}^{\mathrm{i}\frac{\alpha}{\lambda}S^{l}(\gamma_{(i)}(\varrho))}\sum_{n=0}^{\infty}\phi^{(i)l}_{n,01}(\varrho)\left(\frac{\lambda}{\alpha}\right)^{n}\right). \tag{B10}$$

From the lowest order in λ/α, we find that

$$0=\mathrm{Re}\,(\mathrm{e}^{\mathrm{i}\frac{\alpha}{\lambda}S^{r}(\gamma_{(i)}(\varrho))}\phi^{(i)r}_{0,01}(\varrho)+\mathrm{e}^{\mathrm{i}\frac{\alpha}{\lambda}S^{l}(\gamma_{(i)}(\varrho))}\phi^{(i)l}_{0,01}(\varrho)). \tag{B11}$$

Above, we found that the zeroth order amplitude tensors are real. Then, the boundary condition (B11) can only be fulfilled for all ϱ if $\phi^{r}_{0,01}(\varrho)=\phi^{l}_{0,01}(\varrho)$ and $\frac{\alpha}{\lambda}S^{r}(\gamma_{(i)}(\varrho))=\frac{\alpha}{\lambda}S^{l}(\gamma_{(i)}(\varrho))+2\pi m_{(i)}$, where $m_{(i)}\in\mathbb{Z}$.

Appendix C. Deformations of a rod

For isotropic media, the stiffness tensor depends only on the Young's modulus Y, the shear modulus G and the Poisson ratio ν. We have

$$\varepsilon_{xx}=\frac{1}{Y}(\sigma_{xx}-\nu(\sigma_{yy}+\sigma_{zz})), \tag{C1}$$

$$\varepsilon_{yy}=\frac{1}{Y}(\sigma_{yy}-\nu(\sigma_{xx}+\sigma_{zz})), \tag{C2}$$

$$\varepsilon_{zz}=\frac{1}{Y}(\sigma_{zz}-\nu(\sigma_{xx}+\sigma_{yy})), \tag{C3}$$

$$\varepsilon_{ij}=\varepsilon_{ji}=\frac{1}{2G}\sigma_{ij}\quad\text{for } i\neq j. \tag{C4}$$

Since the change of thickness of the rod holding the resonator and its deformations in the x–y-plane are not of interest for us, we can restrict our considerations to ε_{zz}, ε_{xz} and ε_{yz}. The elements of the strain tensor ε_{xz} and ε_{yz} lead to a deformation of the curve $s(\varsigma)$ in the x and y-direction, respectively. Since the corresponding forces are always transversal to the line elements of the rod, they only bend the rod and do not change its proper length. In the proper detector frame, the proper length of the part of the rod in the positive z-direction of the support is approximately given as

[10] We only need the latter to be defined up to rotations around $\epsilon^{(i)\mu}_{1}$ in the spatial slice.

$$\frac{1+\beta}{2}L_p \approx \int \mathrm{d}\varsigma\, ((s'^x)^2 + (s'^y)^2 + (s'^z)^2)^{1/2}$$
$$\approx \int_0^{(1+\beta)L_p/2-\delta b} \mathrm{d}z \left(1 + \frac{1}{2}\left(\left(\frac{s'^x}{s'^z}\right)^2 + \left(\frac{s'^y}{s'^z}\right)^2\right)\right), \tag{C5}$$

where δb is the shift of the z-coordinate of the position of mirror B. For the analysis of the transversal deformations, let us assume that the rod has a rectangular cross section with side lengths w_x and w_y. Furthermore, let us consider the extreme case of $\beta = 1$. An expression for the transversal deformation of such a rod can be found, for example, in equation (2.2) [53]. For the x-direction, we find

$$\frac{\mathrm{d}^2 s^x}{\mathrm{d}z^2} \leqslant 6\frac{\rho}{Y}\mathbf{a}^x_{P\,\max}\frac{(L_p - z)^2}{w_x^2}, \tag{C6}$$

where $\mathbf{a}^x_{P\,\max}$ is the maximal acceleration in x-direction experienced by a part of the rod. With $s' = \mathrm{d}s/\mathrm{d}\varsigma = 0$ at $z = 0$, we obtain that

$$\frac{s'^{\,x}}{s'^{\,z}} = \frac{\mathrm{d}s^x}{\mathrm{d}z} \leqslant 2\frac{\rho}{Y}\mathbf{a}^x_{P\,\max}\frac{L_p^3 - (L_p - z)^3}{w_x^2}. \tag{C7}$$

A similar expression can be found for $s'^{\,y}/s'^{\,z}$. With equation (C5), we obtain the approximate upper bounds for the change of the z-position of the mirror B

$$\delta b \leqslant \frac{9}{7}\frac{L_p^7}{c_s^4}\left(\left(\frac{\mathbf{a}^x_{P\,\max}}{w_x^2}\right)^2 + \left(\frac{\mathbf{a}^y_{P\,\max}}{w_y^2}\right)^2\right). \tag{C8}$$

Then, the new position of mirror B is approximately $(s^x(L_p),\ s^y(L_p),\ L_p - \delta b)$, where we get

$$s^x(L_p) \leqslant \frac{3L_p^4}{2c_s^2}\frac{\mathbf{a}^x_{P\,\max}}{w_x^2} \quad \text{and} \quad s^y(L_p) \leqslant \frac{3L_p^4}{2c_s^2}\frac{\mathbf{a}^y_{P\,\max}}{w_y^2}, \tag{C9}$$

by integration equation (C7) and the corresponding expression for the y-direction. Since δb, $s^x(L_p)$ and $s^y(L_p)$ are already of second and first order in the metric perturbation, respectively, the change of the round trip time can be calculated as

$$\delta T \approx \frac{1}{c}(((L_p - \delta b)^2 + s^x(L_p)^2 + s^y(L_p)^2)^{1/2} - L_p) \tag{C10}$$

$$\approx -\frac{1}{3c}\frac{L_p^7}{c_s^4}\left(\left(\frac{\mathbf{a}^x_{P\,\max}}{w_x^2}\right)^2 + \left(\frac{\mathbf{a}^y_{P\,\max}}{w_y^2}\right)^2\right). \tag{C11}$$

Let us define $\mathbf{a}^z_{P,\mathrm{av}}$ as the larger of the values of $\langle\beta|\mathbf{a}^z(\tau)|\rangle$ and $\langle(3\beta^2+1)L_p c^2|R_{0z0z}(\tau)|/6\rangle$, where $\langle\rangle$ denotes the averaging over the interaction time. Comparison of equation (C8) with equation (28) shows that the effect of the transversal bending on the length of the rod can be neglected in comparison to the effect of the longitudinal deformations if

$$\mathbf{a}^z_{P,\mathrm{av}} \gg \max\{L_p^5\langle|\mathbf{a}^x_{P\,\max}|\rangle^2/c_s^2 w_x^4,\ L_p^5\langle|\mathbf{a}^y_{P\,\max}|\rangle^2/c_s^2 w_y^4\}. \tag{C12}$$

In the gravitational field of a small massive sphere of 100 g of the example in section 9, an observer at rest experiences an acceleration of the order of 10^{-10} ms^{-2}. So we assume $\mathbf{a}^z_{P,\mathrm{av}} = 10^{-10}$ ms^{-2}, $\langle|\mathbf{a}^x_{P\,\max}|\rangle \leqslant 10^{-10}$ ms^{-2} and $\langle|\mathbf{a}^y_{P\,\max}|\rangle \leqslant 10^{-10}$ ms^{-2}[11]. Let us consider an aluminum rod where $c_s = 5 \times 10^3$ms^{-1}. For a rod of length 1 cm, we find that $L_p/w_x \leqslant 10^3$ and $L_p/w_y \leqslant 10^3$ is sufficient to fulfill the conditions in equation (C12). Let us consider the situation for accelerations of the order of 10 ms^{-2} as they are experienced in the gravitational field of the Earth. So we assume $\mathbf{a}^z_{P,\mathrm{av}} = 10$ ms^{-2}, $\langle|\mathbf{a}^x_{P\,\max}|\rangle \leqslant 10$ ms^{-2} and $\langle|\mathbf{a}^y_{P\,\max}|\rangle \leqslant 10$ ms^{-2}. For an aluminum rod of length 10 cm, the conditions in equation (C12) are fulfilled for $L_p/w_x \leqslant 10$ and $L_p/w_y \leqslant 10$. For larger accelerations, the orientation has to be chosen such that $\mathbf{a}^x_{P\,\max} \ll \mathbf{a}^z_{P,\mathrm{av}}$ and $\mathbf{a}^y_{P\,\max} \ll \mathbf{a}^z_{P,\mathrm{av}}$ to fulfill the conditions and still use a rod.

Now, let us consider the longitudinal deformation. From $\mathbf{a}^j_P \approx -c^2\Gamma^j_{00} \approx c^2\partial_j h_{00}$, we obtain the inertial and tidal forces on the rod by multiplication with the mass density ρ. Since h_{00} contains terms that are independent of z and terms that are proportional to z and z^2, we can write the acceleration as

[11] We consider the massive sphere as the only source of a gravitational field here. In an earthbound laboratory, the effect of the Earth's gravitational field has to be taken into account as well.

$$\mathbf{a}_P^z(\tau, x, y, z) = \mathbf{a}_P^z(\tau, x, y, 0) + z\frac{\mathrm{d}}{\mathrm{d}z}\mathbf{a}_P^z(\tau, x, y, z)\Big|_{z=0}. \tag{C13}$$

Let us assume that the rod has a constant cross section A and a constant mass density. Then, the sum of inertial forces and gravitational force along the rod acting on a segment of the rod at $z > 0$ can be approximated as

$$\begin{aligned} F_+^z(\tau, z) &\approx \int_z^b \mathrm{d}z' A\rho\, \mathbf{a}_P^z(\tau, 0, 0, z') \\ &\approx (b - z)A\rho\, \mathbf{a}_P^z(\tau, 0, 0, 0) + \frac{1}{2}(b^2 - z^2)A\rho\frac{\mathrm{d}}{\mathrm{d}z}\mathbf{a}_P^z(\tau, 0, 0, z)\Big|_{z=0}. \end{aligned} \tag{C14}$$

where, by considering the acceleration only at $x = 0 = y$, we neglected terms proportional to the width of the rod. For the force along the rod acting on a segment of the rod at $z < 0$, we find

$$F_-^z(\tau, z) \approx (z - a)A\rho\, \mathbf{a}_P^z(\tau, 0, 0, 0) + \frac{1}{2}(z^2 - a^2)A\rho\frac{\mathrm{d}}{\mathrm{d}z}\mathbf{a}_P^z(\tau, 0, 0, z)\Big|_{z=0}. \tag{C15}$$

Due to the support, this corresponds to the stresses

$$\sigma_{zz}^{\pm}(\tau, z) = \pm\frac{F_\pm^z(\tau, z)}{A}. \tag{C16}$$

The differential force in the x-direction acting on a one-dimensional segment of the rod with coordinates x, y and z induced by all one-dimensional segments with the same z-coordinate, the same y-coordinate and $x' > x$ can be written as

$$\mathrm{d}F_+^x(\tau, x, y, z) = \mathrm{d}z\int_x^{w_x/2}\mathrm{d}x' w_y\rho\mathbf{a}_P^x(\tau, x', y, z).$$

Furthermore, we find

$$\mathrm{d}F_-^x(\tau, x, y, z) = \mathrm{d}z\int_{-w_x/2}^{x}\mathrm{d}x' w_y\rho\mathbf{a}_P^x(\tau, x', y, z)$$

for the differential force induced by all one-dimensional segments with the same z-coordinate, the same y-coordinate and $x' < x$. Since the metric (12) contains constant, linear and quadratic terms in the spatial coordinate and $\mathbf{a}_P^j \approx -c^2\Gamma_{00}^j$, we conclude that $\mathrm{d}\mathbf{a}_P^x(\tau, x, y, z)/\mathrm{d}x$ cannot depend on y in first order in the metric perturbation, and we find that the acceleration in the x-direction can be written as

$$\mathbf{a}_P^x(\tau, x, y, z) = \mathbf{a}_P^x(\tau, 0, y, z) + x\frac{\mathrm{d}}{\mathrm{d}x}\mathbf{a}_P^x(\tau, x, 0, z)|_{x=0}. \tag{C17}$$

The first term corresponds to an acceleration that all segments feel in the same way. Therefore, it does not lead to a stress. Hence, the stress on a segment of the rod at z becomes

$$\sigma_{xx}(\tau, z) = \frac{w_x^2}{8}\rho\frac{\mathrm{d}}{\mathrm{d}x}\mathbf{a}_P^x(\tau, x, 0, z)\Big|_{x=0}.$$

An equivalent expression can be derived for the stress σ_{yy}. The length change of the rod is given as

$$\begin{aligned} \delta L_p(\tau) &\simeq \int_0^b \mathrm{d}z'\varepsilon_{zz}^+(\tau, z') + \int_a^0 \mathrm{d}z'\varepsilon_{zz}^-(\tau, z') \\ &= \frac{1}{Y}\int_0^b \mathrm{d}z'\sigma_{zz}^+(\tau, z') + \frac{1}{Y}\int_a^0 \mathrm{d}z'\sigma_{zz}^-(\tau, z') - \frac{\nu}{Y}\int_a^b \mathrm{d}z'\,(\sigma_{xx}(\tau, z') + \sigma_{yy}(\tau, z')) \end{aligned} \tag{C18}$$

We obtain that

$$\frac{1}{Y}\int_0^b \mathrm{d}z'\sigma_{zz}^+(\tau, z') + \frac{1}{Y}\int_a^0 \mathrm{d}z'\sigma_{zz}^-(\tau, z') \tag{C19}$$

$$= \frac{\rho}{Y}\left(\frac{1}{2}(b^2 - a^2)\mathbf{a}_P^z(\tau, 0, 0, 0) + \frac{1}{3}(b^3 - a^3)\frac{\mathrm{d}}{\mathrm{d}z}\mathbf{a}_P^z(\tau, 0, 0, z)\Big|_{z=0}\right) \tag{C20}$$

$$= \frac{\rho}{Y}L_p\left(\frac{1}{2}\beta L_p\mathbf{a}_P^z(\tau, 0, 0, 0) + \frac{1}{12}(3\beta^2 + 1)L_p^2\frac{\mathrm{d}}{\mathrm{d}z}\mathbf{a}_P^z(\tau, 0, 0, z)\Big|_{z=0}\right). \tag{C21}$$

Since the highest polynomial order of terms in the metric perturbation in the coordinates is 2, $\frac{\mathrm{d}}{\mathrm{d}x}\mathbf{a}_P^x(\tau, x, 0, z)|_{x=0}$ can only contain terms that are independent of z and terms that are linear in z. Hence, we find

$$\frac{\nu}{Y}\int_a^b \mathrm{d}z'\,(\sigma_{xx}(\tau, z') + \sigma_{yy}(\tau, z')), \tag{C22}$$

$$\approx\frac{\nu\rho}{Y}L_p\left(\frac{w_x^2}{8}\frac{\mathrm{d}}{\mathrm{d}x}\mathbf{a}_P^x(\tau,\,x,\,0,\,0,\,0)\,\Big|_{x=0}+\frac{w_y^2}{8}\frac{\mathrm{d}}{\mathrm{d}y}\mathbf{a}_P^y(\tau,\,0,\,y,\,0)\,\Big|_{y=0}\right). \tag{C23}$$

Therefore, the effect of acceleration and curvature on the proper length via σ_{xx} and σ_{yy} is suppressed by a factor $\nu w_x/L_p$ and $\nu\, w_y/L_p$, respectively, in comparison to the effect via σ_{zz}. For most materials $\nu < 1$ and we can assume that $w_x/L_p \ll 1$. Therefore, if $\beta\mathbf{a}_P^z(\tau,\,0,\,0,\,0)$ or $(3\beta^2+1)L_p\frac{\mathrm{d}}{\mathrm{d}z}\mathbf{a}_P^z(\tau,\,0,\,0,\,z)|_{z=0}/6$ is of the same order or larger than $w_x\frac{\mathrm{d}}{\mathrm{d}x}\mathbf{a}_P^x(\tau,\,x,\,0,\,0)_{x=0}/4$ and $w_y\frac{\mathrm{d}}{\mathrm{d}y}\mathbf{a}_P^y(\tau,\,0,\,y,\,0)|_{y=0}/4$ and if the oscillations of the transversal stresses are not on resonant with any elastic mode of the rod that the longitudinal stresses are not on resonance with, we can neglect the effect of the transversal stresses and we can restrict our considerations to σ_{zz}^+ and σ_{zz}^-. Then, we can write the conditions as

$$\mathbf{a}_{P,\mathrm{av}}^z \geqslant \max\{w_x c^2\langle|R_{0x0x}|\rangle,\, w_y c^2\langle|R_{0y0y}|\rangle\}. \tag{C24}$$

Appendix D. The causal deformable rod from relativistic elasticity

In [33], a covariant formulation of the relativistic elastic rod was given. In this section, we show that the definitions of [33] lead to our result equation (31) for the causal rigid rod when applied to the metric in equation (12) in the proper detector frame.

The author of [33] formulates the theory of one-dimensional relativistic elastic bodies by considering a motion of a one-dimensional continuum moving in a $1+1$-dimensional spacetime. Our arguments from sections 2, 4 and 5 lead exactly to such a situation. The rod is dragged along the world line of its support or its center of mass is assumed to move along a geodesic. All accelerations of the rod segments are encoded in the metric in the proper detector frame given by equation (12). Furthermore, our rod is assumed to lie along a spatial geodesic and we neglect all transversal accelerations. What remains is only gravitational effects along the rod encoded by the metric corresponding to the line element

$$\mathrm{d}s^2 = -(1-h_{00}^P(\tau,\,z))\mathrm{d}\tau^2+\mathrm{d}z^2. \tag{D1}$$

Due to our assumption that acceleration and curvature only change very slowly, we find that this situation corresponds to equation (22) of [33]. The coordinate transformation in equation (23) of [33], $\tilde{z}=f(z)$ with $f(z)=\int_0^z \mathrm{d}z'(1-h_{00}^P)^{-1/2}$ leads to

$$\mathrm{d}s^2 \approx -(1-h_{00}^P(\tau,\,f^{-1}(\tilde{z})))(\mathrm{d}\tau^2+\mathrm{d}\tilde{z}^2)\approx(1-h_{00}^P(\tau,\,\tilde{z}))(-\mathrm{d}\tau^2+\mathrm{d}\tilde{z}^2). \tag{D2}$$

in first order in the metric perturbation since $f^{-1}(\tilde{z})=\tilde{z}$ in zeroth order in the metric perturbation. The rigid rod of [33] has constant coordinate length in the coordinates $(\tau,\,\tilde{z})$, which are called conformal coordinates because the line element differs from the that of Minkowski space only by a conformal factor $\mathrm{e}^{2\phi(\tilde{z})}$, where in our case, $\mathrm{e}^{2\phi(\tilde{z})}=(1-h_{00}^P(\tau,\,\tilde{z}))$. This rigid rod can be called a causal rigid rod because the speed of sound in the rod material is equivalent to the speed of light. In contrast, a Born rigid rod would correspond to an infinite speed of sound.

The square root of the conformal factor is the stretch constant of [33]. We obtain the proper length of the causal rigid rod by integrating the stretch constant from one end of the rod to the other. However, we have to note that the stretch factor also contains boundary conditions of the rod; every point at which $\phi(\tilde{z})$ vanishes corresponds to a free end of the rod. Therefore, we cannot just use the expression for h_{00}^P that we used in section 5. We have to consider the two sides of our rod separately, and in each situation, add a constant to h_{00}^P such that the free end is at a or b. Adding a constant to the metric does not change any dynamics and we are free to do such an operation. We define

$$h_{00}^{\mathrm{A}}(\tau,\,\tilde{z}) \coloneqq h_{00}^P(\tau,\,\tilde{z})-h_{00}^P(\tau,\,a) \quad \text{and} \tag{D3}$$

$$h_{00}^{\mathrm{B}}(\tau,\,\tilde{z}) \coloneqq h_{00}^P(\tau,\,\tilde{z})-h_{00}^P(\tau,\,b). \tag{D4}$$

The proper length becomes

$$\begin{aligned} L_p &= \int_a^0 \mathrm{d}\tilde{z}\,(1-h_{00}^{\mathrm{A}}(\tau,\,\tilde{z}))^{1/2}+\int_0^b \mathrm{d}y\,(1-h_{00}^{\mathrm{B}}(\tau,\,\tilde{z}))^{1/2} \\ &\approx \int_a^0 \mathrm{d}\tilde{z}\left(1+\frac{\mathbf{a}^z}{c^2}(\tilde{z}-a)+\frac{R_{0z0z}}{2}(\tilde{z}^2-a^2)\right)+\int_0^b \mathrm{d}\tilde{z}\left(1+\frac{\mathbf{a}^z}{c^2}(\tilde{z}-b)+\frac{R_{0z0z}}{2}(\tilde{z}^2-b^2)\right) \end{aligned} \tag{D5}$$

and we reproduce the result of equation (28) for $c_s=c$.

ORCID iDs

Dennis Rätzel https://orcid.org/0000-0003-3452-6222
Daniel Braun https://orcid.org/0000-0001-8598-2039
Maximilian P E Lock https://orcid.org/0000-0002-8241-8202

References

[1] Tarabrin S P 2007 Interaction of plane gravitational waves with a Fabry–Perot cavity in the local Lorentz frame *Phys. Rev.* D **75** 102002
[2] Reece C E, Reiner P J and Melissinos A C 1982 A detector for high frequency gravitational effects based on parametric conversion at 10-GHz *Proc., 1982 DPF Summer Study on Elementary Particle Physics and Future Facilities (Snowmass 82), eConf* C8206282 *(Snowmass, Colorado, 28 June–16 July, 1982)* pp 394–402
[3] Pegoraro F, Picasso E and Radicati L A 1978 On the operation of a tunable electromagnetic detector for gravitational waves *J. Phys. A: Math. Gen.* **11** 1949
[4] Pegoraro F, Radicati L A, Bernard P and Picasso E 1978 Electromagnetic detector for gravitational waves *Phys. Lett.* A **68** 165–8
[5] Grishchuk L P *et al* 1981 Quantum electromagnetic oscillator in the field of a gravitational wave and the problem of nondemolition measurements *J. Exp. Theor. Phys.* **53** 639
[6] Grishchuk L P and Sazhin M V 1975 Excitation and detection of standing gravitational waves *J. Exp. Theor. Phys.* **41** 787
[7] Gemme G, Chincarini A, Parodi R, Bernard P and Picasso E 2001 Parametric gravity wave detector *Electromagnetic Probes of Fundamental Physics. Proc., Workshop (Erice, Italy, 16–21, October 2001)* pp 75–83
[8] Ju L, Blair D G and Zhao C 2000 Detection of gravitational waves *Rep. Prog. Phys.* **63** 1317–427
[9] Maggiore M 2008 *Gravitational Waves: Volume 1: Theory and Experiments* vol 1 (Oxford: Oxford University Press)
[10] Graham P W, Hogan J M, Kasevich M A and Rajendran S 2013 A new method for gravitational wave detection with atomic sensors *Phys. Rev. Lett.* **110** 171102
[11] Arvanitaki A and Geraci A A 2013 Detecting high-frequency gravitational waves with optically levitated sensors *Phys. Rev. Lett.* **110** 071105
[12] Sabin C, Bruschi D E, Ahmadi M and Fuentes I 2014 Phonon creation by gravitational waves *New J. Phys.* **16** 085003
[13] Goryachev M and Tobar M E 2014 Gravitational wave detection with high frequency phonon trapping acoustic cavities *Phys. Rev.* D **90** 102005
[14] Singh S, Lorenzo L A D, Pikovski I and Schwab K C 2017 Detecting continuous gravitational waves with superfluid ^{4}He *New J. Phys.* **19** 073023
[15] Braginskii V B, Caves C M and Thorne K S 1977 Laboratory experiments to test relativistic gravity *Phys. Rev.* D **15** 2047–68
[16] Howl R, Hackermuller L, Bruschi D E and Fuentes I 2017 Gravity in the quantum lab *Adv. Phys.* X **3** 1383184
[17] Kopeikin S M 2015 Optical cavity resonator in an expanding universe *Gen. Relativ. Gravit.* **47** 5
[18] Kopeikin S M 2014 Einstein's equivalence principle in cosmology *40th COSPAR Scientific Assembly, COSPAR Meeting* vol 40arXiv:1311.4912
[19] Lock M P E and Fuentes I 2016 Relativistic quantum clocks arXiv:1609.09426
[20] Lock M P E and Fuentes I 2017 Dynamical Casimir effect in curved spacetime *New J. Phys.* **19** 073005
[21] Regula B, Lee A R, Dragan A and Fuentes I 2016 Generating entanglement between two-dimensional cavities in uniform acceleration *Phys. Rev.* D **93** 025034
[22] Braun D, Schneiter F and Fischer U R 2017 Intrinsic measurement errors for the speed of light in vacuum *Class. Quantum Grav.* **34** 175009
[23] Born M 1909 Die Theorie des starren Elektrons in der Kinematik des Relativitätsprinzips *Ann. Phys., Lpz.* **335** 1–56
[24] Abraham M 1902 Prinzipien der Dynamik des Elektrons *Ann. Phys., Lpz.* **315** 105–79
[25] Herglotz G 1903 Zur Elektronentheorie *Nachr. Ges. Wiss. Göttingen, Math.-Phys. Kl.* **1903** 357–82
[26] Schwarzschild K 1903 Zur Elektrodynamik: I. Zwei Formen des Princips der Action in der Elektronentheorie *Nachr. Ges. Wiss. Göttingen, Math.-Phys. Kl.* **1903** 126–31
[27] Sommerfeld A 1904 Zur Elektronentheorie: I. Allgemeine Untersuchung des Feldes eines belibig bewegten Elektrons *Nachr. Ges. Wiss. Göttingen, Math.-Phys. Kl.* **1904** 99–130
[28] Sommerfeld A 1904 Zur Elektronentheorie: II. Grundlagen für eine allgemeine Dynamik des Elektrons *Nachr. Ges. Wiss. Göttingen, Math.-Phys. Kl.* **1904** 363–439
[29] Herglotz G 1910 Über den vom Standpunkt des Relativitätsprinzips aus als starr zu bezeichnenden Körper *Ann. Phys., Lpz.* **336** 393–415
[30] Noether F 1910 Zur kinematik des starren körpers in der relativtheorie *Ann. Phys., Lpz.* **336** 919–44
[31] Dixon W G 1970 Dynamics of extended bodies in general relativity: I. Momentum and angular momentum *Proc. R. Soc.* A **314** 499–527
[32] Ehlers J and Rudolph E 1977 Dynamics of extended bodies in general relativity center-of-mass description and quasirigidity *Gen. Relativ. Gravit.* **8** 197–217
[33] Natario J 2014 Relativistic elasticity of rigid rods and strings *Gen. Relativ. Gravit.* **46** 1816
[34] Perlick V 2000 *Ray optics, Fermat's Principle, and Applications to General Relativity* vol 61 (Berlin: Springer)
[35] Straumann N 2012 *General Relativity* (Berlin: Springer)
[36] Rivera S 2012 Tensorial spacetime geometries carrying predictive, interpretable and quantizable matter dynamics *Doctoral Thesis* Universität Potsdam
[37] Audretsch J and Lämmerzahl C 1991 Establishing the Riemannian structure of spacetime by means of light rays and free matter waves *J. Math. Phys.* **32** 2099–105
[38] Plebanski J 1960 Electromagnetic waves in gravitational fields *Phys. Rev.* **118** 1396–408
[39] Manasse F K and Misner C W 1963 Fermi normal coordinates and some basic concepts in differential geometry *J. Math. Phys.* **4** 735–45
[40] Ni W-T and Zimmermann M 1978 Inertial and gravitational effects in the proper reference frame of an accelerated, rotating observer *Phys. Rev.* D **17** 1473–6
[41] Liu M, Artyukhov V I, Lee H, Xu F and Yakobson B I 2013 Carbyne from first principles: chain of c atoms, a nanorod or a nanorope *ACS Nano* **7** 10075–82

[42] Tenev T G and Horstemeyer M F 2018 The mechanics of spacetime—a solid mechanics perspective on the theory of general relativity *Int. J. Mod. Phys.* D **27** 1850083
[43] Gordon W 1923 Zur Lichtfortpflanzung nach der relativitätstheorie *Ann. Phys., Lpz.* **377** 421–56
[44] Hartmann T, Soffel M, Ruder H and Schneider M 1992 *Ausbreitung Elektromagnetischer Signale in Gravitationsfeldern und Medium bei Geodätischen Raumverfahren* (München: Verlag der Bayerischen Akademie der Wissenschaften in Kommission bei der C.H. Beck)
[45] Zubkov M A and Volovik G E 2015 Emergent gravity in graphene *J. Phys.: Conf. Ser.* **607** 012020
[46] Hinkley N, Sherman J A, Phillips N B, Schioppo M, Lemke N D, Beloy K, Pizzocaro M, Oates C W and Ludlow A D 2013 An atomic clock with 10^{-18} instability *Science* **341** 1215–8
[47] Ushijima I, Takamoto M, Das M, Ohkubo T and Katori H 2015 Cryogenic optical lattice clocks *Nat. Photon.* **9** 185–9
[48] Chou C W, Hume D B, Rosenband T and Wineland D J 2010 Optical clocks and relativity *Science* **329** 1630–3
[49] Misner C W, Thorne K S and Wheeler J A 1973 *Gravitation* (London: Macmillan)
[50] Schmöle J 2017 Development of a micromechanical proof-of-principle experiment for measuring the gravitational force of milligram masses *PhD Thesis* Faculty of Physics, University of Vienna
[51] Schmöle J, Mathias D, Hans H and Markus A 2016 A micromechanical proof-of-principle experiment for measuring the gravitational force of milligram masses *Class. Quantum Grav.* **33** 125031
[52] Herglotz G 1911 Über die Mechanik des deformierbaren Körpers vom Standpunkte der Relativitätstheorie *Ann. Phys., Lpz.* **341** 493–533
[53] Srivastava V, Jones H and Greenwood G W 2006 The creep of thin beams under small bending moments *Proc. R. Soc.* A **462** 2863–75

[C] The gravitational field of a laser beam beyond the short wavelength approximation

Fabienne Schneiter, Dennis Rätzel, Daniel Braun
Classical and Quantum Gravity, 35(19), 2018
DOI: 10.1088/1361-6382/aadc81
URL: http://stacks.iop.org/0264-9381/35/i=19/a=195007

The article contains a number of errors, most of them typos and most of them in the appendices, but the main results do not change. The preprint for the erratum is attached.

OPEN ACCESS
IOP Publishing
Classical and Quantum Gravity
Class. Quantum Grav. **35** (2018) 195007 (40pp)
https://doi.org/10.1088/1361-6382/aadc81

The gravitational field of a laser beam beyond the short wavelength approximation

Fabienne Schneiter[1], Dennis Rätzel[2] and Daniel Braun[1]

[1] Eberhard-Karls-Universität Tübingen, Institut für Theoretische Physik, 72076 Tübingen, Germany
[2] Faculty of Physics, University of Vienna, Boltzmanngasse 5, 1090 Vienna, Austria

E-mail: fabienne.schneiter@uni-tuebingen.de and dennis.raetzel@univie.ac.at

Received 30 April 2018, revised 20 July 2018
Accepted for publication 23 August 2018
Published 10 September 2018

Abstract

Light carries energy, and therefore, it is the source of a gravitational field. The gravitational field of a beam of light in the short wavelength approximation has been studied by several authors. In this article, we consider light of finite wavelengths by describing a laser beam as a solution of Maxwell's equations and taking diffraction into account. Then, novel features of the gravitational field of a laser beam become apparent, such as frame-dragging due to its spin angular momentum and the deflection of parallel co-propagating test beams that overlap with the source beam. Even though the effects are too small to be detected with current technology, they are of conceptual interest, revealing the gravitational properties of light.

Keywords: linearized gravity, general relativity, laser beam, paraxial beam, Maxwell's equations, diffraction

(Some figures may appear in colour only in the online journal)

1. Introduction

The gravitational field of a light beam has first been studied by Tolman, Ehrenfest and Podolski in 1931 [36], who described the light beam as a one-dimensional (1D) 'pencil of light'. Later, a description for the gravitational field of a cylindrical beam of light of a finite radius has been presented by Bonnor [4]. In this description, light has been modeled as a continuous fluid moving at the speed of light. A central feature of these two models is the lack of diffraction;

the beams do not diverge. This corresponds to the short wavelength limit where all wavelike properties of light are neglected. Further studies of the gravitational field of light that share this feature include the investigation of two co-directed parallel cylindrical light beams of finite radius [3, 24], spinning non-divergent light beams [23], non-divergent light beams in the framework of gravito-electrodynamics [13], and the gravitational field of a point like particle moving with the speed of light [1, 38].

In contrast, the wavelike properties of light have been taken into account in [37], where the gravitational field of a plane electromagnetic wave has been investigated. An approach to take finite wavelengths into account for the case of a laser pulse has been given in [26, 28], where, however, diffraction has been neglected. In this article we describe the laser beam as a solution to Maxwell's equations. This is done perturbatively by an expansion in the beam divergence, which is considered to be small. The zeroth order of the expansion corresponds to the paraxial approximation and coincides with the result of [4]. In the first order in the beam divergence, frame-dragging due to the spin angular momentum of circularly polarized beams occurs. In the fourth order in the divergence angle, a parallel co-propagating test beam of light overlapping with the source laser beam is found to be deflected by the gravitational field of the laser beam.

The properties of light are inherent in modern physics. They were used to derive special and general relativity and they are often the basis for new approaches to spacetime theories. Furthermore, the gravitational field of laser beams is a phenomenon on the interface of general relativity and quantum mechanics as laser beams can be brought into non-classical states. For the progress of modern physics it is of great importance to study such phenomena, as they may give some insight into quantum gravity. Hence, it is necessary to study the gravitational properties of laser light in sufficient detail. In this article one of the most fundamental features of laser light, its wave properties, is taken into account for the first time. Therefore, even though the effects we present in this article are very small and not measurable with current technology, they are of general interest for the physics community.

We would like to point out that, if detection of the gravitational field of light may be feasable at some point in the future, it is very likely that strongly focussed laser beams will be involved in the corresponding experiments. However, due to the wavelike nature of light, there is a fixed relation between a laser beam's divergence angle and the width of its focus. This feature limits the experimental possibilities further. This has to be taken into account to obtain the sensitivity that would be necessary to detect the gravitational field of light at some point in the future. Therefore, future advanced detection schemes that may be promising to detect the gravitational field of light have to be assessed using the detailed description given in this article. Hence, this article is of importance to future considerations of the possibilities to detect the gravitational field of light.

We proceed as follows: in section 2, we describe a focused laser beam as a solution to Maxwell's equations. This is done perturbatively, as an expansion in the small beam divergence angle θ. Furthermore, we derive the energy–momentum tensor for a circularly polarized laser beam. In section 3, we introduce the framework of linearized gravity. The equations determining the metric perturbation and solutions with Green's functions are given in section 4. Then we discuss the specific effects appearing in the different orders of the expansion in θ of the gravitational field: in section 5, we discuss the zeroth order, which corresponds to the paraxial approximation. Frame-dragging happens in the first order of the metric perturbation and is explained in section 6. The deflection of a co-propagating parallel light ray in the gravitational field of the laser beam is shown in section 7. Some conclusions are given in section 8.

Throughout the article, we use the following notation: for spacetime coordinates we use greek indices, like x^α, and for spatial coordinates we use latin indices, like x^k. For the Minkowski metric, we choose the convention $\eta_{\alpha\beta} = \mathrm{diag}(-1, 1, 1, 1)$.

2. Describing the laser beam

In this section we describe the laser beam as a Gaussian beam, a perturbative solution to Maxwell's equations. The solution is expanded in the beam divergence, which is assumed to be small. Finding a solution for the vector potential, we calculate the energy–momentum tensor, which will be used in the next section to determine the spacetime metric.

2.1. The field strength tensor

The laser beam is a monochromatic plane wave whose intensity distribution in the directions perpendicular to the direction of propagation decreases with a Gaussian factor. It is a perturbative solution of Maxwell's equations: an expansion in the beam divergence, the opening angle of the beam, which is assumed to be small. This solution is obtained by making the ansatz that the vector potential is a plane wave enveloped by a function depending on the spatial position.

More specifically, the vector potential of the Gaussian beam is obtained as follows: it has to satisfy Maxwell's equations in form of the wave equations,

$$\Box A_\alpha(t, x, y, z) = 0, \tag{1}$$

where $\Box = \eta^{\alpha\beta}\partial_\alpha\partial_\beta = -\frac{1}{c^2}\partial_t^2 + \partial_x^2 + \partial_y^2 + \partial_z^2$ is the d'Alembert operator and we choose the Lorenz gauge condition $\eta^{\alpha\beta}\partial_\alpha A_\beta = 0$. For convenience, we work in the dimensionless coordinates $\tau = \frac{ct}{w_0}$, $\xi = \frac{x}{w_0}$, $\chi = \frac{y}{w_0}$, $\zeta = \frac{z}{w_0}$, where w_0 is the beam waist. Writing $\{x^\alpha\}$ for the coordinates $\{ct, x, y, z\}$ and $\{x^{\bar\alpha}\}$ for the coordinates $\{\tau, \xi, \chi, \zeta\}$, we obtain for the Minkowski metric

$$\eta_{\bar\alpha\bar\beta} = \frac{\mathrm{d}x^\alpha}{\mathrm{d}x^{\bar\alpha}}\,\frac{\mathrm{d}x^\beta}{\mathrm{d}x^{\bar\beta}}\,\eta_{\alpha\beta} = w_0^2\,\mathrm{diag}\,(-1, 1, 1, 1)\,. \tag{2}$$

The vector potential transforms as $A_{\bar\alpha} = \frac{\mathrm{d}x^\alpha}{\mathrm{d}x^{\bar\alpha}}A_\alpha$. We make the ansatz that the vector potential is monochromatic and can be written as

$$A_{\bar\alpha}(\tau, \xi, \chi, \zeta) = \mathcal{A}v_{\bar\alpha}(\xi, \chi, \theta\zeta)\mathrm{e}^{\mathrm{i}\frac{2}{\theta}(\zeta-\tau)}, \tag{3}$$

where $\theta = 2/(w_0k)$ is the divergence angle of the beam, k is the wave vector and $\mathcal{A}$ is the amplitude. The vector envelope function $v_{\bar\alpha}$ is assumed to depend on ζ only through the combination $\theta\zeta$. With the ansatz (3), we obtain the Helmholtz equation for the envelope function

$$\left(\partial_\xi^2 + \partial_\chi^2 + \theta^2\partial_{\theta\zeta}^2 + 4\mathrm{i}\partial_{\theta\zeta}\right)v_{\bar\alpha}(\xi, \chi, \theta\zeta) = 0. \tag{4}$$

We consider θ to be small, which implies that the envelope function changes much more slowly in z-direction than in x-direction or in y-direction. Then, we make the ansatz that $v_{\bar\alpha}$ can be written as a power series of θ,[3]

$$v_{\bar\alpha}(\xi, \chi, \theta\zeta) = \sum_{n=0}^{\infty}\theta^n v_{\bar\alpha}^{(n)}(\xi, \chi, \theta\zeta), \tag{5}$$

[3] An expansion in orders of θ^2 has been presented by Davis [12]. Here, we consider the general expansion to allow for helicity eigenstates later on.

where $v_{\bar{\alpha}}^{(n)}$ are the coefficients in the power series. The Helmholtz equation (4) leads to the differential equations

$$\left(\partial_\xi^2 + \partial_\chi^2 + 4\mathrm{i}\partial_{\theta\zeta}\right) v_{\bar{\alpha}}^{(0)}(\xi,\chi,\theta\zeta) = 0, \tag{6}$$

$$\left(\partial_\xi^2 + \partial_\chi^2 + 4\mathrm{i}\partial_{\theta\zeta}\right) v_{\bar{\alpha}}^{(1)}(\xi,\chi,\theta\zeta) = 0, \tag{7}$$

$$\left(\partial_\xi^2 + \partial_\chi^2 + 4\mathrm{i}\partial_{\theta\zeta}\right) v_{\bar{\alpha}}^{(n)}(\xi,\chi,\theta\zeta) = -\partial_{\theta\zeta}^2 v_{\bar{\alpha}}^{(n-2)}(\xi,\chi,\theta\zeta), \text{ for } n > 1. \tag{8}$$

Note, that this set of equations couples components of $v_{\bar{\alpha}}$ of odd n to other components of odd n and components with even n to other components of even n. Therefore, we obtain two independent hierarchies of components of $v_{\bar{\alpha}}$. We will couple odd and even components later when we introduce helicity.

Equation (6) is known as the paraxial Helmholtz equation. It can be interpreted as a Schrödinger equation in two spatial dimensions with $m/\hbar = 2$ when $\theta\zeta$ is seen as a time variable, i.e.

$$\mathrm{i}\partial_{\theta\zeta} v_{\bar{\alpha}}^{(0)}(\xi,\chi,\theta\zeta) = -\frac{1}{4}\Delta_{2d} v_{\bar{\alpha}}^{(0)}(\xi,\chi,\theta\zeta), \tag{9}$$

where $\Delta_{2d} = \partial_\xi^2 + \partial_\chi^2$ is the two dimensional Laplace operator. A solution of equation (9) has to spread similar to the wave packet of a massive particle in quantum mechanics. Here, the spreading of the wave packet corresponds to the divergence of the beam. The solution of equation (9) that we are interested in is a Gaussian wave packet. Furthermore, we want the wave packet to be centered on the optical axis and to be rotationally symmetric about the optical axis. With these conditions, we obtain for the lowest order

$$v_{\bar{\alpha}}^{(0)}(\xi,\chi,\theta\zeta) = \epsilon_{\bar{\alpha}}^{(0)} v_0(\xi,\chi,\theta\zeta), \tag{10}$$

where the function v_0 is given by

$$v_0(\xi,\chi,\theta\zeta) = \mu(\theta\zeta)\mathrm{e}^{-\mu(\theta\zeta)\rho^2}, \tag{11}$$

and where $\rho = \sqrt{\xi^2+\chi^2}$, $\epsilon_{\bar{\alpha}}^{(0)}$ is the constant polarization co-vector and $\mu(\theta\zeta) = 1/(1+\mathrm{i}\theta\zeta)$ relates the spread of the Gaussian wave packet and the divergence angle of the beam. Equation (10) represents the Gaussian beam in lowest order in the divergence angle θ. A graphic representation can be found in figure 1. The first order solution fulfills the same paraxial Helmholtz equation as the zeroth order solution. Therefore, we set

$$v_{\bar{\alpha}}^{(1)}(\xi,\chi,\theta\zeta) = \epsilon_{\bar{\alpha}}^{(1)} v_0(\xi,\chi,\theta\zeta). \tag{12}$$

The equations for the higher order terms in equation (8) correspond to Schrödinger equations with an additional term proportional to the solution of the equation two orders lower, which has the effect of a source term,

$$\mathrm{i}\partial_{\theta\zeta} v_{\bar{\alpha}}^{(n)}(\xi,\chi,\theta\zeta) = -\frac{1}{4}\Delta_{2d} v_{\bar{\alpha}}^{(n)}(\xi,\chi,\theta\zeta) - \frac{1}{4}\partial_{\theta\zeta}^2 v_{\bar{\alpha}}^{(n-2)}(\xi,\chi,\theta\zeta), \quad \text{for } n \geqslant 1. \tag{13}$$

Finally, we have to specify the polarization co-vectors $\epsilon_{\bar{\alpha}}$ and the terms in the expansion of the envelope function of even n. We will do so for a Gaussian beam of circular polarization in the following. First, note that the components of the vector potential are not independent; the Lorenz gauge condition we imposed leads to

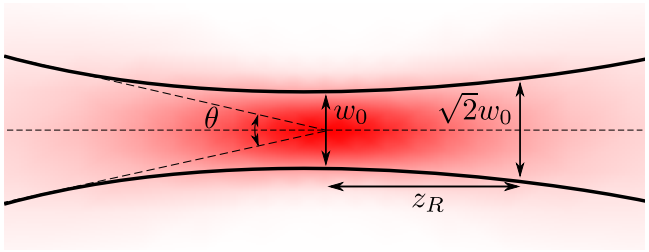

Figure 1. Schematic illustration of the Gaussian beam, the beam waist w_0, the Rayleigh length z_R and the beam divergence θ. More specifically, the figure illustrates the scalar envelope function v_0 of the vector potential of the Gaussian beam in a plane that contains the optical axis (represented by the dashed horizontal line). Due to the rotational symmetry of the envelope function about the optical axis, the vertical axis can be any direction transversal to the optical axis. The thick curved lines mark the distance $w(\zeta) = 1/|\mu(\theta\zeta)|$ from the optical axis at which the absolute value of the envelope function reaches $1/e$ times its maximum.

$$A_\tau = \frac{\mathrm{i}\theta}{2}\partial_\tau A_\tau = \frac{\mathrm{i}\theta}{2}\left(\partial_\xi A_\xi + \partial_\sigma A_\sigma + \theta\partial_{\theta\zeta}A_\zeta\right). \tag{14}$$

With this identity, A_τ can be eliminated from the space-time components of the field strength tensor $F_{\bar\alpha\bar\beta} = \partial_{\bar\alpha}A_{\bar\beta} - \partial_{\bar\beta}A_{\bar\alpha}$ as

$$F_{\tau\bar a} = -F_{\bar a\tau} = -\frac{2\mathrm{i}}{\theta}A_{\bar a} - \frac{\mathrm{i}\theta}{2}\delta^{\bar b\bar c}\partial_{\bar a}\partial_{\bar b}A_{\bar c}, \tag{15}$$

where $\delta^{\bar b\bar c}$ is the Kronecker delta. As the vector potential, the field strength tensor can be expanded as

$$F_{\bar\alpha\bar\beta} = \sum_{n=0}^{\infty}\theta^n\frac{w_0E_0}{\sqrt{2}}f_{\bar\alpha\bar\beta}(\xi,\chi,\theta\zeta)\mathrm{e}^{\mathrm{i}\frac{2}{\theta}(\zeta-\tau)}, \tag{16}$$

where $E_0 = \sqrt{2}\mathcal{A}/(w_0\theta)$ and a direct relation between $v_{\bar\alpha}^{(n)}$ and $f_{\bar\alpha\bar\beta}^{(n)}$ can be established, which is given in appendix A.

2.1.1. Circularly polarized beams. In the last step, we have to specify the polarization of the beam that we want to consider. In this article, we will focus on circularly polarized beams. We define a circularly polarized beam as a helicity state which is an eigenstate of the generator of the duality transformations $F'_{\bar\alpha\bar\beta} = F_{\bar\alpha\bar\beta}\cos\varphi + \star F_{\bar\alpha\bar\beta}\sin\varphi$, where $\star F_{\bar\alpha\bar\beta} = \frac{1}{2}\sqrt{-\det(\eta)}\epsilon_{\bar\alpha\bar\beta\bar\gamma\bar\delta}F^{\bar\gamma\bar\delta}$ is the Hodge dual of $F_{\bar\alpha\bar\beta}$ and $\epsilon_{\bar\alpha\bar\beta\bar\gamma\bar\delta}$ is the completely anti-symmetric Levi-Civita symbol with $\epsilon_{0123} = -1$. The invariance of Maxwell's equations under these duality transformations and the corresponding conservation laws were worked out in [8]. The generator of the duality transformation $D_\theta = \exp(\mathrm{i}\varphi\Lambda) : F_{\bar\alpha\bar\beta} \mapsto F'_{\bar\alpha\bar\beta}$ is $\Lambda : F_{\bar\alpha\bar\beta} \mapsto -\mathrm{i}\star F_{\bar\alpha\bar\beta}$ since $\star\star F_{\bar\alpha\bar\beta} = -F_{\bar\alpha\bar\beta}$.

The vector potentials of well-defined helicity are eigenstates of Λ with eigenvalues $\lambda = \pm 1$. There are two options to obtain these eigenstates. One option is to start with a helicity eigenstate of zeroth order in θ, construct the corresponding higher order terms of the expansion of the envelope function of even n with equation (13), obtain the odd terms in the expansion of the envelope function with the Lorenz gauge condition in equation (14), calculate the field strength tensor and project it with $(1 + \lambda\Lambda)/2$. This option is presented in appendix C.

In the main text of this article, we follow the second option, where a vector potential is constructed order by order by taking into account the condition $(1-\lambda\Lambda)F^{\lambda}_{\bar{\alpha}\bar{\beta}}=0$ and the expansion in equation (16) in each order separately. This construction is presented in appendix A. Starting from $v^{(0)}_{\bar{\alpha}}=\epsilon^{(0)}_{\bar{\alpha}}v_0$, where $\epsilon^{(0)}_{\bar{a}}=w_0(1,-\lambda i,0)/\sqrt{2}$ and $\bar{a}\in\{\xi,\chi,\zeta\}$, and taking the solutions of even orders from [30] into account, we obtain

$$v^{\lambda(0)}_{\bar{a}}=\epsilon^{(0)}_{\bar{a}}v_0, \tag{17}$$

$$v^{\lambda(1)}_{\bar{a}}=-\epsilon^{(1)}_{\bar{a}}\frac{\mathrm{i}w_0\mu}{2\sqrt{2}}\left(\xi-\mathrm{i}\lambda\chi\right)v_0, \tag{18}$$

$$v^{\lambda(2)}_{\bar{a}}=\frac{\mu}{2}\left(1-\frac{1}{2}\mu^2\rho^4\right)v^{\lambda(0)}_{\bar{a}}, \tag{19}$$

$$v^{\lambda(3)}_{\bar{a}}=\frac{\mu}{4}\left(4+\mu\rho^2-\mu^2\rho^4\right)v^{\lambda(1)}_{\bar{a}}, \tag{20}$$

$$v^{\lambda(4)}_{\bar{a}}=\frac{\mu^2}{16}\left(6-3\mu^2\rho^4-2\mu^3\rho^6+\frac{1}{2}\mu^4\rho^8\right)v^{\lambda(0)}_{\bar{a}}, \tag{21}$$

where $\epsilon^{(1)}_{\bar{a}}=w_0(0,0,1)$. The corresponding vector potential is given as $A^{\lambda}_{\bar{\alpha}}=\sum_{n=0}^{4}\theta^n\mathcal{A}v^{\lambda(n)}_{\bar{\alpha}}(\xi,\chi,\theta\zeta)\mathrm{e}^{\mathrm{i}\frac{2}{\theta}(\zeta-\tau)}$, where the component A^{λ}_{τ} is given through the Lorenz gauge condition in equation (14). Linearly polarized Gaussian beams are obtained as linear combinations of helicity eigenstates; for example, $A^{\xi}_{\bar{\alpha}}:=(A^{+}_{\bar{\alpha}}+A^{-}_{\bar{\alpha}})/\sqrt{2}$ is the vector potential of a laser beam that is linearly polarized in the ξ-direction. Note that all terms of higher than leading order in equation (17) decay faster than $v^{\lambda(0)}_{\bar{a}}$ for $\theta\zeta\to\infty$. Hence, $v_{\bar{a}}\approx v^{\lambda(0)}_{\bar{a}}$ for large $\theta\zeta$.

2.2. Three distinct scenarios

The beam divergence θ, which is assumed to be small, is related to the wave vector k, the beam waist w_0 and the Rayleigh length z_R through

$$k=\frac{2}{w_0\theta}=\frac{2}{z_R\theta^2}. \tag{22}$$

The beam waist w_0 describes the width of the beam at its focal point, i.e. at $\zeta=0$, and the Rayleigh length is the distance from the focal point along the direction of propagation such that the cross section of the beam is doubled, as illustrated in figure 1. There are basically three scenarios for which the condition that θ is small is satisfied:

1. $k=$ constant: if the wave vector k is kept constant, the beam waist w_0 and the Rayleigh length z_R have to be large, and $z_R\gg w_0$ has to hold. Keeping the wave vector constant is the characteristic feature of a plane wave. If the beam is very long, its gravitational field may be compared to that of infinitely extended plane waves, which are described by particular pp-wave metrics[4].
2. $w_0=$ constant: keeping the beam waist w_0 fixed, the wave vector k and the Rayleigh length z_R have to be large, and in addition we find $z_R\gg\frac{1}{k}$. This situation describes an almost parallel beam of a given waist. If the beam is very long and the beam waist is

[4] See chapter 35 in [9].

considered to be small, such that it is approximately a cylinder of light, its gravitational field may be compared to the solution found by Bonnor [4] for an infinitely long cylinder of light.

3. $z_R = \text{constant}$: keeping the Rayleigh length fixed, the wave vector k has to be large and the beam waist w_0 has to be small. This case corresponds to a very thin and almost parallel beam along the z-axis, whose energy-density is accordingly high. The corresponding gravitational field is the solution given by Tolman, Ehrenfest and Podolski [36].

In the following, we will keep the beam waist w_0 constant.

2.3. The energy–momentum tensor

To derive the gravitational field of the laser beam, we have to derive its energy–momentum tensor first. Let us define the real part of $F_{\bar{\alpha}\bar{\beta}}$ as $\mathrm{Re}(F)_{\bar{\alpha}\bar{\beta}}$. In terms of $\mathrm{Re}(F)_{\bar{\alpha}\bar{\beta}}$, the energy–momentum tensor is defined as $T_{\bar{\alpha}\bar{\beta}} = c^2\varepsilon_0(\mathrm{Re}(F)_{\bar{\alpha}}{}^{\bar{\sigma}}\mathrm{Re}(F)_{\bar{\beta}\bar{\sigma}} - \frac{1}{4}\eta_{\bar{\alpha}\bar{\beta}}\mathrm{Re}(F)^{\bar{\delta}\bar{\rho}}\mathrm{Re}(F)_{\bar{\delta}\bar{\rho}})$. Therefore, the energy–momentum tensor can be decomposed into the real term

$$(T^r)_{\bar{\alpha}\bar{\beta}} = \frac{c^2\varepsilon_0}{2}\mathrm{Re}\left(F_{\bar{\alpha}}{}^{\bar{\sigma}}F^*_{\bar{\beta}\bar{\sigma}} - \frac{1}{4}\eta_{\bar{\alpha}\bar{\beta}}F^{\bar{\delta}\bar{\rho}}F^*_{\bar{\delta}\bar{\rho}}\right), \tag{23}$$

the complex term

$$(T^c)_{\bar{\alpha}\bar{\beta}} = \frac{c^2\varepsilon_0}{4}\left(F_{\bar{\alpha}}{}^{\bar{\sigma}}F_{\bar{\beta}\bar{\sigma}} - \frac{1}{4}\eta_{\bar{\alpha}\bar{\beta}}F^{\bar{\delta}\bar{\rho}}F_{\bar{\delta}\bar{\rho}}\right), \tag{24}$$

and its complex conjugate $(T^c)^*_{\bar{\alpha}\bar{\beta}}$. The term $(T^c)_{\bar{\alpha}\bar{\beta}}$ is highly oscillating with $\mathrm{i}(\zeta-\tau)/\theta$ while these oscillations cancel in $(T^r)_{\bar{\alpha}\bar{\beta}}$. For eigenstates of the helicity operator with eigenvalue $\lambda = \pm 1$, the highly oscillating terms in $(T^c)_{\bar{\alpha}\bar{\beta}}$ and its complex conjugate vanish and it remains $T_{\bar{\alpha}\bar{\beta}} = (T^r)_{\bar{\alpha}\bar{\beta}}$. Therefore, the highly oscillating parts of the energy–momentum tensor can be interpreted as a result of the interference of contributions of different helicity in the field strength that come into play for linear or elliptical polarization. In the following, we will only consider circular polarization.

The components of the energy–momentum tensor are directly related to the energy density $\mathcal{E}^\lambda$, the Poynting vector $\vec{S}^\lambda$ and the Maxwell stress tensor σ^λ_{ij} of the electromagnetic field,

$$T^\lambda_{\bar{\alpha}\bar{\beta}} = \begin{pmatrix} \mathcal{E}^\lambda & -S^\lambda_\xi/c & -S^\lambda_\chi/c & -S^\lambda_\zeta/c \\ -S^\lambda_\xi/c & \sigma^\lambda_{11} & \sigma^\lambda_{12} & \sigma^\lambda_{13} \\ -S^\lambda_\chi/c & \sigma^\lambda_{12} & \sigma^\lambda_{22} & \sigma^\lambda_{23} \\ -S^\lambda_\zeta/c & \sigma^\lambda_{13} & \sigma^\lambda_{23} & \sigma^\lambda_{33} \end{pmatrix}. \tag{25}$$

For the field strength tensor $F^\lambda_{\bar{\alpha}\bar{\beta}} = \partial_{\bar{\alpha}}A^\lambda_{\bar{\beta}} - \partial_{\bar{\beta}}A^\lambda_{\bar{\alpha}}$ of a circularly polarized laser beam, which we specified in section 2.1.1, the energy density, the Poynting vector and the stress tensor components are given in appendix B.

The power transmitted in the direction of propagation is given by $P = \int_0^{2\pi}\mathrm{d}\phi\int_0^\infty \mathrm{d}\rho\,\rho S_\zeta$. In the leading order in the expansion in θ, we obtain $P_0 = \pi c\varepsilon_0 E_0^2 w_0^2/2$, where E_0 is the amplitude of the electric field in the leading order at the beamline. We may then express the amplitude in terms of the power as $E_0 = \sqrt{\frac{2P_0}{\pi c\varepsilon_0 w_0^2}}$. For a power of $P_0 \sim 10^{15}$ W and a beam waist of $w_0 \sim 10^{-3}$ m, the amplitude is $E_0 \sim 10^{12}$ V m^{-1}.

As the field strength tensor, the energy–momentum tensor can be expanded in orders of θ as $T^{\lambda}_{\bar{\alpha}\bar{\beta}} = \sum_n \theta^n t^{\lambda(n)}_{\bar{\alpha}\bar{\beta}}$. Then, the gravitational field of the laser beam can be calculated for each order and effects of different orders can be identified. We will present this analysis up to fourth order in θ in the following sections.

3. Linearized gravity

Assuming that the energy of the laser beam is sufficiently small, we use the linearized theory of general relativity[5] to describe its gravitational field. In appendix D, we make a rough estimation to show that this is reasonable. The metric $g_{\alpha\beta}$ consists of the metric for flat spacetime $\eta_{\alpha\beta}$ plus a small perturbation $h_{\alpha\beta}$ with $|h_{\alpha\beta}| \ll 1$,

$$g_{\alpha\beta} = \eta_{\alpha\beta} + h_{\alpha\beta}. \tag{26}$$

Therefore one neglects terms quadratic in the metric perturbation. In this case, one sees that the inverse of the metric reads $g^{\alpha\beta} = \eta^{\alpha\beta} - h^{\alpha\beta}$. The Einstein equations can be simplified to a set of linear equations in the metric perturbation. As the full general relativity has an invariance under coordinate transformation, its linearized approximation is invariant under linear coordinate transformations $x^{\alpha} \to \tilde{x}^{\alpha} = x^{\alpha} + \xi^{\alpha}$, where the metric perturbation transforms as $h_{\alpha\beta} \to \tilde{h}_{\alpha\beta} = h_{\alpha\beta} - \partial_{\alpha}\xi_{\beta} - \partial_{\beta}\xi_{\alpha}$.[6] Since curvature is described by the second derivatives of the metric, quantities depending on the curvature are invariant under linear coordinate transformations.

To derive the linearized version of the Einstein equations, we assume the Lorenz gauge condition, $\partial^{\alpha}h_{\alpha\beta} = \partial_{\beta}h_{\alpha}{}^{\alpha}/2$. The energy–momentum tensor has to be conserved, $\eta^{\alpha\beta}\partial_{\alpha}T_{\beta\gamma} = 0$, which implies that the continuity equation is satisfied [21, 26]. The remaining gauge freedom is given by linear coordinate transformations ξ_{α} that satisfy $\Box\xi_{\alpha} = 0$. Taking into account that the trace of the energy–momentum tensor $T_{\sigma}{}^{\sigma}$ is identically zero for the electromagnetic field, we obtain the linearized Einstein equations[7]

$$\Box h_{\alpha\beta} = -\kappa T_{\alpha\beta}, \tag{27}$$

where $\kappa = 16\pi G/c^4$ and G is Newton's constant.

In general relativity, coordinates have no physical meaning. Since the values of the components of the metric tensor depend on the choice of coordinates, we cannot extract physical information directly from them. Therefore, we have to investigate effects on test particles to learn about the gravitational field. The motion of test particles is governed by the geodesic equation

$$\frac{\mathrm{d}^2\gamma^{\mu}}{\mathrm{d}\varrho^2} = -\Gamma^{\mu}_{\nu\rho}\frac{\mathrm{d}\gamma^{\nu}}{\mathrm{d}\varrho}\frac{\mathrm{d}\gamma^{\rho}}{\mathrm{d}\varrho}, \tag{28}$$

where, in linearized gravity, the Christoffel symbols are given as

$$\Gamma^{\mu}_{\nu\rho} = \frac{1}{2}\eta^{\mu\sigma}\left(\partial_{\nu}h_{\sigma\rho} + \partial_{\rho}h_{\sigma\nu} - \partial_{\sigma}h_{\nu\rho}\right). \tag{29}$$

A more direct way to analyse gravitational effects is through the spread and the contraction of the trajectories of test particles. This way, the test particles serve as each others reference.

[5] See chapter 18 in [9].
[6] It is assumed that $|\partial_{\alpha}\xi_{\beta}|$ is of the same order of magnitude as $h_{\alpha\beta}$.
[7] See equation (18.8b) in [9].

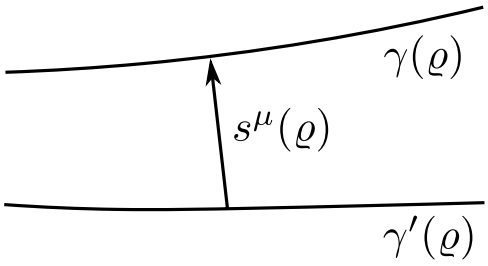

Figure 2. Schematic illustration of the geodesic deviation equation: two nearby geodesics $\gamma(\varrho)$ and $\gamma'(\varrho)$ are seperated by the vector $s^\mu(\varrho)$.

The relative acceleration between two infinitesimally close geodesics $\gamma(\varrho)$ and $\gamma'(\varrho)$ parameterized by ϱ is given by the geodesic deviation equation

$$a^\mu = \frac{D^2 s^\mu}{\mathrm{d}\varrho^2} = R^\mu{}_{\rho\sigma\alpha}(\gamma)\dot\gamma^\rho\dot\gamma^\sigma s^\alpha, \tag{30}$$

where s is the separation vector between the geodesics, $D/\mathrm{d}\varrho = \dot\gamma^\mu\nabla_\mu$ is the covariant derivative along the geodesic $\gamma(\varrho)$ and $R^\mu{}_{\rho\sigma\alpha}$ is the Riemann curvature tensor. This is illustrated in figure 2. In the linearized theory, the pulled down Riemann curvature tensor is given by

$$R_{\alpha\beta\gamma\delta} = \frac{1}{2}\left(\partial_\beta\partial_\gamma h_{\delta\alpha} - \partial_\beta\partial_\delta h_{\gamma\alpha} - \partial_\gamma\partial_\alpha h_{\beta\delta} + \partial_\delta\partial_\alpha h_{\beta\gamma}\right) . \tag{31}$$

Since the metric perturbation transforms as $h_{\alpha\beta} \to \tilde h_{\alpha\beta} = h_{\alpha\beta} - \partial_\alpha\xi_\beta - \partial_\beta\xi_\alpha$, we find that $R_{\alpha\beta\gamma\delta}$ is invariant under a linearized coordinate transformation.

4. The metric of the laser beam

Solving equation (27) for the energy–momentum tensor (25) with emitter and absorber[8] at general positions can be quite cumbersome. In the following, we will consider two different limiting situations instead; we consider the case of the distance between emitter and absorber of the laser beam being very large and very small.

In the first situation, we can neglect the rapid change of the field strength at the emitter and the absorber of the laser beam. Then we can take into account that $T_{\bar\alpha\bar\beta}$ is changing slowly in ζ. In particular, we have $T^\lambda_{\bar\alpha\bar\beta} = \bar T^\lambda_{\bar\alpha\bar\beta}(\xi,\chi,\theta\zeta)$. Therefore, we can expand the metric perturbation similar to equation (5) as

$$h^\lambda_{\bar\alpha\bar\beta}(\xi,\chi,\theta\zeta) = \sum_{n=0}^{\infty}\theta^n h^{\lambda(n)}_{\bar\alpha\bar\beta}(\xi,\chi,\theta\zeta), \tag{32}$$

and the linearized Einstein equations (27) lead to the differential equations

$$\Delta_{2d} h^{\lambda(0)}_{\bar\alpha\bar\beta} = -\kappa w_0^2\,\bar t^{\lambda(0)}_{\alpha\beta}, \tag{33}$$

$$\Delta_{2d} h^{\lambda(1)}_{\bar\alpha\bar\beta} = -\kappa w_0^2\,\bar t^{\lambda(1)}_{\bar\alpha\bar\beta}, \tag{34}$$

[8] In this article, emitter and absorber always refers to the emitter and the absorber of the source laser beam for the case of a finitely extended beam. The emitter can be associated with the laser resonator and the active material and the absorber can be imagined as a beam dump.

$$\Delta_{2d} h^{\lambda(n)}_{\bar{\alpha}\bar{\beta}} = -\kappa w_0^2 \bar{t}^{\lambda(n)}_{\bar{\alpha}\bar{\beta}} - \partial^2_{\theta\zeta} h^{\lambda(n-2)}_{\bar{\alpha}\bar{\beta}}, \text{ for } n > 1. \tag{35}$$

The solutions $h^{\lambda(n)}_{\bar{\alpha}\bar{\beta}}$ of equations (33)–(35) can be given by using the free space Green's function for the Poisson equation in two dimensions as

$$h^{\lambda(n)}_{\bar{\alpha}\bar{\beta}}(\xi,\chi,\theta\zeta) = -\frac{\kappa}{4\pi}\int_{-\infty}^{\infty} \mathrm{d}\xi'\mathrm{d}\chi' \log\left((\xi-\xi')^2+(\chi-\chi')^2\right) Q^{\lambda(n)}_{\bar{\alpha}\bar{\beta}}(\xi',\chi',\theta\zeta), \tag{36}$$

where $Q^{\lambda(n)}$ is the source term on the right hand side of equations (33)–(35), respectively. The form of the solutions in equation (36) was fixed by an additional condition that we did not discuss yet; we want the components of the Riemann curvature tensor to vanish at infinite distance from the beamline. As stated in section 3, the Riemann curvature tensor governs the spread and the contraction of the trajectories of test particles. This means, if the Riemann tensor vanishes, parallel geodesics stay parallel and there is no physical effect as the only reference for a test particle in linearized gravity can be another test particle. We can assume that there is no gravitational effect for infinite spatial distances from the beamline. Therefore, we assume that the Riemann curvature tensor $R^{\mu}{}_{\rho\sigma\alpha}$ vanishes for $\rho \to \infty$. The full discussion of the curvature condition and its implications are given in appendix F. Additionally, appendix F contains expressions for the components of the metric perturbation up to third order in θ.

As we did before for the vector potential, the field strength tensor, the energy–momentum tensor and the metric perturbation, we expand the Christoffel symbols and the Riemann tensor in orders of θ,

$$(\Gamma^{\lambda})^{\bar{\alpha}}_{\bar{\beta}\bar{\gamma}}(\xi,\chi,\theta\zeta) = \sum_{n=0}^{\infty} \theta^n (\gamma^{\lambda(n)})^{\bar{\alpha}}_{\bar{\beta}\bar{\gamma}}(\xi,\chi,\theta\zeta), \tag{37}$$

and

$$R^{\lambda}_{\bar{\alpha}\bar{\beta}\bar{\gamma}\bar{\delta}}(\xi,\chi,\theta\zeta) = \sum_{n=0}^{\infty} \theta^n r^{\lambda(n)}_{\bar{\alpha}\bar{\beta}\bar{\gamma}\bar{\delta}}(\xi,\chi,\theta\zeta), \tag{38}$$

respectively. With equations (31), (29) and (32), we can derive direct relations between the terms of the expansions $r^{\lambda(n)}_{\bar{\alpha}\bar{\beta}\bar{\gamma}\bar{\delta}}$ and $(\gamma^{\lambda(n)})^{\bar{\alpha}}_{\bar{\beta}\bar{\gamma}}$ and terms in the expansion of the metric perturbation $h^{\lambda(n)}_{\alpha\beta}$. They are given in appendix E.

4.1. Small distance between emitter and absorber

In the second situation, where we assume a short distance between emitter and absorber of the laser beam, the rapid change of the field strength at emitter and absorber of the laser beam cannot be neglected. Then, we solve the Einstein equations (27) by use of their retarded solution

$$h^{\lambda}_{\bar{\alpha}\bar{\beta}}(\tau,\xi,\chi,\zeta) = \frac{\kappa}{4\pi}\int_{-\infty}^{\infty} \mathrm{d}\xi'\mathrm{d}\chi'\mathrm{d}\zeta' \frac{T^{\lambda}_{\bar{\alpha}\bar{\beta}}\left(\tau-\sqrt{(\xi-\xi')^2+(\chi-\chi')^2+(\zeta-\zeta')^2},\xi',\chi',\theta\zeta'\right)}{\sqrt{(\xi-\xi')^2+(\chi-\chi')^2+(\zeta-\zeta')^2}}. \tag{39}$$

Furthermore, we can set $\theta\zeta \ll 1$ and we can expand the function $\mathrm{e}^{-|\mu(\theta\zeta)|^2\rho^2}$ appearing in the energy–momentum tensor in θ before the integration, which simplifies the calculations significantly[9]. Expressions for $h^{\lambda}_{\bar{\alpha}\bar{\beta}}$ up to second order in θ for the case of small distances between emitter and absorber of the laser beam can be found in appendix H.

[9] Due to the Gaussian profile of the beam, large values of ρ do not contribute significantly and $(\theta\zeta)^n\rho^2$ can be considered as small for all $n \geqslant 1$.

In the following, we discuss the metric perturbation in different orders in θ and present its physical effects. As already the effects in the leading order of our expansion are too small to be measurable with current technology [26], this will also be the case for the effects in the higher orders. However, the effects are of conceptual interest, as they illustrate the gravitational properties of light.

5. Zeroth/leading order

The metric in the leading order corresponds to the full metric at $\theta = 0$, and thus to the metric for the laser beam in the paraxial approximation. Then, the components of the Poynting vector transversal to the beamline vanish and the only non-zero component of the Maxwell stress tensor is $\sigma^{\lambda}_{\zeta\zeta}$. Furthermore, $\sigma^{\lambda}_{\zeta\zeta} = \mathcal{E}^{\lambda} = -S^{\lambda}_{\zeta}/c$, which leads to

$$T^{\lambda(0)}_{\bar{\alpha}\bar{\beta}} = \mathcal{E}^{(0)} \begin{pmatrix} 1 & 0 & 0 & -1 \\ 0 & 0 & 0 & 0 \\ 0 & 0 & 0 & 0 \\ -1 & 0 & 0 & 1 \end{pmatrix} =: \mathcal{E}^{(0)} M^{0}_{\bar{\alpha}\bar{\beta}}, \tag{40}$$

where $\mathcal{E}^{(0)} = \varepsilon_0 w_0^2 E_0^2 |v_0|^2 = 2P_0|v_0|^2/(\pi c)$. Therefore, the metric perturbation is found as

$$h^{\lambda(0)}_{\bar{\alpha}\bar{\beta}} = I^{(0)} M^{0}_{\bar{\alpha}\bar{\beta}}, \tag{41}$$

where, for the case that the emitter and absorber of the laser beam are far away from each other, we find from equation (36)

$$I^{(0)} = \frac{\kappa w_0^2 P_0}{2\pi c} \left(\frac{1}{2} \mathrm{Ei}\left(-2|\mu|^2\rho^2\right) - \log(\rho) \right), \tag{42}$$

where $\mathrm{Ei}(x)$ is the exponential integral function. The solution (42) can be compared with the exact solution derived by Bonnor for an infinitely extended beam of a light-like medium without divergence. The derivation of the metric for a Gaussian profile of the energy density of the medium is given in appendix G. Bonnor's solution is split into an interior and an exterior solution that are matched at a finite transversal radius a. If the beam is infinitely extended in the transverse direction, we are left with an interior solution only which reads

$$g^{\mathrm{B}}_{\bar{\alpha}\bar{\beta}} = \eta_{\bar{\alpha}\bar{\beta}} - \frac{\kappa w_0^2 P_0}{2\pi c} \left(\log(\rho) - \frac{1}{2} \mathrm{Ei}\left(-2\rho^2\right) \right) M^{0}_{\bar{\alpha}\bar{\beta}}. \tag{43}$$

For $\theta = 0$, we have $\mu(\theta\zeta) = 1$, and the solution in equation (41) coincides with (43).

5.1. Small distance between emitter and absorber of the laser beam

For the case when the emitter and absorber of the laser beam are close to each other, we have to take the second approach described in section 4. With $\theta\zeta \ll 1$, the retarded potential (39) in leading order in θ becomes

$$I^{(0)} = \frac{\kappa w_0^2 P_0}{2\pi c} \mathrm{e}^{-2\rho^2} \int_0^{\infty} \mathrm{d}\rho'\, \rho' \log\left(\frac{\beta - \zeta + \sqrt{(\beta-\zeta)^2 + \rho'^2}}{\alpha - \zeta + \sqrt{(\alpha-\zeta)^2 + \rho'^2}} \right) J_0\left(\mathrm{i}4\rho\rho'\right) \mathrm{e}^{-2\rho'^2}, \tag{44}$$

where J_0 is the Bessel function of the first kind. For small beam waists, $w_0 \ll 1$, the solution for the laser beam (44) approaches the solution for the infinitely thin beam (45), as shown in appendix I. We obtain

$$I^{(0)}_{w_0\to 0} = \frac{\kappa w_0^2 P_0}{2\pi c} \log\left(\frac{\beta-\zeta+\sqrt{(\beta-\zeta)^2+\rho^2}}{\alpha-\zeta+\sqrt{(\alpha-\zeta)^2+\rho^2}}\right). \tag{45}$$

Thus, in the paraxial approximation, we may say that the solution for the laser beam approaches the solution for the infinitely thin beam of constant energy per length of [36] as the beam waist goes to zero. Note that the limit $w_0 \to 0$ can only be considered for the leading order of the laser beam here. This is because $\theta = 0$ implies that the condition $\theta\zeta \ll 1$ can be satisfied for all w_0. In contrast, for any non-vanishing θ, the conditions $w_0 \to 0$ and $\theta z/w_0 = \theta\zeta \ll 1$ imply $z \to 0$.

In figure 3, the function $I^{(0)}$ and its derivatives are illustrated for the three cases of the infinitely long Gaussian beam, the Gaussian beam with short distance between emitter and absorber of the laser beam with a Gaussian profile, and the infinitely thin beam.

5.2. Acceleration of a test particle at rest

Let us consider the acceleration a massive test particle would experience if it was initially at rest at given ρ and ζ. Then, the initial normalized tangent to its worldline $\gamma(\tilde\tau)$, where $\tilde\tau$ is the proper time, is given as $\dot\gamma = cw_0^{-1}\big(1 + h^{\lambda(0)}_{\tau\tau}/(2w_0^2), 0, 0, 0\big)$, where the dot refers to the derivative with respect to proper time. From the geodesic equation (28) and the form of the metric in zeroth order, we find

$$\ddot\gamma^\rho \simeq \frac{c^2}{2w_0^4}\partial_\rho I^{(0)} \quad \text{and} \quad \ddot\gamma^\zeta \simeq \frac{c^2}{2w_0^4}\partial_\zeta I^{(0)}. \tag{46}$$

Plots of $\partial_\rho I^{(0)}$ and $\partial_\zeta I^{(0)}$ for the three different cases above are given in figure 3. As a numerical example for the long beam, for the power $P_0 \sim 10^{15}$ W, the beam waist $w_0 \sim 10^{-3}$ m, a particle at rest at the location $z = 0$ and $r = \sqrt{x^2+y^2} = w_0$ is accelerated by $\ddot\gamma^r \sim -10^{-18}$ ms^{-2}.[10] This is of the same order of magnitude as for the infinitely thin beam [26].

5.3. Curvature

For the leading order, we can find the components of the curvature tensor using equation (E.2) in appendix E and equation (41). The only non-zero independent components of the Riemann curvature tensor for the metric perturbation given in equations (42) and (44) and the limit of an infinitely thin beam in equation (45) are

$$R^{(0)}_{\tau i\tau j} = R^{(0)}_{\zeta i\zeta j} = -R^{(0)}_{\tau i\zeta j} = -\frac{1}{2}\partial_i\partial_j I^{(0)}. \tag{47}$$

For the case of a far extended beam neglecting emitter and absorber of the laser beam that was given in equation (42), we obtain

[10] Here and in the following numerical examples, in order to express the acceleration in the coordinates $\{ct, x, y, z\}$, the Leibnitz rule has been applied and it has been used that the difference between proper time and coordinate time is proportional to the metric perturbation.

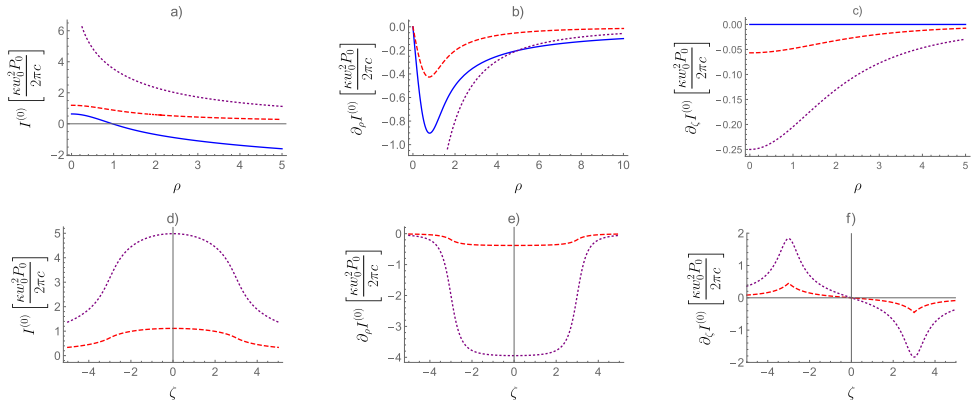

Figure 3. These plots show the value of the leading order of the metric perturbation $I^{(0)}$ (part a, d) and its first derivatives (part b, c, e, f) for the Gaussian beam with infinite distance between (plain, blue), the Gaussian beam with short distance between emitter and absorber of the laser beam (dashed, red), and the infinitely thin beam (dotted, purple) in units of $\kappa P_0 w_0^2/(2\pi c)$. In the second and the third cases, the distance between laser beam's emitter and absorber is chosen to be 6. In the first row, the functions are plotted for $\zeta = 1$ and in the second row for $\rho = 1/2$. The second row does not contain plots for the case of large distances between emitter and absorber of the laser beam as there is no dependence of $I^{(0)}$ on ζ in that case. We find that the values for $I^{(0)}$ and its first derivatives are usually larger for the infinitely thin beam than for the other two cases. This is due to the divergence at the beamline for the case of the infinitely thin beam. In the other two cases, the gravitational field is spread out as the sources are. In (b), we see that the absolute value of the first ρ-derivative of $I^{(0)}$ reaches a maximum at a finite distance from the beamline. Note that $\partial_\rho I^{(0)}$ is proportional to the acceleration that a test particle experiences if it is initially at rest at a given distance ρ to the beamline. We see that acceleration is always directed towards the beamline. It is larger in the case of an infinite distance between emitter and absorber of the laser beam than in the case of a finite distance, which we can attribute to the larger extension of the source (and thus the larger amount of energy) in the former than in the latter. In (e), which shows plots for the cases of finite distance between laser beam's emitter and absorber, we see that $\partial_\rho I^{(0)}$ still is the largest at the center between emitter and absorber of the laser beam and decays quickly once their positions at $\zeta = \pm 3$ are passed. $\partial_\zeta I^{(0)}$ is proportional to the acceleration in the ζ-direction. As expected it vanishes for infinite distance between emitter and absorber of the laser beam. In (f), we see that the acceleration is directed towards the center between the laser beam's emitter and absorber and its absolute values reaches its maximum at $\zeta = -3$ and $\zeta = 3$, the ζ-coordinates of emitter and absorber of the laser beam respectively.

$$R^{(0)}_{\tau\xi\tau\xi} = R^{(0)}_{\zeta\xi\zeta\xi} = -R^{(0)}_{\tau\xi\zeta\xi} = -\frac{\kappa w_0^2 P_0}{4\pi c}\,\frac{|\mu|^2}{\rho^4}\left((\xi^2-\chi^2) - \left(4\xi^2\rho^2 + \xi^2 - \chi^2\right)\mathrm{e}^{-2|\mu|^2\rho^2}\right), \tag{48}$$

$$R^{(0)}_{\tau\chi\tau\chi} = R^{(0)}_{\zeta\chi\zeta\chi} = -R^{(0)}_{\tau\chi\zeta\chi} = \frac{\kappa w_0^2 P_0}{4\pi c}\,\frac{|\mu|^2}{\rho^4}\left((\xi^2-\chi^2) + \left(4\chi^2\rho^2 - \xi^2 + \chi^2\right)\mathrm{e}^{-2|\mu|^2\rho^2}\right), \tag{49}$$

$$R^{(0)}_{\tau\xi\tau\chi} = R^{(0)}_{\zeta\xi\zeta\chi} = -R^{(0)}_{\tau\xi\zeta\chi} = -\frac{\kappa w_0^2 P_0}{2\pi c}\,\frac{|\mu|^2\xi\chi}{\rho^4}\left(1 - (1+2\rho^2)\mathrm{e}^{-2|\mu|^2\rho^2}\right). \tag{50}$$

5.4. Comparison to the infinitely thin beam

In the paraxial approximation (i.e. for $\theta = 0$) and for small beam waists, the Riemann curvature tensor of the infinitely long laser beam approaches the Riemann curvature tensor of the infinitely thin beam, as does the metric. It is also interesting to compare the curvature for the infinitely thin beam with that for the full solution given in [4] by Bonnor. The analysis can be found in appendix G for a beam with a Gaussian profile cut off at a radius a. The corresponding solution splits into an interior solution and an exterior solution. For $a \to \infty$, we obtain the solution in equation (43) that we compared with our leading order metric perturbation already. In appendix G, we give the components of the curvature tensor in the exterior region ($r > a$) in equation (G.8). We show that it coincides with the components of the curvature tensor of an infinitely thin beam. In particular, the curvature is independent of the radial dependence of the beam intensity; only the total power of the beam is important.

6. First order and frame dragging

The metric perturbation for large distances between emitter and absorber of the laser beam in first order in θ is determined by the first order of the energy–momentum tensor, $\bar{t}^{\lambda(1)}_{\bar{\alpha}\bar{\beta}}$, which has the only independent non-zero components

$$\begin{aligned} \theta\bar{t}^{\lambda(1)}_{\tau\xi} &= -\theta\bar{t}^{\lambda(1)}_{\zeta\xi} = -S^{\lambda(1)}_{\xi} = -\mathcal{E}^{(0)}\theta|\mu|^2(\theta\zeta\xi + \lambda\chi), \\ \theta\bar{t}^{\lambda(1)}_{\tau\chi} &= -\theta\bar{t}^{\lambda(1)}_{\zeta\chi} = -S^{\lambda(1)}_{\chi} = \lambda\mathcal{E}^{(0)}\theta|\mu|^2(\xi - \lambda\theta\zeta\chi). \end{aligned} \tag{51}$$

Note that $\tilde{\zeta} = \theta\zeta$ is the coordinate that is considered for the asymptotic expansion in equations (6)–(8). Therefore, $S^{\lambda(1)}_{\xi}$ and $S^{\lambda(1)}_{\chi}$ are indeed of first order in θ regarding the expansion (5).

From equation (34), we obtain for the metric perturbation in first order in θ

$$h^{\lambda(1)}_{\bar{\alpha}\bar{\beta}} = \begin{pmatrix} 0 & I^{\lambda(1)}_{\xi} & I^{\lambda(1)}_{\chi} & 0 \\ I^{\lambda(1)}_{\xi} & 0 & 0 & -I^{\lambda(1)}_{\xi} \\ I^{\lambda(1)}_{\chi} & 0 & 0 & -I^{\lambda(1)}_{\chi} \\ 0 & -I^{\lambda(1)}_{\xi} & -I^{\lambda(1)}_{\chi} & 0 \end{pmatrix}, \tag{52}$$

where

$$I^{\lambda(1)}_{\xi} = \frac{1}{4}(\theta\zeta\partial_{\xi} + \lambda\partial_{\chi})I^{(0)} = -\frac{\kappa P_0 w_0^2(\theta\zeta\xi + \lambda\chi)}{8\pi c\rho^2}\left(1 - \mathrm{e}^{-2|\mu|^2\rho^2}\right), \tag{53}$$

$$I^{\lambda(1)}_{\chi} = -\frac{1}{4}(\lambda\partial_{\xi} - \theta\zeta\partial_{\chi})I^{(0)} = \frac{\kappa P_0 w_0^2(\lambda\xi - \theta\zeta\chi)}{8\pi c\rho^2}\left(1 - \mathrm{e}^{-2|\mu|^2\rho^2}\right). \tag{54}$$

For small $\theta\zeta$, the terms proportional to $\theta\zeta$ can be neglected in (53) such that we find

$$I^{\lambda(1)}_{\xi} = \frac{\lambda}{4}\partial_{\chi}I^{(0)} \quad \text{and} \quad I^{\lambda(1)}_{\chi} = -\frac{\lambda}{4}\partial_{\xi}I^{(0)}. \tag{55}$$

It is interesting to note that our solution coincides with the exact solution of Einstein's equations presented in [5] by Bonnor for a rotating null fluid. In particular, we can identify our functions in the metric with those of [5] as $\alpha = \theta I^{\lambda(1)}_{\chi}/\sqrt{2}$, $\beta = \theta I^{\lambda(1)}_{\xi}/\sqrt{2}$ and $A = I^{(0)}$. Our

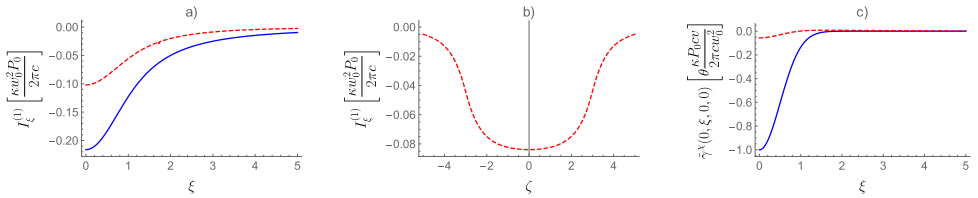

Figure 4. Considering $\theta\zeta \ll 1$, the first two plots show the function $I^{(1)}_{\xi}$ for an infinite distance between emitter and absorber of the laser beam (plain, blue) and a short distance between laser beam's emitter and absorber (dashed, red) as a function of ξ for $\zeta = 0.1$ and $\chi = 0$ (plot (a)) and as a function of ζ at $\xi = 1/2$ and $\chi = 1$ (plot (b)). The functions are plotted in units of $\kappa w_0^2 P_0/(2\pi c)$. In (b) there is no plot for the case of infinite distance between emitter and absorber of the laser beam as the result does not depend on $\theta\zeta$. Plot (c) shows the deflection in the χ-direction a light test particle would experience if it would move radially outwards in the ξ-direction at $\chi = 0$ for an infinite distance between emitter and absorber of the laser beam (plain, blue) and a short distance between laser beam's emitter and absorber (dashed, red). This effect is induced by frame dragging. We see that the effect changes sign for the case of a short distance between the laser beam's emitter and absorber.

equation (34) corresponds to the equations (2.16) and (2.17) in [5]. Similar expressions for the metric of a circularly polarized light beam are presented in [15].

6.1. Small distance between emitter and absorber of the laser beam

For small distances between emitter and absorber of the laser beam, we find directly equation (55), where $I^{(0)}$ has to be taken from equation (44). In figure 4, the function $I^{\lambda(1)}_{\xi}$ is illustrated as a function of ξ and ζ for $\chi = 1$. The plots for $I^{\lambda(1)}_{\chi}$ would look similar when plotted as a function of χ and ζ for $\xi = 1$.

6.2. Curvature

It was shown in [5] that the rotation of the null fluid leads to frame dragging. This has been shown to be the case as well in [34] for a laser beam of light with angular momentum. Here, we obtain the frame dragging effect in the curvature tensor components. The only non-zero components of first order (see equation (E.2)) are

$$\begin{aligned} r^{\lambda(1)}_{\bar{j}\zeta\bar{k}} &= -\frac{1}{2}\partial_{\bar{j}}\left(\partial_{\bar{j}} h^{\lambda(1)}_{\zeta\bar{k}} - \partial_{\bar{k}} h^{\lambda(1)}_{\zeta\bar{j}}\right), \\ r^{\lambda(1)}_{\bar{j}\tau\bar{k}} &= -\frac{1}{2}\partial_{\bar{j}}\left(\partial_{\bar{j}} h^{\lambda(1)}_{\tau\bar{k}} - \partial_{\bar{k}} h^{\lambda(1)}_{\tau\bar{j}}\right), \\ r^{\lambda(1)}_{\bar{j}\tau\zeta\tau} &= -\frac{1}{2}\partial_{\bar{j}}\partial_{\theta\zeta} h^{\lambda(0)}_{\tau\tau}, \end{aligned} \tag{56}$$

where $\bar{j} \neq \bar{k}$. For small $\theta\zeta$, we can neglect $r^{\lambda(1)}_{\bar{j}\tau\zeta\tau}$ and we find

$$r^{\lambda(1)}_{\xi\zeta\xi\chi} = -\lambda\frac{\kappa w_0^2}{2}\xi\mathcal{E}^{(0)} = -r^{\lambda(1)}_{\xi\tau\xi\chi} \quad \text{and} \quad r^{\lambda(1)}_{\chi\zeta\chi\xi} = \lambda\frac{\kappa w_0^2}{2}\chi\mathcal{E}^{(0)} = -r^{\lambda(1)}_{\chi\tau\chi\xi}. \tag{57}$$

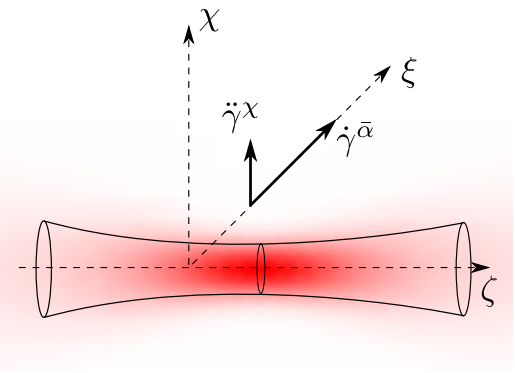

Figure 5. Schematic illustration of the frame dragging effect: a massive particle moving radially outwards from the beamline (here in ξ-direction) is accelerated in the transverse direction (here in χ-direction).

The non-zero curvature components $r^{\lambda(1)}_{\xi\tau\xi\chi}$ and $r^{\lambda(1)}_{\chi\tau\chi\xi}$ lead to the precession of gyroscopes, which can be seen most straight forward in the framework of gravitomagnetism [22]; they can be interpreted as gravitomagnetic fields that govern the motion of test particles in a gravitational Lorentz force law.

6.3. Deflection of test particles

The frame dragging effect can be studied alternatively using the geodesic equation (28) and the expressions for the Christoffel symbols in equation (E.1). Let us consider a test particle moving radially outwards with velocity v. We will only consider terms linear in v in the following. Then, the initial tangent $\dot{\gamma}(0) = cw_0^{-1}\big(1-f, v/c, 0, 0\big)$ to the test particle's world line $\gamma(\bar{\tau})$ at $\gamma(0) = (0, \xi, 0, 0)$ and $f(v, \xi, \chi, \theta\zeta)$ is chosen such that $\dot{\gamma}(\bar{\tau})$ fulfills the condition $g_{\bar{\mu}\bar{\nu}}(\gamma(\bar{\tau}))\dot{\gamma}^{\bar{\mu}}(\bar{\tau})\dot{\gamma}^{\bar{\nu}}(\bar{\tau}) = -c^2$ at $\bar{\tau} = 0$, where again $\bar{\tau}$ is the proper time and the dot represents the derivative with respect to it. In first order in the metric perturbation, we find that

$$\ddot{\gamma}^{\chi}(0) = \frac{cv}{w_0^4}\theta\left(\partial_{\chi}h^{(1)}_{\tau\xi} - \partial_{\xi}h^{(1)}_{\tau\chi}\right) = -\lambda v\,\theta\,\frac{\kappa P_0}{2\pi w_0^2}|\mu|^2 \mathrm{e}^{-2|\mu|^2\rho^2}. \tag{58}$$

We see that massive test particles do not propagate radially. Their trajectories are transversally bent, where the sign of the bending depends on the polarization of the laser beam. This is the effect of frame dragging. For $v \sim 10\mathrm{ms}^{-1}$, $P_0 \sim 10^{15}$ W, $\theta \sim 10^{-3}$, $w_0 \sim 10^{-3}$ m, $z = 0$ and $x = w_0$, the acceleration is of the order of magnitude $\mathrm{d}^2\gamma^y(0)/\mathrm{d}t^2 \sim \pm 10^{-29}$ ms^{-2}.

The effect in equation (58) decreases exponentially with the distance to the beamline. The same is true for the curvature components in equation (57). The effect is due to the spin angular momentum due to the helicity of the beam. In contrast, in [34], frame dragging effects for $\rho \gg 1$ have been shown to arise from the orbital angular momentum of optical vortices. In figure 5, the above deflection is illustrated. It is interesting to note that, by direct calculation from the expressions for the metric perturbation up to third order in θ in appendix F, we find for $\rho \gg 1$

$$R_{\bar{\alpha}\bar{\beta}\bar{\gamma}\bar{\delta}} \approx \left(1 + \frac{\theta^2}{2}\right) R^{(0)}_{\bar{\alpha}\bar{\beta}\bar{\gamma}\bar{\delta}}, \tag{59}$$

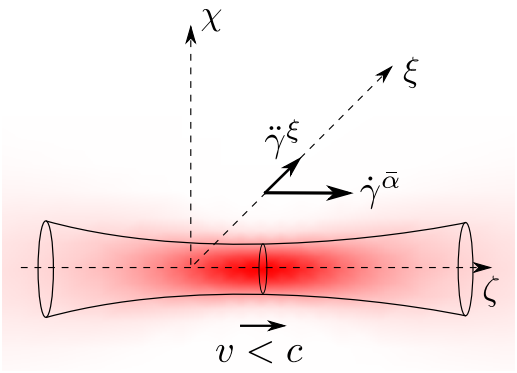

Figure 6. Schematic illustration of the source laser beam and the parallel co-propagating test ray of light: we look at the deflection of the test ray of light due to the gravitational field of the laser beam.

up to third order in θ. All other terms decay exponentially with ρ^2. Therefore, far away from the beam and up to third order in θ, there are no effects beyond those that already exist in zeroth order. All additional effects appear only where the energy distribution of the source beam is non-vanishing; they are effects of a local gravitational coupling between the source and test particles. In the next section, we will discuss another such effect in fourth order in θ, the deflection of parallel co-propagating test rays.

7. Fourth order—the deflection of parallel co-propagating test rays

As discussed in [36] for a finitely long and infinitely thin light beam, a test ray propagating parallel to it is not deflected. It has also been shown [4] that the superposition of two exact solutions of the Einstein equations for pp-waves travelling in the same direction is again a solution, confirming the result of the linearized theory. In our description, there are two more important characteristics of the laser beam playing an important role, both of them coming from the wave-like nature of light: first, the laser beam is diverging. Second, in [14], it was argued that light in a laser beam does not move with the speed of light along the beamline, but with a slightly smaller velocity. The origin of the effect is the superposition of plane waves with different wave vectors, which leads to a reduced effective propagation speed. This was confirmed experimentally in [11]. In [14], the difference between the speed of light and the group velocity of light in a laser beam was found to be[11] $\delta v_\theta = c - v_\theta = c/(k^2 w_0^2) = c\theta^2/4$. It has been shown by Scully that two parallel co-propagating thin beams in a wave-guide, since they are propagating slower than the speed of light, do gravitationally interact with each other [32]. Therefore one may wonder whether the source laser beam deflects an originally parallel co-propagating test ray. We will investigate this question in the following. The setup is illustrated in figure 6.

A parallel co-propagating test light ray is described by the light-like tangent vector $\dot{\gamma}^{\bar{\alpha}} = w_0^{-1} c(1, 0, 0, 1 - f)$, where f is determined by the null-condition and found to be of the same order of magnitude as the metric perturbation, and therefore does not contribute in the

[11] In [14], a different definition of the beam waist is used (see equation (28) of [14]) such that $w = w_0/\sqrt{2}$ in equation (40) of [14].

following, and again the curve is parametrized with proper time and the dot stands for the derivative with respect to it. With the geodesic equation, we obtain

$$\ddot{\gamma}^{\bar{j}}_{+} = -c^2 w_0^{-2} \left[\Gamma^{\bar{j}}_{\tau\tau} + 2\Gamma^{\bar{j}}_{\tau\zeta} + \Gamma^{\bar{j}}_{\zeta\zeta}\right] \tag{60}$$

$$= -c^2 w_0^{-4} \theta^4 \left[-\frac{1}{2}\partial_{\bar{j}} \left(h^{(4)}_{\tau\tau} + 2h^{(4)}_{\tau\zeta} + h^{(4)}_{\zeta\zeta}\right) + \partial_{\theta\zeta} \left(h^{(3)}_{\tau\bar{j}} + h^{(3)}_{\zeta\bar{j}}\right)\right]. \tag{61}$$

From the expression for the components of the energy–momentum tensor in appendix B and equation (35), we find

$$\Delta_{2\mathrm{d}} \left(h^{(4)}_{\tau\tau} + 2h^{(4)}_{\tau\zeta} + h^{(4)}_{\zeta\zeta}\right) = -\frac{\kappa w_0^2 P_0}{2\pi c} |\mu|^6 \rho^4 \mathrm{e}^{-2|\mu|^2\rho^2}, \tag{62}$$

which is solved by equation (36) as

$$h^{(4)}_{\tau\tau} + 2h^{(4)}_{\tau\zeta} + h^{(4)}_{\zeta\zeta} = \frac{\kappa w_0^2 P_0}{32\pi c} \left(\mathrm{Ei}\left(-2|\mu|^2\rho^2\right) - 2\log(\rho) - \left(\frac{3}{2} + |\mu|^2\rho^2\right) \mathrm{e}^{-2|\mu|^2\rho^2}\right). \tag{63}$$

The components of the metric perturbation in third order in θ which appear in the second term in equation (61) can be found in appendix F. We obtain for $\bar{j} \in \{\xi, \chi\}$, assuming that $\theta\zeta \ll 1$,

$$\ddot{\gamma}^{\bar{j}} = \frac{c\kappa P_0}{32\pi w_0^2} \theta^4 \frac{x^{\bar{j}}}{\rho^2} \left(1 - (1-\rho^4)\mathrm{e}^{-2\rho^2}\right). \tag{64}$$

For large distances from the beamline ($\rho \gg 1$) and $j \in \{x, y\}$, the acceleration becomes

$$\ddot{\gamma}^{\bar{j}} = \frac{c\kappa P_0}{32\pi w_0^2} \theta^4 \frac{x^{\bar{j}}}{\rho^2}, \tag{65}$$

which is an apparent repulsion. This is due to the second term in equation (61). If we had considered only the first term in equation (61), we would have obtained the same absolute acceleration as in equation (65), but with the opposite sign. Hence, the first term in equation (61) induces an attraction and the second term a repulsion.

However, coordinate acceleration does not have any physical meaning in general relativity. Therefore, we have to investigate the geodesic deviation to learn about the meaning of the coordinate acceleration (65). With the separation vector $s^{\bar{\alpha}} = (0, 1, 0, 0)$ and the tangent $\dot{\gamma}^{\bar{\alpha}} = w_0^{-1} c(1, 0, 0, 1-f)$, we obtain for the acceleration of the separation vector in ξ-direction from equation (30)

$$a^{\xi} = \frac{\theta^4 c^2}{2w_0^4} \left(\partial_\xi^2 \left(h^{(4)}_{\tau\tau} + 2h^{(4)}_{\tau\zeta} + h^{(4)}_{\zeta\zeta}\right) - 2\partial_\xi \partial_{\theta\zeta} \left(h^{(3)}_{\tau\xi} + h^{(3)}_{\xi\zeta}\right) + \partial^2_{\theta\zeta} h^{(2)}_{\xi\xi}\right). \tag{66}$$

With the expressions for the combinations of the metric perturbation given above and in appendix F, we obtain in the case of $\theta\zeta \ll 1$

$$a^{\xi} = -\frac{\kappa c P_0 \theta^4}{16\pi w_0^2} \mathrm{e}^{-2\rho^2} \left(\rho^2(4\xi^2 + 3) - 6\xi^2\right), \tag{67}$$

which vanishes far from the beamline. Therefore, we found that the deflection in equation (64) is a coordinate effect. More precisely, the geodesic deviation in equation (66) can be split into two parts. The first part is the ξ-derivative of the coordinate acceleration $\ddot{\gamma}^{\bar{j}}$ in equation (64). The second part is the second $\theta\zeta$-derivative of $h^{(2)}_{\zeta\zeta}$ which corresponds to the change of the

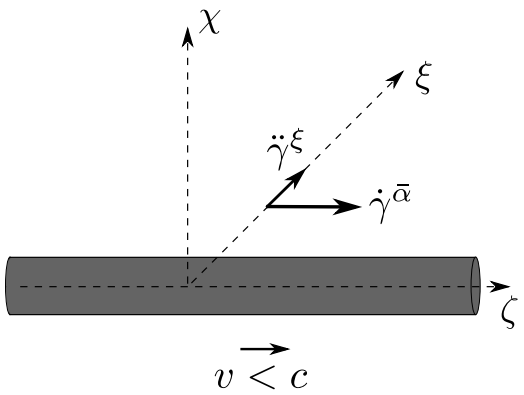

Figure 7. A massive cylinder moving at the speed $v < c$ and a parallel co-propagating test light beam: we investigate the gravitational deflection of the test beam due to the gravitational field of the cylinder.

definition of length in the ξ-direction. The contributions of the two parts to the geodesic deviation cancel for large distances from the beamline. As a numerical example, for $P_0 \sim 10^{15}$ W, $\theta \sim 10^{-3}$, $w_0 \sim 10^{-3}$ m, $x = w_0$ and $y = 0$, one has $a^x \sim -10^{-31}$ ms^{-2}. Notice that this is the relative acceleration of two test light rays. The interesting point is that it is non-zero.

7.1. Comparison to the boosted infinitely long massive cylinder

The reduced propagation speed argued for in [14] suggests that the result in equation (64) may be compared to the deflection of a parallel test ray by a cylindrically symmetric mass distribution moving with $v = c - \delta v_\theta$ along the cylinder axis (see figure 7). That is the content of this subsection.

The exterior gravitational field of a cylindrically symmetric mass distribution of rest of mass per unit length $\mathfrak{m}$ (dimensionless units) is described by the Levi-Civita metric [18],

$$\mathrm{d}s^2 = -\rho^{4\mathfrak{m}}c^2\mathrm{d}t^2 + \rho^{8\mathfrak{m}^2-4\mathfrak{m}}\left(\mathrm{d}\rho^2 + \mathrm{d}z^2\right) + P^2\rho^{2-4\mathfrak{m}}\mathrm{d}\phi^2, \tag{68}$$

in the cylindrical coordinates (ct, ρ, ϕ, z), where $\rho = \sqrt{x^2 + y^2}$ and we set $P = 1$. The parameter $\mathfrak{m}$ can be considered to be a dimensionless quantity representing the mass or energy per unit length for $0 < \mathfrak{m} < \frac{1}{2}$ [6]. Now, we let the cylinder move in positive ζ-direction with normalized velocity $\beta = v/c$, and thus make the coordinate transformation

$$\begin{aligned} ct &\to \gamma(ct - \beta z), \\ z &\to \gamma(z - \beta ct), \end{aligned} \tag{69}$$

where $\gamma = (1 - \beta^2)^{-1/2}$ and $\beta = v/c$. The line density of energy $\mathfrak{m}$ is a quotient of an energy scale $\mathcal{E}$ and a length scale L. The energy seen by an observer in the rest frame is $\mathcal{E}' = \gamma\mathcal{E}$. Due to Lorentz contraction, the length scale seen in the rest frame becomes $L' = L/\gamma$. Therefore, the line density of energy seen in the rest frame becomes $\mathfrak{m}' = \gamma^2\mathfrak{m}$. Then, the metric becomes

$$\begin{aligned} \mathrm{d}s^2 = {} & \gamma^2\left(-\rho^{4\gamma^{-2}\mathfrak{m}'} + \beta^2\rho^{8\gamma^{-4}\mathfrak{m}'^2-4\gamma^{-2}\mathfrak{m}'}\right)c^2\mathrm{d}t^2 - 2\gamma^2\beta\left(-\rho^{4\gamma^{-2}\mathfrak{m}'} + \rho^{8\gamma^{-4}\mathfrak{m}'^2-4\gamma^{-2}\mathfrak{m}'}\right)c\mathrm{d}t\mathrm{d}z \\ & + \gamma^2\left(-\beta^2\rho^{4\gamma^{-2}\mathfrak{m}'} + \rho^{8\gamma^{-4}\mathfrak{m}'^2-4\gamma^{-2}\mathfrak{m}'}\right)\mathrm{d}z^2 + \rho^{8\gamma^{-4}\mathfrak{m}'^2-4\gamma^{-2}\mathfrak{m}'}\mathrm{d}\rho^2 + P^2\rho^{2-4\gamma^{-2}\mathfrak{m}'}\mathrm{d}\phi^2. \end{aligned} \tag{70}$$

Transforming to cylindrical coordinates according to $\rho = \sqrt{x^2 + y^2}$ and $\mathrm{d}\rho = \frac{1}{\rho^2}(x\mathrm{d}x + y\mathrm{d}y)$, as well as $\mathrm{d}\phi = \frac{1}{\rho^2}(-y\mathrm{d}x + x\mathrm{d}y)$, and assuming $\gamma^{-2}\mathfrak{m}'$ to be small and expanding the terms $\rho^{\gamma^{-2}\mathfrak{m}'}$ as $\rho^{\mathfrak{m}} = 1 + \gamma^{-2}\mathfrak{m}'\log(\rho)$ and neglecting quadratic terms in $\gamma^{-2}\mathfrak{m}'$, we obtain

$$\begin{aligned}\mathrm{d}s^2 = &-\left(1 + (1+\beta^2)4\mathfrak{m}'\log(\rho)\right)c^2\mathrm{d}t^2 + 16\beta\mathfrak{m}\log(\rho)c\mathrm{d}t\mathrm{d}z + \left(1 - (1+\beta^2)4\mathfrak{m}'\log(\rho)\right)\mathrm{d}z^2 \\ &+ \left(1 - (1-\beta^2)4\mathfrak{m}'\log(\rho)\right)\left(\mathrm{d}x^2 + \mathrm{d}y^2\right). \end{aligned} \tag{71}$$

This metric can be decomposed into the Minkowski metric plus the small perturbation

$$h_{\alpha\beta} = -4\mathfrak{m}'\log(\rho)\begin{pmatrix} 1+\beta^2 & 0 & 0 & -2\beta \\ 0 & 1-\beta^2 & 0 & 0 \\ 0 & 0 & 1-\beta^2 & 0 \\ -2\beta & 0 & 0 & 1+\beta^2 \end{pmatrix}. \tag{72}$$

We can identify the line density of energy with that of a beam of light as $\mathfrak{m}'c^4/G = P_0/c$. Then, the metric $\eta_{\alpha\beta} + h_{\alpha\beta}$ coincides with the metric of an infinitely long beam of light with constant energy density $P_0/(\pi(w_0/2)^2 c)$ confined to a cross section of $\pi(w_0/2)^2$ for $\beta = 1$ given in [4], up to constants.

From the metric (72), we find that the parallel test ray with tangent $\dot{\gamma}^\mu = c(1,0,0,1)$ is deflected in x-direction according to

$$\ddot{\gamma}^x = -\frac{4GP_0}{c^3}\frac{x}{\sqrt{x^2+y^2}}(1-\beta)^2. \tag{73}$$

Assuming $1 - \beta = \delta v/c = \theta^2/4$, we find that the result in equation (73) differs from equation (65) by its sign and a factor 1/2. Considering the geodesic deviation with the separation vector $s^\alpha = (0,1,0,0)$, we obtain

$$a^x = \frac{1}{2}\partial_x^2\left(h_{tt} + 2h_{tz} + h_{zz}\right), \tag{74}$$

and, inserting the expressions for the metric,

$$a^x = \frac{4GP_0}{c^3}\frac{x^2 - y^2}{(x^2+y^2)^2}(1-\beta)^2. \tag{75}$$

In contrast, for the gravitational field of the focused laser beam, we did not find a deflection for large distances. From this result, we see that the gravitational field of light in a Gaussian beam does not simply behave as massive matter moving with the velocity derived in [14] along the beamline. The reason is that the divergence of the laser beam does not only lead to a reduced group velocity, but also to a change of the metric along the beamline. This leads to the appearance of the second and third term in equation (66), which cancel the effect of the first term for large distances from the beamline. In particular, we mentioned above that the first term in equation (61) induces an attraction with the same absolute value as the acceleration in equation (64). Accordingly, if we had considered the first term in equation (61) only, we would have obtained an expression that would coincide with that for the geodesic deviation induced by the boosted rod given in equation (75) up to a factor 2. Therefore, we can conclude that the additional effects due to the divergence of the light beam cancel the attraction due to the reduced propagation speed of the light in the beam.

8. Conclusion

We analyzed the gravitational field of a focused laser beam, describing the laser beam as a solution to Maxwell's equations. We calculated the five leading orders of the metric perturbation expanded in the divergence angle θ of the beam explicitly and discussed the difference to the solutions when the laser beam is treated in the paraxial approximation. Already in the paraxial approximation, the gravitational field of a laser beam turns out to be too small to be detected with current technology [26]. This is also the case for the effects we describe. However, they are of conceptual interest as they reveal the gravitational properties of light, and with the progress of technology, they may possibly be measurable in future experiments.

For small values of the beam waist and for $\theta = 0$, which corresponds to the paraxial approximation in our case, our solution for the laser beam corresponds to the solution for the infinitely thin beam [36]. If in addition we consider the laser beam to be infinitely long, we recover the solution for an infinitely long cylinder [4].

In first order in the divergence angle, we found frame dragging due to spin angular momentum of the circular polarized laser beam. This is similar to the result of [34] for beams with orbital angular momentum. In contrast to frame dragging induced by orbital angular momentum, the effect we find decays exponentially with the distance squared from the beamline divided by the beam waist parameter w_0. This property coincides with the decay of the energy density of the beam. Hence, frame dragging due to the spin angular momentum of the beam is proportional to the local energy density of the beam. During the peer reviewing process for the publication of this article, the article [35] by Strohaber appeared on the Arxiv preprint server. In the article, frame dragging due to intrinsic angular momentum including spin of light beams is derived and discussed.

The statement of [36] by Tolman *et al* that a non-divergent light beam does not deflect gravitationally a co-directed parallel light beam has been recovered in different contexts: two co-directed parallel cylindrical light beams of finite radius [3, 4, 24], spinning non-divergent light beams [23], non-divergent light beams in the framework of gravito-electrodynamics [13], parallel co-propagating light-like test particles in the gravitational field of a 1D light pulse [26]. In fourth order in the divergence angle, we found a deflection of parallel co-propagating test beams. This shows that the result of [36] and [4] only holds up to the third order in the divergence angle. This could have been expected from the fact that the group velocity of light in a Gaussian beam along the beamline is not the speed of light [11, 14]. However, the deflection of parallel co-propagating light beams by light in a focused source laser beam decays like the distribution of energy of the source beam with the distance from the beamline. This means that the effect does not persist outside of the distribution of energy given by the source laser beam like the frame dragging effect due to spin angular momentum. This is in contrast to the deflection that one obtains from a rod of matter boosted to a speed close to the speed of light. Therefore, we conclude that focused light does not simply behave like massive matter moving with the reduced velocity identified in [26, 34]. This is due to the divergence of the laser beam along the beamline which leads to additional contributions to the metric perturbations which do not appear in the case of the boosted rod. These additional contributions cancel the effect induced by the reduced propagation speed of light in the focused beam.

9. Outlook

As an extension of the research presented in this article, it would be interesting to study the gravitational interaction of two parallel co-propagating focused laser beams in the description

presented here. The result could be compared to the corresponding results presented in [3, 4, 24]. In particular, it would be interesting to see if there exists a contribution to the gravitational interaction of the two beams that does not decay exponentially with the square of the distance between the beamlines of the beams.

It would be interesting to know if the solutions to Maxwell's equations developed in this article can be used as a basis for a quantum field theoretical description of the gravitational interaction of two laser beams in the framework of perturbative quantum gravity (PQG). Then, the effect of localization on light-light interactions could be considered for light with quantum properties. For example, in [25, 27] it is shown that the differential cross section for gravitational photon scattering can be amplified or suppressed when the scattering photons are in specific polarization entangled states initially. It would be interesting to see how this effect depends on the distance between the beams. Furthermore, in [7], the effect of entanglement in the position of a source of a gravitational field was investigated in the framework of semiclassical gravity. Similar questions could be considered in the framework of PQG using focused laser beams in spatial superposition states or with squeezed light as sources.

Another step from the results presented in this article into a different direction could be the consideration of a pulse of light in a focused laser mode. The framework used in this article would need to be extended to envelope functions that depend on time and the position along the beamline. Approaches for the description of such beams are given for example in [2, 19, 31, 39]. An expression for the gravitational field of a focused laser pulse could be used to have a closer look at the implications of focusing for possible experiments trying to detect the gravitational field of light. In particular, the pulsed beams would produce a pulsed gravitational signal that could be detected with resonator systems like small scale gravitational wave detectors (for example [16, 29, 33]) or quantum optomechanical systems.

The gravitational field of a focused laser pulse could be used as well to check the results of [26] where the laser pulse is modeled as a 1D rod of light with an energy density that is modulated as that of a plane wave. In particular, for the model used in [26], all gravitational effects are induced by the emission and the absorption of the light pulse alone; there is no gravitational effect related to the propagation of the pulse. This situation may change once divergence of the beam is taken into account.

It could be worthwhile to see whether a similar solution for the gravitational field of a focused laser beam as we derived in this article could be derived considering the full coupled set of the Einstein–Maxwell equations. The resulting metric could be compared to the one in [20] and it could be investigated if the results of [20] about the effective gravitating mass and angular momentum can be reproduced when divergence of the beam is taken into account. It would also be interesting to consider the gravitational field of the electromagnetic field distribution used in this article to model a focused laser beam in dynamical spacetime theories with spacetime torsion like Einstein–Cartan-theory and the Poincaré-gauge-theory of gravity [17]. In particular, we found that frame dragging due to the spin angular momentum of light is proportional to the local energy density of the beam. This is similar to the effect of spin angular momentum on test particles or fields via spacetime torsion as torsion is not a propagating degree of freedom in Einstein–Cartan-theory and Poincaré-gauge-theory.

Acknowledgments

We would like to thank Robert Beig, Piotr T Chruściel, Peter C Aichelburg, David M Fajman, Julien Fraïsse, Lars Andersson, Jirí Bičák, Marius Oancea, Ralf Menzel and Martin Wilkens for interesting discussions and useful remarks. DR thanks the Humboldt foundation for its support.

Appendix A. Vector potential of a circularly polarized laser beam

From the expansion of the field strength $F^{\lambda}_{\bar{\alpha}\bar{\beta}} = \sum_{n=0}^{\infty} \theta^n \frac{w_0 E_0}{\sqrt{2}} f^{\lambda(n)}_{\bar{\alpha}\bar{\beta}}(\xi,\chi,\theta\zeta) \mathrm{e}^{\mathrm{i}\frac{2}{\theta}(\zeta-\tau)}$, where $E_0 = \sqrt{2}\mathcal{A}/w_0\theta$, and the Lorenz gauge condition

$$A_\tau = \frac{\mathrm{i}\theta}{2}\partial_\tau A_\tau = \frac{\mathrm{i}\theta}{2}\left(\partial_\xi A_\xi + \partial_\chi A_\chi + \theta\partial_{\theta\zeta} A_\zeta\right), \tag{A.1}$$

we obtain a direct relation between $v^{\lambda(n)}_{\bar{\alpha}}$ and $f^{\lambda(n)}_{\bar{\alpha}\bar{\beta}}$ (where λ refers to the polarization state) as

$$\begin{aligned} f^{\lambda(n)}_{0\zeta} &= \partial_\xi v^{\lambda(n-1)}_\xi + \partial_\chi v^{\lambda(n-1)}_\chi + 2\partial_{\theta\zeta} v^{\lambda(n-2)}_\zeta \\ &\quad - \frac{\mathrm{i}}{2}\partial_{\theta\zeta}\left(\partial_\xi v^{\lambda(n-3)}_\xi + \partial_\chi v^{\lambda(n-3)}_\chi + \partial_{\theta\zeta} v^{\lambda(n-4)}_\zeta\right), \end{aligned} \tag{A.2}$$

$$f^{\lambda(n)}_{0\bar{j}} = -2\mathrm{i} v^{\lambda(n)}_{\bar{j}} + \partial_{\bar{j}} v^{(n-1)}_\zeta - \frac{\mathrm{i}}{2}\partial_{\bar{j}}\left(\partial_\xi v^{\lambda(n-2)}_\xi + \partial_\chi v^{\lambda(n-2)}_\chi + \partial_{\theta\zeta} v^{\lambda(n-3)}_\zeta\right), \tag{A.3}$$

$$f^{\lambda(n)}_{\bar{j}\zeta} = -2\mathrm{i} v^{\lambda(n)}_{\bar{j}} + \partial_{\bar{j}} v^{\lambda(n-1)}_\zeta - \partial_{\theta\zeta} v^{\lambda(n-2)}_{\bar{j}}, \tag{A.4}$$

$$f^{\lambda(n)}_{\xi\chi} = \partial_\xi v^{\lambda(n-1)}_\chi - \partial_\chi v^{\lambda(n-1)}_\xi. \tag{A.5}$$

Since the vector potential fulfills the wave equation (1), we have that $\Box F_{\bar{\alpha}\bar{\beta}} = 0$. In particular,

$$\left(\partial^2_\xi + \partial^2_\chi + 4\mathrm{i}\partial_{\theta\zeta}\right) f^{(0)}_{\bar{\alpha}\bar{\beta}}(\xi,\chi,\theta\zeta) = 0, \tag{A.6}$$

$$\left(\partial^2_\xi + \partial^2_\chi + 4\mathrm{i}\partial_{\theta\zeta}\right) f^{(1)}_{\bar{\alpha}\bar{\beta}}(\xi,\chi,\theta\zeta) = 0, \tag{A.7}$$

$$\left(\partial^2_\xi + \partial^2_\chi + 4\mathrm{i}\partial_{\theta\zeta}\right) f^{(n)}_{\bar{\alpha}\bar{\beta}}(\xi,\chi,\theta\zeta) = -\partial^2_{\theta\zeta} f^{(n-2)}_{\bar{\alpha}\bar{\beta}}(\xi,\chi,\theta\zeta), \text{ for } n > 1. \tag{A.8}$$

The components of the Hodge dual of the field strength tensor are given as

$$\star f^{\lambda(n)}_{0\zeta} = -f^{\lambda(n)}_{\xi\chi} \quad , \quad \star f^{\lambda(n)}_{0\xi} = -f^{\lambda(n)}_{\chi\zeta} \quad , \quad \star f^{\lambda(n)}_{0\chi} = f^{\lambda(n)}_{\xi\zeta}, \tag{A.9}$$

$$\star f^{\lambda(n)}_{\xi\zeta} = -f^{\lambda(n)}_{0\chi} \quad , \quad \star f^{\lambda(n)}_{\chi\zeta} = f^{\lambda(n)}_{0\xi} \quad \text{and} \quad \star f^{\lambda(n)}_{\xi\chi} = f^{\lambda(n)}_{0\zeta}, \tag{A.10}$$

and we obtain that a helicity eigenstate has to fulfill the conditions

$$\begin{aligned} 0 &= f^{\lambda(n)}_{0\zeta} + \mathrm{i}\lambda \star f^{\lambda(n)}_{0\zeta} = f^{\lambda(n)}_{0\zeta} - \mathrm{i}\lambda f^{\lambda(n)}_{\xi\chi} \\ &= -\mathrm{i}\lambda\left(\partial_\xi v^{\lambda(n-1)}_\chi - \partial_\chi v^{\lambda(n-1)}_\xi\right) + \partial_\xi v^{\lambda(n-1)}_\xi + \partial_\chi v^{\lambda(n-1)}_\chi + 2\partial_{\theta\zeta} v^{\lambda(n-2)}_\zeta \\ &\quad - \frac{\mathrm{i}}{2}\partial_{\theta\zeta}\left(\partial_\xi v^{\lambda(n-3)}_\xi + \partial_\chi v^{\lambda(n-3)}_\chi + \partial_{\theta\zeta} v^{\lambda(n-4)}_\zeta\right), \end{aligned} \tag{A.11}$$

$$\begin{aligned} 0 &= f^{\lambda(n)}_{0\xi} + \mathrm{i}\lambda \star f^{\lambda(n)}_{0\xi} = f^{\lambda(n)}_{0\xi} - \mathrm{i}\lambda f^{\lambda(n)}_{\chi\zeta} \\ &= -2\mathrm{i} v^{\lambda(n)}_\xi + \partial_\xi v^{(n-1)}_\zeta - \frac{\mathrm{i}}{2}\partial_\xi\left(\partial_\xi v^{\lambda(n-2)}_\xi + \partial_\chi v^{\lambda(n-2)}_\chi + \partial_{\theta\zeta} v^{\lambda(n-3)}_\zeta\right) \\ &\quad - \mathrm{i}\lambda\left(-2\mathrm{i} v^{\lambda(n)}_\chi + \partial_\chi v^{\lambda(n-1)}_\zeta - \partial_{\theta\zeta} v^{\lambda(n-2)}_\chi\right), \end{aligned} \tag{A.12}$$

$$
\begin{aligned}
0 &= f_{0\chi}^{\lambda(n)} + \mathrm{i}\lambda \star f_{0\chi}^{\lambda(n)} = f_{0\chi}^{\lambda(n)} + \mathrm{i}\lambda f_{\xi\zeta}^{\lambda(n)} \\
&= -2\mathrm{i}v_{\chi}^{\lambda(n)} + \partial_{\chi} v_{\zeta}^{(n-1)} - \frac{\mathrm{i}}{2}\partial_{\chi}\left(\partial_{\xi} v_{\xi}^{\lambda(n-2)} + \partial_{\chi} v_{\chi}^{\lambda(n-2)} + \partial_{\theta\zeta} v_{\zeta}^{\lambda(n-3)}\right) \\
&\quad + \mathrm{i}\lambda\left(-2\mathrm{i}v_{\xi}^{\lambda(n)} + \partial_{\xi} v_{\zeta}^{\lambda(n-1)} - \partial_{\theta\zeta} v_{\xi}^{\lambda(n-2)}\right),
\end{aligned} \tag{A.13}
$$

$$
0 = f_{\xi\zeta}^{\lambda(n)} + \mathrm{i}\lambda \star f_{\xi\zeta}^{\lambda(n)} = f_{\xi\zeta}^{\lambda(n)} - \mathrm{i}\lambda f_{0\chi}^{\lambda(n)} = -\mathrm{i}\lambda\left(f_{0\chi}^{\lambda(n)} + \mathrm{i}\lambda f_{\xi\zeta}^{\lambda(n)}\right), \tag{A.14}
$$

$$
0 = f_{\chi\zeta}^{\lambda(n)} + \mathrm{i}\lambda \star f_{\chi\zeta}^{\lambda(n)} = f_{\xi\zeta}^{\lambda(n)} + \mathrm{i}\lambda f_{0\xi}^{\lambda(n)} = \mathrm{i}\lambda\left(f_{0\xi}^{\lambda(n)} - \mathrm{i}\lambda f_{\chi\zeta}^{\lambda(n)}\right), \tag{A.15}
$$

$$
0 = f_{\xi\chi}^{\lambda(n)} + \mathrm{i}\lambda \star f_{\xi\chi}^{\lambda(n)} = f_{\xi\chi}^{\lambda(n)} + \mathrm{i}\lambda f_{0\zeta}^{\lambda(n)} = \mathrm{i}\lambda\left(f_{0\zeta}^{\lambda(n)} - \mathrm{i}\lambda f_{\xi\chi}^{\lambda(n)}\right), \tag{A.16}
$$

where the last three conditions are fulfilled if the first three conditions are fulfilled. The remaining conditions can be rewritten as

$$
\begin{aligned}
0 &= (\partial_{\xi} + \mathrm{i}\lambda\partial_{\chi})\left(v_{\xi}^{\lambda(n-1)} - \mathrm{i}\lambda v_{\chi}^{\lambda(n-1)}\right) + 2\partial_{\theta\zeta} v_{\zeta}^{\lambda(n-2)} \\
&\quad - \frac{\mathrm{i}}{2}\partial_{\theta\zeta}\left(\partial_{\xi} v_{\xi}^{\lambda(n-3)} + \partial_{\chi} v_{\chi}^{\lambda(n-3)} + \partial_{\theta\zeta} v_{\zeta}^{\lambda(n-4)}\right),
\end{aligned} \tag{A.17}
$$

$$
\begin{aligned}
0 &= -2\mathrm{i}\left(v_{\xi}^{\lambda(n)} - \mathrm{i}\lambda v_{\chi}^{\lambda(n)}\right) + (\partial_{\xi} - \mathrm{i}\lambda\partial_{\chi}) v_{\zeta}^{(n-1)} \\
&\quad - \frac{\mathrm{i}}{2}\partial_{\xi}\left(\partial_{\xi} v_{\xi}^{\lambda(n-2)} + \partial_{\chi} v_{\chi}^{\lambda(n-2)}\right) + \mathrm{i}\lambda\partial_{\theta\zeta} v_{\chi}^{\lambda(n-2)} - \frac{\mathrm{i}}{2}\partial_{\xi}\partial_{\theta\zeta} v_{\zeta}^{\lambda(n-3)},
\end{aligned} \tag{A.18}
$$

$$
\begin{aligned}
0 &= -2\mathrm{i}\left(v_{\xi}^{\lambda(n)} - \mathrm{i}\lambda v_{\chi}^{\lambda(n)}\right) + (\partial_{\xi} - \mathrm{i}\lambda\partial_{\chi}) v_{\zeta}^{(n-1)} \\
&\quad - \frac{\lambda}{2}\partial_{\chi}\left(\partial_{\xi} v_{\xi}^{\lambda(n-2)} + \partial_{\chi} v_{\chi}^{\lambda(n-2)}\right) - \partial_{\theta\zeta} v_{\xi}^{\lambda(n-2)} - \frac{\lambda}{2}\partial_{\chi}\partial_{\theta\zeta} v_{\zeta}^{\lambda(n-3)}.
\end{aligned} \tag{A.19}
$$

The sum and the difference of equations (A.18) and (A.19) lead to

$$
\begin{aligned}
0 &= -4\mathrm{i}\left(v_{\xi}^{\lambda(n)} - \mathrm{i}\lambda v_{\chi}^{\lambda(n)}\right) + 2(\partial_{\xi} - \mathrm{i}\lambda\partial_{\chi}) v_{\zeta}^{(n-1)} - \frac{\mathrm{i}}{2}(\partial_{\xi} - \mathrm{i}\lambda\partial_{\chi})\left(\partial_{\xi} v_{\xi}^{\lambda(n-2)} + \partial_{\chi} v_{\chi}^{\lambda(n-2)}\right) \\
&\quad - \partial_{\theta\zeta}\left(v_{\xi}^{\lambda(n-2)} - \mathrm{i}\lambda v_{\chi}^{\lambda(n-2)}\right) - \frac{\mathrm{i}}{2}(\partial_{\xi} - \mathrm{i}\lambda\partial_{\chi})\partial_{\theta\zeta} v_{\zeta}^{\lambda(n-3)},
\end{aligned} \tag{A.20}
$$

and

$$
\begin{aligned}
0 &= -\frac{\mathrm{i}}{2}(\partial_{\xi} + \mathrm{i}\lambda\partial_{\chi})\left(\partial_{\xi} v_{\xi}^{\lambda(n-2)} + \partial_{\chi} v_{\chi}^{\lambda(n-2)}\right) + \partial_{\theta\zeta}\left(v_{\xi}^{\lambda(n-2)} + \mathrm{i}\lambda v_{\chi}^{\lambda(n-2)}\right) \\
&\quad - \frac{\mathrm{i}}{2}(\partial_{\xi} + \mathrm{i}\lambda\partial_{\chi})\partial_{\theta\zeta} v_{\zeta}^{\lambda(n-3)} \\
&= -\frac{\mathrm{i}}{2}(\partial_{\xi} + \mathrm{i}\lambda\partial_{\chi})\left(\partial_{\xi} v_{\xi}^{\lambda(n-2)} + \partial_{\chi} v_{\chi}^{\lambda(n-2)}\right) + \frac{\mathrm{i}}{4}\left(\partial_{\xi}^2 + \partial_{\chi}^2\right)\left(v_{\xi}^{\lambda(n-2)} + \mathrm{i}\lambda v_{\chi}^{\lambda(n-2)}\right) \\
&\quad + \frac{\mathrm{i}}{4}\partial_{\theta\zeta}^2\left(v_{\xi}^{\lambda(n-4)} + \mathrm{i}\lambda v_{\chi}^{\lambda(n-4)}\right) - \frac{\mathrm{i}}{2}(\partial_{\xi} + \mathrm{i}\lambda\partial_{\chi})\partial_{\theta\zeta} v_{\zeta}^{\lambda(n-3)} \\
&= -\frac{\mathrm{i}}{4}(\partial_{\xi} + \mathrm{i}\lambda\partial_{\chi})^2\left(v_{\xi}^{\lambda(n-2)} - \mathrm{i}\lambda v_{\chi}^{\lambda(n-2)}\right) \\
&\quad - \frac{\mathrm{i}}{2}(\partial_{\xi} + \mathrm{i}\lambda\partial_{\chi})\partial_{\theta\zeta} v_{\zeta}^{\lambda(n-3)} + \frac{\mathrm{i}}{4}\partial_{\theta\zeta}^2\left(v_{\xi}^{\lambda(n-4)} + \mathrm{i}\lambda v_{\chi}^{\lambda(n-4)}\right),
\end{aligned} \tag{A.21}
$$

respectively. For the leading/zeroth order envelope function, we find from equation (A.20) that $v_\xi^{\lambda(0)} = \mathrm{i}\lambda v_\chi^{\lambda(0)}$. For the first order envelope function, we obtain from equation (A.17) the condition

$$0 = (\partial_\xi + \mathrm{i}\lambda\partial_\chi)\left(v_\xi^{\lambda(0)} - \mathrm{i}\lambda v_\chi^{\lambda(0)}\right),$$

which is fulfilled for $v_\xi^{\lambda(0)} = \mathrm{i}\lambda v_\chi^{\lambda(0)}$. Furthermore from equation (A.20), we find the condition

$$0 = -2\mathrm{i}\left(v_\xi^{\lambda(1)} - \mathrm{i}\lambda v_\chi^{\lambda(1)}\right) + (\partial_\xi - \mathrm{i}\lambda\partial_\chi)\, v_\zeta^{(0)}. \tag{A.22}$$

For the second order, we obtain from equation (A.17)

$$\begin{aligned} 0 &= (\partial_\xi + \mathrm{i}\lambda\partial_\chi)\left(v_\xi^{\lambda(1)} - \mathrm{i}\lambda v_\chi^{\lambda(1)}\right) + 2\partial_{\theta\zeta} v_\zeta^{\lambda(0)} \\ &= -\frac{\mathrm{i}}{2}\Delta_{2\mathrm{d}} v_\zeta^{\lambda(0)} + 2\partial_{\theta\zeta} v_\zeta^{\lambda(0)}, \end{aligned}$$

which is always fulfilled since $v_\zeta^{\lambda(0)}$ fulfills equation (6). Additionally from equation (A.20) and with $v_\xi^{\lambda(0)} = \mathrm{i}\lambda v_\chi^{\lambda(0)}$, we find the condition

$$\begin{aligned} 0 &= -2\mathrm{i}\left(v_\xi^{\lambda(2)} - \mathrm{i}\lambda v_\chi^{\lambda(2)}\right) + (\partial_\xi - \mathrm{i}\lambda\partial_\chi)\, v_\zeta^{(1)} - \frac{\mathrm{i}}{4}(\partial_\xi - \mathrm{i}\lambda\partial_\chi)(\mathrm{i}\lambda\partial_\xi + \partial_\chi)\, v_\chi^{\lambda(0)} \\ &= -2\mathrm{i}\left(v_\xi^{\lambda(2)} - \mathrm{i}\lambda v_\chi^{\lambda(2)}\right) + (\partial_\xi - \mathrm{i}\lambda\partial_\chi)\, v_\zeta^{(1)} + \frac{\lambda}{4}(\partial_\xi - \mathrm{i}\lambda\partial_\chi)^2 v_\chi^{\lambda(0)}. \end{aligned} \tag{A.23}$$

Assuming $v_\xi^{\lambda(2)} = \mathrm{i}\lambda v_\chi^{\lambda(2)}$, we find that the first term in the condition vanishes and we can solve for $v_\zeta^{(1)}$ as

$$v_\zeta^{(1)} = -\frac{\lambda}{4}(\partial_\xi - \mathrm{i}\lambda\partial_\chi)\, v_\chi^{\lambda(0)}. \tag{A.24}$$

The condition in equation (A.21) is automatically fulfilled in second order due to $v_\xi^{\lambda(2)} = \mathrm{i}\lambda v_\chi^{\lambda(2)}$. For the third order, we find from equation (A.17)

$$0 = \partial_{\theta\zeta} v_\zeta^{\lambda(1)} + \frac{\lambda}{4}\partial_{\theta\zeta}(\partial_\xi - \mathrm{i}\lambda\partial_\chi)\, v_\chi^{\lambda(0)}, \tag{A.25}$$

which is just the $\theta\zeta$-derivative of equation (A.24). From equation (A.20) follows that

$$\begin{aligned} 0 &= -4\mathrm{i}\left(v_\xi^{\lambda(3)} - \mathrm{i}\lambda v_\chi^{\lambda(3)}\right) + 2(\partial_\xi - \mathrm{i}\lambda\partial_\chi)\, v_\zeta^{(2)} - \frac{\mathrm{i}}{2}(\partial_\xi - \mathrm{i}\lambda\partial_\chi)\left(\partial_\xi v_\xi^{\lambda(1)} + \partial_\chi v_\chi^{\lambda(1)}\right) \\ &\quad - \partial_{\theta\zeta}\left(v_\xi^{\lambda(1)} - \mathrm{i}\lambda v_\chi^{\lambda(1)}\right) - \frac{\mathrm{i}}{2}(\partial_\xi - \mathrm{i}\lambda\partial_\chi)\,\partial_{\theta\zeta} v_\zeta^{\lambda(0)}, \\ &= -4\mathrm{i}\left(v_\xi^{\lambda(3)} - \mathrm{i}\lambda v_\chi^{\lambda(3)}\right) + 2(\partial_\xi - \mathrm{i}\lambda\partial_\chi)\, v_\zeta^{(2)} - \frac{\mathrm{i}}{2}(\partial_\xi - \mathrm{i}\lambda\partial_\chi)\left(\partial_\xi v_\xi^{\lambda(1)} + \partial_\chi v_\chi^{\lambda(1)}\right), \end{aligned} \tag{A.26}$$

where we used equation (A.22). The last condition of third order comes from equation (A.21) as

$$\begin{aligned} 0 &= -\frac{\mathrm{i}}{4}(\partial_\xi + \mathrm{i}\lambda\partial_\chi)^2\left(v_\xi^{\lambda(1)} - \mathrm{i}\lambda v_\chi^{\lambda(1)}\right) - \frac{\mathrm{i}}{2}(\partial_\xi + \mathrm{i}\lambda\partial_\chi)\,\partial_{\theta\zeta} v_\zeta^{\lambda(0)} \\ &= -\frac{1}{8}(\partial_\xi + \mathrm{i}\lambda\partial_\chi)\,\Delta_{2\mathrm{d}} v_\zeta^{\lambda(0)} - \frac{\mathrm{i}}{2}(\partial_\xi + \mathrm{i}\lambda\partial_\chi)\,\partial_{\theta\zeta} v_\zeta^{\lambda(0)}, \end{aligned} \tag{A.27}$$

which is fulfilled since equation (9) has to hold. In fourth order, we find from (A.17)

$$\begin{aligned}0 =& \left(\partial_\xi + \mathrm{i}\lambda\partial_\chi\right)\left(v_\xi^{\lambda(3)} - \mathrm{i}\lambda v_\chi^{\lambda(3)}\right) + 2\partial_{\theta\zeta}v_\zeta^{\lambda(2)} \\ &- \frac{\mathrm{i}}{2}\partial_{\theta\zeta}\left(\partial_\xi v_\xi^{\lambda(1)} + \partial_\chi v_\chi^{\lambda(1)} + \partial_{\theta\zeta}v_\zeta^{\lambda(0)}\right) \\ =& -\Delta_{2\mathrm{d}}\left(\frac{\mathrm{i}}{2}v_\zeta^{(2)} + \frac{1}{8}\left(\partial_\xi v_\xi^{\lambda(1)} + \partial_\chi v_\chi^{\lambda(1)}\right)\right) + 2\partial_{\theta\zeta}v_\zeta^{\lambda(2)} \\ &- \frac{\mathrm{i}}{2}\partial_{\theta\zeta}\left(\partial_\xi v_\xi^{\lambda(1)} + \partial_\chi v_\chi^{\lambda(1)} + \partial_{\theta\zeta}v_\zeta^{\lambda(0)}\right) \\ =& -\frac{\mathrm{i}}{2}\left(\Delta_{2\mathrm{d}}v_\zeta^{(2)} + 4\mathrm{i}\partial_{\theta\zeta}v_\zeta^{\lambda(2)} + \partial_{\theta\zeta}^2 v_\zeta^{\lambda(0)}\right) \\ &- \frac{1}{8}\left(\Delta_{2\mathrm{d}}\left(\partial_\xi v_\xi^{\lambda(1)} + \partial_\chi v_\chi^{\lambda(1)}\right) + 4\mathrm{i}\partial_{\theta\zeta}\left(\partial_\xi v_\xi^{\lambda(1)} + \partial_\chi v_\chi^{\lambda(1)}\right)\right), \end{aligned} \tag{A.28}$$

which is satisfied due to equations (7) and (8). From equation (A.20), we obtain in fourth order

$$\begin{aligned}0 =& -4\mathrm{i}\left(v_\xi^{\lambda(4)} - \mathrm{i}\lambda v_\chi^{\lambda(4)}\right) + 2\left(\partial_\xi - \mathrm{i}\lambda\partial_\chi\right)v_\zeta^{(3)} - \frac{\mathrm{i}}{2}\left(\partial_\xi - \mathrm{i}\lambda\partial_\chi\right)\left(\partial_\xi v_\xi^{\lambda(2)} + \partial_\chi v_\chi^{\lambda(2)}\right) \\ &- \partial_{\theta\zeta}\left(v_\xi^{\lambda(2)} - \mathrm{i}\lambda v_\chi^{\lambda(2)}\right) - \frac{\mathrm{i}}{2}\left(\partial_\xi - \mathrm{i}\lambda\partial_\chi\right)\partial_{\theta\zeta}v_\zeta^{\lambda(1)}. \end{aligned} \tag{A.29}$$

Assuming $v_\xi^{\lambda(4)} = \mathrm{i}\lambda v_\chi^{\lambda(4)}$ and taking into account $v_\xi^{\lambda(2)} = \mathrm{i}\lambda v_\chi^{\lambda(2)}$, which we assumed before, we obtain

$$0 = 2\left(\partial_\xi - \mathrm{i}\lambda\partial_\chi\right)v_\zeta^{(3)} - \frac{\mathrm{i}}{2}\left(\partial_\xi - \mathrm{i}\lambda\partial_\chi\right)\left(\partial_\xi v_\xi^{\lambda(2)} + \partial_\chi v_\chi^{\lambda(2)}\right) - \frac{\mathrm{i}}{2}\left(\partial_\xi - \mathrm{i}\lambda\partial_\chi\right)\partial_{\theta\zeta}v_\zeta^{\lambda(1)}. \tag{A.30}$$

With equation (A.24), we obtain that

$$v_\zeta^{(3)} = -\frac{\lambda}{4}\left(\partial_\xi - \mathrm{i}\lambda\partial_\chi\right)\left(v_\chi^{\lambda(2)} + \frac{\mathrm{i}}{4}\partial_{\theta\zeta}v_\chi^{\lambda(0)}\right). \tag{A.31}$$

Again with equation (A.24), we can check that the higher order Helmholtz equation (8) is fulfilled by $v_\zeta^{(3)}$ given in (A.31). The last condition that we have to check is the fourth order condition in equation (A.21), which becomes

$$\begin{aligned}0 =& -\frac{\mathrm{i}}{4}\left(\partial_\xi + \mathrm{i}\lambda\partial_\chi\right)^2\left(v_\xi^{\lambda(2)} - \mathrm{i}\lambda v_\chi^{\lambda(2)}\right) \\ &- \frac{\mathrm{i}}{2}\left(\partial_\xi + \mathrm{i}\lambda\partial_\chi\right)\partial_{\theta\zeta}v_\zeta^{\lambda(1)} + \frac{\mathrm{i}}{4}\partial_{\theta\zeta}^2\left(v_\xi^{\lambda(0)} + \mathrm{i}\lambda v_\chi^{\lambda(0)}\right), \end{aligned} \tag{A.32}$$

which may be written as, using $v_\xi^{\lambda(2)} = \mathrm{i}\lambda v_\chi^{\lambda(2)}$ and $v_\xi^{\lambda(0)} = \mathrm{i}\lambda v_\chi^{\lambda(0)}$,

$$0 = -\frac{\mathrm{i}}{2}\left(\partial_\xi + \mathrm{i}\lambda\partial_\chi\right)\partial_{\theta\zeta}v_\zeta^{\lambda(1)} - \frac{\lambda}{2}\partial_{\theta\zeta}^2 v_\chi^{\lambda(0)}, \tag{A.33}$$

and is fulfilled due to equations (A.24) and (6). We conclude that a vector potential for a circularly polarized laser beam up to fourth order in the divergence angle θ is given by equations (6)–(8), equations (A.24) and (A.31) and the additional sufficient conditions $v_\xi^{\lambda(2n)} = \mathrm{i}\lambda v_\chi^{\lambda(2n)}$ and $v_\zeta^{\lambda(2n)} = 0$ for $n \in \{0, 1, 1\}$ and $v_\xi^{\lambda(2n+1)} = 0 = v_\chi^{\lambda(2n+1)}$ for $n \in \{0, 1\}$.

Starting from $v_{\bar{\alpha}}^{(0)} = \epsilon_{\bar{\alpha}}v_0$, where $\epsilon_{\bar{\alpha}} = w_0(0, 1, -\lambda i, 0)/\sqrt{2}$ and the solutions of even orders that can be found in [30],

$$v_{\bar{\alpha}}^{(0)}(\xi, \chi, \theta\zeta) = \epsilon_{\bar{\alpha}}^{(0)}v_0(\xi, \chi, \theta\zeta), \tag{A.34}$$

$$v_{\bar{\alpha}}^{(2)}(\xi,\chi,\theta\zeta) = \frac{\mu(\theta\zeta)}{2}\left(1-\frac{1}{2}\mu(\theta\zeta)^2\rho^4\right)v_{\bar{\alpha}}^{(0)}(\xi,\chi,\theta\zeta), \tag{A.35}$$

$$v_{\bar{\alpha}}^{(4)}(\xi,\chi,\theta\zeta) = \frac{\mu(\theta\zeta)^2}{16}\left(6-3\mu(\theta\zeta)^2\rho^4-2\mu(\theta\zeta)^3\rho^6+\frac{1}{2}\mu(\theta\zeta)^4\rho^8\right)v_{\bar{\alpha}}^{(0)}(\xi,\chi,\theta\zeta), \tag{A.36}$$

where $v_0(\xi,\chi,\theta\zeta) = \mu(\theta\zeta)\mathrm{e}^{-\mu(\theta\zeta)\rho^2}$. This leads to the expressions for the odd orders

$$v_{\zeta}^{(1)}(\xi,\chi,\theta\zeta) = -\frac{\mathrm{i}w_0\mu(\theta\zeta)}{2\sqrt{2}}\,(\xi-\mathrm{i}\lambda\chi)\,v_0(\xi,\chi,\theta\zeta), \tag{A.37}$$

$$v_{\zeta}^{(3)}(\xi,\chi,\theta\zeta) = \frac{\mu(\theta\zeta)}{4}\left(4+\mu(\theta\zeta)\rho^2-\mu(\theta\zeta)^2\rho^4\right)v_{\zeta}^{(1)}(\xi,\chi,\theta\zeta). \tag{A.38}$$

Appendix B. Poynting vector, Maxwell stress tensor and energy

For the vector potential of a circularly polarized laser beam given by equation (17), the energy density, the Poynting vector and the stress tensor components are given as

$$\begin{aligned}\mathcal{E}^{\lambda} = \mathcal{E}^{(0)}\Bigg[1+\frac{|\mu|^2\theta^2}{2}\left(1+|\mu|^2(2-(4|\mu|^2-3)\rho^2)\rho^2\right)+\frac{|\mu|^2\theta^4}{16}\Big(-3+2|\mu|^2(4-\rho^2+\rho^4)\\ +4|\mu|^4(4-\rho^2-5\rho^4)\rho^2+2|\mu|^6(8+52\rho^2+9\rho^4)\rho^4-48|\mu|^8(2+\rho^2)\rho^6+32|\mu|^{10}\rho^8\Big)\Bigg],\end{aligned} \tag{B.1}$$

$$\begin{aligned}S_{\xi}^{\lambda} = \mathcal{E}^{(0)}\theta|\mu|^2\Bigg[(\theta\zeta\xi+\lambda\chi)\\ -\frac{\theta^2}{4}\left(\lambda\chi-2|\mu|^2(2-\rho^2)\theta\zeta\xi+2(1-\rho^2)\lambda\chi+(\theta\zeta\xi+\lambda\chi)(4+3\rho^2-4|\mu|^2\rho^2)|\mu|^2\rho^2\right)\Bigg],\end{aligned} \tag{B.2}$$

$$\begin{aligned}S_{\chi}^{\lambda} = -\lambda\mathcal{E}^{(0)}\theta|\mu|^2\Bigg[(\xi-\theta\zeta\lambda\chi)\\ -\frac{\theta^2}{4}\left(\xi-2|\mu|^2 2(1-\rho^2)\xi-(2-\rho^2)\theta\zeta\lambda\chi+(\xi-\theta\zeta\lambda\chi)(4+3\rho^2-4|\mu|^2\rho^2)|\mu|^2\rho^2\right)\Bigg],\end{aligned} \tag{B.3}$$

$$S_{\zeta}^{\lambda} = \mathcal{E}^{\lambda}-\frac{1}{2}\mathcal{E}^{(0)}(\theta\rho|\mu|)^2\left[1+\left(\frac{\theta|\mu|}{2}\right)^2\left(4-3\rho^2+(8+6\rho^2-8\rho^2|\mu|^2)\rho^2|\mu|^2\right)\right], \tag{B.4}$$

$$\begin{aligned}\sigma_{\xi\xi}^{\lambda} = \mathcal{E}^{(0)}\theta^2|\mu|^4(\theta\zeta\xi+\lambda\chi)\Bigg[(\theta\zeta\xi+\lambda\chi)+\frac{\theta^2}{2}\Big(-\lambda\chi+3|\mu|^2(\theta\zeta\xi+\lambda\chi)\\ +\rho^2|\mu|^2\left(-2\lambda\chi-2(1-3|\mu|^2)(\theta\zeta\xi+\lambda\chi)+\left(3-4|\mu|^2\right)\rho^2|\mu|^2(\theta\zeta\xi+\lambda\chi)\right)\Big)\Bigg],\end{aligned} \tag{B.5}$$

$$\begin{aligned}\sigma_{\chi\chi}^{\lambda} = \mathcal{E}^{(0)}\theta^2|\mu|^4(\xi-\theta\zeta\lambda\chi)\Bigg[(\xi-\theta\zeta\lambda\chi)+\frac{\theta^2}{2}\Big(-\xi+3|\mu|^2(\xi-\theta\zeta\lambda\chi)\\ +\rho^2|\mu|^2\left(-2\xi-2(1-3|\mu|^2)(\xi-\theta\zeta\lambda\chi)+\left(3-4|\mu|^2\right)\rho^2|\mu|^2(\xi-\theta\zeta\lambda\chi)\right)\Big)\Bigg],\end{aligned} \tag{B.6}$$

$$\sigma^{\lambda}_{\xi\chi} = \mathcal{E}^{(0)}\lambda\theta^2|\mu|^4\Bigg[(\theta\zeta\xi+\lambda\chi)(\theta\zeta\lambda\chi-\xi) - \frac{\theta^2}{4}\Bigg(\theta\zeta\left(6|\mu|^2-1\right)\left(\xi^2-\chi^2\right) + 4(3(|\mu|^2-2))\lambda\xi\chi + 2\rho^2\Bigg(3\theta\zeta\left(2|\mu|^2-1\right)|\mu|^2\left(\xi^2-\chi^2\right) + 2\left(6|\mu|^4-6|\mu|^2+1\right)\lambda\xi\chi + \left(4|\mu|^2-3\right)\rho^2|\mu|^4(\theta\zeta\xi+\lambda\chi)(\theta\zeta\lambda\chi-\xi)\Bigg)\Bigg)\Bigg], \tag{B.7}$$

$$\sigma^{\lambda}_{\xi\zeta} = S^{\lambda}_{\xi} - \mathcal{E}^{(0)}\frac{\theta^3}{2}(\theta\zeta\xi+\lambda\chi)|\mu|^4\rho^2, \tag{B.8}$$

$$\sigma^{\lambda}_{\chi\zeta} = S^{\lambda}_{\chi} + \lambda\mathcal{E}^{(0)}\frac{\theta^3}{2}(\xi-\theta\zeta\lambda\chi)|\mu|^4\rho^2, \tag{B.9}$$

$$\sigma^{\lambda}_{\zeta\zeta} = \mathcal{E}^{\lambda} - \mathcal{E}^{(0)}(\theta\rho|\mu|)^2\left[1+\left(\frac{\theta|\mu|}{2}\right)^2\left(4-4\rho^2+(8+6\rho^2-8\rho^2|\mu|^2)\rho^2|\mu|^2\right)\right], \tag{B.10}$$

where $\mathcal{E}^{(0)} = \varepsilon_0 w_0^2 E_0^2|v_0|^2 = 2P_0|v_0|^2/(\pi c)$.

Appendix C. The projected solution

Following the second option to construct the field strength tensor for a circularly polarized beam described in section 2.1, we start from the zeroth order envelope function $v^{(0)}_{\bar\alpha} = \epsilon^{(0)}_{\bar\alpha} v_0$, where $\epsilon^{(0)}_{\bar\alpha} = (0,1,-\lambda i,0)w_0/\sqrt{2}$. We define cylindrical coordinates (ρ,ϕ,ζ) such that $\xi = \rho\cos\phi$ and $\chi = \rho\sin\phi$. Then, the components of the field strength tensor of the helicity eigenfunction $F^{\lambda,\mathrm{pro}}_{\bar\alpha\bar\beta} = (1+\lambda\Lambda)F^{\lambda}_{\bar\alpha\bar\beta}/2$ become

$$F^{\lambda,\mathrm{pro}}_{\tau\xi} = -\mathrm{i}\lambda F^{\lambda,\mathrm{pro}}_{\zeta\chi} = -\mathrm{i}w_0^2E_0v_0\,\mathrm{e}^{\mathrm{i}\frac{2}{\theta}(\zeta-\tau)}\left[1+\left(\frac{\theta\mu\rho}{2}\right)^2\left(2+\mathrm{e}^{-2\mathrm{i}\lambda\phi}-\mu\rho^2\right) + \left(\frac{\theta\mu\rho}{2}\right)^4\left(6+4\mathrm{e}^{-2\mathrm{i}\lambda\phi}-\left(4+\mathrm{e}^{-2\mathrm{i}\lambda\phi}\right)\mu\rho^2+\frac{1}{2}\mu^2\rho^4\right)\right], \tag{C.1}$$

$$F^{\lambda,\mathrm{pro}}_{\tau\chi} = -\mathrm{i}\lambda F^{\lambda,\mathrm{pro}}_{\xi\zeta} = -\lambda w_0^2E_0v_0\,\mathrm{e}^{\mathrm{i}\frac{2}{\theta}(\zeta-\tau)}\left[1+\left(\frac{\theta\mu\rho}{2}\right)^2\left(2-\mathrm{e}^{-2\mathrm{i}\lambda\phi}-\mu\rho^2\right) + \left(\frac{\theta\mu\rho}{2}\right)^4\left(6-4\mathrm{e}^{-2\mathrm{i}\lambda\phi}-\left(4-\mathrm{e}^{-2\mathrm{i}\lambda\phi}\right)\mu\rho^2+\frac{1}{2}\mu^2\rho^4\right)\right], \tag{C.2}$$

$$F^{\lambda,\mathrm{pro}}_{\tau\zeta} = -\mathrm{i}\lambda F^{\lambda,\mathrm{pro}}_{\chi\xi} = -w_0^2E_0v_0\,\mathrm{e}^{\mathrm{i}\frac{2}{\theta}(\zeta-\tau)}\theta\mu\rho\mathrm{e}^{-\mathrm{i}\lambda\phi}\left[1+\left(\frac{\theta\mu\rho}{2}\right)^2(3-\mu\rho^2)\right]. \tag{C.3}$$

Since $\Lambda F_{\bar\alpha\bar\beta} = -\mathrm{i}\star F_{\bar\alpha\bar\beta}$, the projection $(1+\lambda\Lambda)/2$ is equivalent to adding the dual field of $F_{\bar\alpha\bar\beta}$. In the approach of complex source points presented in [10], adding the dual corresponds

to adding a magnetic dipole to the electric dipole that would create $F_{\bar{\alpha}\bar{\beta}}$. In contrast to [10], we add the dual with a phase shift of $-\pi/2$ to add $-\mathrm{i}\star F_{\bar{\alpha}\bar{\beta}}$ and not just $\star F_{\bar{\alpha}\bar{\beta}}$.[12]

C.1. Poynting vector, Maxwell stress tensor and energy

For the field strength tensor $F^{\lambda,\mathrm{pro}}_{\bar{\alpha}\bar{\beta}}$ of a circularly polarized laser beam given in equation (C.1), the energy density, the Poynting vector and the stress tensor components are given as

$$\mathcal{E}^{\lambda} = \mathcal{E}^{(0)}\left[1+\frac{(\theta\rho|\mu|)^2}{2}\left(2+(4|\mu|^2-3)(1-\rho^2|\mu|^2)\right)\right.$$
$$\left.+\frac{(\theta\rho|\mu|)^4}{16}\left(96|\mu|^4-72|\mu|^2+5-2\rho^2|\mu|^2\left(2(32|\mu|^4-36|\mu|^2+8)-(4|\mu|^2-3)^2\rho^2|\mu|^2\right)\right)\right], \tag{C.4}$$

$$S^{\lambda}_{\xi} = -\mathcal{E}^{(0)}\theta|\mu|^2\left[(\theta\zeta\xi+\lambda\chi)+\frac{(\theta\rho|\mu|)^2}{2}\left((6|\mu|^2-2)\theta\zeta\xi+(6|\mu|^2-3)\lambda\chi-(4|\mu|^2-3)(\theta\zeta\xi+\lambda\chi)\rho^2|\mu|^2\right)\right],$$
$$S^{\lambda}_{\chi} = \lambda\mathcal{E}^{(0)}\theta|\mu|^2\left[(\xi-\lambda\theta\zeta\chi)+\frac{(\theta\rho|\mu|)^2}{2}\left((6|\mu|^2-3)\xi-(6|\mu|^2-2)\lambda\theta\zeta\chi-(4|\mu|^2-3)(\xi-\lambda\theta\zeta\chi)\rho^2|\mu|^2\right)\right],$$
$$S^{\lambda}_{\zeta} = -E^{\lambda}+\frac{1}{2}\mathcal{E}^{(0)}(\theta\rho|\mu|)^2\left[1+\left(\frac{\theta\rho|\mu|}{2}\right)^2 2\left(2|\mu|^2+\frac{1}{2}+(4|\mu|^2-3)\left(1-\rho^2|\mu|^2\right)\right)\right], \tag{C.5}$$

$$\sigma^{\lambda}_{\xi\xi} = \mathcal{E}^{(0)}\theta^2|\mu|^4(\theta\zeta\xi+\lambda\chi)\left[(\theta\zeta\xi+\lambda\chi)\right. \tag{C.6}$$
$$\left.+\frac{(\theta\rho|\mu|)^2}{2}\left((8|\mu|^2-3)\theta\zeta\xi+(8|\mu|^2-5)\lambda\chi-(4|\mu|^2-3)(\theta\zeta\xi+\lambda\chi)\rho^2|\mu|^2\right)\right], \tag{C.7}$$

$$\sigma^{\lambda}_{\chi\chi} = \mathcal{E}^{(0)}\theta^2|\mu|^4(\xi-\lambda\theta\zeta\chi)\left[(\xi-\lambda\theta\zeta\chi)\right.$$
$$\left.+\frac{(\theta\rho|\mu|)^2}{2}\left((8|\mu|^2-3)\xi-(8|\mu|^2-5)\lambda\theta\zeta\chi-(4|\mu|^2-3)(\xi-\lambda\theta\zeta\chi)\rho^2|\mu|^2\right)\right], \tag{C.8}$$

$$\sigma^{\lambda}_{\xi\chi} = \mathcal{E}^{(0)}\lambda\theta^2|\mu|^4\left[(\theta\zeta\xi+\lambda\chi)(\theta\zeta\lambda\chi-\xi)-\frac{1}{2}\theta^2\rho^2\left((\theta\zeta\lambda\chi-\xi)(\theta\zeta\xi+\lambda\chi)(4|\mu|^2-3)\rho^2|\mu|^4\right.\right.$$
$$\left.\left.+4\theta\zeta\xi^2(2|\mu|^2-1)|\mu|^2-4\theta\zeta\chi^2(2|\mu|^2-1)|\mu|^2+\lambda\xi\chi\left(16|\mu|^4-16|\mu|^2+3\right)\right)\right], \tag{C.9}$$

$$\sigma^{\lambda}_{\xi\zeta} = -S^{\lambda}_{\xi}-\mathcal{E}^{(0)}\frac{(\theta\rho|\mu|)^2}{2}\theta(\theta\zeta\xi+\lambda\chi)|\mu|^2, \tag{C.10}$$

$$\sigma^{\lambda}_{\chi\zeta} = -S^{\lambda}_{\xi}+\mathcal{E}^{(0)}\lambda\frac{(\theta\rho|\mu|)^2}{2}\theta(\xi-\lambda\theta\zeta\chi)|\mu|^2, \tag{C.11}$$

[12] Note that this symmetrization of the field strength tensor done in [10] is also performed in [12] without giving reference to a magnetic dipole moment.

$$\sigma^{\lambda}_{\zeta\zeta} = E^{\lambda} - \mathcal{E}^{(0)}(\theta\rho|\mu|)^2 \left[1 + \left(\frac{\theta\rho|\mu|}{2}\right)^2 2\left(2|\mu|^2 + (4|\mu|^2 - 3)\left(1 - \rho^2|\mu|^2\right)\right)\right], \tag{C.12}$$

where $\mathcal{E}^{(0)} = c^2\varepsilon_0 w_0^2 E_0^2 |v_0|^2$.

Appendix D. Validity of the linear approximation of general relativity

In the linearized version of general relativity, we decompose the metric into the Minkowski metric plus a perturbation, which is assumed to be small, equation (26). In this section, we make a rough calculation (just considering orders of magnitude) to verify that the linear approximation is justified, i.e. that it is possible to neglect terms quadratic in the metric perturbation.

From the Einstein equations it follows that the second derivative of the metric perturbation is proportional to $\frac{8\pi G}{c^4}$ times the energy–momentum tensor,

$$\partial^2 h \sim \frac{8\pi G}{c^4} T. \tag{D.1}$$

When considering spatial components (the other components can be considered to be of the same order of magnitude), we integrate to obtain an area A on the right hand side,

$$h \sim \frac{8\pi G}{c^4} TA. \tag{D.2}$$

Identifying TAc as the Power P, we obtain

$$h \sim \frac{8\pi G}{c^5} P. \tag{D.3}$$

In our calculation, we wrote the metric perturbation in the form (where we write ϵ for all expressions of order $O(\theta^0)$

$$h \sim \varepsilon + \theta\varepsilon + \theta^2\varepsilon. \tag{D.4}$$

The linearized theory is valid if one can neglect terms of the order $O(h^2)$, i.e. if $h^2 \ll h$. In our case, this condition translates to $\epsilon \ll \theta^2$. From the above equations, we see that $\epsilon \sim \frac{8\pi G}{c^5} P$. The condition then becomes

$$\frac{8\pi G}{c^5} P \ll \theta^2. \tag{D.5}$$

For a power of the order of magnitude $P \sim 10^{15}$ W, we thus have to require $\theta \gg 10^{-18}$. If we consider θ to be equal to zero, the condition becomes $\epsilon^2 \ll \epsilon$, which is also satisfied.

Appendix E. Expansion of Christoffel symbols and curvature tensor

With the equations (29) and (32), we can derive a direct relation between the terms of the expansions $(\gamma^{\lambda(n)})^{\bar{\alpha}}_{\bar{\beta}\bar{\gamma}}$ and $h^{\lambda(n)}_{\alpha\beta}$. We obtain for $\bar{i},\bar{j},\bar{k} \in \{\xi,\chi\}$

$$
\begin{aligned}
&(\gamma^{\lambda(n)})^{\tau}_{\tau\zeta} = (\gamma^{\lambda(n)})^{\zeta}_{\tau\tau} = -\tfrac{1}{2w_0^2}\partial_{\theta\zeta} h^{\lambda(n-1)}_{\tau\tau},\\
&(\gamma^{\lambda(n)})^{\zeta}_{\zeta\zeta} = \tfrac{1}{2w_0^2}\partial_{\theta\zeta} h^{\lambda(n-1)}_{\zeta\zeta},\\
&(\gamma^{\lambda(n)})^{\tau}_{\zeta\zeta} = -\tfrac{1}{w_0^2}\partial_{\theta\zeta} h^{\lambda(n-1)}_{\zeta\tau}\\
&(\gamma^{\lambda(n)})^{\bar{j}}_{\zeta\zeta} = -\tfrac{1}{2w_0^2}\partial_{\bar{j}} h^{\lambda(n)}_{\zeta\zeta} + \tfrac{1}{w_0^2}\partial_{\theta\zeta} h^{\lambda(n-1)}_{\bar{j}\zeta},\\
&(\gamma^{\lambda(n)})^{\bar{j}}_{\zeta\tau} = -\tfrac{1}{2w_0^2}\partial_{\bar{j}} h^{\lambda(n)}_{\zeta\tau} + \tfrac{1}{2w_0^2}\partial_{\theta\zeta} h^{\lambda(n-1)}_{\bar{j}\tau},\\
&(\gamma^{\lambda(n)})^{\bar{j}}_{\tau\tau} = -\tfrac{1}{2w_0^2}\partial_{\bar{j}} h^{\lambda(n)}_{\tau\tau},\\
&(\gamma^{\lambda(n)})^{\zeta}_{\bar{j}\zeta} = \tfrac{1}{2w_0^2}\partial_{\bar{j}} h^{\lambda(n)}_{\zeta\zeta},
\end{aligned}
\qquad
\begin{aligned}
&(\gamma^{\lambda(n)})^{\zeta}_{\bar{i}\bar{j}} = \tfrac{1}{2w_0^2}\left(\partial_{\bar{i}} h^{\lambda(n)}_{\bar{j}\zeta} + \partial_{\bar{j}} h^{\lambda(n)}_{\bar{i}\zeta} - \partial_{\theta\zeta} h^{\lambda(n-1)}_{\bar{i}\bar{j}}\right),\\
&(\gamma^{\lambda(n)})^{\zeta}_{\bar{j}\tau} = \tfrac{1}{2w_0^2}\left(\partial_{\bar{j}} h^{\lambda(n)}_{\tau\zeta} - \partial_{\theta\zeta} h^{\lambda(n-1)}_{\bar{j}\tau}\right),\\
&(\gamma^{\lambda(n)})^{\tau}_{\bar{j}\zeta} = -\tfrac{1}{2w_0^2}\left(\partial_{\bar{j}} h^{\lambda(n)}_{\tau\zeta} + \partial_{\theta\zeta} h^{\lambda(n-1)}_{\bar{j}\tau}\right),\\
&(\gamma^{\lambda(n)})^{\tau}_{\bar{i}\bar{j}} = -\tfrac{1}{2w_0^2}\left(\partial_{\bar{i}} h^{\lambda(n)}_{\tau\bar{j}} + \partial_{\bar{j}} h^{\lambda(n)}_{\tau\bar{i}}\right),\\
&(\gamma^{\lambda(n)})^{\bar{i}}_{\bar{j}\tau} = \tfrac{1}{2w_0^2}\left(\partial_{\bar{j}} h^{\lambda(n)}_{\tau\bar{i}} - \partial_{\bar{i}} h^{\lambda(n)}_{\tau\bar{j}}\right),\\
&(\gamma^{\lambda(n)})^{\bar{i}}_{\zeta\bar{j}} = \tfrac{1}{2w_0^2}\left(\partial_{\bar{j}} h^{\lambda(n)}_{\bar{i}\zeta} - \partial_{\bar{i}} h^{\lambda(n)}_{\bar{j}\zeta} + \partial_{\theta\zeta} h^{\lambda(n-1)}_{\bar{i}\bar{j}}\right),\\
&(\gamma^{\lambda(n)})^{\bar{k}}_{\bar{i}\bar{j}} = \tfrac{1}{2w_0^2}\left(\partial_{\bar{i}} h^{\lambda(n)}_{\bar{j}\bar{k}} + \partial_{\bar{j}} h^{\lambda(n)}_{\bar{i}\bar{k}} - \partial_{\bar{k}} h^{\lambda(n)}_{\bar{i}\bar{j}}\right),
\end{aligned}
\tag{E.1}
$$

where $h^{n}_{\bar{\alpha}\bar{\beta}} = 0$ if $n < 0$. With the equations (31) and (32), we can derive a direct relation between the terms of the expansions $r^{\lambda(n)}_{\bar{\alpha}\bar{\beta}\bar{\gamma}\bar{\delta}}$ and $h^{\lambda(n)}_{\alpha\beta}$. With $\bar{j}, \bar{k} \in \{\xi, \chi\}$, we obtain

$$
\begin{aligned}
&r^{\lambda(n)}_{\xi\chi\xi\chi} = \partial_{\xi}\partial_{\chi} h^{\lambda(n)}_{\xi\chi} - \tfrac{1}{2}\left(\partial^2_{\xi} h^{\lambda(n)}_{\chi\chi} + \partial^2_{\chi} h^{\lambda(n)}_{\xi\xi}\right),\\
&r^{\lambda(n)}_{\bar{j}\zeta\bar{k}} = \tfrac{1}{2}\partial_{\theta\zeta}\left(\partial_{\bar{j}} h^{\lambda(n-1)}_{\bar{j}\bar{k}} - \partial_{\bar{k}} h^{\lambda(n-1)}_{\bar{j}\bar{j}}\right) - \tfrac{1}{2}\partial_{\bar{j}}\left(\partial_{\bar{j}} h^{\lambda(n)}_{\zeta\bar{k}} - \partial_{\bar{k}} h^{\lambda(n)}_{\zeta\bar{j}}\right),\\
&r^{\lambda(n)}_{\bar{j}\zeta\bar{k}\zeta} = \tfrac{1}{2}\left(\partial_{\theta\zeta}\partial_{\bar{k}} h^{\lambda(n-1)}_{\bar{j}\zeta} - \partial^2_{\theta\zeta} h^{\lambda(n-2)}_{\bar{j}\bar{k}} - \partial_{\theta\zeta}\partial_{\bar{j}} h^{\lambda(n-1)}_{\bar{k}\zeta} + \partial_{\bar{j}}\partial_{\bar{k}} h^{\lambda(n)}_{\zeta\zeta}\right),\\
&r^{\lambda(n)}_{\bar{j}0\bar{j}\bar{k}} = \tfrac{1}{2}\partial_{\bar{j}}\left(\partial_{\bar{k}} h^{\lambda(n)}_{0\bar{j}} - \partial_{\bar{j}} h^{\lambda(n)}_{0\bar{k}}\right),\\
&r^{\lambda(n)}_{\bar{j}0\bar{k}0} = -\tfrac{1}{2}\partial_{\bar{j}}\partial_{\bar{k}} h^{\lambda(n)}_{00},
\end{aligned}
\qquad
\begin{aligned}
&r^{\lambda(n)}_{\bar{j}0\zeta 0} = -\tfrac{1}{2}\partial_{\bar{j}}\partial_{\theta\zeta} h^{\lambda(n-1)}_{00},\\
&r^{\lambda(n)}_{\bar{j}0\zeta\bar{k}} = \tfrac{1}{2}\partial_{\bar{j}}\left(\partial_{\bar{k}} h^{\lambda(n)}_{0\zeta} - \partial_{\theta\zeta} h^{\lambda(n-1)}_{0\bar{k}}\right),\\
&r^{\lambda(n)}_{\zeta 0\zeta\bar{k}} = \tfrac{1}{2}\partial_{\theta\zeta}\left(\partial_{\bar{k}} h^{\lambda(n-1)}_{0\zeta} - \partial_{\theta\zeta} h^{\lambda(n-2)}_{0\bar{k}}\right),\\
&r^{\lambda(n)}_{\zeta 0\zeta 0} = -\tfrac{1}{2}\partial^2_{\theta\zeta} h^{\lambda(n-2)}_{00}.
\end{aligned}
\tag{E.2}
$$

Appendix F. Metric perturbation for large distances between emitter and absorber of the laser beam up to third order in the divergence angle

As stated in section 4, solutions of equations (33)–(35) can be given by equation (36). However, the Green's function of the Poisson equation in two dimensions is only specified up to a constant which for our degenerate equation (33) in three dimensions becomes a function of $\theta\zeta$. This leads to an additional term $h^{\lambda(n)\mathrm{rest}}_{\bar{\alpha}\bar{\beta}}(\theta\zeta)$ that we have to specify by a further condition. Here, we use the physical condition that the Riemann curvature tensor has to vanish at an infinite distance from the beamline to ensure that no physical effects are induced by the gravitational field of the laser beam at infinity. We find

$$
h^{\lambda(n)\mathrm{gen}}_{\bar{\alpha}\bar{\beta}}(\xi, \chi, \theta\zeta) = h^{\lambda(n)}_{\bar{\alpha}\bar{\beta}}(\xi, \chi, \theta\zeta) + h^{\lambda(n)\mathrm{rest}}_{\bar{\alpha}\bar{\beta}}(\theta\zeta), \tag{F.1}
$$

where $h^{\lambda(n)}_{\bar{\alpha}\bar{\beta}}(\xi, \chi, \theta\zeta)$ is given in equation (36). Since the Riemann curvature tensor is linear in the metric perturbation, it consists of a term induced by $h^{\lambda(n)}_{\bar{\alpha}\bar{\beta}}$ and a term induced by $h^{\lambda(n)\mathrm{rest}}_{\bar{\alpha}\bar{\beta}}$. The term induced by $h^{\lambda(n)\mathrm{rest}}_{\bar{\alpha}\bar{\beta}}(\theta\zeta)$ does not depend on the distance to the beamline. Let us assume that the term in the curvature tensor induced by the first term in equation (31) vanishes for $\rho \to \infty$. Then, the term in the curvature tensor induced by $h^{\lambda(n)\mathrm{rest}}_{\bar{\alpha}\bar{\beta}}(\theta\zeta)$ has to vanish everywhere for the curvature to vanish for $\rho \to \infty$. Therefore, $h^{\lambda(n)\mathrm{rest}}_{\bar{\alpha}\bar{\beta}}(\theta\zeta)$ cannot contribute to the curvature tensor and can be set to zero in equation (F.1). It turns out that the contribution of the first term in equation (F.1) to the curvature tensor vanishes at infinity, indeed, up to the fourth order in θ, as we will show in the following. Therefore, we assume $h^{\lambda(n)\mathrm{rest}}_{\bar{\alpha}\bar{\beta}}(\theta\zeta) = 0$ in this article. In the following, we give expressions for $h^{\lambda(n)}_{\bar{\alpha}\bar{\beta}}(\xi, \chi, \theta\zeta)$ up to third order in θ.

In zeroth order, we have (see section 5 for comparison)

$$h^{\lambda(0)}_{\bar{\alpha}\bar{\beta}} = \frac{\kappa w_0^2 P_0}{2\pi c}\left(\frac{1}{2}\mathrm{Ei}\left(-2|\mu|^2\rho^2\right) - \log(\rho)\right)\begin{pmatrix} 1 & 0 & 0 & -1 \\ 0 & 0 & 0 & 0 \\ 0 & 0 & 0 & 0 \\ -1 & 0 & 0 & 1 \end{pmatrix}. \tag{F.2}$$

In first order, we have

$$h^{\lambda(1)}_{\bar{\alpha}\bar{\beta}} = \frac{\kappa P_0 w_0^2}{8\pi c\rho^2}\left(1-\mathrm{e}^{-2|\mu|^2\rho^2}\right)\begin{pmatrix} 0 & -(\theta\zeta\xi+\lambda\chi) & (\lambda\xi-\theta\zeta\chi) & 0 \\ -(\theta\zeta\xi+\lambda\chi) & 0 & 0 & (\theta\zeta\xi+\lambda\chi) \\ (\lambda\xi-\theta\zeta\chi) & 0 & 0 & -(\lambda\xi-\theta\zeta\chi) \\ 0 & (\theta\zeta\xi+\lambda\chi) & -(\lambda\xi-\theta\zeta\chi) & 0 \end{pmatrix}. \tag{F.3}$$

In second order, we find for the only non-vanishing independent components of the metric perturbation

$$h^{\lambda(2)}_{\tau\tau} = \frac{\kappa w_0^2 P_0}{32\pi c}\left(4\mathrm{Ei}\left(-2|\mu|^2\rho^2\right) - 8\log(\rho) - (5-(4-6\rho^2)|\mu|^2 - 8\rho^2|\mu|^4)\mathrm{e}^{-2|\mu|^2\rho^2}\right), \tag{F.4}$$

$$h^{\lambda(2)}_{\tau\zeta} = -\frac{\kappa w_0^2 P_0}{32\pi c}\left(2\mathrm{Ei}\left(-2|\mu|^2\rho^2\right) - 4\log(\rho) - (3-(4-6\rho^2)|\mu|^2 - 8\rho^2|\mu|^4)\mathrm{e}^{-2|\mu|^2\rho^2}\right), \tag{F.5}$$

$$h^{\lambda(2)}_{\zeta\zeta} = -\frac{\kappa w_0^2 P_0}{32\pi c}\left(1-(4-6\rho^2)|\mu|^2 - 8\rho^2|\mu|^4\right)\mathrm{e}^{-2|\mu|^2\rho^2}, \tag{F.6}$$

$$\begin{aligned} h^{\lambda(2)}_{\xi\xi} = \frac{\kappa w_0^2 P_0}{32\pi\rho^4|\mu|^2 c}\Big(&\rho^4|\mu|^2\mathrm{Ei}\left(-2|\mu|^2\rho^2\right) - 2\rho^4|\mu|^2\log(\rho) + (\xi^2-\chi^2) - 2(\xi^2-\chi^2-2\theta\zeta\lambda\xi\chi)|\mu|^2 \\ &+\left(-(\xi^2-\chi^2) + 2(\xi^2-\chi^2-2\theta\zeta\lambda\xi\chi-2\rho^2\xi^2)|\mu|^2 + 4\rho^2(\xi^2-\chi^2-2\theta\zeta\lambda\chi\xi)|\mu|^4\right)\mathrm{e}^{-2|\mu|^2\rho^2}\Big), \end{aligned} \tag{F.7}$$

$$\begin{aligned} h^{\lambda(2)}_{\chi\chi} = \frac{\kappa w_0^2 P_0}{32\pi\rho^4|\mu|^2 c}\Big(&\rho^4|\mu|^2\mathrm{Ei}\left(-2|\mu|^2\rho^2\right) - 2\rho^4|\mu|^2\log(\rho) - (\xi^2-\chi^2) + 2(\xi^2-\chi^2-2\theta\zeta\lambda\xi\chi)|\mu|^2 \\ &-\left(-(\xi^2-\chi^2) + 2(\xi^2-\chi^2-2\theta\zeta\lambda\xi\chi-2\rho^2\chi^2)|\mu|^2 + 4\rho^2(\xi^2-\chi^2-2\theta\zeta\lambda\chi\xi)|\mu|^4\right)\mathrm{e}^{-2|\mu|^2\rho^2}\Big), \end{aligned} \tag{F.8}$$

$$h^{\lambda(2)}_{\xi\chi} = -\frac{\kappa w_0^2 P_0}{16\pi\rho^4|\mu|^2 c}\left(1-(1+\rho^2|\mu|^2)\mathrm{e}^{-2|\mu|^2\rho^2}\right)\left(-\xi\chi + (2\xi\chi+\theta\zeta\lambda(\xi^2-\chi^2))|\mu|^2\right). \tag{F.9}$$

In third order, we obtain the only non-vanishing independent components

$$\begin{aligned} h^{\lambda(3)}_{\tau\xi} = -\frac{\kappa P_0 w_0^2}{32\pi c\rho^2}\Big((4\theta\zeta\xi+3\lambda\chi) + \Big(&-(4\theta\zeta\xi+3\lambda\chi) - 2\rho^2(3\theta\zeta\xi+2\lambda\chi)|\mu|^2 \\ &-2\rho^2(-2+3\rho^2)(\theta\zeta\xi+\lambda\chi)|\mu|^4 + 8\rho^4(\theta\zeta\xi+\lambda\chi)|\mu|^6\Big)\mathrm{e}^{-2|\mu|^2\rho^2}\Big), \end{aligned} \tag{F.10}$$

$$h^{\lambda(3)}_{\tau\chi} = -\frac{\kappa P_0 w_0^2}{32\pi c\rho^2}\Bigg((4\theta\zeta\chi - 3\lambda\xi) + \Bigg(- (4\theta\zeta\xi + 3\lambda\chi) - 2\rho^2(3\theta\zeta\chi - 2\lambda\xi)|\mu|^2 \\ - 2\rho^2(-2+3\rho^2)(\theta\zeta\chi - \lambda\xi)|\mu|^4 + 8\rho^4(\theta\zeta\chi - \lambda\chi)|\mu|^6\Bigg)\mathrm{e}^{-2|\mu|^2\rho^2}\Bigg), \tag{F.11}$$

$$h^{\lambda(3)}_{\zeta\xi} = \frac{\kappa P_0 w_0^2}{32\pi c\rho^2}\Bigg((2\theta\zeta\xi + \lambda\chi) + \Bigg(- (2\theta\zeta\xi + \lambda\chi) - 2\rho^2(2\theta\zeta\xi + \lambda\chi)|\mu|^2 \\ - 2\rho^2(-2+3\rho^2)(\theta\zeta\xi + \lambda\chi)|\mu|^4 + 8\rho^4(\theta\zeta\xi + \lambda\chi)|\mu|^6\Bigg)\mathrm{e}^{-2|\mu|^2\rho^2}\Bigg), \tag{F.12}$$

$$h^{\lambda(3)}_{\zeta\chi} = \frac{\kappa P_0 w_0^2}{32\pi c\rho^2}\Bigg((2\theta\zeta\chi - \lambda\xi) + \Bigg(- (2\theta\zeta\xi + \lambda\chi) - 2\rho^2(2\theta\zeta\chi - \lambda\xi)|\mu|^2 \\ - 2\rho^2(-2+3\rho^2)(\theta\zeta\chi - \lambda\xi)|\mu|^4 + 8\rho^4(\theta\zeta\chi - \lambda\chi)|\mu|^6\Bigg)\mathrm{e}^{-2|\mu|^2\rho^2}\Bigg). \tag{F.13}$$

Now, with the expressions for the terms in the expansion of the curvature tensor given in appendix E, we can show that the contribution of $h^{\lambda(n)}_{\bar\alpha\bar\beta}(\xi,\chi,\theta\zeta)$ to the curvature vanishes for $\rho\to\infty$. From equation (F.1), we obtain that

$$\partial_{\bar j} h^{\lambda(n)}_{\bar\alpha\bar\beta} = -\frac{\kappa}{4\pi}\int_{-\infty}^{\infty}\mathrm{d}\xi'\mathrm{d}\chi'\,\frac{x^{\bar j}}{(\xi-\xi')^2+(\chi-\chi')^2}\mathcal{Q}^{\lambda(n)}_{\bar\alpha\bar\beta}(\xi',\chi',\theta\zeta), \tag{F.14}$$

where $x^{\bar j}\in\{\xi,\chi\}$. From the expressions in appendix B, we see that all terms in the energy–momentum tensor decay like $\exp(-2|\mu|^2\rho^2)$ for $\rho\to\infty$. From the expressions above, we find that this is true for $\partial^2_{\theta\zeta}h^{\lambda(0)}_{\bar\alpha\bar\beta}$ and $\partial^2_{\theta\zeta}h^{\lambda(1)}_{\bar\alpha\bar\beta}$ as well. Furthermore, $\partial^2_{\theta\zeta}h^{\lambda(2)}_{\bar\alpha\bar\beta}$ decays at least as ρ^{-2} for $\rho\to\infty$. Hence, for $n\leqslant 4$ we find that the sources $\mathcal{Q}^{\lambda(n)}_{\bar\alpha\bar\beta}$ (the terms on the right hand side of the differential equations in equations (33)–(35)) are falling off at least as ρ^{-2} for $\rho\to\infty$. Therefore, the first derivatives of $h^{\lambda(n)}_{\bar\alpha\bar\beta}(\xi,\chi,\theta\zeta)$ in the directions ξ and χ will go to zero for $\rho\to\infty$ for $n\leqslant 4$. From the expressions above, we find that $\partial^2_{\theta\zeta}h^{\lambda(n-2)}_{\tau\tau}$ and $\partial^2_{\theta\zeta}h^{\lambda(n-2)}_{\tau\bar k}$ decay like $\exp(-2|\mu|^2\rho^2)$ for $\rho\to\infty$ for $n\leqslant 4$. Therefore, we find that the contribution of $h^{\lambda(n)}_{\bar\alpha\bar\beta}(\xi,\chi,\theta\zeta)$ to the curvature vanishes for $\rho\to\infty$ and $n\leqslant 4$. Hence, the term $h^{\lambda(n)\mathrm{rest}}_{\bar\alpha\bar\beta}(\theta\zeta)$ can be set to zero as argued above.

Appendix G. An exact solution for the infinitely long laser beam with boundary in the paraxial approximation

An exact solution for the infinitely long laser beam in the paraxial approximation, i.e. for $\theta=0$, is constructed as follows: we make the ansatz of a plane wave metric [4],

$$\mathrm{d}s^2 = w_0^2\left(-\mathrm{d}\tau^2+\mathrm{d}\xi^2+\mathrm{d}\eta^2+\mathrm{d}\zeta^2\right)+K\left(\mathrm{d}\tau-\mathrm{d}\zeta\right)^2, \tag{G.1}$$

in the dimensionless coordinates $(\tau,\xi,\chi,\zeta)=(ct,x,y,z)/w_0$. The radius of the beam is supposed to be a, such that the energy density ϱ is given by $\varrho w_0^2 = T_{\tau\tau} = T_{\zeta\zeta} = -T_{\tau\zeta}$ within this radius, and vanishes outside of it. Then the function $K = K(\xi,\eta)$ in the interior region, for $\rho \leqslant a$, and in the exterior region, for $a < \rho$, is determined by

$$\begin{aligned}\varrho w_0^2 &= -\frac{1}{\kappa w_0^2}\left(\partial_\xi^2+\partial_\eta^2\right)K_{\text{int}},\\ 0 &= -\frac{1}{\kappa w_0^2}\left(\partial_\xi^2+\partial_\eta^2\right)K_{\text{ext}}.\end{aligned} \tag{G.2}$$

For the laser beam for $\theta = 0$, the energy density is given by $\varrho w_0^2 = \mathcal{E}^{(0)} = \frac{2P_0}{\pi c}\mathrm{e}^{-2\rho^2}$. Writing equation (G.2) in cylindrical coordinates, we obtain

$$\begin{aligned}\frac{1}{\rho}\partial_\rho\left(\rho\,\partial_\rho K_{\text{int}}\right) &= -\frac{2\kappa P_0 w_0^2}{\pi c}\mathrm{e}^{-2\rho^2},\\ \frac{1}{\rho}\partial_\rho\left(\rho\partial_\rho K_{\text{ext}}\right) &= 0.\end{aligned} \tag{G.3}$$

Integrating twice over ρ leads to

$$\begin{aligned}K_{\text{int}}(\rho) &= \frac{\kappa P_0 w_0^2}{4\pi c}\mathrm{Ei}\left(-2\rho^2\right) + C_1\log(\rho) + C_2,\\ K_{\text{ext}}(\rho) &= D_1\log(\rho) + D_2,\end{aligned} \tag{G.4}$$

where $\mathrm{Ei}(x) = \gamma + \log(|x|) + \mathrm{i}\arg(x) + x + \frac{x^2}{4} + \frac{x^3}{18} + \ldots$ is the exponential integral. For the metric to be finite at $r = 0$, we set $C_1 = -\kappa E_0^2 w_0^2/(2\pi c)$, and for the interior solution to match the exterior solution at $r = a$, i.e. to be continuous and differentiable, we choose $D_2 = 0$ and $C_2 = \kappa P_0 w_0^2 (2\pi c)^{-1}\left(\mathrm{e}^{-2a^2}\log(a) - \frac{1}{2}\mathrm{Ei}(-2a^2)\right)$, s.t. the final solution reads

$$\begin{aligned}K_{\text{int}} &= -\frac{\kappa P_0 w_0^2}{2\pi c}\left(\log(\rho) - \frac{1}{2}\mathrm{Ei}(-2\rho^2) - \mathrm{e}^{-2a^2}\log(a) + \frac{1}{2}\mathrm{Ei}(-2a^2)\right),\\ K_{\text{ext}} &= -\frac{\kappa P_0 w_0^2}{2\pi c}\left(1-\mathrm{e}^{-2a^2}\right)\log(\rho).\end{aligned} \tag{G.5}$$

If the beam is infinitely extended in the transverse direction, we are left with an interior solution only which reads

$$K(\rho) = -\frac{\kappa P_0 w_0^2}{2\pi c}\left(\log(\rho) - \frac{1}{2}\mathrm{Ei}\left(-2\rho^2\right)\right). \tag{G.6}$$

The metric may be written as the Minkowski metric plus a small perturbation $h_{\mu\nu} = K(\rho)M_0$, s.t. the only non-vanishing independent components of the Riemann curvature tensor $R_{\tau i\tau j} = R_{\zeta i\zeta j} = -R_{\tau i\zeta j} = -\frac{1}{2}\partial_i\partial_j K(\rho)$ (for $i,j\in\{\xi,\eta\}$) are given by

$$\begin{aligned}R^{\text{int}}_{\tau\xi\tau\xi} = R^{\text{int}}_{\zeta\xi\zeta\xi} &= -R^{\text{int}}_{\tau\xi\zeta\xi} = -\frac{\kappa P_0 w_0^2}{4\pi c}\frac{1}{\rho^4}\left((\xi^2-\eta^2) - \left(4\xi^2\rho^2+\xi^2-\eta^2\right)\mathrm{e}^{-2\rho^2}\right),\\ R^{\text{int}}_{\tau\eta\tau\eta} = R^{\text{int}}_{\zeta\eta\zeta\eta} &= -R^{\text{int}}_{\tau\eta\zeta\eta} = \frac{\kappa P_0 w_0^2}{4\pi c}\frac{1}{\rho^4}\left((\xi^2-\eta^2) + \left(4\eta^2\rho^2-\xi^2+\eta^2\right)\mathrm{e}^{-2\rho^2}\right),\\ R^{\text{int}}_{\tau\xi\tau\eta} = R^{\text{int}}_{\zeta\xi\zeta\eta} &= -R^{\text{int}}_{\tau\xi\zeta\eta} = -\frac{\kappa P_0 w_0^2}{2\pi c}\frac{\xi\eta}{\rho^4}\left(1-(1+2\rho^2)\mathrm{e}^{-2\rho^2}\right),\end{aligned} \tag{G.7}$$

in the interior region and

$$R^{\text{ext}}_{\tau\xi\tau\xi} = R^{\text{ext}}_{\zeta\xi\zeta\xi} = -R^{\text{ext}}_{\tau\xi\zeta\xi} = -\frac{\kappa P_0 w_0^2}{4\pi c}\frac{\xi^2-\eta^2}{\rho^4}\left(1-\mathrm{e}^{-2a^2}\right),$$
$$R^{\text{ext}}_{\tau\eta\tau\eta} = R^{\text{ext}}_{\zeta\eta\zeta\eta} = -R^{\text{ext}}_{\tau\eta\zeta\eta} = \frac{\kappa P_0 w_0^2}{4\pi c}\frac{\xi^2-\eta^2}{\rho^4}\left(1-\mathrm{e}^{-2a^2}\right),$$
$$R^{\text{ext}}_{\tau\xi\tau\eta} = R^{\text{ext}}_{\zeta\xi\zeta\eta} = -R^{\text{ext}}_{\tau\xi\zeta\eta} = -\frac{\kappa P_0 w_0^2}{2\pi c}\frac{\xi\eta}{\rho^4}\left(1-\mathrm{e}^{-2a^2}\right), \tag{G.8}$$

in the exterior region. We see that the result for the exterior region corresponds to the Riemann curvature tensor for the infinitely thin beam plus a contribution proportional to e^{-2a^2}, which vanishes in the limit as $a \to 0$. The factor

$$P_0 = \frac{1}{2}\pi c\varepsilon_0 E_0^2 w_0^2(1-\mathrm{e}^{-2a^2}) = c\varepsilon_0 E_0^2 w_0^2\int_0^{2\pi}\mathrm{d}\phi\int_0^a \mathrm{d}\rho\,\rho\mathrm{e}^{-2\rho^2} \tag{G.9}$$

is the total power in the circular region with radius a that contains the source of the gravitation field seen in the exterior region. Therefore, expressing the curvature in the exterior region through the total power P_0, we obtain the same result as for the infinitely thin beam. This coincides with the result from Newtonian gravity that the gravitational field outside of a spherical symmetric source distribution does not depend on the radial dependence of its density.

Appendix H. Metric perturbation for small distances between emitter and absorber of the laser beam

In this appendix we provide the calculations for the metric perturbation for the case of a small distance between the emitter and absorber of the laser beam up to the second order in more detail. In the beginning we calculate the integrals we would need to calculate if the mirrors at $\zeta = \alpha$ and $\zeta = \beta$ were not curved. In a next step we will include the correction for the case when they are curved. The beam is assumed to be emitted at the location of the wavefront for which $\zeta = \alpha$ on the ζ-axis, propagate along the ζ-axis and be absorbed at the location of the wavefront for which $\zeta = \beta$ on the ζ-axis. The mirrors at the emission and absorption are curved such that the phase along them is constant. The phase of the Gaussian beam (without the term including the time) is given by

$$\varphi(\rho,\zeta) = \frac{\theta\zeta\rho^2}{1+\theta^2\zeta^2} + \frac{2}{\theta}\zeta. \tag{H.1}$$

For the ζ-coordinate of the mirror at the emission at $\zeta = \alpha$, which we call $\bar{\zeta}_\alpha$, setting $\varphi(0,\alpha) = \varphi\big(\rho,\bar{\zeta}_\alpha(\rho)\big)$, and for the $\bar{\zeta}_\beta$-coordinate of the mirror at the absorption, setting $\varphi(0,\beta) = \varphi\big(\rho,\bar{\zeta}_\beta(\rho)\big)$, we obtain

$$\bar{\zeta}_\alpha(\rho) = \alpha\left(1-\frac{\theta^2}{2}\rho^2\right),$$
$$\bar{\zeta}_\beta(\rho) = \beta\left(1-\frac{\theta^2}{2}\rho^2\right). \tag{H.2}$$

We start by calculating two integrals that will be useful in the following. The first one is

$$\mathcal{I}_a = \int_{-\infty}^{\infty} \mathrm{d}\xi' \int_{-\infty}^{\infty} \mathrm{d}\chi' \int_{\alpha}^{\beta} \mathrm{d}\zeta' \, \frac{1}{\sqrt{(\xi-\xi')^2+(\chi-\chi')^2+(\zeta-\zeta')^2}} \mathrm{e}^{-2(\xi'^2+\chi'^2)}. \tag{H.3}$$

Introducing for any quantity u a shifted quantity u'' by $u'' = u' - u$, and changing to cylindrical coordinates $(\xi'', \chi'', \zeta'') = (\rho'' \cos(\phi''), \rho'' \sin(\phi''), z'')$, we obtain

$$\mathcal{I}_a = \int_{\alpha''}^{\beta''} \mathrm{d}\zeta'' \int_{0}^{2\pi} \mathrm{d}\phi'' \int_{0}^{\infty} \mathrm{d}\rho'' \frac{\rho''}{\sqrt{\rho''^2+\zeta''^2}} \mathrm{e}^{-2(\rho''^2+\rho^2-2\rho\rho''\cos(\phi''-\phi))}. \tag{H.4}$$

Using the Bessel function of the first kind, $J_0(ix) = \frac{1}{\pi}\int_0^{\pi} \mathrm{d}\phi \mathrm{e}^{x\cos(\phi)}$, leads to

$$\mathcal{I}_a = 2\pi \mathrm{e}^{-2\rho^2} \int_0^{\infty} \mathrm{d}\rho'' \, \rho'' \log\left(\frac{\beta-\zeta+\sqrt{(\beta-\zeta)^2+\rho''^2}}{\alpha-\zeta+\sqrt{(\alpha-\zeta)^2+\rho''^2}}\right) J_0\left(\mathrm{i}4\rho\rho''\right) \mathrm{e}^{-2\rho''^2}. \tag{H.5}$$

The second integral we calculate is the same as before but with a factor ζ' in the nominator,

$$\mathcal{I}_b = \int_{\alpha}^{\beta} \mathrm{d}\zeta' \int_{-\infty}^{\infty} \mathrm{d}\xi' \int_{-\infty}^{\infty} \mathrm{d}\chi' \, \frac{\zeta'}{\sqrt{(\xi-\xi')^2+(\chi-\chi')^2+(\zeta-\zeta')^2}} \mathrm{e}^{-2(\xi'^2+\chi'^2)}. \tag{H.6}$$

In the same way as before, we obtain

$$\mathcal{I}_b = \zeta\, \mathcal{I}_a + 2\pi \mathrm{e}^{-2\rho^2} \int_0^{\infty} \mathrm{d}\rho'' \, \rho'' \left(\sqrt{\rho''^2+(\beta-\zeta)^2} - \sqrt{\rho''^2+(\alpha-\zeta)^2}\right) J_0(\mathrm{i}4\rho\rho'') \mathrm{e}^{-2\rho''^2}. \tag{H.7}$$

Every other integral we need to solve to calculate the metric perturbation can be expressed through derivatives of these integrals, using the following identities (and equivalently for $\mathcal{I}_b$ if there is an additional factor ζ' in the numerator):

$$\begin{aligned}
&\int_{\alpha}^{\beta} \mathrm{d}\zeta' \int_{-\infty}^{\infty} \mathrm{d}\xi' \int_{-\infty}^{\infty} \mathrm{d}\chi' \, \frac{\xi'}{\sqrt{(\xi-\xi')^2+(\chi-\chi')^2+(\zeta-\zeta')^2}} \mathrm{e}^{-2(\xi'^2+\chi'^2)} \\
&\quad = \int_{\alpha''}^{\beta''} \mathrm{d}\zeta'' \int_{-\infty}^{\infty} \mathrm{d}\xi'' \int_{-\infty}^{\infty} \mathrm{d}\chi'' \, \frac{\xi''+\xi}{\sqrt{\xi''^2+\chi''^2+\zeta''^2}} \mathrm{e}^{-2(\xi''+\xi)^2+(\chi''+\chi)^2} = -\frac{1}{4}\partial_\xi \mathcal{I}_a, \\
&\int_{\alpha}^{\beta} \mathrm{d}\zeta' \int_{-\infty}^{\infty} \mathrm{d}\xi' \int_{-\infty}^{\infty} \mathrm{d}\chi' \, \frac{\xi'^2}{\sqrt{(\xi-\xi')^2+(\chi-\chi')^2+(\zeta-\zeta')^2}} \mathrm{e}^{-2(\xi'^2+\chi'^2)} = \frac{1}{4}\left(1+\frac{1}{4}\partial_\xi^2\right)\mathcal{I}_a, \\
&\int_{\alpha}^{\beta} \mathrm{d}\zeta' \int_{-\infty}^{\infty} \mathrm{d}\xi' \int_{-\infty}^{\infty} \mathrm{d}\chi' \, \frac{\xi'^4}{\sqrt{(\xi-\xi')^2+(\chi-\chi')^2+(\zeta-\zeta')^2}} \mathrm{e}^{-2(\xi'^2+\chi'^2)} = \frac{1}{16}\left(\frac{1}{16}\partial_\xi^4+\frac{3}{2}\partial_\xi^2+3\right)\mathcal{I}_a.
\end{aligned} \tag{H.8}$$

Including the correction of the boundaries of the integral due to the curvature of the mirrors, we obtain for the first integral

$$\begin{aligned}
\mathcal{I}_A &= \int_{-\infty}^{\infty} \mathrm{d}\xi' \int_{-\infty}^{\infty} \mathrm{d}\chi' \int_{\bar{\zeta}_\alpha(\rho')}^{\bar{\zeta}_\beta(\rho')} \mathrm{d}\zeta' \, \frac{1}{\sqrt{(\xi-\xi')^2+(\chi-\chi')^2+(\zeta-\zeta')^2}} \mathrm{e}^{-2(\xi'^2+\chi'^2)} \\
&= \int_{-\infty}^{\infty} \mathrm{d}\xi' \int_{-\infty}^{\infty} \mathrm{d}y' \, \log\left(\frac{\zeta-\bar{\zeta}_\beta(\rho')+\sqrt{(\zeta-\bar{\zeta}_\beta(\rho'))^2+(\xi-\xi')^2+(\chi-\chi')^2}}{\zeta-\bar{\zeta}_\alpha(\rho')+\sqrt{(\zeta-\bar{\zeta}_\alpha(\rho'))^2+(\xi-\xi')^2+(\chi-\chi')^2}}\right) \mathrm{e}^{-2(\xi'^2+\chi'^2)}.
\end{aligned} \tag{H.9}$$

Inserting $\bar{\zeta}_\beta(\rho') = \beta\left(1 - \frac{\theta^2}{2}(\xi'^2 + \chi'^2)\right)$ and $\bar{\zeta}_\alpha(\rho') = \alpha\left(1 - \frac{\theta^2}{2}(\xi'^2 + \chi'^2)\right)$ and expanding to the second order of θ leads to

$$\mathcal{I}_A = \mathcal{I}_a + \theta^2 \delta\mathcal{I}_a, \tag{H.10}$$

where we defined

$$\delta\mathcal{I}_a = -\frac{1}{2}\int_{-\infty}^{\infty} \mathrm{d}\xi' \int_{-\infty}^{\infty} \mathrm{d}\chi' \, (\xi'^2 + \chi'^2)\mathrm{e}^{-2(\xi'^2+\chi'^2)} \left(\frac{\beta}{\sqrt{(\beta-\zeta)^2 + (\xi'-\xi)^2 + (\chi'-\chi)^2}} - \frac{\alpha}{\sqrt{(\alpha-\zeta)^2 + (\xi'-\xi)^2 + (\chi-\chi)^2}}\right). \tag{H.11}$$

Changing the coordinates as done previously and using equation (H.8), we obtain

$$\begin{aligned}\delta\mathcal{I}_a &= -\frac{1}{8}\left(1 + \frac{1}{4}(\partial_\xi^2 + \partial_\chi^2)\right) \int_0^{2\pi} \mathrm{d}\phi'' \int_0^{\infty} \mathrm{d}\rho'' \, \rho'' \left(\frac{\beta}{\sqrt{(\beta-\zeta)^2 + \rho''^2}} - \frac{\alpha}{\sqrt{(\alpha-\zeta)^2 + \rho''^2}}\right) \mathrm{e}^{-2\left(\rho''^2 + \rho^2 - 2\rho\rho''\cos(\phi - \phi'')\right)} \\ &= -\frac{\pi}{4}\left(1 + \frac{1}{4}(\partial_\xi^2 + \partial_\chi^2)\right)\left(\mathrm{e}^{-2\rho^2}\int_0^{\infty} \mathrm{d}\rho'' \, \rho'' \left(\frac{\beta}{\sqrt{(\beta-\zeta)^2 + \rho''^2}} - \frac{\alpha}{\sqrt{(\alpha-\zeta)^2 + \rho''^2}}\right) J_0(\mathrm{i}4\rho\rho'')\mathrm{e}^{-2\rho''^2}\right),\end{aligned} \tag{H.12}$$

where we express again the integration over the angle through the Bessel function of the first kind. Adjusting the boundaries in the second integral, we obtain

$$\begin{aligned}\mathcal{I}_B &= \int_{-\infty}^{\infty} \mathrm{d}\xi' \int_{-\infty}^{\infty} \mathrm{d}\chi' \int_{\bar{\zeta}_\alpha(\rho')}^{\bar{\zeta}_\beta(\rho')} \mathrm{d}\zeta' \, \frac{\zeta'}{\sqrt{(\xi-\xi')^2 + (\chi-\chi')^2 + (\zeta-\zeta')^2}} \mathrm{e}^{-2(\xi'^2+\chi'^2)} \\ &= \zeta\mathcal{I}_A + \int_{-\infty}^{\infty} \mathrm{d}\xi' \int_{-\infty}^{\infty} \mathrm{d}\chi' \, \mathrm{e}^{-2(\xi'^2+\chi'^2)} \left(\sqrt{(\xi-\xi')^2 + (\chi-\chi')^2 + \left(\bar{\zeta}_\beta(\rho') - \zeta\right)^2} - \sqrt{(\xi-\xi')^2 + (\chi-\chi')^2 + \left(\bar{\zeta}_\alpha(\rho') - \zeta\right)^2}\right).\end{aligned} \tag{H.13}$$

Since the integral $\mathcal{I}_B$ only appears in the second order of the metric perturbation, it is enough to expand it to the first order in θ,

$$\mathcal{I}_B = \mathcal{I}_b + O(\theta). \tag{H.14}$$

The metric perturbation, which is given by integrating over the retarded energy–momentum tensor divided by the distance from the observer to the source point,

$$h^\lambda_{\alpha\beta} = 4G\int_{-\infty}^{\infty} \mathrm{d}\xi' \int_{-\infty}^{\infty} \mathrm{d}\chi' \int_{\bar{\zeta}_\alpha(\rho')}^{\bar{\zeta}_\beta(\rho')} \mathrm{d}\zeta' \, \frac{T^\lambda_{\alpha\beta}\left(\tau - \sqrt{(\xi-\xi')^2 + (\chi-\chi')^2 + (\zeta-\zeta')^2}, \xi', \chi', \zeta'\right)}{\sqrt{(\xi-\xi')^2 + (\chi-\chi')^2 + (\zeta-\zeta')^2}}, \tag{H.15}$$

is then found to be, expressed in terms of the integrals calculated above,

$$h^{\lambda}_{\alpha\beta} = \frac{\kappa w_0^2 P_0}{4\pi^2 c}\left(\mathcal{I}_a M_0 + \lambda\theta\frac{1}{4}\left(\begin{pmatrix} 0 & -\partial_\chi & \partial_\xi & 0 \\ -\partial_\chi & 0 & 0 & \partial_\chi \\ \partial_\xi & 0 & 0 & -\partial_\xi \\ 0 & \partial_\chi & -\partial_\xi & \end{pmatrix}\right)\mathcal{I}_a \right.$$
$$+\theta^2\left(\frac{1}{2}\left(1-\frac{1}{16}\left(\frac{1}{16}\left(\partial_\xi^4+\partial_\chi^4\right)+\frac{3}{2}\left(\partial_\xi^2+\partial_\chi^2\right)+3\right)+\frac{1}{8}\left(1+\frac{1}{4}\left(\partial_\xi^2+\partial_\chi^2\right)+\frac{1}{16}\partial_\xi^2\partial_\chi^2\right)\right)\right)\mathcal{I}_a M_0$$
$$\begin{pmatrix} 0 & \partial_\xi & \partial_\chi & 0 \\ -\partial_\xi & 0 & 0 & -\partial_\xi \\ \partial_\chi & 0 & 0 & -\partial_\chi \\ 0 & -\partial_\xi & -\partial_\chi & 0 \end{pmatrix}\mathcal{I}_b + \frac{1}{4}\begin{pmatrix} 0 & 0 & 0 & 0 \\ 0 & 1+\frac{1}{4}\partial_\chi^2 & -\frac{1}{4}\partial_\xi\partial_\chi & 0 \\ 0 & -\frac{1}{4}\partial_\xi\partial_\chi & 1+\frac{1}{4}\partial_\xi^2 & 0 \\ 0 & 0 & 0 & 0 \end{pmatrix}$$
$$\left.\mathcal{I}_a + \frac{1}{8}\left(2+\frac{1}{4}\left(\partial_\xi^2+\partial_\chi^2\right)\right)\mathcal{I}_a\begin{pmatrix} 1 & 0 & 0 & -\frac{1}{2} \\ 0 & 0 & 0 & 0 \\ 0 & 0 & 0 & 0 \\ -\frac{1}{2} & 0 & 0 & 0 \end{pmatrix}\right). \tag{H.16}$$

Appendix I. The infinitely thin beam as the limit of small beam waists in the laser beam

For $\theta = 0$, the condition $\theta\zeta \ll 1$, which is equivalent to $\theta z \ll w_0$, is satisfied also for small beam waists, more specifically for $w_0 \ll l_{\text{var}}$, where the length scale l_{var} is defined by $l_{\text{var}} = \min\{x, y\}$. In this case, only the zeroth order of the solution for the laser beam is non-zero, and one recovers the solution of the infinitely thin beam: equation (44) written in the coordinates (x, y, z) reads (as can be seen from the expression for $\mathcal{I}_a$ in appendix H)

$$I^{(0)} = \frac{\kappa P_0}{2\pi c}\int_a^b \mathrm{d}z' \int_{-\infty}^{\infty}\mathrm{d}x'\mathrm{d}y' \, \frac{1}{\sqrt{(x-x')^2+(y-y')^2+(z-z')^2}}\mathrm{e}^{-2\frac{x'^2+y'^2}{w_0^2}}. \tag{I.1}$$

Applying twice the saddle point approximation in the form

$$\lim_{N\to\infty}\int_{-\infty}^{\infty}\mathrm{d}x\, g(x)\mathrm{e}^{-Nf(x)} = \lim_{N\to\infty}\mathrm{e}^{-Nf(x_0)}g(x_0)\sqrt{\frac{2\pi}{Nf''(x)}}, \tag{I.2}$$

where x_0 is a stationnary point of f, we obtain

$$\lim_{w_0\to 0} I^{(0)} = \lim_{w_0\to 0}\frac{\kappa w_0^2 P_0}{2\pi c}\log\left(\frac{b-z+\sqrt{(b-z)^2+r^2}}{a-z+\sqrt{(a-z)^2+r^2}}\right). \tag{I.3}$$

For small enough w_0, we thus have approximately

$$I^{(0)} = \frac{\kappa w_0^2 P_0}{2\pi c}\log\left(\frac{b-z+\sqrt{(b-z)^2+r^2}}{a-z+\sqrt{(a-z)^2+r^2}}\right), \tag{I.4}$$

and, written again in dimensionless coordinates,

$$I^{(0)} = \frac{\kappa w_0^2 P_0}{2\pi c}\log\left(\frac{\beta-\zeta+\sqrt{(\beta-\zeta)^2+\rho^2}}{\alpha-\zeta+\sqrt{(\alpha-\zeta)^2+\rho^2}}\right). \tag{I.5}$$

ORCID iDs

Dennis Rätzel https://orcid.org/0000-0003-3452-6222
Daniel Braun https://orcid.org/0000-0001-8598-2039

References

[1] Aichelburg P C and Sexl R U 1971 On the gravitational field of a massless particle *Gen. Relativ. Gravit.* **2** 303–12
[2] April A 2010 Ultrashort, strongly focused laser pulses in free space *Coherence and Ultrashort Pulse Laser Emission* (London: InTechOpen) (https://doi.org/10.5772/12930)
[3] Banerjee A 1975 Cylindrically symmetric stationary beam of electromagnetic radiation *J. Math. Phys.* **16** 1188
[4] Bonnor W B 1969 The gravitational field of light *Commun. Math. Phys.* **13** 163–74
[5] Bonnor W B 1970 Spinning null fluid in general relativity *Int. J. Theor. Phys.* **3** 257–66
[6] Bonnor W B 2009 The gravitational field of photons *Gen. Relativ. Gravit.* **41** 77–85
[7] Bruschi D E 2016 On the weight of entanglement *Phys. Lett.* B **754** 182–6
[8] Calkin M G 1965 An invariance property of the free electromagnetic field *Am. J. Phys.* **33** 958–60
[9] Misner C W, Thorne K S and Wheeler J A 1973 *Gravitation* (San Francisco, CA: W H Freeman and Co.)
[10] Cullen A L and Yu P K 1979 Complex source-point theory of the electromagnetic open resonator *Proc. R. Soc. Lond.* A **366** 155–71
[11] Giovannini D, Romero J, Potoček V, Ferenczi G, Speirits F, Barnett S M, Faccio D and Padgett M J 2015 Spatially structured photons that travel in free space slower than the speed of light *Science* **347** 857–60
[12] Davis L W 1979 Theory of electromagnetic beams *Phys. Rev.* A **19** 1177–9
[13] Faraoni V and Dumse R 1999 The gravitational interaction of light: from weak to strong fields *Gen. Relativ. Gravit.* **31** 91–105
[14] Federov M V and Vintskevich S V 2017 Diverging light pulses in vacuum: Lorentz-invariant mass and mean propagation speed *Laser Phys.* **27** 036202
[15] Frolov V P and Fursaev D V 2005 Gravitational field of a spinning radiation beam pulse in higher dimensions *Phys. Rev.* D **71** 104034
[16] Goryachev M and Tobar M E 2014 Gravitational wave detection with high frequency phonon trapping acoustic cavities *Phys. Rev.* D **90** 102005
[17] Hehl F W, von der Heyde P, Kerlick G D and Nester J M 1976 General relativity with spin and torsion: foundations and prospects *Rev. Mod. Phys.* **48** 393–416
[18] Levi-Civita T 1919 *Atti Accad. Lincei Rend.* **28** 101
[19] Li J X, Salamin Y I, Hatsagortsyan K Z and Keitel C H 2016 Fields of an ultrashort tightly focused laser pulse *J. Opt. Soc. Am.* B **33** 405–11
[20] Lynden-Bell D and Bičák J 2017 Komar fluxes of circularly polarized light beams and cylindrical metrics *Phys. Rev.* D **96** 104053
[21] Maggiore M 2008 *Gravitational Waves. Theory and Experiments* vol 1 (Oxford: Oxford University Press)
[22] Mashhoon B 2003 Gravitoelectromagnetism: a brief review (arXiv:gr-qc/0311030)
[23] Mitskievic N V and Kumaradtya K K 1989 The gravitational field of a spinning pencil of light *J. Math. Phys.* **30** 1095–9
[24] Nackoney R W 1973 The gravitational influence of a beam of light. I *J. Math. Phys.* **14** 1239–47
[25] Rätzel D, Wilkens M and Menzel R 2016 The effect of entanglement in gravitational photon-photon scattering *Europhys. Lett.* **115** 51002
[26] Rätzel D, Wilkens M and Menzel R 2016 Gravitational properties of light—the gravitational field of a laser pulse *New J. Phys.* **18** 023009
[27] Rätzel D, Wilkens M and Menzel R 2017 Effect of polarization entanglement in photon-photon scattering *Phys. Rev.* A **95** 012101
[28] Rätzel D, Wilkens M and Menzel R 2017 Gravitational properties of light: the emission of counter-propagating laser pulses from an atom *Phys. Rev.* D **95** 084008

[29] Sabín C, Bruschi D E, Ahmadi M and Fuentes I 2014 Phonon creation by gravitational waves *New J. Phys.* **16** 085003
[30] Salamin Y I 2007 Fields of a gaussian beam beyond the paraxial approximation *Appl. Phys.* B **86** 319
[31] Salamin Y I, Mocken G R and Keitel C H 2002 Electron scattering and acceleration by a tightly focused laser beam *Phys. Rev. Spec. Top. Accel. Beams* **5** 101301
[32] Scully M O 1979 General-relativistic treatment of the gravitational coupling between laser beams *Phys. Rev.* D **19** 3582–91
[33] Singh S, De Lorenzo L A, Pikovski I and Schwab K C 2017 Detecting continuous gravitational waves with superfluid ^{4}He *New J. Phys.* **19** 073023
[34] Strohaber J 2013 Frame dragging with optical vortices *Gen. Relativ. Gravit.* **45** 2457–65
[35] Strohaber J 2018 General relativistic manifestations of orbital angular and intrinsic hyperbolic momentum in electromagnetic radiation (arXiv:1807.00933)
[36] Tolman R C, Ehrenfest P and Podolsky B 1931 On the gravitational field produced by light *Phys. Rev.* **37** 602–15
[37] van Holten J W 2011 The gravitational field of a light wave *Fortschr. Phys.* **59** 284–95
[38] Voronov N and Kobzarev I Y 1973 On the gravitational field of a massless particle *JETP* **39** 575
[39] Ziolkowski R W and Judkins J B 1992 Propagation characteristics of ultrawide-bandwidth pulsed gaussian beams *J. Opt. Soc. Am.* A **9** 2021–30

Erratum: The gravitational field of a laser beam beyond the short wavelength approximation

Fabienne Schneiter,[1,*] Dennis Rätzel,[2,†] and Daniel Braun[1]

[1] *Eberhard-Karls-Universität Tübingen, Institut für Theoretische Physik, 72076 Tübingen, Germany*
[2] *University of Vienna, Faculty of Physics, Boltzmanngasse 5, 1090 Vienna, Austria*

The paper contains a number of errors, most of them typos and most of them in the appendix, which we herewith correct. The main results and conclusions presented in the paper are unchanged.

- Fig. 1: The angle θ is defined as only half the angle shown. The beam waist w_0 is defined as the radius, not the diameter, of the laser beam.

- Eq. (14): The index σ should be replaced by χ.

- Section 2.1.1: The sentence "The vector potentials of well-defined helicity (...)" should read "The field tensors corresponding to the vector potentials of well-defined helicity (...)".

- Eq. (18): The factor w_0 should be removed.

- Section 2.1.1, at the end: The sentence "Note that all terms of higher than leading order in equation (17) decay (...)" should be replaced by "Note that all contributions to v_α except the leading order decay (...)".

- Eq. (36): The right hand side (rhs) has to be multiplied by $-\kappa^{-1}$, and the phrase after the equation should read "the $Q^{\lambda(n)}$ are the right hand sides of Eqs. (33), (34) and (35) for $n = 0, 1$ or $n > 1$, respectively, and the $\bar{t}^{\lambda(n)}$ are defined through the expansion $\bar{T}^{\lambda}_{\bar{\alpha}\bar{\beta}}(\xi, \chi, \theta\zeta) = \sum_{n=0}^{\infty} \theta^n \bar{t}^{\lambda(n)}_{\bar{\alpha}\bar{\beta}}(\xi, \chi, \theta\zeta)$."

- Eq. (39): The rhs has to be multiplied by w_0^2.

- Eq. (44): The rhs has to be multiplied by 2.

- Eq. (45): The rhs has to be multiplied by 1/2.

- Fig. 3 has to be updated:

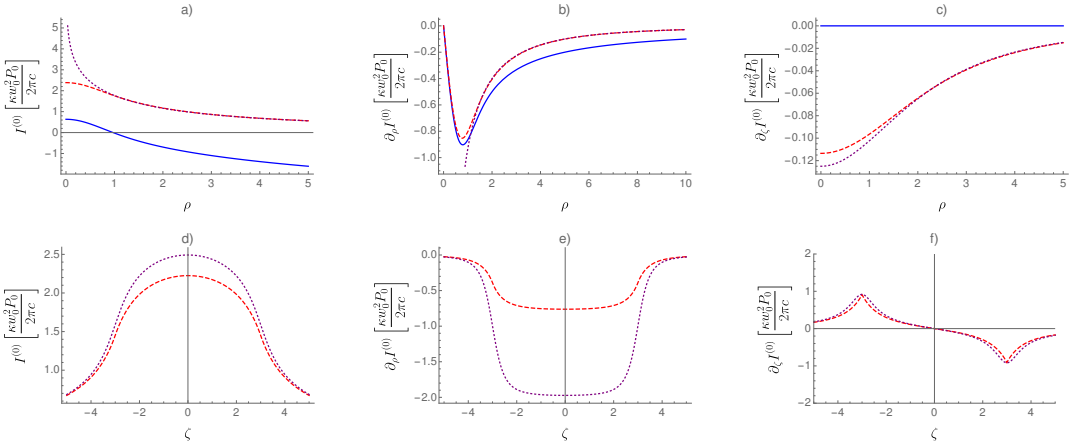

* fabienne.schneiter@uni-tuebingen.de
† dennis.raetzel@univie.ac.at

- Fig. 4 has to be updated:

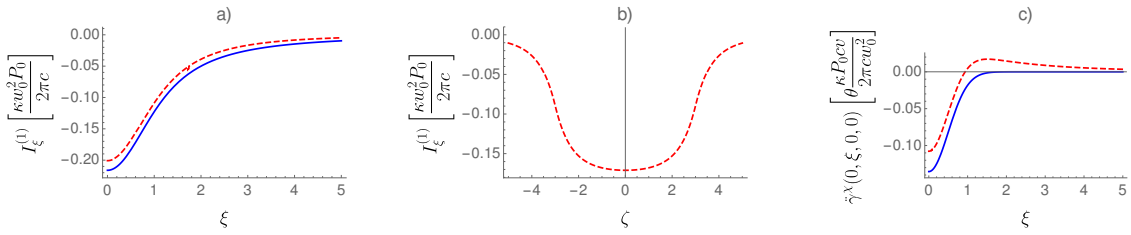

- Eq. (47): The expansion coefficients of the Riemann curvature tensor should be denoted by a small letter r, and the indices i and j should have bars.

- Eq. (48), (49) and (50): The factor $|\mu|^2$ is at the wrong position. Furthermore, the expansion coefficients of the curvature tensor should be denoted by a small r. The equations should read

$$r^{(0)}_{\tau\xi\tau\xi} = r^{(0)}_{\zeta\xi\zeta\xi} = -r^{(0)}_{\tau\xi\zeta\xi} = -\frac{\kappa w_0^2 P_0}{4\pi c}\,\frac{1}{\rho^4}\left((\xi^2-\chi^2) - \left(4|\mu|^2\xi^2\rho^2 + \xi^2 - \chi^2\right) e^{-2|\mu|^2\rho^2}\right)\,, \tag{1}$$

$$r^{(0)}_{\tau\chi\tau\chi} = r^{(0)}_{\zeta\chi\zeta\chi} = -r^{(0)}_{\tau\chi\zeta\chi} = \frac{\kappa w_0^2 P_0}{4\pi c}\,\frac{1}{\rho^4}\left((\xi^2-\chi^2) + \left(4|\mu|^2\chi^2\rho^2 - \xi^2 + \chi^2\right) e^{-2|\mu|^2\rho^2}\right)\,, \tag{2}$$

$$r^{(0)}_{\tau\xi\tau\chi} = r^{(0)}_{\zeta\xi\zeta\chi} = -r^{(0)}_{\tau\xi\zeta\chi} = -\frac{\kappa w_0^2 P_0}{2\pi c}\,\frac{\xi\chi}{\rho^4}\left(1 - (1+2|\mu|^2\rho^2)e^{-2|\mu|^2\rho^2}\right)\,. \tag{3}$$

- Eq. (51): $S^{\lambda(1)}_\xi$ and $S^{\lambda(1)}_\chi$ have to be multiplied by $1/c$.

- Eq. (64): The term ρ^4 has to be multiplied by 2.

- Eq. (68), the reference [6] in the following paragraph: It should be "Bonnor et al, Interpreting the Levi-Civita vacuum metric, Classical and Quantum Gravity 9 (1992) 2065-2068".

- Eq. (71): $\mathfrak{m}$ has to be replaced by $\mathfrak{m}'$, and in the sentence before, the rhs of the equation for $d\rho$ has to be multiplied by ρ.

- Eq. (72), the second sentence after the equation: $w_0/2$ has to be replaced by w_0.

- Eq. (73): The rhs has to be multiplied by $\rho^{-1} = (x^2+y^2)^{-\frac{1}{2}}$.

- Eq.(74) and (75) and the sentence before should read "(...) $s^\alpha = dL(0,1,0,0)$, where dL is an infinitesimal length, we obtain $a^x = \frac{c^2 dL}{2}\partial_x^2\left(\frac{1}{c^2}h_{tt} + \frac{2}{c}h_{tz} + h_{zz}\right)$, and, inserting the expressions for the metric, $a^x = \frac{4GP_0 dL}{c^3}\frac{x^2-y^2}{(x^2+y^2)^2}(1-\beta)^2$."

- Appendix A: The coordinate-indices "0" should be replaced by "τ".

- Eq. (A.28): The upper index λ of $v^{\lambda(2)}_\zeta$ is missing in the first term in the fifth line.

- Eq. (B.1): There was a wrong sign in front of one of the terms. It should read

$$\mathcal{E}^\lambda = \mathcal{E}^{(0)}\left[1 + \frac{|\mu|^2\theta^2}{2}\left(1 + |\mu|^2(2-(4|\mu|^2-3)\rho^2)\rho^2\right) + \frac{|\mu|^2\theta^4}{16}\Big(-3 + 2|\mu|^2(4-\rho^2-\rho^4)\right.$$
$$\left. +4|\mu|^4(4-\rho^2-5\rho^4)\rho^2 + 2|\mu|^6(8+52\rho^2+9\rho^4)\rho^4 - 48|\mu|^8(2+\rho^2)\rho^6 + 32|\mu|^{10}\rho^8\Big)\right]\,. \tag{4}$$

- Eqs. (B.2), (B.3) and (B.4): The left hand side has to be multiplied by $1/c$. In Eqs. (B.2) and (B.3), there are brackets missing. These two equations should read

$$\frac{S^\lambda_\xi}{c} = \mathcal{E}^{(0)}\theta|\mu|^2\left[(\theta\zeta\xi + \lambda\chi) - \frac{\theta^2}{4}\left(\lambda\chi - 2|\mu|^2\left((2-\rho^2)\theta\zeta\xi + 2(1-\rho^2)\lambda\chi + (\theta\zeta\xi+\lambda\chi)(4+3\rho^2-4|\mu|^2\rho^2)|\mu|^2\rho^2\right)\right)\right] \tag{5}$$

$$\frac{S^\lambda_\chi}{c} = -\lambda\mathcal{E}^{(0)}\theta|\mu|^2\left[(\xi - \theta\zeta\lambda\chi) - \frac{\theta^2}{4}\left(\xi - 2|\mu|^2\left(2(1-\rho^2)\xi - (2-\rho^2)\theta\zeta\lambda\chi + (\xi-\theta\zeta\lambda\chi)(4+3\rho^2-4|\mu|^2\rho^2)|\mu|^2\rho^2\right)\right)\right] \tag{6}$$

- Eq. (B.7): There was a bracket too much. It should read

$$\sigma^{\lambda}_{\xi\chi} = \mathcal{E}^{(0)}\lambda\theta^2|\mu|^4\Big[(\theta\zeta\xi+\lambda\chi)(\theta\zeta\lambda\chi-\xi) - \frac{\theta^2}{4}\Big(\theta\zeta\left(6|\mu|^2-1\right)\left(\xi^2-\chi^2\right) + 4(3|\mu|^2-2)\lambda\xi\chi \\ +2\rho^2\Big(3\theta\zeta\left(2|\mu|^2-1\right)|\mu|^2\left(\xi^2-\chi^2\right) + 2\left(6|\mu|^4-6|\mu|^2+1\right)\lambda\xi\chi + \left(4|\mu|^2-3\right)\rho^2|\mu|^4(\theta\zeta\xi+\lambda\chi)(\theta\zeta\lambda\chi-\xi)\Big)\Big)\Big] .$$

- Eqs. (B.8) and (B.9): S^{λ}_{ξ} and S^{λ}_{χ} have to be multiplied by $1/c$
- Eq. (C.5): The right hand sides of the equations for S^{λ}_{ξ}, S^{λ}_{χ} and S^{λ}_{ζ} have to be multiplied by $-c$.
- Eq. (C.8): Two factors were interchanged. It should read

$$\sigma^{\lambda}_{\chi\chi} = \mathcal{E}^{(0)}\theta^2|\mu|^4(\xi-\lambda\theta\zeta\chi)\Big[(\xi-\lambda\theta\zeta\chi) + \frac{(\theta\rho|\mu|)^2}{2}\left((8|\mu|^2-5)\xi - (8|\mu|^2-3)\lambda\theta\zeta\chi - (4|\mu|^2-3)(\xi-\lambda\theta\zeta\chi)\rho^2|\mu|^2\right)\Big] \quad (7)$$

- Eqs. (C.10) and (C.11): There was a wrong sign, a factor c missing, and an index ξ that should be replaced by χ. They should read

$$\sigma^{\lambda}_{\xi\zeta} = S^{\lambda}_{\xi}/c - \mathcal{E}^{(0)}\frac{(\theta\rho|\mu|)^2}{2}\theta(\theta\zeta\xi+\lambda\chi)|\mu|^2 \quad \text{and} \quad \sigma^{\lambda}_{\chi\zeta} = \mathrm{S}^{\lambda}_{\chi}/\mathrm{c} + \mathcal{E}^{(0)}\lambda\frac{(\theta\rho|\mu|)^2}{2}\theta(\xi-\lambda\theta\zeta\chi)|\mu|^2 \quad (8)$$

- Eq. (D.4) should read $h \sim \epsilon + \theta\epsilon + \theta^2\epsilon + \theta^3\epsilon + \theta^4\epsilon$. Accordingly, the sentence in the paragraph below should be changed to "In our case, this condition translates to $\epsilon \ll \theta^4$."
- Eq. (D.5) should read $8\pi GP/c^5 \ll \theta^4$. Then, the sentence below should be changed to "For a power of the order of magnitude $P \sim 10^{15}$ W, we thus have to require $\theta \gg 10^{-10}$."
- Appendix E, first line and the sentence after Eq. (E.1): The indices of the metric perturbation should have bars. The metric perturbation should have a superscript "$\lambda(n)$" instead of "n".
- Eq. (E.2): The indices "0" should be replaced by "τ" and the third equation in the left column should read

$$r^{\lambda(n)}_{\bar{j}\zeta\bar{k}\zeta} = \frac{1}{2}\left(\partial_{\theta\zeta}\partial_{\bar{k}}h^{\lambda(n-1)}_{\bar{j}\zeta} - \partial^2_{\theta\zeta}h^{\lambda(n-2)}_{\bar{j}\bar{k}} + \partial_{\theta\zeta}\partial_{\bar{j}}h^{\lambda(n-1)}_{\bar{k}\zeta} - \partial_{\bar{j}}\partial_{\bar{k}}h^{\lambda(n)}_{\zeta\zeta}\right) , \quad (9)$$

- Eq. (F.7) and Eq. (F.8): There are two factors 2 missing in each of them and there is a wrong sign in Eq. (F.8). They should read

$$h^{\lambda(2)}_{\xi\xi} = \frac{\kappa w_0^2 P_0}{32\pi\rho^4|\mu|^2 c}\Big(2\rho^4|\mu|^2\mathrm{Ei}\left(-2|\mu|^2\rho^2\right) - 4\rho^4|\mu|^2\log(\rho) + (\xi^2-\chi^2) - 2(\xi^2-\chi^2-2\theta\zeta\lambda\xi\chi)|\mu|^2 \\ + \left(-(\xi^2-\chi^2) + 2(\xi^2-\chi^2-2\theta\zeta\lambda\xi\chi-2\rho^2\xi^2)|\mu|^2 + 4\rho^2(\xi^2-\chi^2-2\theta\zeta\lambda\chi\xi)|\mu|^4\right)e^{-2|\mu|^2\rho^2}\Big) , \quad (10)$$

$$h^{\lambda(2)}_{\chi\chi} = \frac{\kappa w_0^2 P_0}{32\pi\rho^4|\mu|^2 c}\Big(2\rho^4|\mu|^2\mathrm{Ei}\left(-2|\mu|^2\rho^2\right) - 4\rho^4|\mu|^2\log(\rho) - (\xi^2-\chi^2) + 2(\xi^2-\chi^2-2\theta\zeta\lambda\xi\chi)|\mu|^2 \\ - \left(-(\xi^2-\chi^2) + 2(\xi^2-\chi^2-2\theta\zeta\lambda\xi\chi+2\rho^2\chi^2)|\mu|^2 + 4\rho^2(\xi^2-\chi^2-2\theta\zeta\lambda\chi\xi)|\mu|^4\right)e^{-2|\mu|^2\rho^2}\Big) . \quad (11)$$

- Eq. (F.9): There is a factor two missing in front of the term $\rho^2|\mu|^2$.
- Eqs. (F.11) and (F.13): In each of them there is a wrong sign and χ's have to be replaced/interchanged with ξ's in a few terms. The equations should read

$$h^{\lambda(3)}_{\tau\chi} = -\frac{\kappa P_0 w_0^2}{32\pi c\rho^2}\Big((4\theta\zeta\chi-3\lambda\xi) + \Big(-(4\theta\zeta\chi-3\lambda\xi) - 2\rho^2(3\theta\zeta\chi-2\lambda\xi)|\mu|^2 \\ -2\rho^2(-2+3\rho^2)(\theta\zeta\chi-\lambda\xi)|\mu|^4 + 8\rho^4(\theta\zeta\chi-\lambda\xi)|\mu|^6\Big)e^{-2|\mu|^2\rho^2}\Big) , \quad (12)$$

$$h^{\lambda(3)}_{\zeta\chi} = \frac{\kappa P_0 w_0^2}{32\pi c\rho^2}\Big((2\theta\zeta\chi-\lambda\xi) + \Big(-(2\theta\zeta\chi-\lambda\xi) - 2\rho^2(2\theta\zeta\chi-\lambda\xi)|\mu|^2 \\ -2\rho^2(-2+3\rho^2)(\theta\zeta\chi-\lambda\xi)|\mu|^4 + 8\rho^4(\theta\zeta\chi-\lambda\xi)|\mu|^6\Big)e^{-2|\mu|^2\rho^2}\Big) . \quad (13)$$

- Eq. (F.14): The rhs has to be multiplied by $2/\kappa$.
- Appendix G: The coordinate "η" should be called "χ".
- Eq. (G.4), two lines after, E_0^2 in the constant C_1 should be replaced by P_0.
- Eq. (G.9): P_0 should read P_0^a.
- Eq. (H.1): Expanded up to second order in θ, the phase should read

$$\varphi(\rho,\zeta) = \theta\zeta\left(\rho^2-1\right) + \frac{2}{\theta}\zeta + \mathrm{sgn}(\zeta)\frac{\pi}{2}\,. \tag{14}$$

  The sentence before Eq. (H.1) should read "The phase of the electric field of the Gaussian beam (...)".
- Eq. (H.4), the sentence before: It should read "Introducing for any coordinate $u \in \{\xi,\chi,\zeta\}$ a shifted coordinate u'' by $u'' = u' - u$, and changing to cylindrical coordinates $(\xi'',\chi'',\zeta'') = (\rho''\cos(\phi''),\rho''\sin(\phi''),z'')$, we obtain, with $\alpha'' = \alpha - \zeta$ and $\beta'' = \beta - \zeta$,".
- Eq. (H.7): After the equation, we should insert "The third integral we define is" and the equation

$$\mathcal{I}_c = \int_{-\infty}^{\infty} d\xi' \int_{-\infty}^{\infty} d\chi' \int_{\alpha}^{\beta} d\zeta' \, \frac{\zeta'^2}{\sqrt{(\xi-\xi')^2+(\chi-\chi')^2+(\zeta-\zeta')^2}} e^{-2(\xi'^2+\chi'^2)}\,. \tag{15}$$

  Accordingly, the sentence in parenthesis before Eq. (H.8) should read "(and correspondingly for $\mathcal{I}_b$ or $\mathcal{I}_c$)".
- Eq. (H.9): In the second line, the integral $\int_{-\infty}^{\infty} dy'$ should be replaced by $-\int_{-\infty}^{\infty} d\chi'$.
- Eq. (H.12): The factors $\left(1+\frac{1}{4}\left(\partial_\xi^2+\partial_\chi^2\right)\right)$ should be replaced by $\left(2+\frac{1}{4}\left(\partial_\xi^2+\partial_\chi^2\right)\right)$.
- Eq. (H.14), sentence before the equation: "first order" should read "lowest order".
- Eq. (H.15): The rhs has to be multiplied by c^{-4}.
- Eq. (H.16): There are a few typos and terms missing in the equation. It should read

$$\begin{aligned} h^{\lambda}_{\alpha\beta} = \frac{\kappa w_0^2 P_0}{2\pi^2 c}\Bigg[& \mathcal{I}_a \begin{pmatrix} 1 & 0 & 0 & -1 \\ 0 & 0 & 0 & 0 \\ 0 & 0 & 0 & 0 \\ -1 & 0 & 0 & 1 \end{pmatrix} + \frac{\lambda\theta}{4} \begin{pmatrix} 0 & \partial_\chi & -\partial_\xi & 0 \\ \partial_\chi & 0 & 0 & -\partial_\chi \\ -\partial_\xi & 0 & 0 & \partial_\xi \\ 0 & -\partial_\chi & \partial_\xi & 0 \end{pmatrix} \mathcal{I}_a \\ & + \frac{\theta^2}{4}\Bigg(\left(\frac{1}{2}\left(\partial_\xi^2+\partial_\chi^2\right)\mathcal{I}_c + \left(1 - \frac{1}{4}\left(\partial_\xi^2+\partial_\chi^2\right) - \frac{2}{16^2}\left(\partial_\xi^2+\partial_\chi^2\right)^2\right)\mathcal{I}_a + 4\delta\mathcal{I}_a \right) \begin{pmatrix} 1 & 0 & 0 & -1 \\ 0 & 0 & 0 & 0 \\ 0 & 0 & 0 & 0 \\ -1 & 0 & 0 & 1 \end{pmatrix} \\ & + \left(1+\frac{1}{8}\left(\partial_\xi^2+\partial_\chi^2\right)\right)\mathcal{I}_a \begin{pmatrix} 2 & 0 & 0 & -1 \\ 0 & 0 & 0 & 0 \\ 0 & 0 & 0 & 0 \\ -1 & 0 & 0 & 0 \end{pmatrix} + \begin{pmatrix} 0 & \partial_\xi & \partial_\chi & 0 \\ \partial_\xi & 0 & 0 & -\partial_\xi \\ \partial_\chi & 0 & 0 & -\partial_\chi \\ 0 & -\partial_\xi & -\partial_\chi & 0 \end{pmatrix} \mathcal{I}_b + \begin{pmatrix} 0 & 0 & 0 & 0 \\ 0 & 1+\frac{1}{4}\partial_\chi^2 & -\frac{1}{4}\partial_\xi\partial_\chi & 0 \\ 0 & -\frac{1}{4}\partial_\xi\partial_\chi & 1+\frac{1}{4}\partial_\xi^2 & 0 \\ 0 & 0 & 0 & 0 \end{pmatrix} \mathcal{I}_a \Bigg)\Bigg]\,. \end{aligned} \tag{16}$$

- Eq. (I.1): The rhs has to be multiplied by π^{-1}.
- Eq. (I.3), (I.4) and (I.5): The rhs of the equations have to be multiplied by $1/2$.

[D] Rotation of polarization in the gravitational field of a focused laser beam - Faraday effect and optical activity

Fabienne Schneiter, Dennis Rätzel, Daniel Braun
arXiv: 1812.04505

Rotation of polarization in the gravitational field of a laser beam - Faraday effect and optical activity

Fabienne Schneiter,[1,*] Dennis Rätzel,[2,†] and Daniel Braun[1]

[1] *Eberhard-Karls-Universität Tübingen, Institut für Theoretische Physik, 72076 Tübingen, Germany*
[2] *Institut für Physik, Humboldt-Universität zu Berlin, 12489 Berlin, Germany*

We investigate the rotation of the polarization of a light ray propagating in the gravitational field of a circularly polarized laser beam. The rotation consists of a reciprocal part due to gravitational optical activity, and a non-reciprocal part due to the gravitational Faraday effect. We discuss how to distinguish the two effects: Letting light propagate back and forth between two mirrors, the rotation due to gravitational optical activity cancels while the rotation due to the gravitational Faraday effect accumulates. In contrast, the rotation due to both effects accumulates in a ring cavity and a situation can be created in which gravitational optical activity dominates. Such setups amplify the effects by up to five orders of magnitude, which however is not enough to make them measurable with state of the art technology. The effects are of conceptual interest as they reveal gravitational spin-spin coupling in the realm of classical general relativity, a phenomenon which occurs in perturbative quantum gravity.

I. INTRODUCTION

The gravitational field of a light beam was first studied in 1931 by Tolman, Ehrenfest and Podolski [1], who described the laser beam in the simplest way, namely as a single light ray of constant energy density and without polarization. Since then, various models for light beams have been considered, such as in [2–4], all of them having in common that the short-wavelength approximation is used. This means that the light is either described as a thin pencil or as a continuous fluid moving at the speed of light and without any wave-like properties. Recently, we studied the gravitational field of a laser beam beyond the short-wavelength approximation [5]: The laser beam is modeled as a solution of Maxwell's equations, and therefore, has wave-like properties. In this case, there appear gravitational effects of light that were not visible in the previous models, such as frame-dragging due to the light's spin angular-momentum, the deflection of a parallel propagating test ray, and the rotation of polarization of test rays. The latter is the subject of this article.

Effects of gravitational rotation of polarization were first described in 1957 independently by Skrotsky [6] and by Balazs [7]. In 1960, Plebanski found a coordinate-invariant expression for the change of the polarization for a light ray coming from flat spacetime, passing through a weak gravitational field, and going to flat spacetime again [8]. The gravitational rotation of polarization has been studied for several systems: for moving objects, moving gravitational lenses [9–11] and other astrophysical situations [12, 13], in the context of gravitational waves [14], for rotating rings [15], for ring lasers [16] and for linearly polarized lasers in a waveguide [17]. It was also treated more formally in [18–20].

Rotation of polarization is well-known from classical optics, when light rays pass through certain media (see e.g.[21]). For this, the medium needs broken inversion symmetry, a property certain materials have naturally. Such media with "natural optical activity" lead to different phase velocities of right- and left-circularly polarized light. The effect is "reciprocal", i.e. when the light ray is reflected back through the medium, the rotation of polarization is undone. In contrast hereto is the Faraday effect, which can be created even in isotropic media by applying a magnetic field. Here, the rotation is "non-reciprocal", i.e. the polarization keeps rotating in the same direction relative to the original frame when the light propagates back along the path. In this article, we consider the rotation of the polarization vector of test rays in the gravitational field of a circularly polarized laser beam in free space. It turns out that the rotation of polarization contains both a reciprocal and a non-reciprocal part. The former can hence be interpreted as gravitational optical activity and the latter as a gravitational Faraday effect, also called Skrotsky effect.

The laser beam is described as a perturbative solution to Maxwell's equations, an expansion in the beam divergence angle θ, which is assumed to be smaller than one radian. The description of the laser beam and its gravitational field is given in detail in [5] and summarized below. We look at the rotation of the polarization of test rays which are parallel co-propagating, parallel counter-propagating, or propagating transversally to the beamline of the source laser-beam, and consider a cavity where the rotation of the polarization vector accumulates after each roundtrip. We thus propose a measurement scheme which may possibly be realized in a laboratory in the future, when the sensitivity in experiments has improved accordingly.

The description of the gravitational field of a laser beam is reviewed in section II, and the calculation of the rotation of light polarization in curved spacetime in section III. In section IV, we calculate the Faraday effect for test rays. As already mentioned, only the non-reciprocal

* fabienne.schneiter@uni-tuebingen.de
† dennis.raetzel@physik.hu-berlin.de

part of the rotation which is not due to the deflection can be associated with the Faraday effect, which is discussed in section V. Considering a cavity in a certain arrangement, the rotation angles acquired after each roundtrip of the light inside the cavity sum up. This is the subject of section VI, where we look at a one-dimensional cavity and a ring cavity and discuss the possible measurement precision of the rotation angle. We give a conclusion and an outlook in section VII.

To keep track of the orders of magnitude, we introduce dimensionless coordinates by dividing them by the beam waist w_0 as $\tau = ct/w_0$, $\xi = x/w_0$, $\chi = y/w_0$ and $\zeta = z/w_0$, where c is the speed of light. Greek indices like x^α refer to dimensionless spacetime coordinates and latin indices like x^a refer to dimensionless spatial coordinates. For the spacetime metric, we choose the sign convention $(-,+,+,+)$, such that the Minkowski metric η in the dimensionless coordinates reads $\eta = w_0^2\mathrm{diag}(-1,1,1,1)$. In the numerical examples and plots, we use the following values: the beam waist $w_0 = 10^{-6}\,\mathrm{m}$, the beam divergence $\theta = 0.3\,\mathrm{rad}$ (this determines the wavelength, which is given by $\pi\theta w_0 \simeq 1\,\mu\mathrm{m}$), the polarization $\lambda = 1$, and the power of the source laser-beam, which is directed in the positive z-direction, $P_0 = 10^{15}\,\mathrm{W}$.

II. THE GRAVITATIONAL FIELD OF A LASER BEAM BEYOND THE SHORT WAVELENGTH APPROXIMATION

In this section, we summarize the description of the laser beam and its gravitational field presented in [5]. A laser beam is accurately described by a Gaussian beam. The Gaussian beam is a monochromatic electromagnetic, almost plane wave whose intensity distribution decays with a Gaussian factor with the distance to the beamline. It is obtained as a perturbative solution of Maxwell's equations, namely an expansion in the beam divergence θ, the opening angle of the beam, which is assumed to be smaller than one radian. The electromagnetic four-vector potential describing the Gaussian beam is obtained by a plane wave multiplied by an envelope function that is assumed to vary slowly in the direction of propagation, in agreement with the property that the divergence of the beam is small. Corresponding to these features, one makes the ansatz for the four-vector potential $A_\alpha(\tau,\xi,\chi,\zeta) = \tilde{\mathcal{A}} v_\alpha(\xi,\chi,\theta\zeta)e^{i\frac{2}{\theta}(\zeta-\tau)}$, where $\tilde{\mathcal{A}}$ is the amplitude and v_α the envelope function.[1] The exponential factor describes a plane wave propagating in ζ-direction with wave number $k = 2/(\theta w_0)$, where w_0 is the beam waist at its focal point. The laser beam propagates in positive ζ-direction such that its beamline concides with the ζ-axis. The beam is illustrated in figure 1.

[1] More precisely, the complex-valued vector potential A we consider is the analytical signal of the real-valued physical vector potential, which is obtained by taking the real part of A.

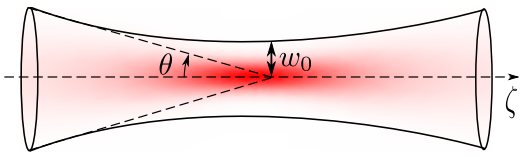

Figure 1. Schematic illustration of the laser beam propagating in the positive ζ-direction: The beam divergence θ describes the opening angle of the laser beam and is assumed to be a small parameter (smaller than 1 rad), and the beam waist w_0 is a measure for the radius of the laser beam at its focal point. The intensity of the laser beam decreases with a Gaussian factor with the distance from the beamline.

Like the four-vector potential for any radiation, A_α satisfies the Maxwell equations, which, in vacuum, are given by the wave equations

$$\left(-\partial_\tau^2 + \partial_\xi^2 + \partial_\chi^2 + \partial_\zeta^2\right) A_\mu(\tau,\xi,\chi,\zeta) = 0\,, \qquad (1)$$

where the Lorenz-gauge condition is chosen. Since the envelope function varies slowly in the direction of propagation, the wave equations (1) reduce to a Helmholtz equation for each component of the envelope function,

$$\left(\partial_\xi^2 + \partial_\chi^2 + \theta^2\partial_{\theta\zeta}^2 + 4iw_0\partial_{\theta\zeta}\right) v_\alpha(\xi,\chi,\theta\zeta) = 0\,. \qquad (2)$$

This Helmholtz equation is solved by writing the envelope function as a power series in the small parameter θ. One obtains an equation for each order of the expansion of the envelope function, with a source term consisting of the solution for a lower order, where even and odd orders do not mix. The beam is assumed to have left- or right-handed circular polarization, which we label by $\lambda = \pm 1$.[2] We define this to be the case if its field strength, defined as $F_{\alpha\beta} = \partial_\alpha A_\beta - \partial_\beta A_\alpha$, is an eigenfunction with eigenvalue ± 1 of the generator of the duality transformation of the electromagnetic field given by $F_{\alpha\beta} \mapsto -i\epsilon_{\alpha\beta\gamma\delta}F^{\gamma\delta}/2$, where $\epsilon_{\alpha\beta\gamma\delta}$ is the completely anti-symmetric tensor with $\epsilon_{0123} = -1$. Our definition of helicity is based on the invariance of Maxwell's equations under the duality transformation and the conservation of the difference between photon numbers of right- and left-polarized photons shown in [22] (see also [23–26]). For $\theta = 0$, this leads to the usual expressions for the field strength of a circularly polarized laser beam.

It turns out that the energy-momentum tensor, which one may expect to be oscillating at the frequency of the laser beam, does not contain any oscillating terms when

[2] The vector potential describing the laser beam thus depends on the parameter λ, and so do its energy-momentum tensor, the induced metric perturbation and the effects we calculate in the following sections. Therefore, these quantities can be thought of as being labelled by an index λ, which we suppress in the following, except for appendix A, where we write the index λ explicitly.

circular polarization is assumed. The energy-momentum tensor reads (see appendix A for the explicit expressions)

$$T_{\alpha\beta} = \frac{c^2\epsilon_0}{2}\,\mathrm{Re}\left(F_\alpha{}^\sigma F^*_{\beta\sigma} - \frac{1}{4}\eta_{\alpha\beta}F^{\delta\rho}F^*_{\delta\rho}\right). \qquad (3)$$

The power series expansion of the envelope function induces a power series expansion of the energy-momentum tensor and the expansion coefficients are identified as different order terms of $T_{\alpha\beta}$ in θ.

Since the energy density of a laser beam is small compared to the one of ordinary matter, one may expect its gravitational field to be weak. The spacetime metric describing the gravitational field is thus assumed to consist of the metric for flat spacetime $\eta_{\alpha\beta}$ plus a small perturbation $h_{\alpha\beta}$. Terms quadratic in the metric perturbation are neglected; this is the linearized theory of general relativity. In this case, the Einstein field equations reduce to wave equations for the metric perturbation [27]

$$\frac{1}{w_0^2}\left(-\partial_\tau^2 + \partial_\xi^2 + \partial_\chi^2 + \partial_\zeta^2\right)h_{\alpha\beta} = -\frac{16\pi G}{c^4}T_{\alpha\beta}\,, \qquad (4)$$

where G is Newton's constant and where the Lorenz-gauge has been chosen. Like the envelope function and the energy-momentum tensor, the metric perturbation is expanded in the beam divergence,

$$h_{\alpha\beta}(\xi,\chi,\theta\zeta) = \sum_{n=0}^{\infty}\theta^n h^{(n)}_{\alpha\beta}(\xi,\chi,\theta\zeta)\,. \qquad (5)$$

For a laser beam extending from minus to plus spatial infinity, the wave equations (4) result in a two-dimensional Poisson equation for each $h^{(n)}_{\alpha\beta}$, with a source term consisting of a term of the energy-momentum tensor of the same order and a term proportional to $h^{(n-2)}_{\alpha\beta}$, where even and odd orders do not mix. Details and the solutions for the zeroth, the first and the third order, which are relevant for our purposes, are given in appendix A.

For a finitely extended source beam, the solution of (4) with time-independent energy-momentum tensor of the source laser-beam can be calculated using the Green's function of the three-dimensional Poisson equation,

$$h_{\alpha\beta} = \frac{4Gw_0^2}{c^4}\int d\xi' d\chi' d\zeta' \frac{T_{\alpha\beta}\left(\xi',\chi',\theta\zeta'\right)}{|\vec{x}-\vec{x}'|}\,, \qquad (6)$$

where $\vec{x} = (\xi,\chi,\zeta)$ and $\vec{x}' = (\xi',\chi',\zeta')$. The solution (6) is discussed in detail in [5].

III. ROTATION OF POLARIZATION IN A WEAKLY CURVED SPACETIME

In this section, we explain the expression presented in [8] for the rotation angle that the polarization vector of a test ray acquires when propagating in a gravitational field.

For a light ray propagating through a gravitational field and starting and ending at spatial infinity, the rotation angle of polarization within a plane perpendicular to the propagation direction (in the following called ray-transverse plane) is given by equation (5.33) in [8]. For our set of coordinates, it takes the form

$$\Delta = \frac{1}{2w_0^2}\int_{-\infty}^{\infty} d\tau\; t_0^a\epsilon_{abc}\partial_b h_{c\alpha}(\tau, \varrho_\perp + \tau t_0)t_0^\alpha\,, \qquad (7)$$

where ϵ_{abc} is the Levi-Civita symbol in three dimensions with $\epsilon_{123} = 1$, $t_0^a = \dot{\gamma}^a(\tau_0)$ is the initial tangent to the curve describing the light ray parametrized by the dimensionless parameter τ, and the line $\varrho_\perp + \tau t_0$ with $\varrho_\perp = (\xi_0,\chi_0,0)$ constant is equivalent to the spatial part of the ray γ including terms up to linear order in the metric perturbation. Therefore, the evaluation of the metric perturbation along the line $\varrho_\perp + \tau t_0$ instead of γ the actual, possibly deflected trajectory of a light ray in the gravitational field of the source is justified as the correction would be of higher order in the metric perturbation.

The sign of the rotation angle Δ is chosen such that the positive sign refers to right-handedness (handedness of rotation as inferred from equation (5.20) of [8]). Equation (7) was obtained using the formal analogy of Maxwell's equations in a dielectric medium and Maxwell's equations in a gravitational field and using geometric ray optics for vectors. It is shown in [8] that the expression in equation (7) is invariant under coordinate transformations that approach the identity at spatial infinity. For equation (7) to be valid, the metric perturbation and all its first derivatives have to vanish at least as $\tilde{\rho}^{-1}$ for $\tilde{\rho}\to\infty$, where $\tilde{\rho} = \sqrt{\xi^2+\chi^2+\zeta^2}$.

For a light ray that is not deflected by the gravitational field, i.e. that does not change its direction of propagation, the ray-transverse plane is the same everywhere far away from the laser beam, where spacetime is flat. However, when the light ray is deflected, this plane is tilted after passing the gravitational field with respect to the one before entering the gravitational field. Therefore, the rotation of the polarization vector within the ray-transverse plane given in equation (7) is superimposed with a change of the polarization vector $\delta\vec{\omega}$ due to the deflection of the light ray. The latter consists of a rotation plus a deformation which depend on the initial polarization vector $\vec{\omega}$.[3] It does not contribute to the gravitational Faraday effect or the optical activity. An experimentalist who wants to measure these effect would thus have to correct for the deflection effects. The change of the polarization vector is illustrated in figure 2.

[3] See section 6 in [8].

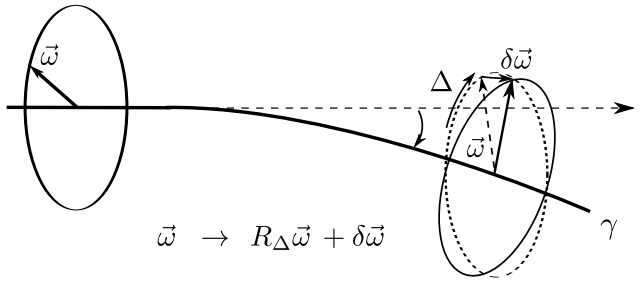

Figure 2. Change of the initial polarization vector $\vec{\omega}$ of a light ray γ: The initial polarization vector $\vec{\omega}$ in the initial ray-transverse plane (represented by the solid circle on the left and the dashed circle on the right) is rotated by the angle Δ into $R_\Delta\vec{\omega}$ (dashed arrow on the right) due to the gravitational field, where R_Δ is the corresponding rotation matrix. Additionally, the deflection of the laser beam tilts the ray-transverse plane into its final orientation (solid circle on the right) such that it stays orthogonal to the tangent of the deflected laser beam. The tilt leads to an additional change $\delta\vec{\omega}$ of the polarization vector $\vec{\omega}$. The rotation by the angle Δ consists of a reciprocal part due to the gravitational optical activity and a non-reciprocal part due to the gravitational Faraday effect.

Another approach how to describe the rotation of polarization is described in appendix B. It agrees with the results presented in this section.

For a linearly polarized test ray, the interpretation of the rotation of the polarization vector is clear: For example, for a test light-ray propagating in ζ-direction, the polarization vector describing linear polarization in ξ-direction, $\vec{\epsilon}_\xi = (1,0,0)$, is rotated into $R_\Delta\vec{\epsilon}_\xi = (\cos(\Delta),\sin(\Delta),0)$, where R_Δ stands for the matrix rotating by the angle Δ about the ζ-axis. For a circularly polarized test ray with helicity $\lambda_{\text{test}} = \pm 1$ and with the corresponding polarization vector $\vec{\epsilon}_{\lambda_{\text{test}}} = (1, -\lambda_{\text{test}} i, 0)/\sqrt{2}$, one obtains $R_\Delta\vec{\epsilon}_{\lambda_{\text{test}}} = e^{i\lambda_{\text{test}}\Delta}\vec{\epsilon}_{\lambda_{\text{test}}}$. This means that the circularly polarized test ray acquires the phase $\lambda_{\text{test}}\Delta$. In general, for an elliptically polarized test light ray, the acquired phases of the circular components lead to a rotation of the major axis of the ellipse by an angle Δ.

IV. ROTATION OF POLARIZATION IN THE GRAVITATIONAL FIELD OF A LASER BEAM

In this section, we investigate the rotation of the polarization vector of a test ray passing through the gravitational field of a source laser-beam according to equation (7).

We consider different orientations of the test ray with respect to the source beam: parallel co-propagating, parallel counter-propagating, and transversal test rays. We find that the effect depends strongly on the orientation of the test ray. In particular, we obtain that the order of the metric expansion[4] that causes the rotation of polarization depends on the orientation of the test ray.

The source laser-beam is assumed to propagate along the ζ-axis, to be emitted at $\zeta = \alpha$ and absorbed at $\zeta = \beta$. The parallel co-propagating test ray is emitted at $\zeta = A$ and absorbed at $\zeta = B$ and the parallel counter-propagating test ray is emitted at $\zeta = B$ and absorbed at $\zeta = A$. The test ray that is oriented transversally to the beamline of the source laser-beam is emitted at $\xi = A$ and absorbed at $\xi = B$ or vice versa.

In subsection IV A we focus on an ideal situation of infinitely long test rays. The source laser-beam is considered to be either finitely or infinitely extended. In subsection IV B we look at finitely long test rays and a finitely extended source laser-beam, and we discuss the the long-range behavior of the rotation of polarization of the test rays. In subsection IV C, we discuss the gravitational coupling between the spin of the source laser-beam and the spin of the test ray.

A. Infinitely extended test ray

For the infinitely extended test rays, the conditions for the application of equation (7) are immediately seen to be fulfilled for the finitely extended source beam, as the metric perturbation and all its first derivatives vanish at least as $\tilde{\rho}^{-1}$ for $\tilde{\rho} \to \infty$. This follows directly from the Green's function which is proportional to $1/\tilde{\rho}$ in three dimensions.

For the parallel test rays, for an infinitely extended source beam and an infinitely extended test ray it will always be understood that the emitter and absorber of the test ray are sent to infinity more rapidly than those of the source-beam, i.e. $|A|, |B| \gg |\alpha|, |\beta| \to \infty$, such that also here the test ray indeed begins and ends in flat spacetime. For the transversal test rays, for an infinitely extended source beam and infinitely extended test rays, it is assumed that $|A|$ and $|B|$ approach infinity fast enough for them to be in flat spacetime.

Besides the strict validity of equation (7), the infinite test-ray has also the advantage to lead to relatively simple analytical expressions for the rotation angles.

1. *Parallel test rays*

We start by looking at the rotation of the polarization vector of test rays which are parallel co-propagating or counter-propagating with respect to the source laser-beam as illustrated in figure 3.

[4] Generally, with the order of the metric expansion, we refer to the order in θ. Any higher order terms of the metric perturbation itself are neglected in the linearized theory of general relativity.

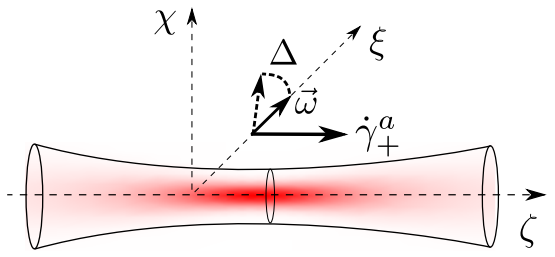

Figure 3. Schematic illustration of the rotation of the polarization vector $\vec{\omega}$ (here it originally has only a component in ξ-direction) of a parallel co-propagating test ray with tangent $\dot\gamma_+$ in the gravitational field of the laser beam.

The parallel co- and counter-propagating test rays are assumed to have a distance $\rho = \sqrt{\xi^2 + \chi^2}$ from the beamline, and to travel from $\zeta = -\infty$ to $\zeta = \infty$ and from $\zeta = \infty$ to $\zeta = -\infty$, respectively. They are considered to have transversal polarization described by the polarization vector $w^\mu = (0, w^\xi, w^\chi, 0)$. The initial tangents to their worldlines are given by $\dot\gamma_\pm(\tau_0) = (1, 0, 0, \pm(1 - f^\pm))$, where the "+" corresponds to the co-propagating test ray and the "−" to the counter-propagating test ray. The parameter $f^\pm$ ensures that $\dot\gamma_\pm$ satisfies the null condition. It is proportional to the metric perturbation, which means that it does not contribute in equation (7) and can be neglected in the following calculations. Since the integration in equation (7) is along the line $\varrho_\perp + \tau t_0 = (\xi_0, \chi_0, \pm\tau)$, we can change the integration variable from τ to ζ when neglecting terms quadratic in the metric perturbation. Then, for the parallel propagating test rays we obtain (see equation (D1))

$$\Delta_\pm = -\frac{1}{2w_0^2}\int_{-\infty}^{\infty} d\zeta \Big(\partial_\chi \left(h_{\xi\zeta} \pm h_{\tau\xi}\right) - \partial_\xi \left(h_{\chi\zeta} \pm h_{\tau\chi}\right)\Big) . \tag{8}$$

Notice that the metric perturbation contains a factor w_0^2, such that $\Delta_\pm$ is dimensionless. For the co-propagating test ray, the contribution coming from the first order of the metric perturbation cancels, and one obtains in leading order (the third order in θ)

$$\Delta_+ = \lambda \frac{G P_0 \theta^3}{c^5} \int_\alpha^\beta d\zeta\, |\mu|^2 (1 + 2|\mu|^2\rho^2) e^{-2|\mu|^2\rho^2} , \tag{9}$$

where $|\mu|^2 = (1 + (\theta\zeta)^2)^{-1}$. Note that ζ in (9) parametrizes the source beam (i.e. corresponds to ζ' in (6)). The derivation of (9) (see appendix E for details) uses an asymptotic expansion in $1/B$, i.e. assumes that $B \gg |\zeta'|, |\rho'|$, as well as a finite cut-off ρ_0 of the energy density in radial direction that is then sent to infinity. The expression with ρ_0 kept finite is given by (E15). For an infinitely extended source beam, we can then simply evaluate the limit $\alpha \to -\infty$ and $\beta \to \infty$. An alternative derivation that starts from an infinitely extended source beam and an infinitely extended test ray is given in appendix D.

The integrand in (9) decreases as a Gaussian with the distance to the beamline. The Gaussian factor is the same as the one that appears as a global factor in the energy-momentum tensor of the source beam (see [5] or appendix A), which implies that significant contributions to Δ_+ for the infinitely extended test ray are only accumulated in regions where the energy distribution of the source beam does not vanish. In addition, (E15) shows that there is no effect outside of a finite beam when a cut-off of the energy-momentum distribution is considered.

The sign of the rotation angle in equation (9) depends on λ, which specifies the handedness of the light in the source laser-beam. The dependence of the rotation angle Δ_+ on the distance to the beamline is illustrated in the upper graph of figure 4.

For the counter-propagating test ray, we obtain in leading order (the first order in θ)

$$\Delta_- = -\lambda \frac{8 G P_0 \theta}{c^5} \int_\alpha^\beta d\zeta\, |\mu|^2 e^{-2|\mu|^2\rho^2} . \tag{10}$$

for the finitely extended source beam and the infinitely extended test ray. Equation (10) is derived with the same limiting procedures as (9). Its version with finite radial cut-off of $T_{\mu\nu}$ is given in (E8). The integrand in equation (10) decreases in the same way as the one in equation (9) with the same Gaussian factor with the distance to the beamline that can be found as a global factor in the energy-momentum tensor of the laser beam. We find that there are no significant contributions to the rotation angle Δ_- outside of the energy distribution for an infinitely extended test ray (see equation (E8)) when introducing a cut-off of the energy-momentum distribution in transversal direction. The dependence of the rotation angle Δ_- on the distance to the beamline is illustrated in the lower graph in figure 4. The two orders of magnitude larger values for Δ_- compared to those for Δ_+ arise due to the factor $\theta^2/8$ present in the expression for Δ_+ but not in the one for Δ_- (compare equations (9) and (10)).

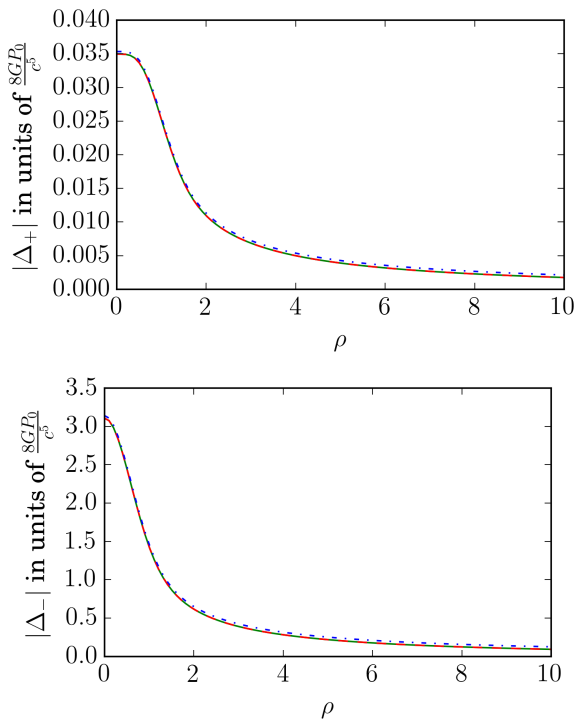

Figure 4. The absolute value of the polarization rotation angle Δ_+ (upper graph) for a parallel co-propagating light ray and Δ_- (lower graph) for a parallel counter-propagating light ray as a function of the transversal distance ρ from the beamline. The blue (dashed-dotted) line gives the rotation angle for the infinitely extended source beam and test ray. The green (unbroken) line gives the rotation angle for a source beam with emitter and absorber at $\zeta = -200$ and $\zeta = 200$, respectively, and infinitely extended test ray. The red (dashed) line gives the numerical values for the same extensions of the test beam and a finitely extended test light-ray with emitter (absorber) and absorber (emitter) at $\zeta = A = -600$ and $\zeta = B = 600$, respectively, for the co-propagating (counter-propagating) beam. For the parameters given in the introduction, the factor $8GP_0/c^5$ is of the order 10^{-37}. The plots show good agreement between our results for finitely and infinitely extended beams close to the beamline.

2. *Transversally propagating test rays*

The transversally propagating test ray is described by the initial tangent $\dot{\gamma}_\pm = (1, \pm(1-f^\pm), 0, 0)$. Due to the same argument as before, we do not have to take into account the parameter $f^\pm$. For the rotation angle of the polarization vector, we obtain for the infinitely extended source beam and infinitely extended test ray (see appendix D for the detailed derivation) including terms up to first order

$$\begin{aligned}\Delta_{t^\pm} &= \pm \frac{1}{2w_0^2}\int_{-\infty}^{\infty} d\xi\, \partial_\chi h^{(0)}_{\tau\zeta} + \frac{\theta}{2w_0^2}\int_{-\infty}^{\infty} d\xi\, \partial_\chi h^{(1)}_{\xi\zeta} \\ &= \pm \frac{4\pi G P_0}{c^5}\,\mathrm{erf}\left(\sqrt{2}|\mu|\chi\right) + \lambda\frac{2\sqrt{2\pi}GP_0\theta}{c^5}|\mu| e^{-2|\mu|^2\chi^2}\,. \end{aligned} \tag{11}$$

Let us denote the first term in equation (11) as $\Delta^{(0)}_{t^\pm}$ and the second term as $\Delta^{(1)}_{t^\pm}$. Then, we find that $\Delta^{(1)}_{t^\pm} = \frac{\lambda\theta}{4}\partial_\chi \Delta^{(0)}_{t^+}$. One might think that the symmetry of the beam geometry implies that $\Delta^{(0)}_{t^\pm}$ should vanish at $\zeta = 0$ as the term is independent of the helicity of the source beam. However, the symmetry is broken due to the direction of propagation of the source laser-beam. This can also be seen from the fact that only the $\tau\zeta$-component of the metric perturbation contributes to the effect, which would vanish for a massive medium at rest (see for example the Levi-Civita metric for an infinitely extended rod of matter [28]). The effect is similar to the deflection of a transversally propagating test ray, which is both deflected radially towards the laser beam as well as in ζ-direction [1]. To illustrate the ζ-dependence of $\Delta^{(1)}_{t^\pm}$, a numerical evaluation and a comparison to results for a finitely extended source beam (see the following subsection) are given in figure 5.

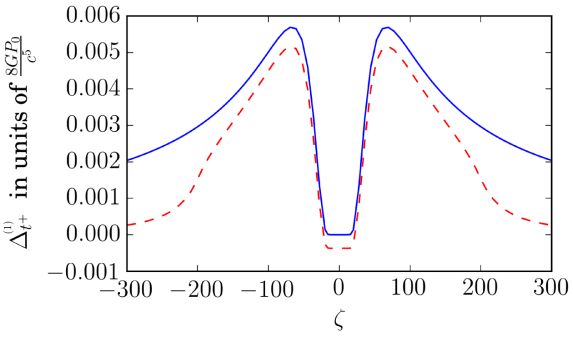

Figure 5. First order contribution (corresponding to the leading order effect of gravitational optical activity) to the rotation angle Δ_{t^+} for the polarization vector of an transversally propagating test ray with $\lambda = +1$: The blue, continuous line corresponds to the infinitely extended source beam, and the red, dashed line corresponds to the finitely extended source beam, emitted at $\alpha = -200$ and absorbed at $\beta = 200$. The test ray runs from $\xi = A = -600$ to $\xi = B = 600$ at $\chi = 10$. We find that the results for the infinitely extended source beam and test ray can be used to describe the effect in the case of the finitely extended source beam and test ray to some approximation for ζ-positions that are in between emitter and absorber, but far from them. It can be seen that the rotation decreases fast at the ends of the finitely extended source beam.

The first and the second term in equation (11) are fundamentally different in their dependence on the variable χ, which can be interpreted as the impact parameter of the scattering of the test light-ray with respect to the source beam. $\Delta^{(1)}_{t^\pm}$ is proportional to the same Gaussian function of χ that appears as a global factor in the energy-momentum tensor of the source beam for $\xi = 0$, which means that it vanishes if there is no overlap of the source beam and the test ray in the same way as in the case of Δ_+ and Δ_- above. Instead, the first term in equation (11) vanishes at $\chi = 0$ and saturates for large

values of χ at a finite value, see figure 6 for plots showing numerical values for the first term in (11) and for the finitely extended source beam.

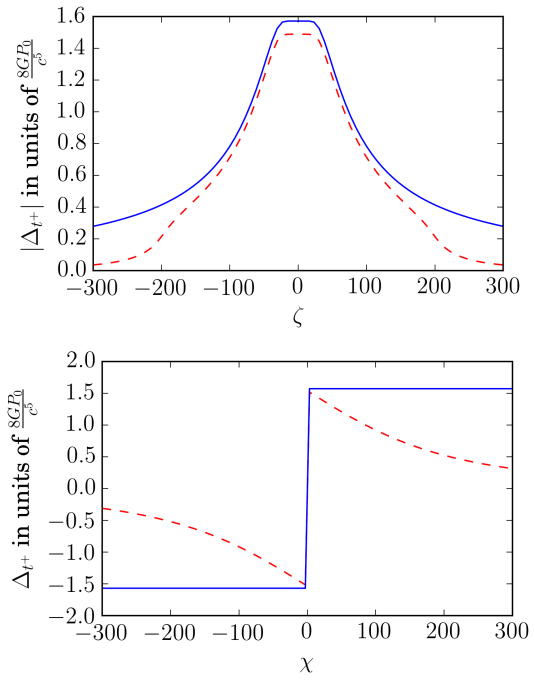

Figure 6. The rotation angle Δ_{t^+} (zeroth and first order) for the polarization vector of an transversally propagating test ray: The blue, plain line corresponds to the infinitely extended source beam, and the red, dashed line corresponds to the finitely extended source beam, emitted at $\alpha = -200$ and absorbed at $\beta = 200$. For the finitely extended source beam, the test ray is emitted at $\xi = A = -600$ and absorbed at $\xi = B = 600$. In the first plot, $|\Delta_{t^+}|$ is given as a function of the coordinate ζ along the beamline for $\chi = 10$. For the parameters given in the introduction, the factor $8GP_0/c^5$ is of the order 10^{-37}. We find that the results for the infinitely extended beam approximate those for the finitely extended beam for ζ-positions in between emitter and absorber that are far from emitter and absorber. It can be seen that $|\Delta_{t^+}|$ decays quickly outside of the range of the finitely extended source beam and test ray in contrast to $|\Delta_{t^+}|$ for the infinitely extended ones that always overlap. In both cases, the maximal effect is obtained close to $\zeta = 0$. In the second plot, the angle Δ_{t^+} is given as a function of χ at $\zeta = 0$. For large values of χ, it reaches a constant value for the infinitely extended source beam and test ray (undashed, blue) and decreases for the finitely extended source beam and test ray (dashed, red). A dependence on χ as $1/\chi^2$ is found for larger values of χ using a multipole expansion presented in appendix F.

Up to numerical factors of order 1, the prefactors in equations (9), (10), and (11) can be interpreted as the ratio of the power P_0 of the source laser-beam to the Planck power $E_p/t_p = E_p^2/\hbar$, where $E_p = \sqrt{\hbar c^5/G}$ is the Planck energy, which explains the smallness of the effect.

B. Finite vs. infinite source beams and test rays and the long range behavior

For potential future experiments, finitely extended test-rays are relevant. It may even not be possible to realize extensions of the test ray much larger than that of the source beam or one may need to know details about the decay of the effect for large distances from the beamline. It should then be kept in mind that (7) holds for test rays that begin and end in flat spacetime. This is a condition which can be fulfilled only approximatively for a finitely extended test-ray. Furthermore, only under this condition has the rotation of the polarization a clear physical, coordinate-invariant meaning. To give a physical meaning to the rotation angle for a finitely extended test-ray, a physical reference system may be considered that extends from emitter to absorber. To this end, matter properties of the reference system like its density and stiffness have to be taken into account to obtain a reliable result. This is very similar to the considerations we made in [29] for the frequency shift of an optical resonator in a curved spacetime. We do not follow such an approach in this article.

Here we rather focus on the question under which conditions equation (7), when integrated over a finitely extended test ray, leads to results comparable to those of the infinitely extended test-ray. We will find that sufficiently close to the beamline the results from the finite integration can be very close to those of an infinite test-ray, which suggests that the latter, rigorous results with clear physical meaning, also remain valid for experiments using a finitely extended test-ray close to the source beam. The situation is quite different, however, in the far field, where results from the finite source beam and the infinitely extended one, both evaluated using (7), can differ siginificantly. This can be shown with a multipole expansion based on equation (6) or by numerically evaluating equation (6). The basic expressions for the numerics are given in appendix C and the multipole expansion is performed in apendix F. Here we briefly discuss both approaches and the main results.

The numerical values for the rotation angle for finitely extended test rays and source beams presented in figure 4 are obtained from equations (C6) and (C7). The derivative in equation (7) acting on the metric perturbation is shifted to the energy-momentum tensor by pulling it into the integral, using the symmetry of the function $|\vec{x} - \vec{x}'|$ to replace the derivative for an un-primed coordinate by a derivative for a primed coordinate and partial integration. The resulting expressions are evaluated using Python and the scypy.integrate.quad and scypy.integrate.romberg methods. The results for the finitely extended beam and those for the infinitely extended beam are very similar close to the beamline, see figure 4. The region in the ξ-χ-plane containing most of the energy of the source beam can be defined by a drop of its intensity by a factor e^{-2}, which implies a radius $w(\zeta) = \sqrt{1 + (\theta\zeta)^2}$ of that region. In standard no-

tions $w(\zeta)$ is called the width of the beam as a realistic beam is never infinitely extended in the transversal direction and is usually considered to extend only on length scales of the order of $w(\zeta)$. Equations (9) and (10) imply that there is only a significant rotation angle accumulated along an infinitely extended test ray if the latter overlaps with the region bounded by the source beam's width, as the integrands in equations (9) and (10) are proportional to the same Gaussian function that can be found as a global factor in the energy-momentum tensor of the source beam. In the following, we will call this situation an overlap of the test light ray and the source beam. That Δ_- and Δ_+ are only non-zero for an overlap of test ray and source beam is confirmed by equations (E15) and (E8), where a cut-off of the source beam's energy-momentum distribution is considered. For $\theta\zeta \gg 1$, we find that $w(\zeta) \approx \theta\zeta$. Therefore, a test ray at $\rho \gg 1$ overlaps with the source beam only in regions where $|\theta\zeta| > \rho$. For the infinitely extended source beam and test ray, there is always an overlap, but it does not need to be the case if at least one of the two beams has finite length.

Note that for large values of $\theta\zeta$, the energy-density of the source laser-beam is proportional to $(\theta\zeta)^{-2}$ (while transversally it decreases as a Gaussian with the distance to the beamline). The same is true for the integrands in equations (9) and (10). Therefore, $\Delta_\pm$ in equations (9) and (10) are approximately proportional to $1/(\theta\zeta)$ evaluated at the boundaries of the regions where test ray and source beam overlap. For the infinitely extended beams, this implies that the rotation angles in equations (9) and (10) are approximately proportional to $1/\rho$ for large ρ. The proportionality of Δ_- and Δ_+ to $1/\rho$ holds as well for finitely extended source beams if $\rho \ll -\theta\alpha$ or $\rho \ll \theta\beta$. For larger values of ρ, there is no overlap of test ray and source beam (this is illustrated in figure 7 and figure 8). Then, Δ_- and Δ_+ decay proportional to $e^{-\Sigma\rho^2}/\rho^2$ and $e^{-\Sigma\rho^2}$, respectively, where $\Sigma = 2/(\theta\alpha)^2$ for $\alpha \geq -\beta$ or $\Sigma = 2/(\theta\beta)^2$ for $\beta \geq -\alpha$, as shown in equation (E11) and equation (E17), respectively.

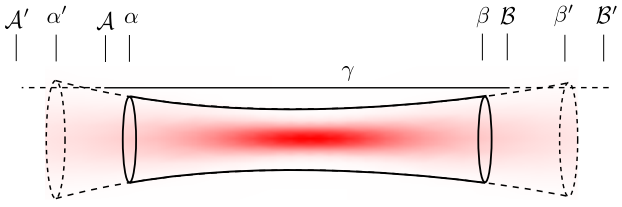

Figure 7. Illustration of the overlap of the test ray with the source laser-beam: A test ray may overlap with the source laser-beam only if the latter is long enough. In the illustration, the path of the test ray is labelled by γ and starts and ends at $\mathcal{A}$ and $\mathcal{B}$ respectively for the short source laser-beam (starting and ending at α and β respectively) or at $\mathcal{A}'$ and $\mathcal{B}'$ for the long source laser-beam (starting and ending at α' and β' respectively).

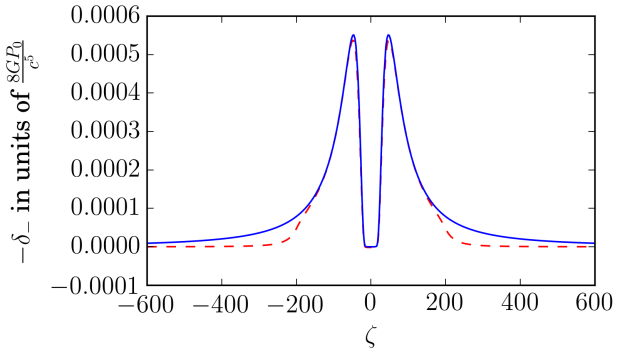

Figure 8. The function $-\delta_-$ (the integrand in equation (10)) for the polarization vector of the parallel counter-propagating light ray is plotted as a function of the coordinate along the beamline ζ for a distance from the beamline $\rho = 10$. The blue (unbroken) line gives the rotation angle for the infinitely extended source beam and test ray as in equation (10). The red (dashed) line gives the numerical values for a finitely extended source beam with emitter and absorber at $\alpha = -200$ and $\beta = 200$, respectively, based on (6). It can be seen that δ_- decays quickly outside of the range of the finitely extended beam in contrast to δ_- for the infinitely extended source beam, which continues to decay like $1/\zeta^2$ for large ζ just as the source beam's energy density. The region left of the steep descent around $\zeta \sim -70$ and the region right of the steep ascent around $\zeta \sim 70$ correspond to the overlap regions of source beam and test light-ray. In the case of an infinitely extended source beam, these regions are infinitely extended. In the case of a finitely extended source beam, the overlap regions end at the end of the source beam as can be seen with the steep ascent close to $\zeta = -200$ and the steep descent close to $\zeta = 200$ for the red (dashed) curve.

The behavior for large distances from the beamline and finitely extended test rays can be analysed with a multipole expansion, assuming that the source term in the form of the derivatives of the energy-stress tensor can be effectively cut-off at $w(\zeta)$. This is presented in appendix F. One finds that for $\Delta_\pm$ the lowest contributing moment is a quadrupole leading to a $1/\rho^3$ decay for finite $B = -A$. At the same time, the prefactor of these terms decay as $1/B^2$ for $B \gg \rho$. Higher multipoles lead to an even faster decay, both with ρ and B. Hence, in the case of a finitely extended source beam and an infinitely extended test ray that does not overlap with the source beam, one expects to recover the fast decay of $\Delta_\pm$ with ρ obtained in equations (9) and (10). However, a resummation of the multipole expansion would be needed to find out its functional form. This is beyond the scope of the present investigation. Nevertheless, the analysis makes clear that $\Delta_\pm$ sensed by a finitely extended test ray in the far-field regime is not captured accurately by the results from the idealized infinitely extended test ray for the cases considered.

For the transversal test ray, the χ-dependence of $\Delta_{t\pm}$ for $\chi \gg 1$ changes drastically for the finitely extended source beam compared to the infinitely extended one. In particular, the result that the first term in equation (11) does

not vanish for large distances from the beamline turns out to be an effect of the infinite extension of source beam and test ray. Alternatively, this can also be seen as follows: As $\Delta^{(0)}_{t^\pm}$ is of zeroth order, it remains present when describing the laser beam in the paraxial approximation, in which the gravitational field of an infinitely extended source beam has the form $h_{00} = h_{33} = -h_{30} \propto \ln(\rho)$ (see [3, 30] and consider an infinite pulse length or see [2], consider an energy distribution localized to the beamline, and subtract the Minkowski metric from the resulting spacetime metric). From equation (7) and for a transversal infinitely extended test ray, we immediately obtain a rotation angle proportional to the first term in equation (11). On the other hand, the solution for the gravitational field for a finitely extended source beam can be found in [1]. In appendix G, using this solution and an infinitely extended test ray, we obtain the radial dependence of the rotation angle as $1/\chi$, and for a finitely extended test ray, we find that the rotation angle is proportional to $1/\chi^2$ for large χ. This is corroborated by the multipole expansion, where we find a monopole contribution responsible for the $1/\chi^2$ behavior to zeroth order in θ for $\chi \gg B$. As function of $B = -A$ it saturates for large B (i.e. $B \gg \chi$) and gives a β/χ behavior, see appendix F. Since $\Delta^{(1)}_{t^\pm} = \frac{\lambda\theta}{4}\partial_\chi \Delta^{(0)}_{t^+}$, we find that $\Delta^{(1)}_{t^\pm}$ decays as $1/\chi^3$ for finitely extended source beams and test rays and as $1/\chi^2$ for finitely extended source beams and infinitely extended test rays. The corresponding multipole expansion is given in appendix F.

C. Rotation of polarization and gravitational spin-spin coupling

The rotation angles $\Delta_\pm$ as well as the first order contribution to $\Delta_{t^\pm}$ are proportional to the helicity λ of the source laser-beam. As explained in the end of section III, the rotation angle is equivalent to a phase for circularly polarized test light rays, which is given by $-\lambda_{\text{test}}\Delta$. This phase contains the product of the helicities of the source laser-beam and the test ray, $\lambda\lambda_{\text{test}}$. Therefore, the phase depends on the relative helicity of the two beams. This is gravitational spin-spin coupling.

We can consider the source beam as its own test beam, $\lambda_{\text{test}} = \lambda$, such that $\lambda_{\text{test}}\Delta_+ = C_+$ where $C_+ > 0$ is a function that increases monotonously with the end of the source beam at $\zeta = \beta$ (see (9)). Since C_+ enters as a phase $\text{Exp}(iC_+)$, it can be combined with the global plane wave factor at the end of the beam $\zeta = \beta$ as $\text{Exp}(i\Phi)$ where $\Phi = 2(\beta-\tau)/\theta + C_+$. This leads to the locally modified wave number $\tilde{k} = \partial_\beta\Phi = (2 + \theta\,\partial_\beta C_+)/\theta$ at $\zeta = \beta$. Effectively, this leads to the interpretation of a locally modified dispersion relation and an effectively reduced speed of light. This self-interaction effect is proportional to the intensity of the electromagnetic field. It is reminiscent of the apparent modification of the speed of light found in [31] based on the eikonal approximation of the solution of the relativistic wave equation of a light-beam in its own gravitational field.

V. FARADAY EFFECT AND OPTICAL ACTIVITY

The electromagnetic Faraday effect is a non-reciprocal phenomenon. Non-reciprocity means that the effect does not cancel when the test ray propagates back and forth along the same path. We investigate this feature for its gravitational analogue.

The rotation angle given in equation (7) is defined with respect to the propagation direction. Therefore, the absolute rotation accumulated on the way back and forth through spacetime seen by an external reference system at the starting point of the test ray's trajectory at spatial infinity is given by the difference between the rotation angle acquired on the outbound trip and the one acquired on the way back. For a tangent vector t^μ_0 with $t^0_0 = 1$ and $t^a_0 = d\,\delta^a_m$ with $m \in \{\xi, \chi, \zeta\}$ and $d = +1$ for outbound and $d = -1$ for back propagation, we obtain from equation (7) the rotation angle

$$\Delta = \frac{1}{2w_0^2}\int_{-\infty}^{\infty} d\tau\ \epsilon_{mbc}\partial_b(h_{cm} + dh_{c\tau})\ , \tag{12}$$

and therefore, the Faraday rotation becomes

$$\Delta^{\text{F}} = \frac{1}{w_0^2}\int_{-\infty}^{\infty} d\tau\ \epsilon_{mbc}\partial_b h_{c\tau}\ . \tag{13}$$

We find that the gravitational Faraday effect is given by the spacetime-mixing component of the metric perturbation $h_{c\tau}$. In contrast, the first term in (12) containing a purely spatial component of the metric perturbation does not depend on the propagation direction and cancels on the way back and forth. This is the gravitational optical activity.

For the rotation due to the gravitational Faraday effect after one roundtrip for the parallel test ray, we obtain from equation (8) to leading order

$$\begin{aligned}\Delta^{\text{F}}_{+-} &= \Delta_+ - \Delta_- \\ &= -\frac{\theta}{w_0^2}\int_{-\infty}^{\infty} d\zeta\Big(\partial_\chi h^{(1)}_{\tau\xi} - \partial_\xi h^{(1)}_{\tau\chi}\Big)\ .\end{aligned} \tag{14}$$

Adding the rotations due to the transversal back and forth propagation leads to (the explicit expression is identical to twice the positive contribution of the first term in equation (11)),

$$\Delta^{\text{F}}_{\text{t}^+\text{t}^-} = \Delta_{\text{t}^+} - \Delta_{\text{t}^-} = \frac{1}{w_0^2}\int_{-\infty}^{\infty} d\xi\ \partial_\chi h^{(0)}_{\tau\zeta}\ , \tag{15}$$

which means that the effect is of zeroth order. The contribution of gravitational optical activity is given as (to leading order and for one direction of propagation)

$$\begin{aligned}\Delta^{\text{Op}}_{+-} &= \frac{\Delta_+ + \Delta_-}{2} \\ &= -\frac{\theta}{2w_0^2}\int_{-\infty}^{\infty} d\zeta\Big(\partial_\chi h^{(1)}_{\zeta\xi} - \partial_\xi h^{(1)}_{\zeta\chi}\Big)\end{aligned} \tag{16}$$

for the parallel test rays, and

$$\Delta^{\rm Op}_{{\rm t}^+{\rm t}^-} = \frac{\Delta_{{\rm t}^+} + \Delta_{{\rm t}^-}}{2} = \frac{\theta}{2w_0^2}\int_{-\infty}^{\infty} d\xi\, \partial_\chi h^{(1)}_{\xi\zeta} \qquad (17)$$

for the transversal test rays.
From the vanishing of Δ_+ in first order in the metric perturbation, we deduce that the first order contributions of optical activity and the Faraday effect to the polarization rotation accumulated along a parallel co-propagating test ray have the same absolute value and cancel each other. In contrast, the two contributions add for the counter-propagating test ray. This situation can be compared to the result of Tolman et al. [1], which states that a test ray is not deflected in the gravitational field of a source light-beam if it is parallel co-propagating, while it is deflected if it is parallel counter-propagating. It is the motion of the source of gravity that breaks the symmetry; its motion with the speed of light leads to the extreme case of equal absolute values of the two effects.

VI. TEST RAYS IN CAVITIES

In a one-dimensional cavity containing light that propagates back and forth, the effect associated with gravitational optical activity cancels while the gravitational Faraday effect adds up. In a ring cavity or an optical fiber coiled around the beamline, the full polarization rotation is accumulated and the gravitational Faraday effect represents the leading order effect. For the case of a transversally oriented ring cavity, a situation can be created in which the Faraday effect vanishes and only the gravitational optical activity accumulates.

A. Parallel linear cavity

We consider a cavity consisting of two mirrors between which the light propagates back and forth, with the axis of the cavity oriented parallel to the beamline and at a distance ρ from the beamline. The setup is illustrated in figure 9.

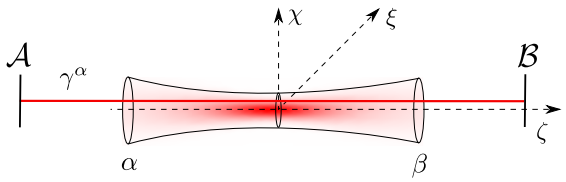

Figure 9. Schematic illustration of the parallel cavity in the gravitational field of the laser beam: The source laser-beam starts at α and ends at β. The test ray propagates on the worldline γ between the mirrors $\mathcal{A}$ and $\mathcal{B}$ of the cavity. The Faraday effect adds up after each roundtrip, while the rotation associated with gravitational optical activity vanishes.

Up to third order in θ, the light travels undeflected from $\zeta = A$ to $\zeta = B$ and picks up a small deflection of zeroth order in θ when travelling from $\zeta = B$ to $\zeta = A$. The deflection vanishes when the light ray propagates at the center of the source beam, at $\rho = 0$. In this case only the angle due to the Faraday effect accumulates. For one back and forth propagation, it is given by equation (14). Letting the light propagate during the time $\tau = LF/(\pi c)$, where F is the finesse of the cavity, the total angle of rotation is given by $\Delta_{{\rm cav},+-} = \Delta^{\rm F}_{+-}F/(2\pi)$. For a cavity of finesse $F = 10^6$ [32] and the parameters given in the introduction, the rotation angle is of the order of magnitude $\Delta_{{\rm cav},+-} \sim \pm 10^{-32}$ rad. For a cavity at distance $\rho > 0$ from the center of the laser beam, the effect is smaller, and one has to take into consideration the deflection when the test ray is counter-propagating to the source laser-beam.

B. Transversal linear cavity

Rotating the parallel cavity by ninety degrees, we obtain a transversal cavity, as illustrated in figure 10. Analogously to the parallel cavity, one finds that the total angle of rotation is given by $\Delta_{{\rm cav},{\rm t}^+{\rm t}^-} = \Delta^{\rm F}_{{\rm t}^+{\rm t}^-}F/(2\pi)$. For a finesse of $F \sim 10^6$ and the parameters given in the introduction, it is of the order $\pm 10^{-32}$ rad.

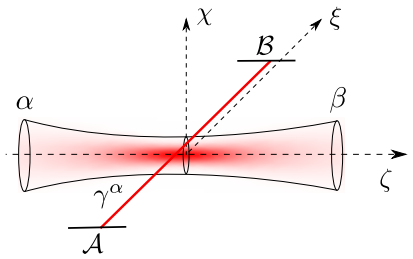

Figure 10. Schematic illustration of the transversal cavity in the gravitational field of the laser beam: The test ray propagates along the worldline γ, marked as a red line, and is reflected at the mirrors $\mathcal{A}$ and $\mathcal{B}$. The source laser-beam is emitted at $\zeta = \alpha$ and absorbed at $\zeta = \beta$. The Faraday effect adds up after each roundtrip, while the rotation associated with gravitational optical activity vanishes.

C. Ring cavity

In order to measure the polarization rotation including the contribution due to optical activity for the transversal light ray, we consider a ring cavity: The light propagates from $\mathcal{A}$ at $(\xi,\chi,\zeta) = (-\infty,\chi_1,0)$, to $\mathcal{B}$ at $(\xi,\chi,\zeta) = (\infty,\chi_1,0)$, to $\mathcal{C}$ at $(\xi,\chi,\zeta) = (\infty,\chi_2,0)$, where χ_1 and χ_2 have opposite sign, to $\mathcal{D}$ at $(\xi,\chi,\zeta) = (-\infty,\chi_2,0)$ and back to $\mathcal{A}$. The $\pm\infty$ can be replaced by distances from the beamline much larger than β. The polarization rotation accumulated when propagating from $\mathcal{A}$ to $\mathcal{B}$ and from $\mathcal{C}$ to $\mathcal{D}$ add up. The setup is illustrated in figure 11.

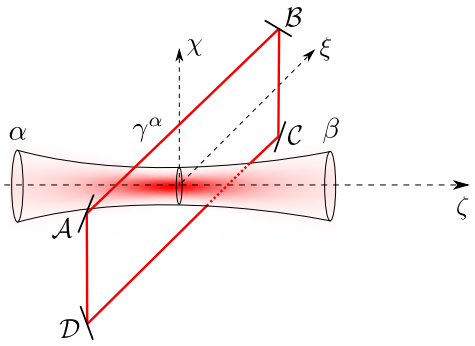

Figure 11. Schematic illustration of the ring cavity setup: The test ray propagates along the path γ and is reflected at the mirrors $\mathcal{A}$, $\mathcal{B}$, $\mathcal{C}$ and $\mathcal{D}$. The source laser-beam is emitted at $\zeta = \alpha$ and absorbed at $\zeta = \beta$. A similar situation can be created with a test ray in a wave guide that is wound many times around the source beam.

The rotation of polarization after one roundtrip is given by twice the expression in equation (11) for $\chi_1 \sim 1$ and $\chi_2 \sim -1$. For $\chi_1 \gg \beta$, $\chi_2 \gg -\beta$ and $\alpha = -\beta$, we have shown that the effect decays as β/χ^2 in appendix F. As the first term in equation (11) corresponding to the gravitational Faraday effect is of zeroth order in θ, it does not depend on the beam waist for the fixed wavelength given by $\pi\theta w_0$. This means that the beam has to be long, but it does not need to be focused. Again for a finesse of $F = 10^6$ and the parameters given in the introduction, the rotation is of the order of magnitude $\Delta_{t^+} F/(2\pi) \sim 10^{-32}$ rad.

For $\chi_1 = 0$ and $\chi_2 = -\infty$ or at least $-\chi_2$ very large, we find that the polarization rotation due to the Faraday effect vanishes (see also equation (E22)) and the rotation due to gravitational optical activity remains (see also equation (E23)). Then, the accumulated effect is by one order smaller than that due to the Faraday effect at $\chi_1 = \chi_2 > 1$.

A ring cavity can also be used to amplify the rotation angle of the polarization the parallel co-propagating test ray acquires: Since it is not deflected, one can let the light ray pass through the gravitational field N times just in the direction of propagation of the source beam, such that the effect is amplified by a factor N.

D. Measurement precision of the rotation angle

The rotation angle Δ is experimentally inferred by measuring the additional phase difference that the right- and left-circularly polarized components of the test ray acquire when propagating in the gravitational field as explained in the end of section III. The measurement precision of the phase $\Phi = -\lambda_{\text{test}}\Delta$ is restricted by the shot noise. Using classical light, the minimal uncertainty in a phase estimation cannot exceed the shot noise limit, which is of the order of magnitude $\delta\Phi \sim \frac{1}{\sqrt{nM}}$, where n is the number of photons of the light inside the cavity and M the number of measurements [33]. For a cavity resonator driven by a laser with frequency $\omega/(2\pi)$ and power P_{dr}, we find a number of photons $n = P_{\text{dr}} T_{\text{av}}/(\hbar\omega)$, where T_{av} is the average time a photon spends in the resonator. Therefore, the number of measurements that can be performed with n photons in an experimental time T_{tot} is given as $M = T_{\text{tot}}/T_{\text{av}}$, giving $nM = P_{\text{dr}} T_{\text{tot}}/(\hbar\omega)$, which is the total number of photons passing the cavity in time T_{tot}.

The measurement precision becomes thus better by increasing the power of the driving laser and lowering its frequency. For cw-laser beams with power $P_{\text{dr}} = 100\,\text{kW}$ [34],[5] for a wavelength of approximately 500 nm and a total experimental time of about two weeks, i.e. $T_{\text{tot}} \sim 10^6\,\text{s}$, the minimal standard deviation is given by $\delta\phi \sim 10^{-15}$ rad. Its order of magnitude does not change when using a squeezed (single mode coherent) state with the currently maximal squeezing of 15 dB [36][6] and analyzing the uncertainty with the corresponding quantum Cramér-Rao bound [37].

The Cramér-Rao bound is a tight bound on the uncertainty of an unbiased phase-estimation that can in principle be achieved in a highly idealized situation, where all other noise sources such as thermal noise, electronic noise, seismic noise etc. are neglected. The sensitivity can be increased by using more than one mode, but without entangling the modes or creating other non-classical states no gain in sensitivity at fixed total energy is possible [38].

For a more practical benchmark of current state-of-the-art measurement precision, consider the LIGO observatory. It obtains a sensitivity for length changes of their arms of the order of $10^{-20}\,\text{m}$ (strains of the order of $10^{-23}\,(\text{Hz})^{-1/2}$ on an arm length of the order of $10^3\,\text{m}$ [39]), which corresponds to a phase sensitivity of the order of 10^{-11} rad at about 1000 nm wavelength. Another obstacle is that the source-laser power of $10^{15}\,\text{W}$ that we considered here can so far only be reached in very short pulses, which means that an extension of our analysis to

[5] Of course the power of the driving laser cannot be unlimited as the cavity mirrors have to withstand the heating due to scattered light. The finesse $F \sim 10^6$ leads to a circulating power in the cavity of the order of $10^{10}\,\text{W}$, which leads to a necessary size of the beam at the mirrors of the order of 1 m [35]. Assuming the transversal setup described in section VI, the waist of the test ray has to be smaller than the waist of the source beam and the divergence angle of the test ray must be smaller than one radian to ensure a complete overlap of the focal regions of the source beam and the test ray. We assumed a waist of the source beam of the order of $10^{-6}\,\text{m}$, which implies a maximum waist of the test ray of the same order. Furthermore, the divergence angle of the test ray below one radian implies that the distance between the mirrors of the test ray has to be of the order of several meters. The situation for the longitudinal cavity turns out to be even more challenging. However, the given parameters serve as an upper limit of what would be possible in the near future.

[6] Note that this degree of squeezing has only been reached for much a smaller beam power of the order of mW, which would actually lead to a decrease in the sensitivity.

pulsed source beams will be required when one day substantially larger powers and more sensitive measurements might become available. We conclude that the angles due to the gravitational Faraday effect of the order of magnitude $\Delta \sim 10^{-32}$ rad cannot be measured with current and near-future technology.

VII. SUMMARY, CONCLUSION AND OUTLOOK

We analyzed the rotation of polarization for a test ray propagating in the gravitational field of a laser beam. We distinguished the non-reciprocal contribution to the rotation due to the gravitational Faraday effect from the reciprocal contribution associated with the gravitational optical activity. As the rotation angle is equivalent to a phase for circularly polarized test rays, the precision of the measurement of the effect investigated in this article is limited by the shot-noise limit when using classical light. With this analysis we found that the rotation of polarization of a test ray induced by the gravitational field of a circularly polarized source laser-beam is too small to be measured with state-of-the-art technology. The effects are of fundamental interest, however.

For an infinitely extended (or at least very long) test ray propagating parallel to the source beam, we found that the local rotation picked up by the polarization vector of the test ray is proportional to the energy density of the source beam. In that case, we concluded that effects are only present for an overlap of the test ray and the source beam's region of highest intensity bounded by its width. Using the approximation of an infinitely extended source beam, such an overlap is always present for parallel propagating test rays and we find a decay of the integrated rotation angle with the inverse of the distance to the beamline of the source beam. In the realistic situation of a finitely extended source beam, this dependence on the distance remains approximately valid as long as there is a significant overlap. However, for the finitely extended source beam, there is no overlap for distances from the beamline larger than the extension of the beamline multiplied by the divergence angle of the source beam. Above that limit, we find that the polarization rotation picked up by a parallel propagating infinitely extended test ray decreases as a Gaussian with the distance to the beamline of the source beam. For a finitely extended test ray far from the beamline of the source beam, we find that the effects decay with the inverse of the third power of the distance using a multipole expansion. However, a finitely extended test ray begins and ends in regions with non-vanishing gravitational effect of the source beam. Hence, the interpretation of the rotation angle is not straight forward. To overcome this problem, a physical reference system could be considered that extends or is moved from the beginning to the end of the test ray.

For transversally propagating test rays, the situation is different: The leading order effect decreases with the inverse of the distance from an finitely extended source beam for an infinitely extended test ray and with the inverse square for a finitely extended test ray. Therefore, of the effects investigated in this article, the rotation of polarization of a transversal test ray should be the easiest to detect, while we reiterate that a detection will not be possible in the near future. It is interesting to note that the effect remains there also in the geometric optical limit and is independent of the source beam's helicity.

Only the gravitational Faraday effect contributes to the leading order effect for the transversal test ray. The gravitational optical activity induces the next to leading order term, and it decays one order more strongly with χ than the gravitational Faraday effect.

It has been shown that for light passing through or being emitted from a rotating spherical body [6, 7] or a rotating spherical shell [12], one obtains a rotation of the polarization proportional to the inverse of the square of the distance to the rotating object. On the other hand, when the light ray is only passing by these objects or any stationary object, there is no rotation of polarization [40, 41]. However, if these objects are in motion, it has been shown that the polarization is rotated (for a moving point mass [42], for gravitational lenses [10, 41], for a moving Schwarzschild object [9], for moving stars [8]). As the laser beam, although its spacetime metric is stationary, consists of an energy-distribution in motion, our results agree with the literature in the sense that the rotation of polarization is non-vanishing.

As another interesting fundamental insight, we found that to first order in the divergence angle θ, the polarization vector of a parallel counter-propagating test ray rotates, while this is not the case for a co-propagating test ray. We argue that this asymmetry is due to the propagation of the source laser-beam. This is similar to the deflection of a parallel test ray by the gravitational field of a laser beam which is non-zero for a counter-propagating ray and vanishes for a co-propagating ray [1].

The gravitational field of the laser beam depends on its polarization. This is in agreement with the gravitational field of a polarized infinitely thin laser beam or pulse derived in [3] and the gravitational field of a polarized electromagnetic plane wave presented in [43]. However, the gravitational field in the models [3, 43] does not depend on the direction of linear polarization and neither on the helicity of light in the case of circular polarization. This is in contrast to gravitational photon-photon scattering in perturbative quantum gravity discussed in [44]. In [5], we showed that the gravitational field of a laser beam considered as a proper perturbative solution of Maxwell's equations beyond the short wavelength approximation does depend on the helicity of the laser beam. In the present article, we showed that, accordingly, the polarizations of two light beams couple gravitationally; two circularly polarized light beams inflict on each other a phase shift depending on the relation between their he-

licity. This is gravitational spin-spin coupling of light (see [45] for a general review on gravitational spin-spin coupling).
Together with frame-dragging and the deflection of a parallel co-propagating test ray discussed in [5], the gravitational Faraday effect and gravitational optical activity are only visible when the source is treated beyond geometric ray optics. It can be expected that angular orbital momentum of light would contribute to the effects mentioned above (see [4] for an investigation of the gravitational field of light beams with orbital angular momentum).

ACKNOWLEDGEMENTS

We thank Julien Fraïsse for proofreading the manuscript. DR would like to thank the Humboldt Foundation for supporting his work with their Feodor Lynen Research Fellowship.

Appendix A: Metric perturbation (from [5])

In this appendix, we give the explicit expressions for the metric perturbation as derived in [5]. The metric perturbation is obtained from the electromagnetic field of a circularly polarized laser beam given in [5], which is determined by the vector potential $A_\alpha(\tau,\xi,\chi,\zeta) = \tilde{\mathcal{A}} v_\alpha(\xi,\chi,\theta\zeta) e^{i\frac{2}{\theta}(\zeta-\tau)}$, where $\tilde{\mathcal{A}}$ is the amplitude, $v_\alpha = \sum_{n=0}^{\infty} \theta^n v_\alpha^{(n)}$ is the envelop function, whose spatial components, $a \in \{\xi,\chi,\zeta\}$, are given up to third order in θ by

$$v_a^{\lambda(0)} = \epsilon_a^{(0)} v_0 \,, \tag{A1}$$

$$v_a^{\lambda(1)} = -\epsilon_a^{(1)} \frac{i\mu}{2\sqrt{2}} \left(\xi - i\lambda\chi\right) v_0 \,, \tag{A2}$$

$$v_a^{\lambda(2)} = \frac{\mu}{2}\left(1 - \frac{1}{2}\mu^2\rho^4\right) v_a^{\lambda(0)} \,, \tag{A3}$$

$$v_a^{\lambda(3)} = \frac{\mu}{4}\left(4 + \mu\rho^2 - \mu^2\rho^4\right) v_a^{\lambda(1)} \,, \tag{A4}$$

where $\mu = 1/(1+i\theta\zeta)$, the function v_0 is given by

$$v_0(\xi,\chi,\theta\zeta) = \mu e^{-\mu\rho^2} \,, \tag{A5}$$

and $\epsilon_a^{(0)} = w_0(1,-\lambda i,0)/\sqrt{2}$, $\epsilon_a^{(1)} = w_0(0,0,1)$ and $\lambda = \pm 1$ refers to the helicity. Since we work in the Lorenz gauge, the τ-component of the vector potential is given as

$$A_\tau = \frac{i\theta}{2}\partial_\tau A_\tau = \frac{i\theta}{2}\left(\partial_\xi A_\xi + \partial_\sigma A_\sigma + \theta\partial_{\theta\zeta} A_\zeta\right) . \tag{A6}$$

The leading order is thus the usual expression for the electromagnetic field of the Gaussian beam in the paraxial approximation. The higher orders are corrections to the paraxial approximation. The corresponding components of the energy-momentum tensor are given as $T_{\tau\tau} = \mathcal{E}$, $T_{\tau j} = -S_j/c$ and $T_{jk} = \sigma_{jk}$ for $j,k \in \{\xi,\chi,\zeta\}$. For the vector potential of a circularly polarized laser beam given by equation (A1), the energy density $\mathcal{E}$, the Poynting vector $\vec{S}$ and the stress tensor components σ_{jk} up to third order in θ are given as

$$\mathcal{E}^\lambda = \mathcal{E}^{(0)}\Bigg[1 + \frac{|\mu|^2\theta^2}{2}\left(1 + |\mu|^2(2-(4|\mu|^2-3)\rho^2)\rho^2\right)\Bigg], \tag{A7}$$

$$S_\xi^\lambda/c = \mathcal{E}^{(0)}\theta|\mu|^2\Bigg[(\theta\zeta\xi + \lambda\chi) - \frac{\theta^2}{4}\Bigg(\lambda\chi - 2|\mu|^2\Bigg((2-\rho^2)\theta\zeta\xi + 2(1-\rho^2)\lambda\chi + (\theta\zeta\xi+\lambda\chi)(4+3\rho^2-4|\mu|^2\rho^2)|\mu|^2\rho^2\Bigg)\Bigg)\Bigg] , \tag{A8}$$

$$S_\chi^\lambda/c = -\lambda\mathcal{E}^{(0)}\theta|\mu|^2\Bigg[(\xi - \theta\zeta\lambda\chi) - \frac{\theta^2}{4}\Bigg(\xi - 2|\mu|^2\Bigg(2(1-\rho^2)\xi - (2-\rho^2)\theta\zeta\lambda\chi + (\xi-\theta\zeta\lambda\chi)(4+3\rho^2-4|\mu|^2\rho^2)|\mu|^2\rho^2\Bigg)\Bigg)\Bigg] , \tag{A9}$$

$$S_\zeta^\lambda/c = \mathcal{E}^\lambda - \frac{1}{2}\mathcal{E}^{(0)}(\theta\rho|\mu|)^2 \,, \tag{A10}$$

$$\sigma_{\xi\xi}^\lambda = \mathcal{E}^{(0)}\theta^2|\mu|^4(\theta\zeta\xi+\lambda\chi)^2 \,, \tag{A11}$$

$$\sigma_{\chi\chi}^\lambda = \mathcal{E}^{(0)}\theta^2|\mu|^4(\xi-\theta\zeta\lambda\chi)^2 \,, \tag{A12}$$

$$\sigma_{\xi\chi}^\lambda = \mathcal{E}^{(0)}\lambda\theta^2|\mu|^4(\theta\zeta\xi+\lambda\chi)(\theta\zeta\lambda\chi-\xi) \,, \tag{A13}$$

$$\sigma_{\xi\zeta}^\lambda = S_\xi^\lambda/c - \mathcal{E}^{(0)}\frac{\theta^3}{2}(\theta\zeta\xi+\lambda\chi)|\mu|^4\rho^2 \,, \tag{A14}$$

$$\sigma_{\chi\zeta}^\lambda = S_\chi^\lambda/c + \lambda\mathcal{E}^{(0)}\frac{\theta^3}{2}(\xi-\theta\zeta\lambda\chi)|\mu|^4\rho^2 \,, \tag{A15}$$

$$\sigma_{\zeta\zeta}^\lambda = \mathcal{E}^\lambda - \mathcal{E}^{(0)}(\theta\rho|\mu|)^2 \,, \tag{A16}$$

where $|\mu|^2 = 1/(1+(\theta\zeta)^2)$ and $\mathcal{E}^{(0)} = \varepsilon_0 w_0^2 E_0^2 |v_0|^2 = 2P_0|\mu|^2\mathrm{Exp}(-2|\mu|^2\rho^2)/(\pi c)$.

1. Field equations

The linearized Einstein equations take the form

$$\Delta_{2d} h_{\alpha\beta}^{\lambda(0)} = -\kappa w_0^2\, t_{\alpha\beta}^{\lambda(0)} \,, \tag{A17}$$

$$\Delta_{2d} h_{\alpha\beta}^{\lambda(1)} = -\kappa w_0^2\, t_{\alpha\beta}^{\lambda(1)} \,, \tag{A18}$$

$$\Delta_{2d} h_{\alpha\beta}^{\lambda(n)} = -\kappa w_0^2\, t_{\alpha\beta}^{\lambda(n)} - \partial_{\theta\zeta}^2 h_{\alpha\beta}^{\lambda(n-2)} \text{ for n} > 1 , \tag{A19}$$

where $t_{\alpha\beta}^{(n)}$ are the coefficients of the power series expansion of the energy-momentum tensor in orders of θ, i.e. $T_{\alpha\beta} = \sum_n \theta^n t_{\alpha\beta}^{(n)}$.

2. Zeroth order

The metric perturbation in the leading (zeroth) order of the expansion in the beam divergence is given by [5]

$$h_{\tau\tau} = h_{\zeta\zeta} = -h_{\tau\zeta} = I^{(0)} \,, \tag{A20}$$

where the function $I^{(0)}$ is given by

$$I^{(0)} = \frac{8GP_0w_0^2}{c^5}\left(\frac{1}{2}\mathrm{Ei}\left(-2|\mu|^2\rho^2\right) - \log(\rho)\right) \,, \tag{A21}$$

where $\mathrm{Ei}(x) = -\int_{-x}^{\infty} dt\ \frac{e^{-t}}{t}$ is the exponential integral.

3. First order

The metric perturbation in the first order of the expansion in the beam divergence is given by [5]

$$h^{\lambda(1)}_{\alpha\beta} = \begin{pmatrix} 0 & I^{\lambda(1)}_{\xi} & I^{\lambda(1)}_{\chi} & 0 \\ I^{\lambda(1)}_{\xi} & 0 & 0 & -I^{\lambda(1)}_{\xi} \\ I^{\lambda(1)}_{\chi} & 0 & 0 & -I^{\lambda(1)}_{\chi} \\ 0 & -I^{\lambda(1)}_{\xi} & -I^{\lambda(1)}_{\chi} & 0 \end{pmatrix} \,, \tag{A22}$$

where the functions $I^{\lambda(1)}_{\xi}$ and $I^{\lambda(1)}_{\chi}$ given by

$$\begin{aligned} I^{\lambda(1)}_{\xi} &= \frac{1}{4}\left(\theta\zeta\partial_{\xi} + \lambda\partial_{\chi}\right) I^{(0)} \\ &= -\frac{2GP_0w_0^2(\theta\zeta\xi + \lambda\chi)}{c^5\rho^2}\left(1 - e^{-2|\mu|^2\rho^2}\right) \,, \end{aligned} \tag{A23}$$

$$\begin{aligned} I^{\lambda(1)}_{\chi} &= -\frac{1}{4}\left(\lambda\partial_{\xi} - \theta\zeta\partial_{\chi}\right) I^{(0)} \\ &= \frac{2GP_0w_0^2(\lambda\xi - \theta\zeta\chi)}{c^5\rho^2}\left(1 - e^{-2|\mu|^2\rho^2}\right) \,. \end{aligned} \tag{A24}$$

4. Third order

The only non-zero components of the metric perturbation in the third order of the expansion in the beam divergence are given by

$$\begin{aligned} h^{\lambda(3)}_{\tau\xi} = &-\frac{GP_0w_0^2}{2c^5\rho^2}\Bigg((4\theta\zeta\xi + 3\lambda\chi) + \Bigg(-(4\theta\zeta\xi + 3\lambda\chi) - 2\rho^2(3\theta\zeta\xi + 2\lambda\chi)|\mu|^2 \\ &- 2\rho^2(-2 + 3\rho^2)(\theta\zeta\xi + \lambda\chi)|\mu|^4 + 8\rho^4(\theta\zeta\xi + \lambda\chi)|\mu|^6\Bigg)e^{-2|\mu|^2\rho^2}\Bigg) \,, \end{aligned} \tag{A25}$$

$$\begin{aligned} h^{\lambda(3)}_{\tau\chi} = &-\frac{GP_0w_0^2}{2c^5\rho^2}\Bigg((4\theta\zeta\chi - 3\lambda\xi) + \Bigg(-(4\theta\zeta\chi - 3\lambda\xi) - 2\rho^2(3\theta\zeta\chi - 2\lambda\xi)|\mu|^2 \\ &- 2\rho^2(-2 + 3\rho^2)(\theta\zeta\chi - \lambda\xi)|\mu|^4 + 8\rho^4(\theta\zeta\chi - \lambda\xi)|\mu|^6\Bigg)e^{-2|\mu|^2\rho^2}\Bigg) \,, \end{aligned} \tag{A26}$$

$$\begin{aligned} h^{\lambda(3)}_{\zeta\xi} = &\frac{GP_0w_0^2}{2c^5\rho^2}\Bigg((2\theta\zeta\xi + \lambda\chi) + \Bigg(-(2\theta\zeta\xi + \lambda\chi) - 2\rho^2(2\theta\zeta\xi + \lambda\chi)|\mu|^2 \\ &- 2\rho^2(-2 + 3\rho^2)(\theta\zeta\xi + \lambda\chi)|\mu|^4 + 8\rho^4(\theta\zeta\xi + \lambda\chi)|\mu|^6\Bigg)e^{-2|\mu|^2\rho^2}\Bigg) \,, \end{aligned} \tag{A27}$$

$$\begin{aligned} h^{\lambda(3)}_{\zeta\chi} = &\frac{GP_0w_0^2}{2c^5\rho^2}\Bigg((2\theta\zeta\chi - \lambda\xi) + \Bigg(-(2\theta\zeta\chi - \lambda\xi) - 2\rho^2(2\theta\zeta\chi - \lambda\xi)|\mu|^2 \\ &- 2\rho^2(-2 + 3\rho^2)(\theta\zeta\chi - \lambda\xi)|\mu|^4 + 8\rho^4(\theta\zeta\chi - \lambda\xi)|\mu|^6\Bigg)e^{-2|\mu|^2\rho^2}\Bigg) \,. \end{aligned} \tag{A28}$$

Appendix B: Another approach to determine the rotation of polarization (as described in [11])

Another result for the rotation of the polarization was obtained in [11], where the polarization vector is parallel transported through the gravitational field, again starting and ending in flat spacetime. The angle of rotation

in the $\alpha\beta$-plane is given by

$$\tilde{\Delta}_{\alpha\beta} = \int_{-\infty}^{\infty} d\tilde{\tau}\ \dot{\gamma}^{\gamma}\Gamma^{\delta}_{\alpha\gamma}g_{\beta\delta}\ , \tag{B1}$$

where $\tilde{\tau}$ is the parameter parametrizing the geodesic γ. It is obtained as follows: The polarization vector ω^{α} is parallel transported if

$$\dot{\gamma}^{\alpha}\partial_{\alpha}\omega^{\gamma} + \dot{\gamma}^{\alpha}\omega^{\beta}\Gamma^{\gamma}_{\alpha\beta} = 0\ . \tag{B2}$$

Integrating along the geodesic γ, the change of polarization is given by

$$\delta\omega^{\gamma} = \int_{-\infty}^{\infty} d\tau\ \dot{\gamma}^{\alpha}\partial_{\alpha}\omega^{\gamma} = -\int_{-\infty}^{\infty} d\tau\ \dot{\gamma}^{\alpha}\omega^{\beta}\Gamma^{\gamma}_{\alpha\beta}\ . \tag{B3}$$

From the change of polarization, the angle of rotation in the plane $\beta\gamma$ is obtained by writing

$$(\omega + \delta\omega)^{\gamma} = \left(g^{\gamma}{}_{\beta} + \tilde{\Delta}^{\gamma}{}_{\beta}\right)\omega^{\beta}\ , \tag{B4}$$

which has the form of an infinitesimal rotation. The rotation angle is given by (B1). This result is coordinate-invariant if the metric perturbation vanishes far away from the source of the gravitational field. This is not the case for the laser beam. However, in some cases the result can be applied, as we will explain. Also, (B1) describes a four-dimensional rotation. If the test light-ray is deflected by the laser beam (as for the parallel counter-propagating and the transversal light ray), one has to be careful when applying this formula, as the ray-transversal plane tilts when the light ray is deflected. In our case, the formula can be applied. Indeed, it leads to the same results as we obtain with equation (7): For the parallel co- and parallel conter-propagating light rays, one obtains (to third and first order in the expansion in θ, respectively)

$$\begin{aligned}\tilde{\Delta}^{+}_{\xi\chi} =& -\frac{\theta^2}{2w_0^2}\int_{-\infty}^{\infty} d(\theta\zeta)\left(\partial_{\chi}\left(h^{(3)}_{\xi\zeta} + h^{(3)}_{\tau\xi}\right)\right.\\ &\left. - \partial_{\xi}\left(h^{(3)}_{\chi\zeta} + h^{(3)}_{\tau\chi}\right) - \partial_{\theta\zeta}h^{(2)}_{\xi\chi}\right)\ ,\end{aligned} \tag{B5}$$

$$\begin{aligned}\tilde{\Delta}^{-}_{\chi\xi} =& -\frac{1}{2w_0^2}\int_{-\infty}^{\infty} d(\theta\zeta)\left(\partial_{\chi}\left(h^{(1)}_{\xi\zeta} - h^{(1)}_{\xi\tau}\right)\right.\\ &\left. - \partial_{\xi}\left(h^{(1)}_{\chi\zeta} - h^{(1)}_{\chi\tau}\right)\right)\ .\end{aligned} \tag{B6}$$

The last term of the integrand in the above equation for $\tilde{\Delta}^{+}_{\xi\chi}$ vanishes when integrating from $\zeta = -\infty$ to $\zeta = \infty$, as in our case $h_{\xi\chi}(\infty) = h_{\xi\chi}(-\infty)$. Therefore, we see that $\tilde{\Delta}^{+}_{\xi\chi} = \Delta_{+}$ and $\tilde{\Delta}^{-}_{\chi\xi} = \Delta_{-}$. The same is the case for the transversally propagating light rays: We find (up to the first order in the expansion in θ)

$$\tilde{\Delta}^{t^+}_{\chi\zeta} = \frac{1}{2w_0^2}\int_{-\infty}^{\infty} d\xi\left(\partial_{\chi}h^{(0)}_{\tau\zeta} - \theta\partial_{\chi}h^{(1)}_{\xi\tau} + \theta\partial_{\xi}h^{(1)}_{\chi\zeta}\right)\ , \tag{B7}$$

$$\tilde{\Delta}^{t^-}_{\zeta\chi} = \frac{1}{2w_0^2}\int_{-\infty}^{\infty} d\xi\left(-\partial_{\chi}h^{(0)}_{\tau\zeta} - \theta\partial_{\chi}h^{(1)}_{\xi\tau} - \theta\partial_{\xi}h^{(1)}_{\chi\zeta}\right)\ . \tag{B8}$$

As $h^{(1)}_{\chi\zeta}(\xi = \infty) = h^{(1)}_{\chi\zeta}(\xi = -\infty)$, we obtain $\tilde{\Delta}^{t^+}_{\chi\zeta} = \Delta_{t^+}$ and $\tilde{\Delta}^{t^-}_{\zeta\chi} = \Delta_{t^-}$.

Appendix C: Derivation for finitely extended source and test beams

Starting from the solution in equation (6) for the linearized Einstein equations, we find with equation (8), using the identity $\partial_{x^a}\frac{1}{|\vec{x}-\vec{x}'|} = -\partial_{x^{a\prime}}\frac{1}{|\vec{x}-\vec{x}'|}$, and partial integration (the energy-momentum tensor vanishes at infinity)

$$\begin{aligned}\Delta_{\pm} =& -\frac{2G}{c^4}\int_A^B d\zeta\int_{-\infty}^{\infty} d\xi' d\chi' d\zeta'\ \frac{1}{|\vec{x}-\vec{x}'|}\\ &\left(\theta\left(\partial_{\chi'}\left(t^{(1)}_{\xi\zeta} \pm t^{(1)}_{\tau\xi}\right) - \partial_{\xi'}\left(t^{(1)}_{\chi\zeta} \pm t^{(1)}_{\tau\chi}\right)\right)\right.\\ &\left. + \theta^3\left(\partial_{\chi'}\left(t^{(3)}_{\xi\zeta} \pm t^{(3)}_{\tau\xi}\right) - \partial_{\xi'}\left(t^{(3)}_{\chi\zeta} \pm t^{(3)}_{\tau\chi}\right)\right)\right)\ .\end{aligned} \tag{C1}$$

The energy-momentum tensor of the finitely extended beam is given by multiplying the expressions in appendix A for the infinitely extended beam with the Heaviside functions $\Theta(\zeta - \alpha(\rho))$ and $\Theta(\beta(\rho) - \zeta)$, where $\alpha(\rho)$ and $\beta(\rho)$ describe the ζ-coordinate of the source beam's emitter and absorber, respectively. This truncation of the energy-momentum tensor leads to a violation of the continuity equation of general relativity, which in our case means neglecting recoil on emitter and absorber. This corresponds to energy and momentum being inserted into the system and dissipated from it, respectively, and can lead to apparent effects close to emitter and absorber that may not be present in practice. The best approximation of reality by our model of the finitely extended beam will be achieved for points far from emitter and absorber but close to the beamline (see also [46] for a detailed analysis of a similar situation).

When the surfaces of emitter and absorber are considered to match the phase fronts of the beam, they are curved and, therefore, depend on ρ. This dependence is of second order in θ. The derivatives in equation (C1) lead to Dirac delta functions $\alpha'(\rho)\delta(\zeta - \alpha(\rho))$ and $\beta'(\rho)\delta(\beta(\rho) - \zeta)$, and hence to evaluation of the integrand at the surfaces of emitter and absorber, respectively, integrated over the transversal directions. For each term in equation (C1), this contributes even higher order terms. In the following, we restrict our considerations to the leading order only (to first order for Δ_{-} and to third order for Δ_{+}). Therefore, the contributions of the curved surfaces of emitter and absorber can be neglected and we set α and β to be constants. From the expressions given in appendix A for the energy-momentum tensor, one sees that $t^{(1)}_{\xi\zeta} = -t^{(1)}_{\tau\xi}$ and $t^{(1)}_{\chi\zeta} = -t^{(1)}_{\tau\chi}$. The derivatives appearing in the expression for $\Delta_{\pm}$ of the first order terms are given by

$$\partial_{\chi}t^{(1)}_{\xi\zeta} = \frac{2P_0}{\pi c}|\mu|^4\Big(-4\chi|\mu|^2(\theta\zeta\xi + \lambda\chi) + \lambda\Big)e^{-2|\mu|^2\rho^2}\ , \tag{C2}$$

$$\partial_{\xi}t^{(1)}_{\chi\zeta} = \frac{2P_0}{\pi c}|\mu|^4\Big(-4\xi|\mu|^2(\theta\zeta\chi - \lambda\xi) - \lambda\Big)e^{-2|\mu|^2\rho^2}\ , \tag{C3}$$

and the derivatives of the third order terms are found to be

$$\partial_\chi\left(t^{(3)}_{\xi\zeta}+t^{(3)}_{\tau\xi}\right)=-\frac{P_0}{\pi c}|\mu|^6\rho^2e^{-2|\mu|^2\rho^2}\Big(\lambda +(-4|\mu|^2+2/\rho^2)\chi(\theta\zeta\xi+\lambda\chi)\Big)\,, \quad \text{(C4)}$$

$$\partial_\xi\left(t^{(3)}_{\chi\zeta}+t^{(3)}_{\tau\chi}\right)=-\frac{P_0}{\pi c}|\mu|^6\rho^2e^{-2|\mu|^2\rho^2}\Big(-\lambda +(-4|\mu|^2+2/\rho^2)\xi(\theta\zeta\chi-\lambda\xi)\Big)\,. \quad \text{(C5)}$$

Considering only the leading order terms in θ, we obtain for the rotation angles of the parallel co- and the parallel counter-propagating test rays

$$\Delta_-=-\frac{8GP_0}{c^5}\frac{2\lambda\theta}{\pi}\int_{-\infty}^{\infty}d\xi'd\chi'\int_\alpha^\beta d\zeta' K(\xi',\chi',\zeta') |\mu(\zeta')|^4(1-2|\mu(\zeta')|^2\rho'^2)e^{-2|\mu(\zeta')|^2\rho'^2}\,, \quad \text{(C6)}$$

$$\Delta_+=\frac{8GP_0}{c^5}\frac{\lambda\theta^3}{\pi}\int_{-\infty}^{\infty}d\xi'd\chi'\int_\alpha^\beta d\zeta' K(\xi',\chi',\zeta') |\mu(\zeta')|^6\rho'^2(1-|\mu(\zeta')|^2\rho'^2)e^{-2|\mu(\zeta')|^2\rho'^2}\,, \quad \text{(C7)}$$

where $|\mu(\zeta')|^2=1/(1+(\theta\zeta')^2)$ and

$$K(\xi',\chi',\zeta')=\log\left(\frac{B-\zeta'+(\rho''^2+(B-\zeta')^2)^{1/2}}{A-\zeta'+(\rho''^2+(A-\zeta')^2)^{1/2}}\right)\,, \quad \text{(C8)}$$

with $\rho''=\sqrt{(\xi'-\xi)^2+(\chi-\chi')^2}$.
For the transversal test ray, we find along the same lines (neglecting again the effect of the curved surfaces of emitter and absorber as they are at least of second order in θ), using equation (D8),

$$\Delta_{t\pm}=\frac{2G}{c^4}\int_A^B d\xi\int_{-\infty}^{\infty}d\xi'd\chi'd\zeta'\,\frac{1}{|\vec{x}-\vec{x}'|}\,\partial_{\chi'}\left(\pm t^{(0)}_{\tau\zeta}+\theta t^{(1)}_{\xi\zeta}\right)\,. \quad \text{(C9)}$$

From the expressions for the energy-momentum tensor in appendix A, we find that the derivatives in the above equation are given by

$$\partial_\chi t^{(0)}_{\tau\zeta}=\frac{8P_0}{\pi c}|\mu|^4\chi e^{-2|\mu|^2\rho^2}\,, \quad \text{(C10)}$$

$$\partial_\chi t^{(1)}_{\xi\zeta}=\frac{2P_0}{\pi c}|\mu|^4(\lambda(1-4|\mu|^2\chi^2) -4\theta\zeta\xi\chi|\mu|^2)e^{-2|\mu|^2\rho^2} \quad \text{(C11)}$$

which leads to the rotation angle for the transversal test ray

$$\Delta_{t\pm}=\frac{8GP_0}{c^5}\frac{1}{2\pi}\int_{-\infty}^{\infty}d\xi'd\chi'\int_\alpha^\beta d\zeta' K_t(\xi',\chi',\zeta') |\mu(\zeta')|^4\Big(\pm4\chi'+\theta(\lambda(1-4|\mu(\zeta')|^2\chi'^2) -4\theta\zeta'\xi'\chi'|\mu(\zeta')|^2)\Big)e^{-2|\mu(\zeta')|^2\rho'^2}\,, \quad \text{(C12)}$$

where the function K_t is given by

$$K_t(\xi',\chi',\zeta') =\log\left(\frac{B-\xi'+(\chi''^2+(\zeta-\zeta')^2+(B-\xi')^2)^{1/2}}{A-\xi'+(\chi''^2+(\zeta-\zeta')^2+(A-\xi')^2)^{1/2}}\right)\,, \quad \text{(C13)}$$

where $\chi''=\chi'-\chi$.
For the numerical analysis, we transform the found expressions for the rotation angles into the cylindrical coordinates $\left(\rho',\phi',\zeta'\right)$ with $\phi'=\arccos(\xi'/\rho')$ or $\left(\rho'',\phi'',\zeta'\right)$ with $\rho''=\sqrt{\xi'^2+\chi''^2}$ and $\phi''=\arccos(\xi'/\rho'')$.

Appendix D: Derivation for infinitely extended source and test beams

For the parallel test rays, we obtain from equation (7) and $t_{0,\pm}=\dot\gamma_\pm(\tau_0)=(1,0,0,\pm(1-f^\pm))$

$$\begin{aligned}\Delta_\pm=&\frac{1}{2w_0^2}\int_{-\infty}^{\infty}d\tau\; t_0^a\epsilon_{abc}\partial_b h_{c\alpha}(\varrho_\perp+\tau t_0)t_0^\alpha \quad \text{(D1)}\\ =&\frac{1}{2w_0^2}\int_{-\infty}^{\infty}d\tau\;\epsilon_{\zeta bc}\partial_b\left(h_{c\zeta}(\xi,\chi,\pm\tau)\pm h_{c\tau}(\xi,\chi,\pm\tau)\right)\\ =&-\frac{1}{2w_0^2}\int_{-\infty}^{\infty}d\zeta\,\Big(\partial_\chi(h_{\xi\zeta}\pm h_{\xi\tau})-\partial_\xi(h_{\chi\zeta}\pm h_{\chi\tau})\Big)\,.\end{aligned}$$

The rotation angle for the parallel counter-propagating test ray is thus given by (considering the leading order only)

$$\Delta_-=-\frac{\theta}{2w_0^2}\int_{-\infty}^{\infty}d\zeta\Big(\partial_\chi\left(h^{(1)}_{\xi\zeta}-h^{(1)}_{\tau\xi}\right) -\partial_\xi\left(h^{(1)}_{\chi\zeta}-h^{(1)}_{\tau\chi}\right)\Big)\,. \quad \text{(D2)}$$

From the expressions for the metric perturbation in appendix A, we see that $h^{(1)}_{\xi\zeta}=-h^{(1)}_{\tau\xi}$, $h^{(1)}_{\chi\zeta}=-h^{(1)}_{\tau\chi}$. For the derivatives in the above expression, we find

$$\partial_\chi h^{(1)}_{\xi\zeta}-\partial_\xi h^{(1)}_{\chi\zeta}=\frac{8GP_0w_0^2}{c^5}\lambda|\mu|^2e^{-2|\mu|^2\rho^2}\,, \quad \text{(D3)}$$

which leads to the rotation angle for the parallel counter-propagating test ray

$$\Delta_-=-\lambda\frac{8GP_0\theta}{c^5}\int_{-\infty}^{\infty}d\zeta\,|\mu|^2e^{-2|\mu|^2\rho^2}\,. \quad \text{(D4)}$$

Along the same lines, we find in leading order

$$\Delta_+=-\frac{\theta^3}{2w_0^2}\int_{-\infty}^{\infty}d\zeta\,\Big(\partial_\chi\left(h^{(3)}_{\xi\zeta}+h^{(3)}_{\tau\xi}\right) -\partial_\xi\left(h^{(3)}_{\chi\zeta}+h^{(3)}_{\tau\chi}\right)\Big)\,. \quad \text{(D5)}$$

From the expressions for the metric perturbation in appendix A, one finds for the derivatives in the above expression

$$\begin{aligned}&\partial_\chi\left(h^{(3)}_{\xi\zeta}+h^{(3)}_{\tau\xi}\right)-\partial_\xi\left(h^{(3)}_{\chi\zeta}+h^{(3)}_{\tau\chi}\right)\\&=-\lambda\frac{2GP_0w_0^2}{c^5}|\mu|^2(1+2\rho^2|\mu|^2)e^{-2|\mu|^2\rho^2}\,.\end{aligned}\tag{D6}$$

Then, the rotation angle for the parallel co-propagating light ray is given by

$$\Delta_+ =\lambda\frac{GP_0\theta^3}{c^5}\int_{-\infty}^{\infty}d\zeta\,|\mu|^2(1+2\rho^2|\mu|^2)e^{-2|\mu|^2\rho^2}\,.\tag{D7}$$

For the transversal test ray, we obtain from equation (7) and $\dot\gamma_\pm=(1,\pm1,0,0)$

$$\begin{aligned}\Delta_{t^\pm} =&\frac{1}{2w_0^2}\int_{-\infty}^{\infty}d\tau\;t_0^a\epsilon_{abc}\partial_b h_{c\alpha}(\tau,\varrho_\perp+\tau t_0)t_0^\alpha\\=&\pm\frac{1}{2w_0^2}\int_{-\infty}^{\infty}d\xi\,(\partial_\chi h_{\tau\zeta}-\theta\partial_{\theta\zeta}h_{\tau\chi})\\&+\frac{1}{2w_0^2}\int_{-\infty}^{\infty}d\xi\,(\partial_\chi h_{\xi\zeta}-\theta\partial_{\theta\zeta}h_{\xi\chi})\,,\end{aligned}\tag{D8}$$

Considering the terms up to first order in θ, it is given by

$$\Delta_{t^\pm}=\pm\frac{1}{2w_0^2}\int_{-\infty}^{\infty}d\xi\,\partial_\chi h^{(0)}_{\tau\zeta}+\frac{\theta}{2w_0^2}\int_{-\infty}^{\infty}d\xi\,\partial_\chi h^{(1)}_{\xi\zeta}\,.\tag{D9}$$

From the expressions for the metric perturbation in appendix A, we obtain for the derivatives appearing in the above expression

$$\partial_\chi h^{(0)}_{\tau\zeta}=\frac{8GP_0w_0^2}{c^5}\frac{\chi}{\rho^2}\left(1-e^{-2|\mu|^2\rho^2}\right),\tag{D10}$$

$$\partial_\chi h^{(1)}_{\xi\zeta}=-\frac{1}{4}(\theta\zeta\partial_\chi\partial_\xi+\lambda\partial_\chi^2)I^{(0)}\,.\tag{D11}$$

The first term in equation (D11) leads to an integration over a derivative, which vanishes,

$$\int_{-\infty}^{\infty}d\xi\,\partial_\chi\partial_\xi I^{(0)}=\partial_\chi I^{(0)}\Big|_{\xi=-\infty}^{\xi=\infty}=0\,.\tag{D12}$$

Then, we obtain for the rotation angle for the transversal test ray

$$\begin{aligned}\Delta_{t^\pm}=&\pm\frac{4\pi GP_0}{c^5}\,\mathrm{erf}\left(\sqrt{2}|\mu|\chi\right)\\&+\lambda\frac{2\sqrt{2\pi}GP_0\theta}{c^5}\,|\mu|e^{-2|\mu|^2\chi^2}\,.\end{aligned}\tag{D13}$$

Appendix E: Derivation for finitely extended source beams and infinitely extended test rays

For an infinitely extended test ray and a finitely extended source beam, we obtain

$$\begin{aligned}\Delta_-=&-\frac{2G}{c^4}\partial_\chi\lim_{B\to\infty}\int_{-B}^{B}d\zeta\int_{-\infty}^{\infty}d\xi'd\chi'd\zeta'\\&\frac{1}{|\vec x-\vec x'|}\Big(t_{\xi\zeta}(\xi',\chi',\zeta')-t_{\tau\xi}(\xi',\chi',\zeta')\Big)\\&+\frac{2G}{c^4}\partial_\xi\lim_{B\to\infty}\int_{-B}^{B}d\zeta\int_{-\infty}^{\infty}d\xi'd\chi'd\zeta'\\&\frac{1}{|\vec x-\vec x'|}\Big(t_{\chi\zeta}(\xi',\chi',\zeta')-t_{\tau\chi}(\xi',\chi',\zeta')\Big)\\=&-\frac{4G\theta}{c^4}\partial_\chi\int_\alpha^\beta d\zeta'\int_0^{\rho_0(\zeta')}d\rho'\,\rho'\int_0^{2\pi}d\phi'\\&\lim_{B\to\infty}K_B(\xi,\chi,\zeta,\rho',\phi',\zeta')t^{(1)}_{\xi\zeta}(\rho',\phi',\zeta')\\&+\frac{4G\theta}{c^4}\partial_\xi\int_\alpha^\beta d\zeta'\int_0^{\rho_0(\zeta')}d\rho'\,\rho'\int_0^{2\pi}d\phi'\\&\lim_{B\to\infty}K_B(\xi,\chi,\zeta,\rho',\phi',\zeta')t^{(1)}_{\chi\zeta}(\rho',\phi',\zeta')\,,\end{aligned}\tag{E1}$$

where cylindrical coordinates $\rho'=\sqrt{\xi'^2+\chi'^2}$ and $\phi'=\arctan(\chi'/\xi')$ are used and the function K_B is given by

$$\begin{aligned}&K_B(\xi,\chi,\zeta,\rho',\phi',\zeta')\\&=\log\left(\frac{B-\zeta'+(\rho''^2+(B-\zeta')^2)^{1/2}}{-B-\zeta'+(\rho''^2+(B+\zeta')^2)^{1/2}}\right),\end{aligned}\tag{E2}$$

where $\rho''^2=(\xi'-\xi)^2+(\chi'-\chi)^2=\rho'^2+\rho^2-2\rho'\rho\cos(\phi-\phi')$, and $\rho_0(\zeta')=\rho_0/|\mu(\zeta')|$ is the finite transversal extension of the beam that is related to the width of emitter and absorber and ρ_0 is a constant. For $\beta/B\ll1$, $-\alpha/B\ll1$ and $\rho_0(\zeta')/B\ll1$ for all $\zeta'\in[\alpha,\beta]$, we obtain

$$\begin{aligned}&K_B(\rho',\phi',\zeta')\\&=\log\left(\frac{B-\zeta'+(\rho''^2+B^2(1-\zeta'/B)^2)^{1/2}}{-B-\zeta'+(\rho''^2+B^2(1+\zeta'/B)^2)^{1/2}}\right)\\&\approx\log\left(\frac{2(B-\zeta')+\rho''^2/(2B(1-\zeta'/B))}{\rho''^2/(2B(1+\zeta'/B))}\right)\\&=\log\left(\frac{1+\zeta'/B}{1-\zeta'/B}+\frac{4B^2}{\rho''^2}(1-(\zeta'/B)^2)\right)\\&\approx\log\left(4\frac{B^2}{\rho''^2}\right).\end{aligned}\tag{E3}$$

In order to evaluate the expression for Δ_-, one needs to take derivatives of the function K_B. One finds

$$\begin{aligned}&\partial_\chi\log\left(4\frac{B^2}{\rho''^2}\right)t^{(1)}_{\xi\zeta}-\partial_\xi\log\left(4\frac{B^2}{\rho''^2}\right)t^{(1)}_{\chi\zeta}\\&=\frac{2P_0}{\pi c}|\mu'|^4e^{-2|\mu'|^2\rho'^2}\Big(\lambda\rho'\partial_{\rho'}+\theta\zeta'\partial_{\phi'}\Big)\log\left(\rho''^2\right).\end{aligned}\tag{E4}$$

Therefore, one finds for the following expression appearing in the expression for Δ_-,

$$\begin{aligned}
&\partial_\chi \int_0^{\rho_0(\zeta')} d\rho'\,\rho' \int_0^{2\pi} d\phi' \lim_{B\to\infty} K_B(\rho',\phi',\zeta') t^{(1)}_{\xi\zeta} \\
&- \partial_\xi \int_0^{\rho_0(\zeta')} d\rho'\,\rho' \int_0^{2\pi} d\phi' \lim_{B\to\infty} K_B(\rho',\phi',\zeta') t^{(1)}_{\chi\zeta} \\
&= \frac{2P_0}{\pi c}|\mu'|^4 \int_0^{\rho_0(\zeta')} d\rho'\,\rho' e^{-2|\mu'|^2\rho'^2} \\
&\int_0^{2\pi} d\phi' \Big(\lambda\rho'\partial_{\rho'} + \theta\zeta'\partial_{\phi'}\Big) \log\left(\rho''^2\right). \qquad \text{(E5)}
\end{aligned}$$

The term containing the ϕ'-derivative vanishes under the integral. With

$$\begin{aligned}
&\rho'\partial_{\rho'} \int_0^{2\pi} d\phi' \log\left(\rho'^2 + \rho^2 - 2\rho\rho'\cos(\phi'-\phi)\right) \\
&= 2\pi\rho'\partial_{\rho'} \left\{ \begin{array}{ll} \log\left(\rho'^2\right) & \text{for} \quad \rho \le \rho' \\ \log\left(\rho^2\right) & \text{for} \quad \rho > \rho' \end{array} \right\} \\
&= 4\pi \left\{ \begin{array}{ll} 1 & \text{for} \quad \rho \le \rho' \\ 0 & \text{for} \quad \rho > \rho' \end{array} \right\} = 4\pi\Theta(\rho'-\rho)\,, \qquad \text{(E6)}
\end{aligned}$$

we obtain

$$\begin{aligned}
&\frac{2P_0\lambda}{\pi c}|\mu'|^4 \int_0^{\rho_0(\zeta')} d\rho'\,\rho' \int_0^{2\pi} d\phi' \qquad \text{(E7)} \\
&e^{-2|\mu'|^2\rho'^2}\rho'\partial_{\rho'}\log\left(\rho''^2\right) \\
&= -\frac{2P_0\lambda}{c}|\mu'|^2 \int_0^{\rho_0(\zeta')} d\rho'\,\Theta(\rho'-\rho)\partial_{\rho'} e^{-2|\mu'|^2\rho'^2} \\
&= -\frac{2P_0\lambda}{c}|\mu'|^2 \left\{ \begin{array}{cc} \int_\rho^{\rho_0(\zeta')} d\rho'\,\partial_{\rho'} e^{-2|\mu'|^2\rho'^2} & : \rho \le \rho_0(\zeta') \\ 0 & : \rho > \rho_0(\zeta') \end{array} \right\} \\
&= \frac{2P_0\lambda}{c}|\mu'|^2\Theta(\rho_0(\zeta')-\rho)\Big(e^{-2|\mu'|^2\rho^2} - e^{-2|\mu'|^2\rho_0^2(\zeta')}\Big).
\end{aligned}$$

Finally, we obtain for the rotation of polarization for the parallel counter-propagating test ray

$$\begin{aligned}
\Delta_- = -\lambda\frac{8GP_0\theta}{c^5}\int_\alpha^\beta d\zeta' \qquad \text{(E8)} \\
\Theta(\rho_0 - |\mu'|\rho)|\mu'|^2\Big(e^{-2|\mu'|^2\rho^2} - e^{-2\rho_0^2}\Big)\,,
\end{aligned}$$

which leads to equation (10) for $\rho_0 \to \infty$. We see that Δ_- vanishes if there is no overlap with the beam, i.e. if $\rho > \rho_0(\alpha)$ and $\rho > \rho_0(\beta)$. For large ρ, there is only an overlap for large ζ' for which $\rho_0(\zeta') \approx \rho_0\theta\zeta'$ and $|\mu'| = |\theta\zeta'|^{-1}$. Evaluating the integral, we find

$$\begin{aligned}
\Delta_- = \lambda\frac{8GP_0}{c^5\rho}\Bigg[&\Theta(-\theta\alpha-\rho/\rho_0)\left(\frac{\sqrt{\pi}}{2\sqrt{2}}\left(\mathrm{erf}\left(-\frac{\sqrt{2}\rho}{\theta\alpha}\right) - \mathrm{erf}\left(\sqrt{2}\rho_0\right)\right) - \mathrm{e}^{-2\rho_0^2}\left(-\frac{\rho}{\theta\alpha} - \rho_0\right)\right) \\
&+\Theta(\theta\beta-\rho/\rho_0)\left(\frac{\sqrt{\pi}}{2\sqrt{2}}\left(\mathrm{erf}\left(\frac{\sqrt{2}\rho}{\theta\beta}\right) - \mathrm{erf}\left(\sqrt{2}\rho_0\right)\right) - \mathrm{e}^{-2\rho_0^2}\left(\frac{\rho}{\theta\beta} - \rho_0\right)\right)\Bigg]. \qquad \text{(E9)}
\end{aligned}$$

For $\rho_0 \to \infty$, we obtain

$$\begin{aligned}
\Delta_- = -\lambda\frac{4GP_0}{c^5\rho}\frac{\sqrt{\pi}}{\sqrt{2}} \\
\left(\mathrm{erfc}\left(\frac{\sqrt{2}\rho}{\theta\beta}\right) + \mathrm{erfc}\left(\frac{\sqrt{2}\rho}{\theta|\alpha|}\right)\right), \qquad \text{(E10)}
\end{aligned}$$

where erfc is the complementary error function. For $\rho \gg \theta\beta$ and $\rho \gg -\theta\alpha$, using the asymptotic expansion of the complementary error function, we obtain

$$\Delta_- \approx -\lambda\frac{2GP_0\theta}{c^5\rho^2}\left(\beta e^{-2(\rho/\theta\beta)^2} + |\alpha| e^{-2(\rho/\theta\alpha)^2}\right). \qquad \text{(E11)}$$

For Δ_+, it follows from equation (C1) that in leading order (third order in θ), the rotation of polarization for

the parallel co-propagating light ray is given by

$$\begin{aligned}\Delta_+ = &-\frac{2G}{c^4}\partial_\chi \lim_{B\to\infty}\int_{-B}^{B} d\zeta \\ &\int_{-\infty}^{\infty} d\xi' d\chi' d\zeta' \,\frac{1}{|\vec{x}-\vec{x}'|}\left(t_{\xi\zeta}+t_{\tau\xi}\right) \\ &+\frac{2G}{c^4}\partial_\xi \lim_{B\to\infty}\int_{-B}^{B} d\zeta \\ &\int_{-\infty}^{\infty} d\xi' d\chi' d\zeta' \,\frac{1}{|\vec{x}-\vec{x}'|}\left(t_{\chi\zeta}+t_{\tau\chi}\right) \\ = &-\frac{2G\theta^3}{c^4}\partial_\chi \int_\alpha^\beta d\zeta' \int_0^{\rho_0(\zeta')} d\rho'\,\rho' \\ &\int_0^{2\pi} d\phi' \lim_{B\to\infty} K_B(\rho',\phi',\zeta')\left(t^{(3)}_{\xi\zeta}+t^{(3)}_{\tau\xi}\right) \\ &+\frac{2G\theta^3}{c^4}\partial_\xi \int_\alpha^\beta d\zeta' \int_0^{\rho_0(\zeta')} d\rho'\,\rho' \\ &\int_0^{2\pi} d\phi' \lim_{B\to\infty} K_B(\rho',\phi',\zeta')\left(t^{(3)}_{\xi\zeta}+t^{(3)}_{\tau\xi}\right)\,. \end{aligned} \tag{E12}$$

The relevant combination of derivatives of the function K_B with the approximation given in equation (E3) is given by

$$\begin{aligned}&\partial_\chi \log\left(4\frac{B^2}{\rho''^2}\right)\left(t^{(3)}_{\xi\zeta}+t^{(3)}_{\tau\xi}\right) \\ &-\partial_\xi \log\left(4\frac{B^2}{\rho''^2}\right)\left(t^{(3)}_{\chi\zeta}+t^{(3)}_{\tau\chi}\right) \\ =&-\frac{P_0}{\pi c}|\mu'|^6\rho'^2 e^{-2|\mu'|^2\rho'^2}\left(\lambda\rho'\partial_{\rho'}+\theta\zeta'\partial_{\phi'}\right)\log\left(\rho''^2\right).\end{aligned} \tag{E13}$$

Again, the term containing the derivative with respect to ϕ' vanishes under the integration over ϕ' and we obtain

$$\begin{aligned}&-\frac{P_0\lambda}{\pi c}|\mu'|^6\int_0^{\rho_0(\zeta')} d\rho'\,\rho'^3\int_0^{2\pi} d\phi' \\ &e^{-2|\mu'|^2\rho'^2}\rho'\partial_{\rho'}\log\left(\rho''^2\right) \\ =&\frac{P_0\lambda}{c}|\mu'|^4\int_0^{\rho_0(\zeta')} d\rho'\,\Theta(\rho'-\rho)\rho'^2\partial_{\rho'}e^{-2|\mu'|^2\rho'^2} \\ =&\frac{P_0\lambda}{c}|\mu'|^4\left\{\begin{array}{cc}\int_\rho^{\rho_0(\zeta')} d\rho'\,\rho'^2\partial_{\rho'}e^{-2|\mu'|^2\rho'^2} & :\ \rho\le\rho_0(\zeta')\\ 0 & :\ \rho>\rho_0(\zeta')\end{array}\right\} \\ =&-\frac{P_0\lambda}{c}|\mu'|^4\Theta(\rho_0(\zeta')-\rho)\Bigg[2\int_\rho^{\rho_0(\zeta')} d\rho'\,\rho' e^{-2|\mu'|^2\rho'^2} \\ &+\left(\rho^2 e^{-2|\mu'|^2\rho^2}-\rho_0(\zeta')^2 e^{-2|\mu'|^2\rho_0(\zeta')^2}\right)\Bigg] \\ =&-\frac{P_0\lambda}{c}|\mu'|^2\Theta(\rho_0(\zeta')-\rho)\Bigg[-\frac{1}{2}\int_\rho^{\rho_0(\zeta')} d\rho'\,\partial_{\rho'}e^{-2|\mu'|^2\rho'^2} \\ &+|\mu'|^2\left(\rho^2 e^{-2|\mu'|^2\rho^2}-\rho_0(\zeta')^2 e^{-2|\mu'|^2\rho_0(\zeta')^2}\right)\Bigg] \\ =&-\frac{P_0\lambda}{2c}|\mu'|^2\Theta(\rho_0(\zeta')-\rho)\Big((1+2|\mu'|^2\rho^2)e^{-2|\mu'|^2\rho^2} \\ &-(1+2|\mu'|^2\rho_0(\zeta')^2)e^{-2|\mu'|^2\rho_0(\zeta')^2}\Big).\end{aligned} \tag{E14}$$

Finally, the rotation of polarization for the parallel co-propagating light ray is given by

$$\begin{aligned}\Delta_+ = &\lambda\frac{GP_0\theta^3}{c^5}\int_\alpha^\beta d\zeta' \\ &\Theta(\rho_0-|\mu'|\rho)|\mu'|^2\Big((1+2|\mu'|^2\rho^2)e^{-2|\mu'|^2\rho^2} \\ &-(1+2\rho_0^2)e^{-2\rho_0^2}\Big),\end{aligned} \tag{E15}$$

which leads to equation (9) for $\rho_0\to\infty$. In this case, we find that

$$\Delta_+ = -\frac{\theta^2}{8}\Big(1-\partial_\sigma\Big)\Delta_-(\sqrt{\sigma}\rho)\Big|_{\sigma=1}\,. \tag{E16}$$

Again, we find that Δ_+ vanishes if there is no overlap with the beam, i.e. if $\rho>\rho_0(\alpha)$ and $\rho>\rho_0(\beta)$. For $\rho_0\to\infty$, $\rho\gg\theta\beta$ and $\rho\gg-\theta\alpha$, we find

$$\begin{aligned}\Delta_+ &= \lambda\frac{GP_0\theta^3}{2c^5}\left(\beta\left(\frac{1}{\rho^2}+\frac{1}{(\theta\beta)^2}\right)e^{-2(\rho/\theta\beta)^2}\right. \\ &\qquad\left.-\alpha\left(\frac{1}{\rho^2}+\frac{1}{(\theta\alpha)^2}\right)e^{-2(\rho/\theta\alpha)^2}\right) \\ &\approx \lambda\frac{GP_0\theta}{2c^5}\left(\frac{1}{\beta}e^{-2(\rho/\theta\beta)^2}+\frac{1}{|\alpha|}e^{-2(\rho/\theta\alpha)^2}\right).\end{aligned} \tag{E17}$$

For $\Delta_{t^\pm}$ for a finitely extended source beam and an infinitely extended test ray we obtain, considering only the

leading order contribution,

$$\Delta^{(0)}_{t^\pm} = \pm\frac{1}{2w_0^2}\int_{-\infty}^{\infty} d\xi\,\partial_\chi h^{(0)}_{\tau\zeta} = \mp\frac{2G}{c^4}\int_\alpha^\beta d\zeta' \int_{\rho\le\rho_0(\zeta')} d\xi' d\chi' \lim_{B\to\infty}\partial_\chi K_{t,B}(\xi',\chi',\zeta')t^{(0)}_{\tau\zeta}\,, \tag{E18}$$

where the function $K_{t,B}$ is given by

$$K_{t,B}(\xi',\chi',\zeta') = \log\left(\frac{B-\xi'+(\chi''^2+(\zeta-\zeta')^2+(B-\xi')^2)^{1/2}}{-B-\xi'+(\chi''^2+(\zeta-\zeta')^2+(B+\xi')^2)^{1/2}}\right), \tag{E19}$$

and where $\chi'' = \chi' - \chi$. For $B \gg 1$, we obtain

$$\begin{aligned}
&K_{t,B}(\xi',\chi',\zeta')\\
&= \log\left(\frac{B-\xi'+(B-\xi')\Big(1+(\chi''^2+(\zeta-\zeta')^2)/(B-\xi')^2\Big)^{1/2}}{-B-\xi'+(B+\xi')\Big(1+(\chi''^2+(\zeta-\zeta')^2)/(B+\xi')^2\Big)^{1/2}}\right)\\
&\approx \log\left(\frac{B-\xi'+(B-\xi')\Big(1+(\chi''^2+(\zeta-\zeta')^2)/(2(B-\xi')^2)\Big)}{-B-\xi'+(B+\xi')\Big(1+(\chi''^2+(\zeta-\zeta')^2)/(2(B+\xi')^2)\Big)}\right)\\
&= \log\left(\frac{2(B-\xi')+(\chi''^2+(\zeta-\zeta')^2)/(2(B-\xi'))}{(\chi''^2+(\zeta-\zeta')^2)/(2(B+\xi'))}\right)\\
&\approx \log\left(\frac{B+\xi'}{B-\xi'}+\frac{4B^2}{\chi''^2+(\zeta-\zeta')^2}(1-\xi'^2/B^2)\right)\\
&\approx \log\left(\frac{4B^2}{\chi''^2+(\zeta-\zeta')^2}\right).
\end{aligned} \tag{E20}$$

With the derivative of $K_{t,B}$ with respect to χ,

$$\partial_\chi \log\left(\frac{4B^2}{\chi''^2+(\zeta-\zeta')^2}\right) = 2\frac{\chi-\chi'}{\chi''^2+(\zeta-\zeta')^2} \tag{E21}$$

we obtain for the zeroth order of the rotation of polarization of the transversal test ray

$$\Delta^{(0)}_{t^\pm} = \mp\frac{4GP_0}{\pi c^5}\int_\alpha^\beta d\zeta' \int_{\rho\le\rho_0(\zeta')} d\xi' d\chi' \frac{\chi-\chi'}{\chi''^2+(\zeta-\zeta')^2}|\mu'|^2 e^{-2|\mu'|^2\rho'^2}\,. \tag{E22}$$

Note that for $\chi = 0$, the integrand is anti-symmetric in χ' and $\Delta^{(0)}_{t^\pm}$ vanishes. For the first order contribution, we find

$$\Delta^{(1)}_{t^\pm} = \lambda\frac{4GP_0}{\pi c^5}\int_\alpha^\beta d\zeta' \int_{\rho\le\rho_0(\zeta')} d\xi' d\chi' \frac{\chi'(\chi-\chi')}{(\chi-\chi')^2+(\zeta-\zeta')^2}|\mu'|^4 e^{-2|\mu'|^2\rho'^2}\,. \tag{E23}$$

For $\chi = 0$, the integrand is symmetric in χ' and $\Delta^{(1)}_{t^\pm}$ does not vanish.

Appendix F: Multipole expansion of the far field for finitely extended source and test beams

For the finitely extended source beam, one can get analytical approximations of Δ in the far field. For simplicity we assume here that the source beam extends from $-\beta$ to β, and the probe beam from $-B$ to B. The maximal radial extension of the source beam, reached at $\zeta' = \pm\beta$, is then given by $\rho' = \theta\beta/\sqrt{2}$. This is the maximum scale on which all components of the energy-stress tensor and its derivatives fall off like a Gaussian (for smaller values of $|\zeta'|$ the decay is even faster). Far field means then that the probe beam should be a distance $\rho \gg \theta\beta/\sqrt{2}$ from the source beam when passing parallel to the source beam. A much shorter distance of order $\rho \simeq 1$ suffices for the transversal beam passing at the beam waist for being in the far field regime.
From eqs.(6,8) we obtain, after shifting derivatives to the prime-coordinates and partial integration,

$$\Delta_\pm = -\frac{2G}{c^4\theta}\int_{-B}^{B} d(\theta\zeta)\int d^3x'\frac{1}{|\vec{x}-\vec{x}'|}\Big[\partial_{\chi'}(T_{\xi\zeta}(\vec{x}')\pm T_{\tau\xi}(\vec{x}')) - \partial_{\xi'}(T_{\chi\zeta}(\vec{x}')\pm T_{\tau\chi}(\vec{x}'))\Big]. \tag{F1}$$

For the partial integration we assume once more that we are in the far-field, so that boundary terms are

exponentially suppressed through the Gaussian factor $\exp(-2|\mu|^2\rho^2)$. The source term relevant for Δ_- is given to first order in θ by (see Appendix A, eqs.(A22)

$$\begin{aligned} S_-(\rho',\zeta') &\equiv \frac{\pi c}{4P_0\theta}\Big[\partial_{\chi'}(T_{\xi\zeta}(\vec{x}') - T_{\tau\xi}(\vec{x}')) \\ &\quad -\partial_{\xi'}(T_{\chi\zeta}(\vec{x}') - T_{\tau\chi}(\vec{x}'))\Big] \\ &= \frac{2e^{-2\frac{\rho'^2}{1+\theta^2\zeta'^2}}\lambda(1+\theta^2\zeta'^2-2\rho'^2)}{(1+\theta^2\zeta'^2)^3}\,. \end{aligned} \tag{F2}$$

Manifestly, S_- enjoys azimuthal symmetry. It is then useful to expand the function $1/|\vec{x}-\vec{x}'|$ as (see e.g. [47] p. 93)

$$\frac{1}{|\vec{x}-\vec{x}'|} = \sum_{l=0}^{\infty}\frac{r_<^l}{r_>^{l+1}}P_l(\cos\vartheta')P_l(\cos\vartheta)\ , \tag{F3}$$

where P_l are the Legendre-polynomials, $r_<$ ($r_>$) is the smaller (larger) of $|\vec{x}|$ and $|\vec{x}'|$, and ϑ (ϑ') the angle between the z-axis and $\vec{x}$ ($\vec{x}'$). For calculating the far field, we can set everywhere $r_> = r = |\vec{x}|$ and $r_< = r' = |\vec{x}'|$. This leads to

$$\begin{aligned} \Delta_- &= \sum_{l=0}^{\infty}\Delta_-^{(l)} \\ &= -\frac{16GP_0\theta}{c^5}\sum_{l=0}^{\infty}\int_{-B}^{B}d\zeta\frac{Q_-^{(l)}}{(\rho^2+\zeta^2)^{(l+1)/2}}P_l(\frac{\zeta}{\sqrt{\rho^2+\zeta^2}})\,, \end{aligned} \tag{F4}$$

where the multipoles $Q_-^{(l)}$ are given by

$$\begin{aligned} Q_-^{(l)} &= \int_{-\beta}^{\beta}d\zeta'\int_0^{\infty}\rho' d\rho'\,(\rho'^2+\zeta'^2)^{l/2} \\ &\quad\times P_l(\frac{\zeta'}{\sqrt{\rho'^2+\zeta'^2}})S_-(\rho',\zeta')\,, \end{aligned} \tag{F5}$$

and we have used that in cylinder coordinates $\vartheta = \arccos(\zeta/\sqrt{\rho^2+\zeta^2})$, and correspondingly for ϑ'. The multipoles and their contributions to Δ_- can be calculated analytically. All odd multipoles vanish, and so do the monopole and dipole contribution ($l = 0, 1$, respectively). Δ_- is then dominated by the quadropole contribution $l = 2$. The correction due to higher order multipoles $l = 4, 6, ...$ decays quickly with l. We therefore limit ourselves to listing the results for $l = 2, 4, 6$. Note that the direct dependence on ζ' of $1/|\vec{x}-\vec{x}'|$ (rather than on $\theta\zeta$ as for the rest of the integrand) brings about additional θ dependence. Neglecting these higher order terms, we find

$$Q_-^{(2)} = \frac{\beta\lambda}{4}\,, \tag{F6}$$

$$Q_-^{(4)} = \frac{\beta\lambda}{8}(-3+4\beta^2)\,, \tag{F7}$$

$$Q_-^{(6)} = \frac{3\beta\lambda}{64}(15-40\beta^2+16\beta^4)\,, \tag{F8}$$

and, with $\Omega \equiv 8\lambda\theta GP_0/c^5$,

$$\Delta_-^{(2)} = \frac{\Omega\beta}{2}\frac{B}{(B^2+\rho^2)^{3/2}}\,, \tag{F9}$$

$$\Delta_-^{(4)} = \frac{\Omega\beta(-3+4\beta^2)}{16}\frac{(2B^3-3B\rho^2)}{(B^2+\rho^2)^{7/2}}\,, \tag{F10}$$

$$\begin{aligned} \Delta_-^{(6)} &= \frac{\Omega\beta(15-40\beta^2+16\beta^4)}{256} \\ &\quad\frac{(8B^4-40B^2\rho^2+15\rho^4)}{(B^2+\rho^2)^{11/2}}\,. \end{aligned} \tag{F11}$$

For Δ_+, the lowest contributing terms are from the derivatives of the third order of the metric. The expression for S_- is replaced by S_+ given by

$$\begin{aligned} S_+(\rho',\zeta') &\equiv \frac{\pi c}{P_0\theta^2}\Big[\partial_{\chi'}(T_{\xi\zeta}(\vec{x}') + T_{\tau\xi}(\vec{x}')) \\ &\quad -\partial_{\xi'}(T_{\chi\zeta}(\vec{x}') + T_{\tau\chi}(\vec{x}'))\Big] \\ &= -\frac{e^{-2\frac{\rho'^2}{1+\theta^2\zeta'^2}}\lambda\rho'^2(1-\rho'^2/(1+\theta^2\zeta'^2))}{(1+\theta^2\zeta'^2)^3}\,. \end{aligned} \tag{F12}$$

Also here the monopole contribution ($l = 0$) and all contributions with odd l, in particular the dipole contribution ($l = 1$) vanish. The lowest order non-vanishing contributions are

$$Q_+^{(2)} = -\frac{\beta\lambda\theta^2}{16}\,, \tag{F13}$$

$$Q_+^{(4)} = \frac{\beta\lambda\theta^2}{64}(9-8\beta^2)\,, \tag{F14}$$

$$Q_+^{(6)} = -\frac{3\beta\lambda\theta^2}{128}(15-30\beta^2+8\beta^4)\,, \tag{F15}$$

to be substituted into the expression corresponding to (F5), i.e.

$$\begin{aligned} \Delta_+ &= \sum_{l=0}^{\infty}\Delta_+^{(l)} \\ &= -\frac{16GP_0\theta}{c^5}\sum_{l=0}^{\infty}\int_{-B}^{B}d\zeta\frac{Q_+^{(l)}}{(\rho^2+\zeta^2)^{(l+1)/2}}P_l(\frac{\zeta}{\sqrt{\rho^2+\zeta^2}})\,. \end{aligned} \tag{F16}$$

This leads to

$$\Delta_+^{(2)} = -\frac{\Omega\theta^2}{8}\frac{B\beta}{(B^2+\rho^2)^{3/2}}\,, \tag{F17}$$

$$\Delta_+^{(4)} = \frac{\Omega\theta^2(-9+8\beta^2)}{128}\frac{(-2B^3+3B\rho^2)}{(B^2+\rho^2)^{7/2}}\,, \tag{F18}$$

$$\begin{aligned} \Delta_+^{(6)} &= -\frac{\Omega\theta^2 B\beta(15-30\beta^2+8\beta^4)}{512} \\ &\quad\frac{(8B^4-40B^2\rho^2+15\rho^4)}{(B^2+\rho^2)^{11/2}}\,, \end{aligned} \tag{F19}$$

where we recall that Ω contains already one factor θ. So both $\Delta_\pm$ fall off as $1/\rho^3$ in the far-field due to the quadrupole contribution. For fixed ρ, β that contribution decays as $1/B$ for large B, i.e. $B \gg \rho$. This can be traced

back to the integral over ζ in and would not be the case for the monopole contribution.

For $\Delta_{t^\pm}$ we start with the lowest, zeroth order in θ. It is then useful to keep the derivatives of the energy-stress tensor outside the calculation of the multipoles, as otherwise the cylindrical symmetry gets spoiled. We find

$$\Delta^{(0)}_{t^\pm} = \mp \frac{8GP_0}{c^5}\int_{-B}^{B} d\xi\, \partial_\chi \sum_{l=0}^{\infty} \frac{P_l(\frac{\zeta}{\sqrt{\rho^2+\zeta^2}})}{(\rho^2+\zeta^2)^{(l+1)/2}} Q^{(0)(l)}_{t^\pm} \,, \tag{F20}$$

$$Q^{(0)(l)}_{t^\pm} = \int_{-\beta}^{\beta} d\zeta' \int_0^\infty d\rho' \rho' (\rho'^2+\zeta'^2)^{l/2} P_l(\frac{\zeta'}{\sqrt{\rho'^2+\zeta'^2}}) \times \frac{1}{1+\theta^2\zeta'^2} e^{-2\frac{\rho'^2}{1+\theta^2\zeta'^2}} \,. \tag{F21}$$

Also here, all the odd-power multipoles ($l = 1, 3, 5, \ldots$) vanish due to the fact that the Legendre-polynomials of odd order are odd, whereas the rest of the integrand in $Q^{(0)(l)}_{t^\pm}$ is even in ζ'. The three lowest non-vanishing multipoles read

$$Q^{(0)(0)}_{t^\pm} = \frac{\beta}{2} \,, \tag{F22}$$

$$Q^{(0)(2)}_{t^\pm} = -\frac{1}{24}\beta(3-4\beta^2) \,, \tag{F23}$$

$$Q^{(0)(4)}_{t^\pm} = \frac{1}{160}\beta(15-40\beta^2+16\beta^4) \,. \tag{F24}$$

The corresponding contributions to $\Delta_{t^\pm}$ at $\zeta = 0$ are

$$\Delta^{(0)(0)}_{t^\pm} = \pm\tilde{\Omega}\frac{B\beta}{\chi\sqrt{B^2+\chi^2}} \,, \tag{F25}$$

$$\Delta^{(0)(2)}_{t^\pm} = \pm\tilde{\Omega}\frac{B\beta(3-4\beta^2)(2B^2+3\chi^2)}{24\chi^3(B^2+\chi^2)^{3/2}} \,, \tag{F26}$$

$$\Delta^{(0)(4)}_{t^\pm} = \pm\tilde{\Omega}\frac{B\beta(15-40\beta^2+16\beta^4)}{640\chi^5(B^2+\chi^2)^{5/2}} (8B^4+20B^2\chi^2+15\chi^4) \,, \tag{F27}$$

where $\tilde{\Omega} = 8GP_0/c^5$. We see that now there is a contribution from the monopole that leads to a decay as $1/\chi^2$ with the minimal distance χ from the beamline when evaluated at $\zeta = 0$ and in the limit of $\chi \gg B$. The next (quadrupole) term contributes a $1/\chi^4$ decay. In the limit of $B \to \infty$ at fixed χ, the monopole contribution converges to a β/χ^2 behavior.

For the first order term in $\Delta_{t^\pm}$, the contribution to the Faraday effect, we obtain with the expressions for the energy-momentum tensor given in appendix A, using the symmetry of $|\vec{x}-\vec{x}'|$ and performing a partial integration,

$$\begin{aligned}\Delta^{(1)}_{t^\pm} &= \frac{2G\theta}{c^4}\partial_\chi \int_{-B}^{B} d\xi \int_{-\infty}^{\infty} d\xi' d\chi' d\zeta' \frac{1}{|\vec{x}-\vec{x}'|} t^{(1)}_{\xi\zeta} \\ &= \frac{\lambda\theta}{4}\partial_\chi \Delta^{(0)}_{t^+} - \frac{GP_0\theta^2}{\pi c^5}\partial_\chi \int_{-B}^{B} d\xi\, \partial_\xi \int_{-\infty}^{\infty} d\xi' d\chi' \\ &\quad \int_{-\beta}^{\beta} d\zeta' \frac{1}{|\vec{x}-\vec{x}'|}\frac{\zeta'}{1+\theta^2\zeta'^2} e^{-2\frac{\rho'^2}{1+\theta^2\zeta'^2}} \,. \end{aligned} \tag{F28}$$

We neglect the second term as it is of higher order in θ. For the first term, we find from the multipole expansion of $\Delta^{(0)}_{t^+}$ for $\zeta = 0$

$$\Delta^{(1)(0)}_{t^\pm} = -\frac{\lambda\theta}{4}\tilde{\Omega}\frac{B\beta(B^2+2\chi^2)}{\chi^2(B^2+\chi^2)^{3/2}} \,, \tag{F29}$$

$$\Delta^{(1)(2)}_{t^\pm} = -\frac{\lambda\theta}{4}\tilde{\Omega}\frac{B\beta(3-4\beta^2)}{8\chi^4(B^2+\chi^2)^{5/2}} (2B^4+5B^2\chi^2+4\chi^4) \,, \tag{F30}$$

$$\Delta^{(1)(4)}_{t^\pm} = -\frac{\lambda\theta}{4}\tilde{\Omega}\frac{B\beta(15-40\beta^2+16\beta^4)}{128\chi^6(B^2+\chi^2)^{7/2}} (8B^6+28B^4\chi^2+35B^2\chi^4+18\chi^6) \,. \tag{F31}$$

In a real experiment, it should be kept in mind that the gravitational effects from emitter and absorber and the power-supplies feeding them, as well as heat-radiation from the absorber may lead to effects that mask the rotation of the polarization of the source beam itself in the far field, if their dipole- or monopole-contributions do not vanish. If one wishes to evaluate these effects, a careful modelling of the entire setup will be necessary.

Appendix G: The infinitely thin beam

The metric perturbation induced by an infinitely thin beam of light that extends along the ζ-axis from $-\beta$ to β is given by the only non-zero components $h_{\tau\tau} = -h_{\tau\zeta} = h_{\zeta\zeta} = h$, where h is given as [1]

$$h = \frac{4GP_0w_0^2}{c^5}\log\left(\frac{\beta-\zeta+(\rho^2+(\beta-\zeta)^2)^{1/2}}{-\beta-\zeta+(\rho^2+(\beta+\zeta)^2)^{1/2}}\right) . \tag{G1}$$

Therefore, we find with equation (7) at $\zeta = 0$ and for large χ

$$\begin{aligned}\Delta_{t^\pm} &\approx \pm\frac{1}{2w_0^2}\int_{-B}^{B} d\xi\, \partial_\chi h^{(0)}_{\tau\zeta} \\ &\approx \pm\frac{8GP_0}{c^5}\frac{\beta B}{\chi\sqrt{B^2+\chi^2}} \,, \end{aligned} \tag{G2}$$

where we considered a test ray extending from $-B$ to B, and

$$\Delta_{t^\pm} \approx \pm\tfrac{8GP_0}{c^5}\tfrac{\beta}{\chi} \,, \tag{G3}$$

for the infinitely extended test ray.

[1] Richard C. Tolman, Paul Ehrenfest, and Boris Podolsky. On the gravitational field produced by light. *Physical Review*, 37(602), 1931.

[2] W. B. Bonnor. The gravitational field of light. *Communications in Mathematical Physics*, 13(3):163–174, 1969.

[3] Dennis Rätzel, Martin Wilkens, and Ralf Menzel. Gravitational properties of light – the gravitational field of a laser pulse. *New Journal of Physics*, 18(2):023009, 2016.

[4] James Strohaber. General relativistic manifestations of orbital angular and intrinsic hyperbolic momentum in electromagnetic radiation. *arXiv: 1807.00933*, 2018.

[5] Fabienne Schneiter, Dennis Rätzel, and Daniel Braun. The gravitational field of a laser beam beyond the short wavelength approximation. *Classical and Quantum Gravity*, 35:195007, 2018.

[6] G. V. Skrotskii. The influence of gravity on the propagation of light. *Doklady Akademii Nauk SSSR*, 114(1):73–76, 1957.

[7] N. L. Balazs. Effect of a gravitational field, due to a rotating body, on the plane of polarization of an electromagnetic wave. *Physical Review*, 110(1), 1958.

[8] Jerzy Plebanski. Electromagnetic waves in gravitational fields. *Physical Review*, 118:1396–1408, 1960.

[9] Maxim Lyutikov. Rotation of polarization by a moving gravitational lens. *Physical Review D*, 95:124003, 2017.

[10] Sergei Kopeikin and Bahram Mashoon. Gravitomagnetic effects in the propagation of electromeagnetic waves in variable gravitational fields of arbitrary-moving and spinning bodies. *Physical Review D*, 65:064025, 2002.

[11] Ue-Li Pen, Xin Wang, and I-Sheng Yang. Gravitational rotation of polarization: Clarifying the gauge dependence and prediction for a double pulsar. *Physical Review D*, 95:044034, 2017.

[12] Mauro Sereno. Gravitational Faraday rotation in a weak gravitational field. *Physical Review D*, 69:087501, 2004.

[13] Bin Chen. Probing the gravitational Faraday rotation using quasar x-ray microlensing. *Scientific Reports*, 5(16860), 2015.

[14] Tsvi Piran and Pedro N. Safier. A gravitational analogue of Faraday rotation. *Nature*, 318(21), 1985.

[15] H. Dehnen. Gravitational Faraday-effect. *International Journal of Theoretical Physics*, 7(6):467–474, 1973.

[16] David Eric Cox, James G. O'Brien, Ronald L. Mallett, and Chandra Roychoudhuri. Gravitational Faraday effect produced by a ring laser. *Foundation of Physics*, (37):723, 2007.

[17] Peiyong Ji and Ying Bai. Gravitational effects induced by high-power lasers. *The European Physical Journal C - Particles and Fields*, 46(3):817–823, 2006.

[18] N. Yu. Gnedin and I. G. Dymnikova. Rotation of the plane of polarization of a photon in a Petrov type $\mathcal{D}$ space-time. *Zh. Eksp. Teor. Fiz.*, 94:26–31, 1988.

[19] Aharon Brodutch, Tommaso F. Demarie, and Daniel R. Terno. Photon polarization and geometric phase in general relativity. *Physical Review D*, 84:104043, 2011.

[20] Aharon Brodutch and Daniel R. Terno. Polarization rotation, reference frames, and Mach's principle. *Physical Review D*, 84:121501(R), 2011.

[21] L. Landau and E. M. Lifschitz. *Lehrbuch der Theoretischen Physik, Band VIII, Elektrodynamik der Kontinua (German edition)*. Akademie Verlag, Berlin, 3rd edition, 1974.

[22] M. G. Calkin. An invariance property of the free electromagnetic field. *American Journal of Physics*, 33(11):958–960, 1965.

[23] Jos L Trueba and Antonio F Raada. The electromagnetic helicity. *European Journal of Physics*, 17(3):141, 1996.

[24] Stephen M. Barnett, Robert P. Cameron, and Alison M. Yao. Duplex symmetry and its relation to the conservation of optical helicity. *Phys. Rev. A*, 86:013845, Jul 2012.

[25] Ivan Fernandez-Corbaton, Xavier Zambrana-Puyalto, and Gabriel Molina- Terriza. Helicity and angular momentum: A symmetry-based framework for the study of light-matter interactions. *Physical Review A*, 86:042103, October 2012.

[26] Lars Andersson, Sajad Aghapour, and Reebhu Bhattacharyya. Helicity and spin conservation in Maxwell theory and Linearized Gravity. *Preprint: arXiv:1812.03292*, 2018.

[27] Charles W. Misner, Kip S. Thorne, and John Archibald Wheeler. *Gravitation*. W. H. Freeman and Company, San Francisco, 1973.

[28] T. Levi-Civita. *Atti Accad. Lincei Rendi*, 28(101), 1919.

[29] Dennis Rätzel, Fabienne Schneiter, Daniel Braun, Tupac Bravo, Richard Howl, Maximilian P. E. Lock, and Ivette Fuentes. Frequency spectrum of an optical resonator in a curved spacetime. *New Journal of Physics*, 20(5):053046, 2018.

[30] Peter C. Aichelburg and Roman Ulrich Sexl. On the gravitational field of a massless particle. *General Relativity and Gravitation*, 2(4):303–312, 1971.

[31] Daniel Braun, Fabienne Schneiter, and Uwe R. Fischer. Intrinsic measurement errors for the speed of light in vacuum. *Class. Quantum Grav.*, 34(17):175009, 2017.

[32] F. Della Valle, E. Milotti, A. Ejlli, U. Gastaldi, G. Messineo, L. Piemontese, G. Zavattini, R. Pengo, and G. Ruoso. Extremely long decay time optical cavity. *Optics Express*, 22(9):11570, 2014.

[33] W. Schottky. Über spontane Stromschwankungen in verschiedenen Elektrizitätsleitern. *Annalen der Physik*, 57:541567, 1918.

[34] E. A. Shcherbakov, V. V. Fomin, A. A. Abramov, A. A. Ferin, D. V. Mochalov, and V. P. Gaspontsev. Industrial grade 100 kw power cw fiber laser. In *Advanced Solid-State Lasers Congress*, page ATh4A.2. Optical Society of America, 2013.

[35] Lei S. Meng, Jason K. Brasseur, and David K. Neumann. Damage threshold and surface distortion measurement for high-reflectance, low-loss mirrors to 100+ mw/cm2 cw laser intensity. *Optics Express*, 13(25):10085–10091, 2005.

[36] Henning Vahlbruch, Moritz Mehmet, Karsten Danzmann, and Roman Schnabel. Detection of 15 db squeezed states of light and their application for the absolute calibration of photoelectric quantum efficiency. *Physical Review Letters*, 117:110801, 2016.

[37] O. Pinel, P. Jian, N. Treps, C. Fabre, and D. Braun. Quantum parameter estimation using general single-mode Gaussian states. *Physical Review A*, 88:040102(R), 2013.

[38] Daniel Braun, Gerardo Adesso, Fabio Benatti, Roberto Floreanini, Ugo Marzolino, Morgan W. Mitchell, and Stefano Pirandola. Quantum-enhanced measurements without entanglement. *Review of Modern Physics*, 90:035006, 2018.

[39] Aasi et al. Enhanced sensitivity of the LIGO gravitational wave detector by using squeezed states of light. *Nature Photonics*, 7:613–619, 2013.

[40] V. Faraoni. On the rotation of polarization by a gravitational lens. *Journal of Astrophysics and Astronomy*, 272:385–388, 1993.

[41] I. Yu. Kobzarev and K. G. Selivanov. Rotation of the polarization vector in a nonstationary gravitational field. *Zh. Eksp. Teor. Fiz.*, 94(1-4), 1988.

[42] Ue-Li Pen, Xin Wang, and I-Sheng Yang. Gravitational rotation of polarization: Clarifying the gauge dependence and prediction for a double pulsar. *Physical Review D*, 95:044034, 2017.

[43] J. W. van Holten. The gravitational field of a light wave. *Fortschritte der Physik*, 59(3-4):284–295, 2011.

[44] B. M. Barker, M. S. Bhatia, and S. N. Gupta. Gravitational scattering of light by light. *Physical Review*, 158:1498, 1967.

[45] Bahram Mashhoon. Gravitational couplings of intrinsic spin. *Classical and Quantum Gravity*, 17:2399, 2000.

[46] Dennis Rätzel, Martin Wilkens, and Ralf Menzel. The effect of entanglement in gravitational photon-photon scattering. *Europhysics Letters*, 115(5):51002, 2016.

[47] John David Jackson. *Classical electrodynamics*. Wiley, New York, 3rd edition, 1999.

Declaration according to §Abs. 2 No. 8 of the PhD regulations of the Faculty of Science

- Collaborative Publications -

Name: Fabienne Schneiter

List of Publications

1. Daniel Braun, Fabienne Schneiter, Uwe R. Fischer. Intrinsic measurement errors for the sped of light in vacuum. Classical and Quantum Gravity, 34(17), 2017. arXiv: 1502.04979.
2. Dennis Rätzel, Fabienne Schneiter, Daniel Braun, Tupac Bravo, Richard Howl, Maximilian P. E. Lock, Ivette Fuentes. Frequency spectrum of an optical resonator in a gravitational field. New Journal of Physics, 20, 2018. arXiv: 1711.11320.
3. Fabienne Schneiter, Dennis Rätzel, Daniel Braun. The gravitational field of a laser beam beyond the short wavelength approximation. Classical and Quantum Gravity, 35(19), 2018. arXiv: 1804.08706.
4. Fabienne Schneiter, Dennis Rätzel, Daniel Braun. Rotation of polarization in the gravitational field of a focused laser beam - optical activity and Faraday effect. arxiv: 1812.04505.

Nr.	Accepted for publication	Number of authors	Position of candidate	Scientific ideas of candidate	Analysis and interpretation by candidate	Paper writing by candidate
1	yes	3	second	20%	30%	5%
2	yes	7	second	40%	40%	10%
3	yes	3	first	50%	50%	50%
4	no	3	first	50%	50%	50%

I certify that the above-stated is correct.

Date, signature of candidate

I/We certify that the above-stated is correct.

Date, signature of doctoral committee or at least one of the supervisors